

ESE 546: Principles of Deep Learning

Fall 2020

Instructor

Pratik Chaudhari pratikac@seas.upenn.edu

Teaching Assistants

Evangelos Chatzipantazis vaghat@seas

Rahul Ramesh rahulram@seas

Dushyant Sahoo sadu@seas

Rongguang Wang rgw@seas

Shiyun Xu shiyunxu@sas

December 10, 2020

Contents

1	What is intelligence?	5
1.1	Key components of intelligence	6
1.1.1	What is learning?	7
1.2	Intelligence: The Beginning (1942-50)	7
1.2.1	Representation Learning	9
1.3	Intelligence: Reloaded (1960-2000)	11
1.4	Intelligence: Revolutions (2006-)	12
1.5	A summary of our goals in this course	13
2	Linear Regression, Perceptron, Stochastic Gradient Descent	14
2.1	Problem setup for machine learning	14
2.1.1	Generalization	15
2.2	Linear regression	16
2.2.1	Maximum Likelihood Estimation	17
2.3	Perceptron	19
2.3.1	Surrogate Losses	19
2.4	Stochastic Gradient Descent	20
2.4.1	The general form of SGD	21
3	Kernels, Beginning of neural networks	22
3.1	Digging deeper into the perceptron	22
3.1.1	Convergence rate	22
3.1.2	Dual representation	23
3.2	Creating nonlinear classifiers from linear ones	24
3.3	Kernels	25
3.3.1	Kernel perceptron	25
3.3.2	Mercer's theorem	26
3.4	Learning the feature vector	27
3.4.1	Random features	28
3.4.2	Learning the feature matrix as well	29
4	Deep fully-connected networks, Backpropagation	31
4.1	Deep fully-connected networks	31
4.1.1	Some deep learning jargon	33
4.1.2	Weights	34
4.2	The backpropagation algorithm	35
4.2.1	One hidden layer with one neuron	35
4.2.2	Implementation of backpropagation	38

5	Convolutional Architectures	39
5.1	Basics of the convolution operation	40
5.1.1	Convolutions of 2D images	42
5.1.2	Some examples	42
5.2	How are convolutions implemented?	44
5.3	Convolutions for multi-channel images in a deep network	45
5.4	Translational equivariance using convolutions	46
5.5	Pooling to build translational invariance	47
6	Data augmentation, Loss functions	49
6.1	Data augmentation	49
6.1.1	Some basic data augmentation techniques	50
6.1.2	How does augmentation help?	50
6.1.3	What kind of augmentation to use when?	51
6.2	Loss functions	51
6.2.1	Regression	52
6.2.2	Classification: Cross-Entropy loss	53
6.2.3	Softmax Layer	55
6.2.4	Label smoothing	55
6.2.5	Multiple ground-truth classes	56
7	Bias-Variance Trade-off, Dropout, Batch-Normalization	57
7.1	Bias-Variance Decomposition	57
7.1.1	Cross-Validation	61
7.2	Weight Decay	63
7.2.1	Do not do weight decay on biases	64
7.2.2	Maximum a posteriori (MAP) Estimation	64
7.3	Dropout	66
7.3.1	Bagging classifiers	67
7.3.2	Some insight into how dropout works	68
7.3.3	Implementation details of dropout	70
7.3.4	Using dropout as a heuristic estimate of uncertainty	70
7.4	Batch-Normalization	71
7.4.1	Covariate shift	71
7.4.2	Internal covariate shift	72
7.4.3	Problems with batch-normalization	75
8	Recurrent Architectures, Attention Mechanism	78
8.1	Recursive updates in a Kalman filter, sufficient statistics	78
8.2	Recurrent Neural Networks (RNNs)	80
8.2.1	Backpropagation in an RNN	82
8.2.2	Handling long-term temporal dependencies	83
8.3	Long Short-Term Memory (LSTM)	86
8.3.1	Gated Recurrent Units (GRUs)	86
8.3.2	LSTMs	87
8.4	Bidirectional architectures	87
8.5	Attention mechanism	88
8.5.1	Weighted regression estimate	89
8.5.2	Attention layer in deep networks	90
8.5.3	Attention as one of the layers of a recurrent networks	91

9	Background on Optimization, Gradient Descent	93
9.1	Convexity	94
9.2	Introduction to Gradient Descent	96
9.2.1	Conditions for optimality	96
9.2.2	Different types of convergence	97
9.3	Convergence rate for gradient descent	98
9.3.1	Some assumptions	98
9.3.2	GD for convex functions	99
9.3.3	Gradient descent for strongly convex functions	102
9.4	Limits on convergence rate of first-order methods	104
10	Accelerated Gradient Descent	105
10.1	Polyak's Heavy Ball method	105
10.1.1	Polyak's method can fail to converge	107
10.2	Nesterov's method	108
10.2.1	Yet another way to write Nesterov's updates	109
10.2.2	How to pick the momentum parameter?	111
11	Stochastic Gradient Descent	113
11.1	SGD for least-squares regression	115
11.2	Convergence of SGD	116
11.2.1	Typical assumptions in the analysis of SGD	117
11.2.2	Convergence rate of SGD for strongly-convex functions	118
11.2.3	When should one use SGD in place of GD?	120
11.3	Accelerating SGD using momentum	121
11.3.1	Momentum methods do not accelerate SGD	122
11.4	Understanding SGD as a Markov Chain	123
11.4.1	Gradient flow	123
11.4.2	Markov chains	124
11.4.3	A Markov chain model of SGD	126
11.4.4	The Gibbs distribution	128
11.4.5	Convergence of a Markov chain to its invariant distribution	130
12	Shape of the energy landscape of neural networks	133
12.1	Introduction	134
12.2	Deep Linear Networks	135
12.3	Extending the picture to deep networks	139
13	Generalization performance of machine learning models	140
13.1	The PAC-Learning model	140
13.2	Concentration of Measure	143
13.2.1	Union Bound (or Boole's Inequality)	143
13.2.2	Chernoff Bound	143
13.3	Uniform convergence	145
13.4	Vapnik-Chernovenkis (VC) dimension	147
14	Variational Inference	150
14.1	The model	150
14.2	Some technical basics	152
14.2.1	Variational calculus	152
14.2.2	Laplace approximation	154
14.2.3	Digging deeper into KL-divergence	155

14.3	Evidence Lower Bound (ELBO)	156
14.3.1	Parameterizing ELBO	158
14.4	Gradient of the ELBO	160
14.4.1	The Reparameterization Trick	161
14.4.2	Score-function estimator of the gradient	162
14.4.3	Gradient of the remaining terms in ELBO	163
14.5	Some comments	164
15	Generative Adversarial Networks	166
15.1	Two-sample tests and Discriminators	167
15.2	Building the Discriminator in a GAN	168
15.3	Building the Generator of a GAN	170
15.4	Putting the discriminator and generator together	170
15.5	How to perform validation for a GAN?	172
15.6	The zoo of GANs	174
	Bibliography	175

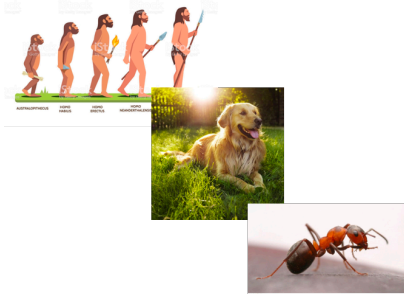
Chapter 1

What is intelligence?

Reading

1. Bishop 1.1-1.5
2. Goodfellow Chapter 1
3. “A logical calculus of the ideas immanent in nervous activity” by Warren McCulloch and Walter Pitts (McCulloch and Pitts, 1943).
4. “Computing machinery and intelligence” by Alan Turing in 1950 (Turing, 2009).

What is intelligence? It is hard to define, I don't know a good definition. We certainly know it when we see it. All humans are intelligent. Dogs are plenty intelligent. Most of us would agree that a house fly or an ant is less intelligent than a dog. What are the common features of these species? They all can gather food, search for mates and reproduce, adapt to changing environments and, in general, the ability to survive.



Let us ask a different question. Are plants intelligent? Plants have sensors, they can measure light, temperature, pressure etc. They possess reflexes, e.g., sunflowers follow the sun. This is an indication of “reactive/automatic intelligence”. The mere existence of a sensory and actuation mechanism is not an indicator of intelligence. Plants cannot perform planned movements, e.g., they cannot travel to new places.

A Tunicate in Figure 1.1 is an interesting plant however. Tunicates are invertebrates. When they are young they roam around the ocean floor in search of nutrients, and they also have a nervous system (ganglion cells) at this point

57 a feed-forward process. Your sensory inputs depend on the previous action
58 you took.

59 **1.1.1 What is learning?**

60 This class will focus on learning. It is a component, not the entirety, of
61 cognition. Learning is in charge of looking at past data and predicting what
62 future data may look like. Cognition is much more than that, it also involves
63 assimilating knowledge, handling situations when the current data does not
64 match past data, e.g., arithmetic problems you solved in elementary school
65 used your skills of algebraic manipulation to handle new problems.

66 Examples of other classes that address various aspects of intelligence are:

- 67 • Perception: CIS 580, CIS 581, CIS 680
- 68 • Learning: CIS 520, CIS 521, CIS 522, CIS 620, CIS 700, ESE 545
- 69 • Control: ESE 650, MEAM 620, ESE 505

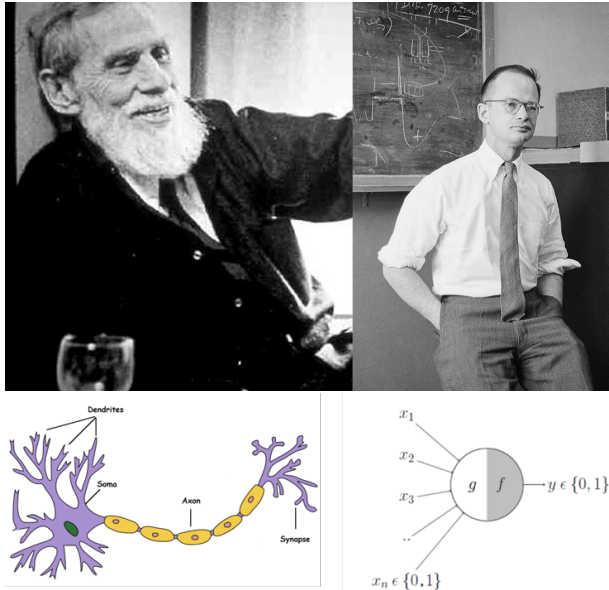
70 Imagine a supreme agent which is infinitely fast and clever can interpret its
71 sensory data and compute the best actions for any task, say driving, it wishes.
72 One would think learning on the past data is not essential to cognition, certainly
73 not for this supreme agent. However, learning is essential to cognition. Priors
74 help you if you are not as fast as the supreme agent or if you want to save
75 some compute time/energy during decision making.

You should not think of a deep network or a machine learning model as a mechanism that directly undertakes the actions. It is better suited to provide a prior on the possible actions that an autonomous agent should take; other algorithms that rely on real-time sensory data will be in charge of picking one action out of these predictions. The objective of the learning process is really to crunch the data and learn a prior.

76 **1.2 Intelligence: The Beginning (1942-50)**

77 Let us give a short account of how our ideas about intelligence have evolved.

78 The story begins in 1942 in Chicago. These are Warren McCulloch who
79 was a neuroscientist and Walter Pitts who studied mathematical logic. They
80 built the first model of a mechanical neuron and propounded the idea that
81 simple elemental computational blocks in your brain work together to perform
82 complex functions. Their paper ([McCulloch and Pitts, 1943](#)) is an assigned
83 reading for this lecture.



**A LOGICAL CALCULUS OF THE IDEAS IMMANENT IN
NERVOUS ACTIVITY***

■ WARREN S. MCCULLOCH AND WALTER PITTS
University of Illinois, College of Medicine,
Department of Psychiatry at the Illinois Neuropsychiatric Institute,
University of Chicago, Chicago, U.S.A.

84 Around the same time in England, Alan Turing was forming his initial
85 ideas on computation and neurons. He had already published his paper on
86 computability by then. This paper (Turing, 2009) is the second assigned
87 reading for this lecture. ¹

VOL. LIX. No. 236.]

[October, 1950

MIND

A QUARTERLY REVIEW

OF

PSYCHOLOGY AND PHILOSOPHY

I.—COMPUTING MACHINERY AND
INTELLIGENCE

By A. M. TURING

88

1. *The Imitation Game.*

89 McCulloch was inspired by Turing's idea that of building a machine that could
90 compute any function in finitely-many steps was powerful. In his mind, the
91 neuron in a human brain, which either fires or does not fire depending upon
92 the stimuli of the neurons connected to it, was a binary object; rules of logic
93 where a natural way to link such neurons, just like the Pitt's hero Bertrand
94 Russell rebuilt modern mathematics using logic.

¹If you need more inspiration to go and read it, the first section is titled "The Imitation Game".

95 Together, McCulloch & Pitts' and Turing's work already had all the germs
 96 of neural networks as we know them today: non-linearities, networks of a
 97 large number of neurons, training the weights *in situ* etc.

98 Let's now move to Cambridge, Massachusetts. Norbert Wiener, who was
 99 a famous professor at MIT, had created a little club of enthusiasts around
 100 1942. They would coin the term "Cybernetics" to study exactly the perception-
 101 cognition-action loop we talked about. You can read more in the original
 102 book titled "Cybernetics: or control and communication in the animal and
 103 the machine" (Wiener, 1965). You can also look at the book "The Cybernetic
 104 Brain" (Pickering, 2010) to read more.



Figure 1.2. The four pioneers of cybernetics (left to right): Ross Ashby, Warren McCulloch, Grey Walter, and Norbert Wiener. Source: de Latil 1956, facing p. 53.

Figure 1.2: The famous four of the first era of intelligence. (From right to left) Norbert Wiener, Grey Walter, Warren McCulloch and Walter Pitts

105 1.2.1 Representation Learning

106 Perceptual agents, from plants to humans, perform measurements of physical
 107 processes ("signals") at a level of granularity that is essentially continuous.
 108 They also perform actions in the physical space, which is again continuous.
 109 Cognitive science on the other hand thinks in terms of discrete entities, "con-
 110 cepts, ideas, objects, categories" etc. These can be manipulated with tools
 111 in logic and inference. What is the information that is transferred from the
 112 perception system to the cognition system, or from cognition to control? An
 113 agent needs to maintain a notion of an internal representation that is the object
 114 being passed around.

115 We will often talk about Claude Shannon and information theory for
 116 studying these kind of ideas. Shannon devised one such representation learning
 117 scheme: that for compressing, coding, decoding and decompressing data. The
 118 key idea to grasp here is that the notion of information in information theory
 119 is slightly different from the one we need in machine learning. Compression,
 120 decompression etc. care about never losing information from the data; machine
 121 learning necessarily requires you forget parts of your data. If the model focuses
 122 too much on the grass next to the dogs in the dataset, it will "over-fit" to the
 123 data and next time when you see grass, it will end up predicting a dog.

CONTENTS

Preface to the Second Edition vii

PART I

ORIGINAL EDITION

1948

Introduction	1
I Newtonian and Bergsonian Time	30
II Groups and Statistical Mechanics	45
III Time Series, Information, and Communication	60
IV Feedback and Oscillation	95
V Computing Machines and the Nervous System	116
VI Gestalt and Universals	133
VII Cybernetics and Psychopathology	144
VIII Information, Language, and Society	155

PART II

SUPPLEMENTARY CHAPTERS

1961

IX On Learning and Self-Reproducing Machines	169
X Brain Waves and Self-Organizing Systems	181
Index	205

Figure 1.3: This course's content is (surprisingly) closely related to Wiener's book on Cybernetics.

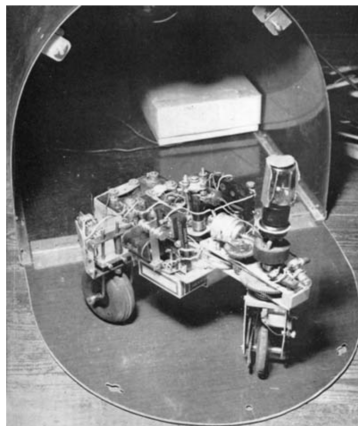


Figure 3.3. Anatomy of a tortoise. Source: de Latil 1956, facing p. 50.

Figure 1.4: Grey Walter's cybernetic tortoises named Elmer and Elsie were one of the first electronic autonomous robots (<https://youtu.be/iLULRImXkKo>). Walter wanted to create an artificial brain, he wanted to show how neuron-like components connected together can give to complex behaviors, in this case this is a light sensitive robot that tracks the source of light.

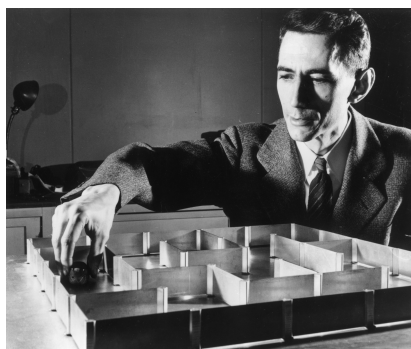


Figure 1.5: Claude Shannon studied information theory. This is a picture of a maze solving mouse that he made around 1950, among the world's first examples of machine learning (read more at <https://www.technologyreview.com/2018/12/19/138508/mighty-mouse>).

124 The study of intelligence has always had this diverse flavor. Computer
 125 scientists trying to understand perception, electrical engineers trying to under-
 126 stand representations and mechanical and control engineers building actuation
 127 mechanisms.

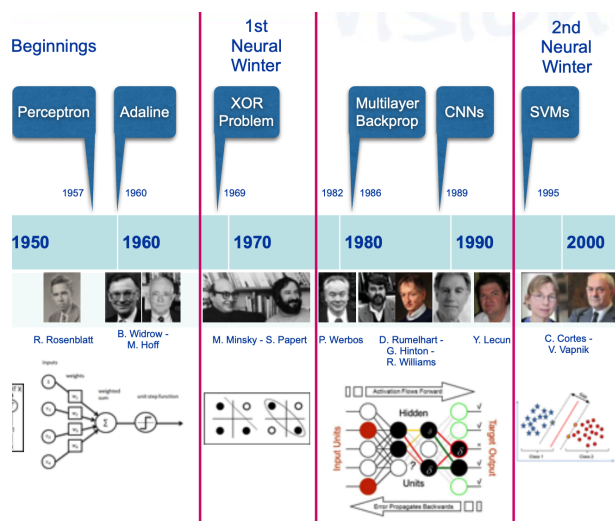
128 1.3 Intelligence: Reloaded (1960-2000)

129 The early period created interest in intelligence and developed some basic
 130 ideas. The first major progress of what one would call the second era was
 131 made by Frank Rosenblatt in 1957. Rosenblatt's model called the perceptron is
 132 a model with a single binary neuron. It was a machine designed to distinguish
 133 punch cards marked on the left from cards marked on the right, and it weighed
 134 5 tons ([https://news.cornell.edu/stories/2019/09/professors-perceptron-paved-
 135 way-ai-60-years-too-soon](https://news.cornell.edu/stories/2019/09/professors-perceptron-paved-way-ai-60-years-too-soon)). The input integration is implemented through the
 136 addition of the weighted inputs that have fixed weights obtained during the
 137 training stage. If the result of this addition is larger than a given threshold, the
 138 neuron fires. When the neuron fires its output is set to 1, otherwise it is set to
 139 0. It looks like the function

$$f(x; w) = \text{sign}(w^T x) = \text{sign}(w_1 x_1 + \dots + x_d x_d).$$

140 Rosenblatt's perceptron (Rosenblatt, 1958) had a single neuron, it cannot
 141 distinguish between complex data. This is what Marvin Minsky and Seymour
 142 Papert discussed in a famous book Minsky and Papert (2017). This book was
 143 widely perceived as a death knell for the perceptron and interest in neuron-
 144 based artificial intelligence (connectionist approach) waned.

145 This coupled with the rise of symbolic reasoning in the early 1970s and
 146 resulted in what one would call the first AI winter.



147

148 There was resurgence of ideas around neural networks, mostly fueled by
 149 the (re)-discovery of back-propagation by Rumelhart et al. (1985). Multi-layer
 150 networks were in vogue due to back-propagation working well. Convolutional
 151 neural networks built upon a large body of work starting from two neuro-
 152 scientists Hubel and Wiesel who did very interesting experiments in the 60s
 153 to discover visual cell types (Hubel and Wiesel, 1968) and Fukushima who
 154 implemented convolutional and downsampling layers in his famous Neocogni-
 155 tron (Fukushima, 1988). Yann LeCun demonstrated classification of handwrit-
 156 ten digits using CNNs in the early 1990s and used it to sort zipcodes (LeCun
 157 et al., 1989, 1998). Neural networks in the late 80s and early 90s was arguably,
 158 as popular a research area as it is in 2020 today.

159 Support Vector Machines (SVMs) were invented in Cortes and Vapnik
 160 (1995). These were (are) brilliant machine learning models with extremely
 161 good performance, were much easier to train than neural networks because
 162 they had a strong foundation in theory and, in general were a delight to use as
 163 compared to neural networks. Kernel methods, although known much before
 164 in the context of the perceptron (Aizerman, 1964; Scholkopf and Smola, 2018),
 165 made SVMs very powerful. The rise of Internet commerce in the late 90s
 166 meant that a number of these algorithms found widespread and impactful
 167 applications. Others such as random forests (Breiman, 2001) further led the
 168 progress in machine learning. Neural networks, which worked well when they
 169 did but required a lot of tuning and expertise to get to work, lost out to this
 170 competition. However, there were other neural network-based models in the
 171 natural language processing (NLP) community such as LSTMs (Hochreiter
 172 and Schmidhuber, 1997) which remained popular through this period.

173 1.4 Intelligence: Revolutions (2006-)

174 The growing quantity of data and computation came together in late 2000s to
 175 create ideas like deep Belief Networks (Hinton et al., 2006), deep Boltzmann
 176 machines (Salakhutdinov and Larochelle, 2010), large-scale training using
 177 GPUs (Raina et al., 2009) etc. The watershed moment that got everyone's
 178 attention was when Krizhevsky et al. (2012) trained a convolutional neural

179 network to show dramatic improvement in the classification performance on
180 a large dataset called ImageNet. This is a dataset with 1.4 million images
181 collected across 1000 different categories. Performing well on this dataset
182 was considered very difficult, the best approaches in 2011 (ImageNet chal-
183 lenge used to be an annual competition until 2016) achieved about 25% error.
184 Krizhevsky et al. (2012) managed to obtain an error of 15.3%. Many signifi-
185 cant results in the world of neural networks have been achieved since 2012.
186 Today, deep networks in their various forms run a large number of applications
187 in computer vision, natural language processing, speech processing, robotics,
188 physical sciences such as chemistry and biology, medical sciences, and many
189 many others (LeCun et al., 2015).

190 This progress in deep learning has been driven by the availability of data
191 and cheap computation. Most importantly, it is driven today by the intense
192 curiosity of people from diverse fields of inquiry. Deep learning in its modern
193 form is a very young field. As is typical in new research fields, consolidation
194 of ideas is difficult to come by. The dramatic progress today is driven by ideas
195 that are often-quixotic and a large number of open problems remain in how
196 we may build a more sophisticated understanding of deep networks.

197 **1.5 A summary of our goals in this course**

198 This course will take off from around late 1990s (kernel methods) and develop
199 ideas in deep learning that bring us to 2020. Our goals are to

- 200 1. become good at using modern deep networks, i.e., implementing them,
201 training them, modeling specific problems using ideas in deep learning;
- 202 2. understanding why techniques in deep networks work.

203 After taking this course, we expect to be able to not only develop methods
204 that use deep learning, but more importantly improve existing ideas using
205 foundational understanding of the mathematics behind these ideas and develop
206 new ways of improving deep learning theory and practice.

207 Chapter 2

208 Linear Regression, 209 Perceptron, Stochastic 210 Gradient Descent

Reading

1. Bishop 3.1, 4.1, 4.3
2. Goodfellow Chapter 5.1-5.4

211 2.1 Problem setup for machine learning

212 Nature gives us data X and targets Y for this data.

$$X \rightarrow Y.$$

213 Nature does not usually tell us what property of a datum $x \in X$ results in a
214 particular prediction $y \in Y$. We would like to learn to imitate Nature, namely
215 predict y given x .

216 What does such learning mean? It is simply a notion of being able to
217 identify patterns in the input data without explicitly programming a computer
218 for prediction. We are often happy with a learning process that identifies
219 correlations: if we learn correlations on a few samples $(x^1, y^1), \dots, (x^n, y^n)$,
220 we may be able to predict the output for a new datum x^{n+1} . We may not need
221 to know *why* the label of x^{n+1} was predicted to be so and so.

222 Let us say that Nature possesses a probability distribution P over (X, Y) .
223 We will formalize the problem of machine learning as Nature drawing n
224 independent and identically distributed samples from this distribution. This is
225 denoted by

$$D_{\text{train}} = \{(x^i, y^i) \sim P\}_{i=1}^n$$

226 is called the “training set”. We use this data to identify patterns that help make
227 predictions on some future data.

228 What is the task in machine learning?

229 Suppose D_{train} consists of $n = 50$ RGB images of size 100×100 of two kinds,
 230 ones with an orange inside them and ones without. 10^4 is a large number of
 231 pixels, each pixel taking any of the possible 255^3 values. Suppose we discover
 232 that one particular pixel, say at location $(25, 45)$, takes distinct values in all
 233 images inside our training set. We can then construct a predictor based on
 234 this pixel. This predictor, it is a binary classifier, perfectly maps the training
 235 images to their labels (orange: +1 or no orange: -1). If x_{ij}^k is the $(ij)^{\text{th}}$ pixel
 236 for image x^k , then we use the function

$$f(x) = \begin{cases} y^k & \text{if } x_{ij}^k = x_{ij} \text{ for some } k = 1, \dots, n \\ -1 & \text{otherwise.} \end{cases}$$

237 This predictor certainly solves the task. It correctly works for all images in the
 238 training set. Does it work for images outside the training set?

239 Our task in machine learning is to learn a predictor that works *outside* the
 240 training set. The training set is only a source of information that Nature gives
 241 us to find such a predictor.

Designing a predictor that is accurate on D_{train} is trivial. A hash function that memorizes the data is sufficient. This is NOT our task in machine learning. We want predictors that generalize to new data outside D_{train} .

242 2.1.1 Generalization

243 If we never see data from outside D_{train} why should we hope to do well on it?
 244 The key is the distribution P . Machine learning is formalized as constructing
 245 a predictor that works well on new data that is also drawn independently from
 246 the distribution P . We will call this set of data the “test set”.

$$D_{\text{test}}.$$

247 This assumption is important. It provides coherence between past and future
 248 samples: past samples that were used to train and future samples that we will
 249 wish to predict upon.

250 How to find such predictors that work well on new data? The central idea
 251 in machine learning is to restrict the set of possible binary functions that we
 252 consider.

We are searching for a predictor that generalizes well but only have the training to ascertain which predictor works well.

253 The *right* class of functions f cannot be too large, otherwise we will find
 254 our binary classifier above as the solution and that is not too useful. The class
 255 of functions cannot be too small either, otherwise we won't be able to predict
 256 difficult images. If the predictor does not even work well on the training set,
 257 why should we expect it to work on the test set!

258 Finding this correct class of functions with the right balance is what
 259 machine learning is all about.

🔗 How many such binary classifiers are there at most?

🔗 Can you now think how is machine learning different from other fields you might know such as statistics or optimization?

2.2 Linear regression

Let us focus on a simpler problem. We fix the class of functions, our predictors, to only have linear classifiers. We will consider that our data $X \subset \mathbb{R}^d$ and labels $Y \subset \mathbb{R}$. If the labels/targets are real-valued, we call it is a regression problem. Our predictor for any $x \in X$ is

$$f(x; w, b) = w^\top x + b. \quad (2.1)$$

This is a linear function in the data x with parameters $w \in \mathbb{R}^d$ and $b \in \mathbb{R}$. Different settings of w and b give access to different functions f . Picking a particular function f is therefore akin to picking particular values of the parameters. Parameters are also called weights. We can visualize what this predictor does in two ways, consider the case of $d = 2$.

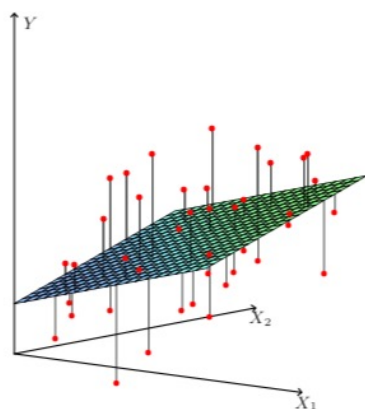


Figure 2.1: Linear least squares with $X \subset \mathbb{R}^2$.

Figure 2.1 shows the hyperplane corresponding to a particular (w, b) with the data x^i, y^i (in red). Each hyperplane is a particular predictor $f(x; w, b)$. You can also think of the function f as a point in three dimensional space $w \in \mathbb{R}^2$ and $b \in \mathbb{R}$.

Predicting the target accurately using this linear model would require us to find values (w, b) that minimize the average distance to the hyperplane of each sample in the training dataset. We write this as an *objective function*.

$$\begin{aligned} \ell(w, b) &:= \frac{1}{2n} \sum_{i=1}^n (y^i - \hat{y}^i)^2 \\ &= \frac{1}{2n} \sum_{i=1}^n (y^i - w^\top x^i - b)^2 \end{aligned} \quad (2.2)$$

where we have written the prediction as

$$\hat{y}^i = w^\top x^i + b.$$

The quadratic term for each datum $\frac{1}{2} (y^i - \hat{y}^i)^2$ is known as the *loss function*.

The objective above is thus an average of the loss for each datum. Finding the

🔗 Why use the average, as opposed to say the maximum value?

280 best weights w, b now boils down to solving the optimization problem

$$w^*, b^* = \underset{w \in \mathbb{R}^d, b \in \mathbb{R}}{\operatorname{argmin}} \ell(w, b) \quad (2.3)$$

281 **How to solve the optimization problem?** We will learn many techniques to
 282 solve problems of the form (2.3). We have a simple case here and therefore
 283 can use what you did in HW0. The solution is given by

$$w^* = (\tilde{\mathbf{X}}^\top \tilde{\mathbf{X}})^{-1} \tilde{\mathbf{X}}^\top \mathbf{Y} \quad (2.4)$$

284 where we have denoted by $\tilde{\mathbf{X}} \in \mathbb{R}^{n \times (d+1)}$ the matrix whose i^{th} row is the
 285 datum with a constant entry 1 appended at the end $[x^i, 1]$. Similarly $\mathbf{Y} \in \mathbb{R}^n$
 286 is a vector whose i^{th} entry is the target y^i .

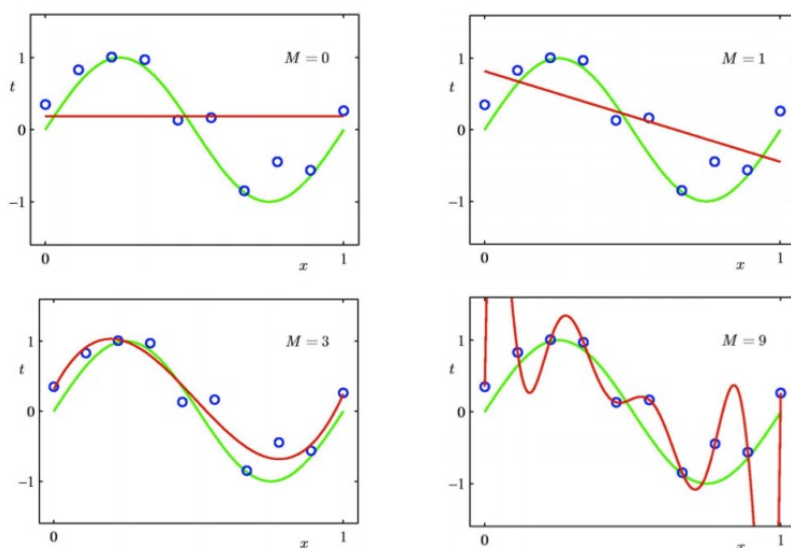


Figure 2.2: Least squares fitting using polynomials. As the degree of the polynomial M increases the predictor f fits the training data (in blue) better and better. But such a well-fitted predictor may be very different from the true model from which Nature generated the data (in green). The red curve in the fourth panel in these cases is said to have been *over-fitted*.

287 2.2.1 Maximum Likelihood Estimation

288 There is another perspective to fitting a machine learning model. We will
 289 *suppose* that our training data was created using a statistical model. We write
 290 this as

$$y = w^\top x + b + \epsilon \quad (2.5)$$

291 Of course we do not know whether Nature used this particular model $f(x; w, b) :=$
 292 $w^\top x + b$ to create the data, it might have created the data using some other
 293 model. This discrepancy between the models is *modeled* as noise ϵ . Noise in
 294 machine learning comes from the fact that we the user do not know Nature's
 295 model.

296 What model is appropriate for the noise ϵ ? There can be many models
 297 depending upon your experiment (think of a model that predicts the arrival

❓ When is our solution to least squares regression in (2.4) not defined?

❓ What are we losing by fitting a linear predictor? Will this work if the true model from which Nature generates the data was different, say a polynomial?

❓ Can you think any other sources of noise? For instance, if you scraped some images from the Internet, how will you label them?

298 time of a bus at the bus stop, what noise would you use?). For our purpose we
299 will use zero-mean Gaussian noise

$$\epsilon \sim N(0, \sigma_\epsilon^2)$$

300 that does not depend on the sample x . The probability that a sample (x^i, y^i)
301 in our dataset D_{train} was created using our statistical model is then

$$p(y^i|x^i, w, b) = N(w^\top x^i + b, \sigma_\epsilon^2).$$

302 We have assumed that the data was drawn iid by Nature so the likelihood of
303 our entire dataset is

$$p(D_{\text{train}}|w, b) = \prod_{i=1}^n p(y^i|x^i, w, b).$$

304 Finding good values of w, b can now be thought of as finding values that
305 maximize the likelihood of our observed data

$$w^*, b^* = \underset{w, b}{\operatorname{argmin}} -\log p(D_{\text{train}}|w, b). \quad (2.6)$$

306 Observe that our objective is written as the minimization of the *negative log-*
307 *likelihood*. This is equivalent to maximizing the likelihood because logarithm
308 is monotonic function. We can now rewrite the objective as

$$-\log p(D_{\text{train}}|w, b) = \frac{n}{2} \log(\sigma_\epsilon^2) + \frac{n}{2} \log(2\pi) + \frac{1}{2\sigma_\epsilon^2} \sum_{i=1}^n (y^i - w^\top x^i - b)^2.$$

309 Notice that only the third term depends on w, b . The first term is a function
310 of our *chosen* value σ_ϵ^2 , the second term is a constant. In other words, finding
311 maximizing the likelihood boils down to solving the optimization problem

$$w^*, \beta^* = \underset{w, b}{\operatorname{argmin}} \frac{1}{2\sigma_\epsilon^2} \sum_{i=1}^n (y^i - w^\top x^i - b)^2. \quad (2.7)$$

312 This objective is nothing other than our least squares regression objective with
313 σ_ϵ^2 set to 1. This objective known as the maximum likelihood objective (MLE).

314

315 Maximum likelihood objective has an interesting offshoot. In the least
316 squares case, given an input x all that our fitted model could predict was

$$\hat{y} = w^{*\top} x + b^*.$$

317 MLE has helped us fit a statistical model to the data. So we can now predict
318 the entire distribution

$$p(y|x, w^*, b^*) = N(w^{*\top} x + b^*, \sigma_\epsilon^2).$$

319 The solution of least squares is the mean of the Gaussian random variable
320 $y|x, w^*, b^*$, the variance of this random variance is σ_ϵ^2 . So instead of just pre-
321 dicting \hat{y} the machine learning model can now give the probability distribution
322 $p(y|x, w^*, b^*)$ as the output and the user is free to use it as they wish, e.g.,
323 compute the mean, the median, the 5% probability value of the right tail etc.

🔗 How does using a different value of σ_ϵ in (2.7) change the least squares solution in (2.4)?

2.3 Perceptron

Let us now solve a classification problem. We will again go around the model selection problem and consider the class of linear classifiers. Assume binary labels $Y \in \{-1, 1\}$. To keep the notation clear, we will use the trick of appending a 1 to the data x and hide the bias term b in the linear classifier. The predictor is now given by

$$\begin{aligned} f(x; w) &= \text{sign}(w^\top x) \\ &= \begin{cases} +1 & \text{if } w^\top x \geq 0 \\ -1 & \text{else.} \end{cases} \end{aligned} \quad (2.8)$$

We have used the sign function denoted as sign to get binary $\{-1, +1\}$ outputs from our real-valued prediction $w^\top x$. This is the famous perceptron model of Frank Rosenblatt. We can visualize the perceptron the same way as we did for linear regression.

Let us now formulate an objective to fit/train the perceptron. As usual, we want the predictions of the model to match those in the training data.

$$\ell_{\text{zero-one}}(w) := \frac{1}{n} \sum_{i=1}^n \mathbf{1}_{\{y^i \neq f(x^i; w)\}}. \quad (2.9)$$

The indicator function inside the summation measures the number of mistakes the perceptron makes on the training dataset. The objective here is designed to find weights w that minimizes the average number of mistakes, also known as the training error. Such a loss that measures the mistakes is called the zero-one loss, it incurs a penalty of 1 for a mistake and zero otherwise.

2.3.1 Surrogate Losses

The zero-one loss is the clearest indication of whether the perceptron is working well. It is however non-differentiable, so we cannot use powerful ideas from optimization theory to minimize it. This is why surrogate losses are constructed in machine learning. These are proxies for the loss function, typically for the classification problems and look as follows.

The hinge loss is one such surrogate loss. It is given by

$$\ell_{\text{hinge}}(w) = \max(0, -y w^\top x).$$

If the predicted label $\hat{y} = \text{sign}(w^\top x)$ have the same sign as the true label y , the hinge-loss is zero. If they have opposite signs, the hinge loss increases linearly. The exponential loss

$$\ell_{\text{exp}}(w) = e^{-y (w^\top x)}$$

or the logistic loss

$$\ell_{\text{logistic}}(w) = \log \left(1 + e^{-y w^\top x} \right)$$

are some other popular losses for classification.

❓ Is a linear model appropriate if our data was natural images? What properties have we lost by restricting the classifier to be linear?

⚠️ The linear classifier remains unchanged if we reorder the pixels of all images consistently in our entire training set and the weights w . The images will look nothing like real images to us. The perceptron does not care about which pixels in the input are close to which others.

❓ Can you think of some quantity other than the zero-one error that we may wish to optimize?

❓ Draw the three losses to observe their differences.

2.4 Stochastic Gradient Descent

We will now fit a perceptron using the hinge loss using a very simple optimization technique. At each iteration, this algorithm updates the weights w in the direction of the negative gradient. So first, let us compute the gradient of the hinge loss. It is easily seen to be

$$\frac{d\ell_{\text{hinge}}(w)}{dw} = \begin{cases} -y x & \text{for incorrect prediction} \\ 0 & \text{else.} \end{cases} \quad (2.10)$$

We will use a naive algorithm to update the weights. Here is how it goes.

The Perceptron algorithm

Perform the following steps for iterations $t = 1, 2, \dots$

1. At the t^{th} iteration, sample a datum with index $\omega_t \in \{1, \dots, n\}$ from D_{train} uniformly randomly, call it $(x^{\omega_t}, y^{\omega_t})$.
2. Update the weights of the perceptron as

$$w^{t+1} = \begin{cases} w^t + y^{\omega_t} x^{\omega_t} & \text{if } \text{sign}(w^{t\top} x^{\omega_t}) \neq y^{\omega_t} \\ w^t & \text{else.} \end{cases} \quad (2.11)$$

In other words, the perceptron weights is changed only if it makes a mistake on the sample $(x^{\omega_t}, y^{\omega_t})$. The updated perceptron improves its mistake on this sample. Observe that a mistake happens if the sign of $w^{t\top} x^{\omega_t}$ and y^{ω_t} are different, the product $y^{\omega_t} w^{t\top} x^{\omega_t}$ is therefore negative. The updated weights of the perceptron now satisfy

$$\begin{aligned} y^{\omega_t} (w^t + y^{\omega_t} x^{\omega_t})^\top x^{\omega_t} &= y^{\omega_t} \langle w^t, x^{\omega_t} \rangle + (y^{\omega_t})^2 \langle x^{\omega_t}, x^{\omega_t} \rangle \\ &= y^{\omega_t} \langle w^t, x^{\omega_t} \rangle + \|x^{\omega_t}\|_2^2. \end{aligned}$$

In simple worlds, the value of $y^{\omega_t} \langle w, x^{\omega_t} \rangle$ increases as a result of the update, it becomes more positive. If the perceptron makes mistakes on the same datum repeatedly, this value is eventually going to become positive. Of course, mistakes on other data in the training set may steer the perceptron towards other directions and it may continue to cycle ad infinitum, but it is easy to show that it ceases its updates when all data are correctly classified. More precisely, if the training data are such that they can be correctly classified using a linear predictor, then the perceptron will find this predictor after a finite number of iterations.

We have seen a powerful algorithm for machine learning. This algorithm is called stochastic gradient descent (SGD) and it is very general: so long as you can take the gradient of the objective you can execute SGD. The algorithm for fitting the perceptron above was given by Rosenblatt in 1957 and is popularly known as the ‘‘perceptron algorithm’’. It is interesting to note that it is simply the instantiation of SGD which was known before [Robbins and Monro \(1951\)](#) for the hinge loss.

🔗 You may have seen the hinge loss written as

$$\ell_{\text{hinge}}(w) = \max(0, 1 - y w^\top x).$$

Why the difference?

2.4.1 The general form of SGD

SGD is a very general algorithm. We can use it so long as you have a dataset and an objective that is differentiable. Consider an optimization problem that looks like

$$w^* = \operatorname{argmin}_w \frac{1}{n} \sum_{i=1}^n \ell^i(w)$$

where the function ℓ^i denotes the loss on the sample (x^i, y^i) and $w \in \mathbb{R}^p$ denotes the weights. Solving this problem using SGD corresponds to iteratively updating the weights using

$$w^{t+1} = w^t - \eta \frac{d\ell^{\omega_t}(w)}{dw} \Big|_{w=w^t}.$$

We have chosen to be a bit more precise and the sample over which we compute the gradient is ω_t . This is a random variable with domain and we will use ω_t to denote its index.

$$\omega_t \in \{1, \dots, n\}.$$

The gradient of the loss $\ell^{\omega_t}(w)$ with respect to w is denoted by

$$\begin{aligned} \nabla \ell^{\omega_t}(w^t) &:= \frac{d\ell^{\omega_t}(w)}{dw} \Big|_{w=w^t} \\ &= \begin{bmatrix} \nabla_{w_1} \ell^{\omega_t}(w^t) \\ \nabla_{w_2} \ell^{\omega_t}(w^t) \\ \vdots \\ \nabla_{w_p} \ell^{\omega_t}(w^t) \end{bmatrix} \\ &\in \mathbb{R}^p. \end{aligned}$$

The gradient $\nabla \ell^{\omega_t}(w^t)$ is therefore a vector in \mathbb{R}^p . We have written

$$\nabla_{w_1} \ell^{\omega_t}(w^t) = \frac{d\ell^{\omega_t}(w)}{dw_1} \Big|_{w=w^t}$$

for the scalar-valued derivative of the objective $\ell^{\omega_t}(w^t)$ with respect to the first weight $w_1 \in \mathbb{R}$. We can therefore write SGD as

$$w^{t+1} = w^t - \eta \nabla \ell^{\omega_t}(w^t). \quad (2.12)$$

The non-negative scalar $\eta \in \mathbb{R}_+$ is called the step-size or the learning rate. It governs the distance traveled along the negative gradient $-\nabla \ell^{\omega_t}(w^t)$ at each iteration.

397

Chapter 3

398

Kernels, Beginning of neural networks

399

Reading

1. Bishop 6.1-6.3
2. Goodfellow 6.1-6.4
3. “Random features for large-scale kernel machines” by [Rahimi and Recht \(2008\)](#).

400

3.1 Digging deeper into the perceptron

401

3.1.1 Convergence rate

402

How many iterations does a perceptron need to fit on a given dataset? We will assume that the training data are bounded, i.e., $\|x^i\| \leq R$ for some R and for all $i \in \{1, \dots, n\}$. Let us also assume that the training dataset is indeed linearly separable, i.e., a solution w^* exists for the perceptron weights with training error exactly zero. This means

403

404

405

406

$$y^i w^{*\top} x^i > 0 \quad \forall i.$$

407

We will also assume that this classifier *separates the data well*. Note that the distance of each input x^i from the decision boundary (i.e., all x such that $w^{*\top} x = 0$) is given by the component of x^i in the direction of w^* if the label is $y^* = +1$ and in the direction $-w^*$ if the label is negative. In other words,

408

409

410

$$\frac{y^i w^{*\top} x^i}{\|w^*\|} = \rho^i$$

411

gives the distance to the decision boundary. The quantity on the right hand side is called the *margin*, it is simply the distance of the sample i from the

412

413 decision boundary. If w^* is the classifier with the largest average margin,

$$\rho = \min_{i \in \{1, \dots, n\}} \rho^i$$

414 is a good measure of how hard a particular machine learning problem is.

415 You can now try to prove that after each update of the perceptron the inner
416 product of the current weights with the true solution $\langle w_t, w^* \rangle$ increases at least
417 linearly and that the squared norm $\|w_t\|^2$ increases at most linearly in the
418 number of updates t . Together the two will give you a result that after t weight
419 updates

$$t \leq \frac{R^2}{\rho^2} \quad (3.1)$$

420 all training data are classified correctly. Notice a few things about this expres-
421 sion.

- 422 1. The quantity $\frac{R^2}{\rho^2}$ is dimension independent; that the number of steps
423 reach a given accuracy is independent of the dimension of the data will
424 be a property shared by optimization algorithms in general.
- 425 2. There are no constant factors, this is also the worst case number of
426 updates; this is rare.
- 427 3. The number of updates scales with the hardness of the problem; if the
428 margin ρ was small, we need lots of updates to drive the training error
429 to zero.

430 3.1.2 Dual representation

431 Let us see how the parameters of the perceptron look after training on the entire
432 dataset. At each iteration, the weights are updated in the direction (x^t, y^t)
433 or they are not updated at all. Therefore, if α^i is the number of times the
434 perceptron sampled the datum (x^i, y^i) during the course of its training and got
435 it wrong, we can write the weights of the perceptron as a linear combination

$$w^* = \sum_{i=1}^n \alpha^i y^i x^i. \quad (3.2)$$

436 where $\alpha^i \in \{0, 1, \dots\}$. The perceptron therefore using the classifier

$$\begin{aligned} f(x, w) &= \text{sign}(\hat{y}) \\ \text{where } \hat{y} &= \left(\sum_{i=1}^n \alpha^i y^i x^i \right)^\top x \\ &= \sum_{i=1}^n \alpha^i y^i x^{i\top} x. \end{aligned} \quad (3.3)$$

437 Remember this special form: the inner product of the new input x with
438 all the other inputs x^i in the training dataset is combined linearly to get the
439 prediction. The weights of this linear combination are the dual variables which
440 is a measure of how many tries it took the perceptron to fit that sample during
441 training.
442

▲ As you see in (3.3), computing the prediction for a new input x involves, either remembering all the weights w at the end of training, or storing all the $\{\alpha^i\}_{i=1, \dots, n}$ along with the training dataset. The latter is called the dual representation of a perceptron and the scalars $\{\alpha^i\}$ are called the dual parameters.

443 3.2 Creating nonlinear classifiers from linear ones

444 Linear classifiers such as the perceptron, or the support vector machine (SVM)
 445 can be extended to nonlinear ones. The trick is essentially the same that we
 446 saw when we fit polynomials (polynomials are nonlinear) using the formula for
 447 linear regression. We are interested in mapping input data x to some different
 448 space, this is usually a higher-dimensional space called the *feature space*.

$$x \mapsto \phi(x).$$

449 The quantity $\phi(x)$ is called a feature vector.

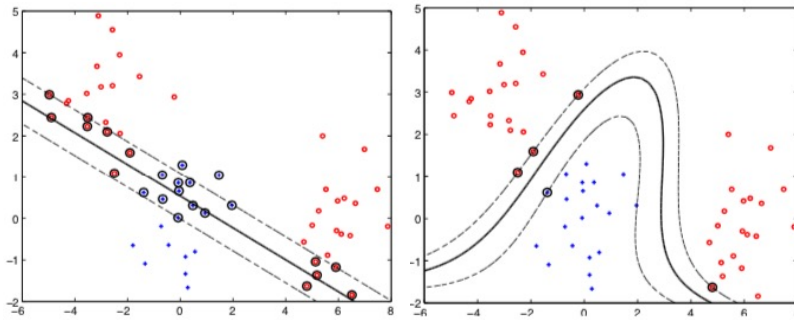


Figure 3.1

450 For example, in the polynomial regression case for scalar input data $x \in \mathbb{R}$
 451 we used

$$\phi(x) := \left[1, \sqrt{2}x, x^2 \right]^\top$$

452 to get a quadratic feature space. The role of $\sqrt{2}$ will become clear shortly.
 453 Certainly this trick of polynomial expansion also works for higher dimensional
 454 input

$$\phi(x) := \left[1, x_1, x_2, \sqrt{2}x_1x_2, x_1^2, x_2^2 \right]^\top.$$

455 Having fixed a feature vector $\phi(x)$, we can now fit a linear perceptron on the
 456 input data $\{\phi(x^i), y^i\}$. This involves updating the weights at each iteration as

$$w_{t+1} = \begin{cases} w_t + y^t \phi(x^t) & \text{if } \text{sign}(w_t^\top \phi(x^t)) \neq y^t \\ w_t & \text{else.} \end{cases} \quad (3.4)$$

457 At the end of such training, the perceptron is

$$w^* = \sum_{i=1}^n \alpha^i y^i \phi(x^i)$$

458 and predictions are made by first mapping the new input to our feature space

$$f(x; w) = \text{sign} \left(\sum_{i=1}^n \alpha^i y^i \phi(x^i)^\top \phi(x) \right). \quad (3.5)$$

459 Notice that we now have a linear combination of the *features* not the data
 460 directly.

🔍 The concept of a feature space seems like a panacea. If we have complex data, we simply map it to some high-dimensional feature and fit a linear function to these features. However, the “curse of dimensionality” coined by Richard Bellman states that to fit a function in \mathbb{R}^d the number of data needs to be exponential in d . It therefore stands to reason that we need a lot more data to fit a classifier in feature space than in the original input space. Why would we still be interested in the feature space then?

3.3 Kernels

Observe the expression of the classifier in (3.5). Each time we make predictions on the new input, we need to compute n inner products of the form

$$\phi(x^i)^\top \phi(x).$$

If the feature dimension is high, we need to enumerate the large number of feature dimensions if we are using the weights of the perceptron, or these inner products if we are using the dual variables. Observe however that even if the feature vector is large, we can compactly evaluate the inner product

$$\begin{aligned}\phi(x) &= [1, \sqrt{2}x, x^2] \\ \phi(x') &= [1, \sqrt{2}x', x'^2] \\ \phi(x)^\top \phi(x') &= 1 + 2xx' + (xx')^2 = (1 + xx')^2.\end{aligned}$$

for input $x \in \mathbb{R}$. Kernels are a formalization of exactly this idea. A kernel

$$k : X \times X \rightarrow \mathbb{R}.$$

is a symmetric, positive semi-definite function of its two arguments for which it holds that

$$k(x, x') = \phi(x)^\top \phi(x')$$

for some feature ϕ . Few examples of kernels are

$$\begin{aligned}k(x, x') &= (x^\top x' + c)^2, \\ k(x, x') &= \exp(-\|x - x'\|^2 / (2\sigma^2)).\end{aligned}$$

3.3.1 Kernel perceptron

We can now give the kernel version of the perceptron algorithm. The idea is to simply replace any inner product in the algorithm that looks like $\phi(x)^\top \phi(x')$ by the kernel $k(x, x')$.

Kernel perceptron

Initialize dual variables $\alpha^i = 0$ for all $i \in \{1, \dots, n\}$. Perform the following steps for iterations $t = 1, 2, \dots$

1. At the t^{th} iteration, sample a data point with index ω_t from D_{train} uniformly randomly, call it $(x^{\omega_t}, y^{\omega_t})$.
2. If there is a mistake, i.e., if

$$\begin{aligned}0 &\geq y^{\omega_t} \left(\sum_{i=1}^n \alpha^i y^i \phi(x^i)^\top \phi(x^{\omega_t}) \right) \\ &= y^{\omega_t} \left(\sum_{i=1}^n \alpha^i y^i k(x^i, x^{\omega_t}) \right),\end{aligned}$$

then update

$$\alpha^{\omega_t} \leftarrow \alpha^{\omega_t} + 1.$$

▲ Feature spaces can become large very quickly. What is the dimensionality of $\phi(x)$ for a tenth-order polynomial with a three-dimensional input data?

476 Notice that we do not ever compute $\phi(x)$ so it does not matter what the
 477 dimensionality of the feature vector is. It can even be infinite, e.g., for the
 478 radial basis function kernel. Observe also that we do not maintain weights
 479 w . We instead maintain the dual variables $\{\alpha^1, \dots, \alpha^n\}$ while running the
 480 algorithm.

481 Note that the kernel perceptron computes the kernel over *all* data samples
 482 in the training set at each iteration. It is expensive and seems wasteful. The
 483 Gram matrix denoted by $G \in \mathbb{R}^{n \times n}$

$$G_{ij} = k(x^i, x^j) \quad (3.6)$$

484 helps address this problem by computing the kernel on all pairs in the training
 485 dataset. With this in hand, we can modify step 2 in the kernel perceptron using

$$y^t \left(\sum_{i=1}^n \alpha^i y^i k(x^i, x^t) \right) = y^t (\alpha \odot Y)^\top G e_t.$$

486 where $e_t = [0, \dots, 0, 1, 0, \dots]$ with a 1 on the t^{th} element, $\alpha = [\alpha^1, \dots, \alpha^n]$
 487 denotes the vector of all the dual variables, $Y = [y^1, \dots, y^n]$ is a vector of all
 488 the labels, and the notation $\alpha \odot Y = [\alpha^1 y^1, \dots, \alpha^n y^n]$ denotes the element-
 489 wise (Hadamard) product. This expression now only involves a matrix-vector
 490 multiplication, which is much easier than computing the kernel at each iteration.
 491 Gram matrices can become very big. If the number of samples is $n = 10^6$, not
 492 an unusual number today, the Gram matrix has 10^{12} elements. The big failing
 493 of kernel methods is that they require a large amount of memory at training
 494 time. Nystrom methods compute low-rank approximations of the Gram matrix
 495 which makes operations with kernels easier.

496 3.3.2 Mercer's theorem

497 This theorem shows that given any kernel that satisfies some regularity proper-
 498 ties can be rewritten as an inner product.

499 **Theorem 3.1 (Mercer's Theorem).** For any symmetric function $k : X \times$
 500 $X \rightarrow \mathbb{R}$ which is square integrable in $X \times X$ and satisfies

$$\int_{X \times X} k(x, x') f(x) f(x') dx dx' \geq 0 \quad (3.7)$$

501 for all square integrable functions $f \in L_2(X)$, there exist functions $\phi_i : X \rightarrow$
 502 \mathbb{R} and numbers $\lambda_i \geq 0$ where

$$k(x, x') = \sum_i \lambda_i \phi_i^\top(x) \phi_i(x')$$

503 for all $x, x' \in X$. The condition in (3.7) is called Mercer's condition. You will
 504 also have seen it written as *for any finite set of inputs $\{x^1, \dots, x^n\}$ and any*
 505 *choice of real-valued coefficients c_1, \dots, c_n a valid kernel should satisfy*

$$\sum_{i,j} c_i c_j k(x^i, x^j) \geq 0.$$

506 There can be an infinite number of coefficients λ_i in the summation.

🔍 Kernels look great, you can fit perceptrons in powerful feature spaces using essentially the same algorithm. How expensive is each iteration of the perceptron?

⚠️ When ML algorithms are implemented in a system, there exist tradeoffs between the feature-space version and the Gram matrix version of linear classifiers. The former is preferable if the number of samples in the dataset is large, while the latter is used when the dimensionality of features is large.

🔍 Logistic regression with a loss function

$$\ell_{\text{logistic}}(w) = \log \left(1 + e^{-yw^\top x} \right)$$

is also a linear classifier. Write down how you will fit a logistic regression using stochastic gradient descent; this is similar to the perceptron algorithm. Write down the feature-space version of the algorithm and a kernelized logistic regression that uses the Gram matrix.

💡 A function $f : X \rightarrow \mathbb{R}$ is square integrable iff

$$\int_{x \in X} |f(x)|^2 dx < \infty.$$

507 **Remark 3.2 (Checking if a function is a valid kernel).** Note that Mercer's
 508 condition states that the Gram matrix of any dataset is positive semi-definite:

$$u^\top G u \geq 0 \quad \text{for all } u \in \mathbb{R}^n.$$

509 This is easy to show.

$$\begin{aligned} u^\top G u &= \sum_{ij} u_i u_j G_{ij} \\ &= \sum_{ij} u_i u_j \phi(x_i)^\top \phi(x_j) \\ &= \left(\sum_i u_i \phi(x_i) \right)^\top \left(\sum_j u_j \phi(x_j) \right) \\ &= \left\| \sum_i u_i \phi(x_i) \right\|^2 \\ &\geq 0. \end{aligned}$$

510 The integral in Theorem 3.1 in Mercer's condition is really just the continuous
 511 analogue of the vector-matrix-vector multiplication above. So if you have a
 512 function that you would like to use as a kernel, checking its validity is easy by
 513 showing that the Gram matrix is positive semi-definite.

514 Kernels are powerful because they do not require you to think of the feature
 515 and parameter spaces. For instance, we may wish to design a machine learning
 516 algorithm for spam detection that takes in a variable length of feature vector
 517 depending on the particular input. If $x[i]$ is the i^{th} character of a string, a good
 518 feature vector to use is to consider the set of all length k subsequences. The
 519 number of components in this feature vector is exponential. However, as you
 520 can imagine, given two strings x, x'

```
521         this string is interesting
522         txws sbhtqg is iyubqtnhpqg
```

523 you can write a Python function to check their similarities with respect to some
 524 rules *you define*. Mercer's theorem is useful here because it says that so long
 525 as your function satisfies the basic properties of a kernel function, there exists
 526 some feature space which your function implicitly constructs.

527 3.4 Learning the feature vector

The central idea behind deep learning is to learn the feature vectors ϕ instead of choosing them a priori.

528 How do we choose what set of feature vectors to learn from? For instance, we
 529 can pick all polynomials; we can pick all possible Gabor filters that you saw
 530 in HW 1; we can also pick all possible string kernels.

3.4.1 Random features

Suppose that we have a finite-dimensional feature $\phi(x) \in \mathbb{R}^p$. We saw in the perceptron that

$$f(x; w) = \text{sign} \left(\sum_i w_i \phi_i(x) \right)$$

where $\phi(x) = [\phi_1(x), \dots, \phi_p(x)]$ and $w = [w_1, \dots, w_p]$ are the feature and weight vectors respectively. We will set

$$\phi(x) = \sigma(S^\top x), \quad (3.8)$$

where $S \in \mathbb{R}^{d \times p}$ is a matrix. The function $\sigma(\cdot)$ is a nonlinear function of its argument and acts on all elements of the argument element-wise

$$\sigma(z) = [\sigma(z_1), \dots, \sigma(z_p)]^\top.$$

We will abuse notation that denote both the vector version of σ and the element-wise version of σ using the same Greek letter. Notice that this is a special type of feature vector (or a special type of kernel), it is a linear combination of the input elements. What matrix S should we pick to combine these input elements? The paper by [Rahimi and Recht \(2008\)](#) proposed the idea that for shift-invariant kernels (which have the property $k(x, x') = k(x - x')$) one may use a matrix with random elements as our S

$$S^\top = \begin{bmatrix} \omega_1 \\ \vdots \\ \omega_p \end{bmatrix}$$

where $\omega_i \in \mathbb{R}^d$ are random variables drawn from, say, a Gaussian distribution and the function

$$\sigma(z) = \cos(z)$$

is a cosine function. Using a random matrix is a cheap trick, it lets us create a lot of features quickly without worrying about their quality. Our classifier is now

$$f(x; w) = \text{sign}(w^\top \sigma(S^\top x)) \quad (3.9)$$

and we can solve the optimization problem

$$w^* = \underset{w}{\text{argmin}} \frac{1}{n} \sum_{i=1}^n \ell_{\text{hinge}}(y^i, \hat{y}^i) \quad (3.10)$$

with $\hat{y}^i = w^\top \sigma(S^\top x^i)$ and fit the weights w using SGD as before.



Figure 3.2

552 As an example consider the heatmap of Gabor-like kernel $k(x, x')$ in Fig-
 553 ure 3.2 on the left. We can think of the decomposition

$$\begin{aligned} \text{left-most picture} &= k(x, x') = \phi(x)^\top \phi(x') \\ &= w_1 \sigma(\omega_1^\top x) + w_2 \sigma(\omega_2^\top x) + w_k \sigma(\omega_k^\top x) + \dots \\ &= \text{right-most picture} \end{aligned}$$

554 In other words, the random elements of the matrix S , namely ω_k can combine
 555 together *linearly* using the trained weights w_k to give us a kernel that looks
 556 like a useful kernel on the left. A large random matrix S allows us to learn
 557 may such kernels and combine their output linearly.

558 3.4.2 Learning the feature matrix as well

559 Random features do not work easily for all kinds of data. For instance, if you
 560 have an image of size 100×100 , and you are trying to find a fruit



561

562 we can design random features of the form

$$\phi_{ij,kl} = \mathbf{1}_{\{\text{mostly red color in a box formed by pixels } (ij) \text{ and } (kl)\}}.$$

563 We will need lots and lots of such features before we can design an object
 564 detector that works well for this image. In other words, random features do
 565 not solve the problem that you need to be clever about picking your feature
 566 space/kernel.

567 We can now simply motivate deep learning as learning the matrix S in (3.9)
 568 in addition to the coefficients w . The classifier now is

$$f(x; w, S) = \text{sign}(w^\top \sigma(S^\top x)) \quad (3.11)$$

569 but we now solve the optimization problem

$$w^*, S^* = \underset{w, S}{\text{argmin}} \frac{1}{n} \sum_{i=1}^n \ell_{\text{hinge}}(y^i, \hat{y}^i) \quad (3.12)$$

570 with $\hat{y}^i = w^\top \sigma(S^\top x^i)$ as before. We have hereby seen our first *deep network*.
 571 The classifier in (3.11) is a two-layer neural network.

572 Moving from the problem in (3.10) to this new problem in (3.12) is a very
 573 big change.

574 1. **Nonlinearity.** The classifier in (3.11) is not linear anymore. It is a
 575 nonlinear function of its parameters w, S (both of which we will call
 576 weights).

🔍 What kind of data do you think random features will work well for?

-
- 577 2. **High-dimensionality.** We added a lot more weights to the classifier,
578 the original classifier had $w \in \mathbb{R}^p$ parameters to learn while the new
579 one also has $S \in \mathbb{R}^{d \times p}$ more weights. The curse of dimensionality
580 suggests that we will need a lot more data to fit the new classifier.
- 581 3. **Non-convex optimization.** The optimization problem in (3.12) much
582 harder than the one in (3.10). The latter is a convex function (we
583 will discuss this soon) which are easy to minimize. The former is
584 a non-convex function in its parameters w, S because they interact
585 multiplicatively, such functions are harder to minimize. We could write
586 down the solution of the perceptron using the final values of the dual
587 variables. We cannot do this for a two-layer neural network.

588 Chapter 4

589 Deep fully-connected 590 networks, Backpropagation

Reading

1. Bishop 5.1, 5.3
2. Goodfellow 6.3-6.5
3. Notes at <http://cs231n.github.io/optimization-2/>

591 4.1 Deep fully-connected networks

592 A deep neural network takes the idea of a two-layer network to the next step.
593 Instead of having one matrix S in the classifier

$$f(x; v, S) = \text{sign}(v^\top \sigma(S^\top x))$$

594 a deep network has many matrices S_1, \dots, S_L

$$f(x; v, S_1, \dots, S_L) = \text{sign}(v^\top \sigma(S_L^\top \dots \sigma(S_2^\top \sigma(S_1^\top x)) \dots)). \quad (4.1)$$

595 We will call each operation of the form $\sigma(S_k^\top \dots)$, as a *layer*. Consider the
596 second layer: it takes the features generated by the first layer, namely $\sigma(S_1^\top x)$,
597 multiplies these features using its feature matrix S_2^\top and applies a nonlinear
598 function $\sigma(\cdot)$ to this result element-wise before passing it on to the third layer.

A deep network creates new features by composing older features.

599 This composition is very powerful. Not only do we not have to pick a
600 particular feature vector, we can create very complex features by sequentially
601 combining simpler ones. For example Figure 4.1 shows the features (more

precisely, the kernel) learnt by a deep neural network. The first layer of features are called Gabor-like, they are similar to ones you constructed in HW 1. These features are *combined* linearly along with a nonlinear operation to give richer features (spirals, right angles) in the middle panel. The third layer combines the lower features to get even more complex features, these look like patterns (notice a soccer ball in the bottom left), a box on the bottom right etc.

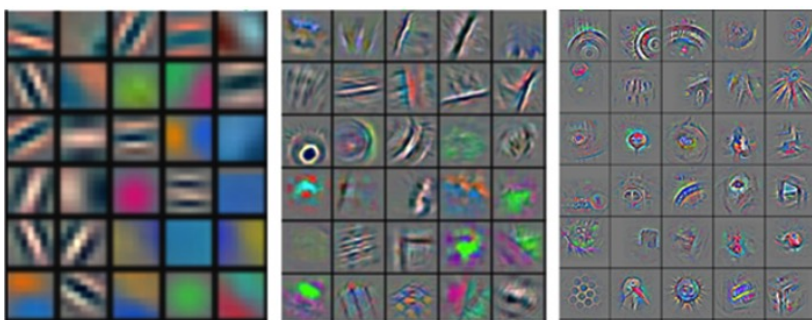


Figure 4.1

The optimization problem for fitting a deep network is written as

$$v^*, S_1^*, \dots, S_L^* = \underset{v, S_1, \dots, S_L}{\operatorname{argmin}} \frac{1}{n} \sum_{i=1}^n \ell_{\text{hinge}}(y^i, \hat{y}^i). \quad (4.2)$$

where the output prediction is now

$$\hat{y} = v^\top \sigma(S_L^\top \dots \sigma(S_2^\top \sigma(S_1^\top x)) \dots).$$

Notice that if fitting a two-layer network was difficult, then fitting a multi-layer neural network like (4.1) is even harder. There are *lots* of parameters and consequently we need a lot more data to fit such a model. The optimization problem in (4.2) is also naturally much harder than its two-layer version. The benefit for going through this difficulty is many fold and quite astounding.

1. Not having to pick features is very powerful. Notice that we do not need to worry about what kind of data x is at the input. So long as we can write it into a vector, the classifier as written in (4.1) works. In other words, the same type of classifier works for image-based data, data from natural language processing, speech processing, and many other types. This is the primary reason why a large number of scientific field are adopting deep networks.
2. Before the resurgence of deep learning, each of these fields essentially had their own favorite kernels they preferred, these kernels were designed across decades of insights from that specific field (wavelets in signal processing, keypoint detectors and descriptors in computer vision, n-grams in NLP etc.). It was very difficult for a researcher to use ideas from a different field. With deep learning, this has become much easier. There is still a significant amount of domain insight that you need to make deep networks work well but the bar for entering a new field is much lower.

632 3. Deep neural networks are universal approximators. In simple words, it
 633 means that provided the deep network has enough number of layers and
 634 enough number of features in each layer, it can fit any dataset. This is a
 635 theorem in approximation theory.

636 4.1.1 Some deep learning jargon

637 We have defined the essential parts of a deep network. Let us briefly take a
 638 look at some typical jargon you will encounter as you read more.

639 **Activation function.** The nonlinear function $\sigma(\cdot)$ in (4.1) is called the acti-
 640 vation function (motivated from the threshold-based activation of McCulloch-
 641 Pitts neuron). It is also called a nonlinearity because it is the only nonlinear
 642 operation in the classifier. There are many activation functions that have been
 643 used over the years.

644 1. Threshold

$$\text{threshold}(x) = \begin{cases} 1 & \text{if } x \geq 0 \\ 0 & \text{else.} \end{cases}$$

645 2. Sigmoid/Logistic

$$\text{sigmoid}(x) = \frac{1}{1 + e^{-x}}.$$

646 3. Hyperbolic tangent

$$\text{tanh}(x) = \frac{e^x - e^{-x}}{e^x + e^{-x}}$$

647 4. Rectified Linear Units (ReLU)

$$\begin{aligned} \text{relu}(x) &= |x|_+ \\ &= \max(0, x). \end{aligned}$$

648 5. Leaky ReLUs

$$\sigma_c(x) = \begin{cases} x & \text{if } x > 0 \\ c x & \text{else.} \end{cases}$$

649 6. Swish

$$\sigma(x) = x \text{ sigmoid}(x).$$

650 Different activation functions work differently. ReLU nonlinearities are the
 651 most popular and we will see the reasons why they work better than older ones
 652 such as sigmoid/tanh nonlinearities in the backpropagation section.

653 **Logits for multi-class classification.** The output

$$\hat{y} = v^\top \sigma(S_L^\top \dots \sigma(S_2^\top \sigma(S_1^\top x)) \dots)$$

654 are called the logits corresponding to the different classes. This name comes
 655 from logistic regression where logits are the log-probabilities of belonging
 656 to one of the two classes. A deep network affords an easy way to solve a
 657 multi-class classification problem, we simply set

$$v \in \mathbb{R}^{p \times C}$$

🔗 How would you use a binary classifier to classify 10 classes?

658 where C is the total number of classes in the data. Just like logistic regression
 659 predicts the logits of the two classes, we would like to *interpret* the vector \hat{y} as
 660 the log-probabilities of an input belonging to one of the classes.

661 **Mid-level features.** The features at any layer can be studied once you create
 662 a deep network. You pass an input image x and compute

$$h^l = S_l^\top \dots \sigma(S_2^\top \sigma(S_1^\top x)) \dots \quad (4.3)$$

663 to get the *pre-activation* output of the l^{th} layer. The *post-activation* output is
 664 given by applying the nonlinearity

$$\sigma(h^l).$$

665 Sometimes people will call the $\sigma(h^L)$ as the *feature* created by a deep network;
 666 the rationale here is that just like a kernel-based classifier uses features $\phi(x)$
 667 and fits a linear classifier to these features we may think of the feature of a
 668 deep network to be $\sigma(h^L)$. These features are often very useful, e.g., you can
 669 use a pre-trained deep network on the ImageNet dataset in PyTorch within
 670 two lines of code and use these features to fit a linear classifier for classifying
 671 fruits. Training a deep network yourself on ImageNet is quite difficult.

672 **Hidden layers/neurons.** The intermediate layers that create the features
 673 h^1, \dots, h^L are called the hidden layers. A feature is the same as a neuron;
 674 think of the McCulloch-Pitts picture, just like a neuron takes input from all the
 675 other neurons connected to it via some weights, a feature is computed using
 676 a weighted combination of the features at the lower layer. We will say that a
 677 neural network is *wide* if it has lots of features/neurons on each hidden layer.
 678 We will say that it is *thin* if it has few features/neurons on each hidden layer.

679 4.1.2 Weights

680 It is customary to not differentiate between the parameters of different layers of
 681 a deep network and simply say *weights* when we want to refer to all parameters.
 682 The set

$$w := \{v, S_1, S_2, \dots, S_L\}$$

683 is the set of *weights*. This set is typically stored in PyTorch as a set of matrices,
 684 one for each layer.

🔗 What would the shape of w be if you were performing regression using a deep network?

Important. Every time we want to write down mathematical equations,

we will imagine w to be a large vector. This is less cumbersome notation. We denote by p the dimensionality of w and imagine that

$$w \in \mathbb{R}^p.$$

The dimensionality p keeps things consistent with linear classifiers where the features were $\phi(x) \in \mathbb{R}^p$. When you use PyTorch to implement an algorithm that requires you to iterate over the weights, you will iterate over elements of the set. Using this new notation, we will write down a deep classifier as simply

$$f(x, w) \tag{4.4}$$

and fitting the deep network to a dataset involves the optimization problem

$$w^* = \operatorname{argmin}_w \frac{1}{n} \sum_{i=1}^n \ell(y^i, \hat{y}^i). \tag{4.5}$$

We will also sometimes denote the loss of the i^{th} sample as

$$\ell^i(w) := \ell(y^i, \hat{y}^i).$$

685 4.2 The backpropagation algorithm

686 We would like to using SGD to fit a deep network on a given dataset. As we
687 saw in Chapter 2, if the loss function is denoted by $\ell^{\omega_t}(w)$ where ω_t was the
688 index of the datum sampled at iteration t , we would like to update the weights
689 using

$$w^{t+1} = w^t - \eta \left. \frac{d\ell^{\omega_t}(w)}{dw} \right|_{w=w^t}.$$

690 We have used a scalar $\eta > 0$ as the step-size or the learning rate. It governs the
691 distance traveled along the negative gradient at each iteration. Let us ignore
692 the index of the datum ω_t in this section, imagine $\omega_t = 1$. Implementing SGD
693 therefore boils down to computing the gradient

$$\frac{d\ell(w)}{dw}.$$

Backpropagation is an algorithm for computing the gradient of the loss function for a deep network.

694 4.2.1 One hidden layer with one neuron

695 Consider the linear regression problem with one layer and one datum:

$$\ell(w) = \frac{1}{2}(y - v\sigma(w^\top x))^2$$

696 where $\sigma(\cdot)$ is some activation function and our weights are $\{v, w\}$. Let us
 697 understand the computational graph of how the loss is computed:

$$w, x \xrightarrow{\text{layer 1}} z \xrightarrow{\text{layer 2}} h \xrightarrow{\text{layer 3}} vh \xrightarrow{\text{layer 4}} \ell. \quad (4.6)$$

698 where $h = \sigma(z)$ and $z = w^\top x$. Each node in this graph is either the input/out-
 699 put or an intermediate result of the computation. The gradient of the loss with
 700 respect to the weights using the chain rule is

$$\frac{\partial \ell}{\partial v} = (y - v\sigma(w^\top x)) (-\sigma(w^\top x)) \quad (4.7)$$

701 and

$$\frac{\partial \ell}{\partial w} = (y - v\sigma(w^\top x)) (-v\sigma'(w^\top x)) (x). \quad (4.8)$$

1. **Caching computations for the chain rule.** The first idea behind backpropagation is to realize that quantities like $(y - v\sigma(w^\top x))$ or $z = w^\top x$ are computed multiple times in the chain rule in (4.7) and (4.8). If we can cache these quantities we can compute the chain rule-based gradient for the different parameters quickly.
2. **Forward computation.** The second idea behind backpropagation is to realize that quantities like $(y - vh)$, $h = \sigma(z)$ and $z = w^\top x$ are outputs of the third, second and first layers respectively. In other words, the quantities we need to cache in the chain rule computation are simply the outputs of the individual layers.
3. **Backward computation.** The third observation is to see that the quantity $\sigma'(z)$ in (4.8) is the derivative of the output of the activation function, namely $h = \sigma(z)$ with respect to z , its input argument

$$\sigma'(z) = \frac{dh}{dz}.$$

This derivative is combined with the forward computation $(y - vh)$ to get the gradient with respect to the weights w .

Backpropagation is simply a book-keeping exercise that caches the forward computation of the graph in (4.6) and uses these cached values to compute the derivative of the loss ℓ with respect to the parameters of each layer sequentially.

702 We will use a clever notation to denote the backprop gradient which will
 703 make all this process very mechanical and easy. Denote by

$$\bar{v} = \frac{d\ell}{dv} \quad (4.9)$$

704 the derivative of the loss ℓ with respect to a parameter v . Effectively, for our
 705 simple two layer (one neuron) neural network, we are interested in computing
 706 the quantities

$$\bar{w}, \quad \bar{v}.$$

707 Let us also denote the output of the second linear layer (layer 3)

$$e = vh.$$

Now observe the following “forward computation”

$$z = w^\top x \quad (4.10)$$

$$h = \sigma(z) \quad (4.11)$$

$$e = vh \quad (4.12)$$

$$\ell = \frac{1}{2} (y - e)^2. \quad (4.13)$$

708 Let us imagine that we have cached all the quantities on the left hand side
709 of the equalities above. We use these quantities to perform the “backward”
710 computation.

$$\begin{aligned} \frac{d\ell}{d\ell} &= \bar{\ell} = 1. \\ \mathbb{R} \ni \bar{e} &= \bar{\ell} \frac{d\ell}{de} \\ &= -1(y - e) = \bar{\ell}(-(y - e)). \quad (\text{from (4.13)}) \\ \mathbb{R} \ni \bar{v} &= \bar{e} \frac{de}{dv} \\ &= -(y - e)h = \bar{e}h. \quad (\text{from (4.12)}) \\ \mathbb{R} \ni \bar{h} &= \bar{e} \frac{de}{dh} \\ &= \bar{e}(v). \quad (\text{from (4.12)}) \\ \mathbb{R} \ni \bar{z} &= \bar{h} \frac{dh}{dz} \\ &= \bar{h} \sigma'(z). \quad (\text{from (4.11)}) \\ \mathbb{R}^d \ni \bar{w} &= \bar{z} \frac{dz}{dw} \\ &= \bar{z}x. \quad (\text{from (4.10)}) \\ \mathbb{R}^d \ni \bar{x} &= \bar{z} \frac{dz}{dx} \\ &= \bar{z}w. \quad (\text{from (4.10)}) \end{aligned}$$

711 **Remark 4.1.** An interesting mnemonic to remember backprop by is to see
712 that if the forward graph is

$$z = w_1x_1 + w_2x_2$$

713 the backprop gradient is $\bar{w}_1 = \bar{z}x_1$ and $\bar{w}_2 = \bar{z}x_2$. If x_1 was large and
714 dominated the computation of z during the forward propagation, then w_1
715 which is the multiplier of x_1 also gets a dominant share of the backprop
716 gradient \bar{z} . The backprop gradient is shared equitably among the different
717 quantities that took part in the forward computation. This is useful to remember
718 when you build neural networks with complex architectures on your own: if
719 there is a part of the network whose activations are very small and it is being
720 combined with another part of the network whose activations have a large
721 magnitude, then the former is not going to get a large enough backprop
722 gradient.

723 **Remark 4.2 (Gradient with respect to the input x).** Notice that we obtain
724 the gradient of the loss with respect to the input x

$$\frac{d\ell}{dx}$$

725 as a by-product of backpropagation. Backpropagation computes the gradient
726 of the input activations to each layer \bar{v} because this is precisely the gradient
727 that is propagated downwards. So the gradient \bar{x} should not be surprising,
728 after all x is nothing but the input activation to the first layer. This gradient
729 is useful, you can use to find what are called adversarial examples, i.e., input
730 images which look like natural images to us humans but contain imperceptible
731 noise that gives a large value of \bar{x} .

732 4.2.2 Implementation of backpropagation

733 Consider our neural network classifier given by

$$f(x; v, S_1, \dots, S_L) = \text{sign}(w^\top \sigma(S_L^\top \dots \sigma(S_2^\top \sigma(S_1^\top x)) \dots)).$$

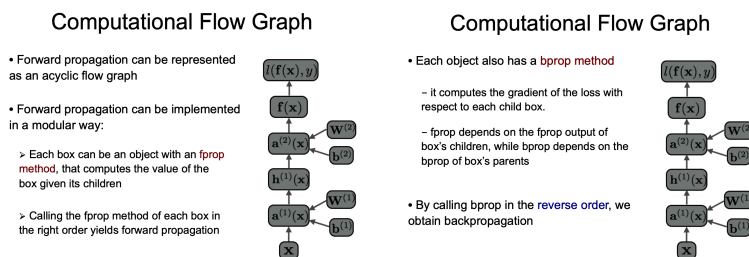


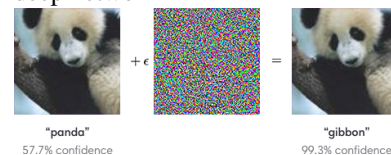
Figure 4.2: A schematic of forward and backward computations in backpropagation.

734 When you build such a multi-layer network in PyTorch, the k^{th} layer is
735 automatically equipped with two member functions.

```
736
737 def forward(self, h^{k-1}, S_k):
738     # computes the output of the k^{th} layer
739     # given output of previous layer h^k and
740     # parameters of current layer S_k
741     return h^k
742
743 def backward(self, h^k, d loss/dh^{k}, S_k):
744     # computes two quantities
745     # 1. d loss/d{S_k}
746     # 2. d loss/d{h^{k-1}}
747     return d loss/d{S_k}, d loss/d{h^{k-1}}
```

749 Such forward and backward functions exist for every layer, including the
750 nonlinearities. If you implement a new type of layer in a neural network, say a
751 new nonlinearity, you only need to write the forward function. The autograd
752 module inside PyTorch automatically writes the backward function by looking
753 at the forward function. This is why PyTorch is so powerful, you can build
754 complex functions inside your deep networks without really bothering to
755 compute the derivatives yourself.

▲ An example adversarial input to a deep network



756

Chapter 5

757

Convolutional Architectures

Reading

1. Goodfellow 9
2. “Striving for simplicity: The all convolutional net”, by (Springenberg et al., 2014)

758

We have been talking about “fully-connected” neural networks till now. There are a few problems that are apparent even in our limited experience.

759

760

761

762

763

764

765

766

767

Fully-connected layers have lot of parameters. If an input image is of size $100 \times 100 = 10^4$ grayscale pixels and we would like to classify it as belonging to one out of 1000 classes, we need 10M parameters. It is difficult to perform so many add-multiply operations quickly even on sophisticated hardware. Further, the curse of dimensionality never goes away; we need lots of data to fit these many parameters.

Natural data is full of “nuisances” that are not useful for tasks such as classification. E.g., illumination, viewpoint, and occlusions



$$I = h(\xi, \nu)$$



$$\tilde{I} = h(\xi, \tilde{\nu}), \quad \tilde{\nu} = \text{illumination}$$



$$\tilde{\nu} = \text{visibility}$$



$$\tilde{\nu} = \text{viewpoint}$$



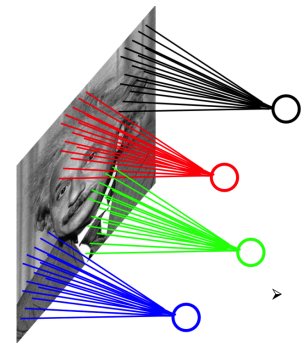
$$\tilde{I} = h(\tilde{\xi}, \tilde{\nu}), \quad \tilde{\xi} \neq \xi$$

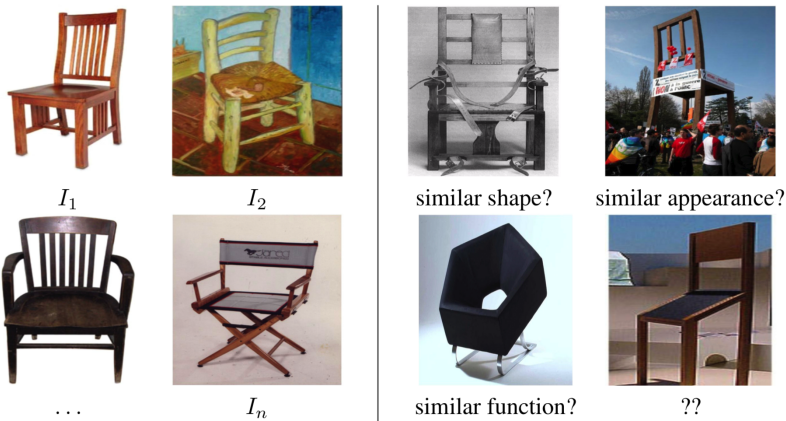
768

769

or even semantic ones shown below

Let us consider an example using local connections instead of a fully-connected layer. If each output neuron is connected to only 25 pixels of the 100×100 image and there are 1000 output neurons, how many weights will this layer have?





770

771 Do fully connected networks work for such different images?

772 Nuisances can be defined as operations that act on the data before you
 773 get to see it (nature creates these nuisances). Some of them are special and
 774 they have a group structure, i.e., they satisfy certain algebraic conditions
 775 [https://en.wikipedia.org/wiki/Group_\(mathematics\)](https://en.wikipedia.org/wiki/Group_(mathematics)). For instance, images of
 776 the same chair taken from different vantage points are projections of different
 777 rigid body transformations of the camera. Some other nuisances such as occlu-
 778 sions do not have a group structure, e.g., there is no rigid body transformation
 779 that allows us to backcalculate the pixels belonging to a person standing behind
 780 a car. Convolutional layers are a simple way to tackle one particular kind of
 781 nuisance, that of translations.

782

5.1 Basics of the convolution operation

783 So far, we have seen that the basic unit of a neural network is

$$\sigma(w^\top x).$$

784 The basic unit of a convolutional neural network is

$$\sigma(x * w)$$

785 where the $*$ denotes a convolution operation. Consider two one-dimensional
 786 vectors $x \in \mathbb{R}^3$ and $w \in \mathbb{R}^3$; we will imagine these to be arrays of infinite
 787 length with all the entries at indices $[4, \infty)$ set to zero; this is known as
 788 zero-padding the input

$$\begin{aligned} x &= [2, -1, 1, 0, 0, \dots] \\ w &= [1, 1, 2, 0, 0, \dots]. \end{aligned}$$

789 The convolution of x with w (which is called the filter) is denoted by

$$(x * w)_k = \sum_{\tau=0}^{\infty} x_\tau w_{k-\tau}. \quad (5.1)$$

790 The element $(x * w)_k$ at the k^{th} index is a composition of all the terms in the
 791 summation on the right hand side. The term $w_{k-\tau}$ for negative arguments is

▲ In the signal processing literature, the words filter and kernels are used equivalently, so convolutional filters are also often called convolutional kernels.

792 interpreted as a mirror flip of the vector w . For continuous functions, you will
793 have seen the expression

$$(x * w)(t) = \int_0^t x(\tau)w(t - \tau) d\tau.$$

794 for the convolution operation. For our vectors x, w with three entries the
795 convolution operation looks as follows.

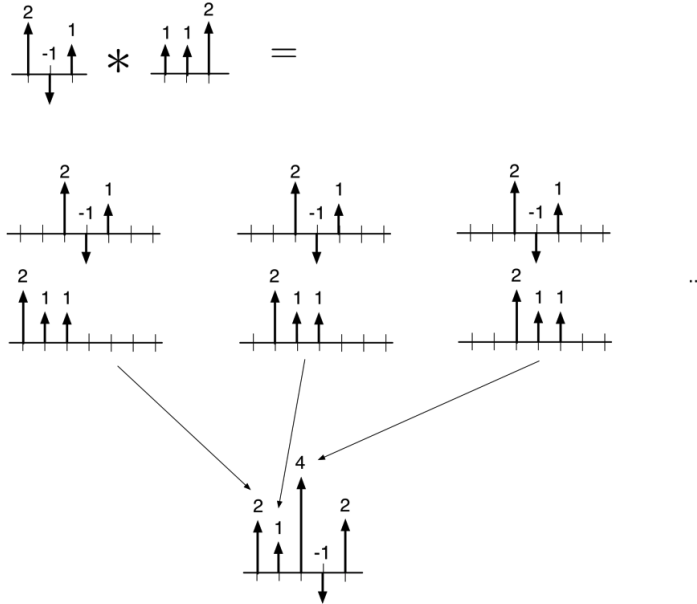


Figure 5.1: Flip and filter style computation of a convolution corresponding to the summation in (5.1).

796 **Remark 5.1 (Some identities regarding convolutions).** Notice that we can
797 change the variable of integration and set $s = t - \tau$ to get

$$\begin{aligned} (x * w)(t) &= \int_0^t x(\tau)w(t - \tau) d\tau \\ &= - \int_t^0 x(t - s) w(s) ds \\ &= \int_0^t w(s) x(t - s) ds \\ &= (w * x)(t). \end{aligned}$$

798 Convolutions are therefore commutative; you can show similarly that they are
799 also distributive $(f * g) * h = f * (g * h)$. Convolution is a linear operator,
800 you can show that

$$(f + g) * h = (f * h) + (g * h)$$

801 for any integrable functions f, g, h .

🔍 Discuss the convolution of two square waves x, w .

802 **Remark 5.2 (Padding for implementing convolutions).** In order to imple-
 803 ment the summation in convolution, we need to pad the input vector x by
 804 zeros. How many zeros should we pad it by? You will notice that if the kernel
 805 w has $2k + 1$ elements, the input vector x need not be padded all the way to
 806 infinity, we only need to pad it with k extra elements.

807 5.1.1 Convolutions of 2D images

808 Convolutions work in the same way for two-dimensional or three-dimensional
 809 input signals. The kernel w will be a matrix of size $k \times k$ in the former case
 810 and of size $k \times k \times k$ in the latter.

$$(x * w)_{i,j} = \sum_{s=0}^{\infty} \sum_{t=0}^{\infty} x_{s,t} w_{i-s,j-t}. \quad (5.2)$$

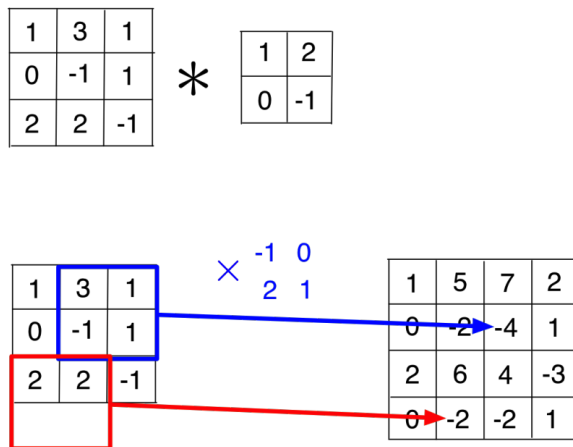


Figure 5.2: Flip and filter style computation of a convolution for a 2D input image corresponding to the summation in (5.2).

811 5.1.2 Some examples

- 812 1. Since convolution is a linear operator we should be able to write it as a
 813 matrix-vector multiplication. We take the kernel, flip it and sweep it left
 814 and right to get the rows of the matrix.

$$(2, -1, 1) * (1, 1, 2) = \begin{bmatrix} 1 & & & \\ 1 & 1 & & \\ 2 & 1 & 1 & \\ & 2 & 1 & 2 \end{bmatrix} \begin{bmatrix} 2 \\ -1 \\ 1 \end{bmatrix}.$$

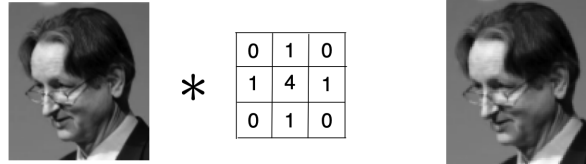
815 The matrix is called a Toeplitz matrix https://en.wikipedia.org/wiki/Toeplitz_matrix.
 816 Two-dimensional convolutions can be written as a matrix-matrix multi-
 817 plication using a similar construction; see [https://stackoverflow.com/questions/16798888/2-](https://stackoverflow.com/questions/16798888/2-d-convolution-as-a-matrix-matrix-multiplication)
 818 [d-convolution-as-a-matrix-matrix-multiplication](https://stackoverflow.com/questions/16798888/2-d-convolution-as-a-matrix-matrix-multiplication).

▲ Most deep learning libraries implement a slightly different operation instead of convolution, even though they call it a convolution. They implement the cross-correlation operation

$$(x * w)_k = \sum_{\tau=0}^{\infty} x_{\tau} w_{k+\tau}.$$

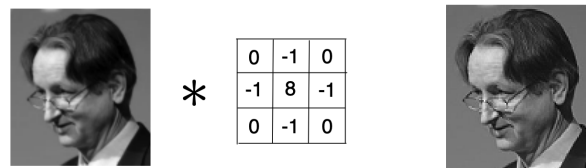
In simple words, the kernel w is not mirror flipped about the Y axis before computing the summation in (5.1). While such an operation is not strictly a convolution (you can see the difference if you consider an asymmetric kernel w , cross-correlation and convolution are the same for symmetric kernels), the difference does not matter for deep learning because the kernel w is learned during training. You can mirror flip the kernel after training and interpret the network as indeed performing a convolution with the flipped kernel.

- 819 2. Lots of non-trivial transformations of the image are possible using slight
820 changes in the weights. E.g., blurring



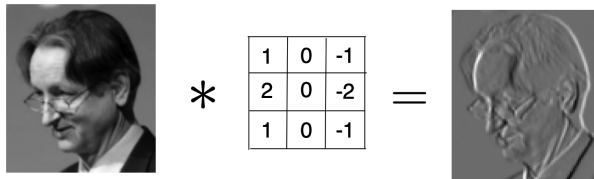
821

- 822 or sharpening using a slight change in the weights



823

- 824 We can also detect edges

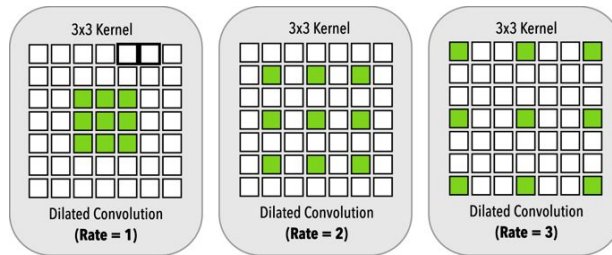


825

826 This filter is called the Sobel filter and is an integral part of image
827 pre-processing pipelines in computer vision.

- 828 3. Just like fully-connected layers, we can also stack up convolutions. The
829 effective receptive field, i.e., the pixels that are considered by the kernel
830 in the convolutional operation increases as we go up the layers.
- 831 4. The operation $S^\top x$ has $S \in \mathbb{R}^{d \times p}$ weights and returns a vector in \mathbb{R}^p . A
832 convolution operator returns a vector $(x * w) \in \mathbb{R}^d$ using K parameters
833 in the kernel w . It is important to note that a lot of parameter sharing
834 is happening while computing the values of the output neurons. You
835 can find some animations at <https://colah.github.io/posts/2014-07-Conv-Nets-Modular> and <https://colah.github.io/posts/2014-07-Understanding-Convolutions>.
836
837
- 838 5. Padding the input by zeros is common in signal processing because
839 the signals are usually a function of time. We can do a bit better for
840 images than zero padding ($\text{RGB} = (0, 0, 0)$) which is akin to creating
841 an artifact of a dark black border around the image. Reflection padding
842 is a technique (`torch.nn.ReflectionPad2d` in PyTorch) that mirrors the
843 pixels at the boundary and does not create such artifacts.

844 **Remark 5.3 (Dilated convolutions).** You don't need to use a kernel that
 845 looks like a contiguous array. We can create holes in the kernel and expand
 846 the receptive field. Dilated convolutions do precisely this.



847

848 These operators are very useful for image segmentation because they capture
 849 correlations across large parts of the input image while still enabling the
 850 parameter sharing of a convolutional layer.

851 **Remark 5.4 (Separable convolutions).** There are 9 weights in a 3×3 kernel.
 852 Even convolutional layers can get really big, e.g., a standard CNN used for
 853 ImageNet has about 25M weights and is almost entirely convolutional. Thus
 854 we might want to reduce the number of weights even further. Separable
 855 convolutions are a trick to doing so. Consider a 3×3 kernel and split it into
 856 two kernels of 3×1 and 1×3

$$\begin{bmatrix} 3 & 6 & 9 \\ 4 & 8 & 12 \\ 5 & 10 & 15 \end{bmatrix} = \begin{bmatrix} 3 \\ 4 \\ 5 \end{bmatrix} \times [1 \quad 2 \quad 3].$$

857 Using the original kernel requires 9 multiply operations to compute each pixel
 858 value. Using the split kernels requires only 6, it also has fewer weights. These
 859 are called separable convolutions. The Sobel filter which we saw before can
 860 be written as a separable convolution

$$\begin{bmatrix} 1 & 0 & -1 \\ 2 & 0 & -2 \\ 1 & 0 & -1 \end{bmatrix} = \begin{bmatrix} 1 \\ 2 \\ 1 \end{bmatrix} [1 \quad 0 \quad -1]$$

861 because it measures the gradient of the image intensity independently in the
 862 two directions. Separable convolutions are very useful when you can use
 863 high-dimensional data in deep learning, e.g., medical images out of MRI are
 864 4-dimensional images (width, height, depth, channel).

865 5.2 How are convolutions implemented?

866 Convolutions are the most heavily used operator in a deep network. We
 867 therefore need to implement them as efficiently as we can. There are a few
 868 different ways of implementing convolutions.

- 869 1. Write a simple for loop. This works well if the kernel is small in size.
- 870 2. We can expand out the kernel as a matrix and in this way a convolutional
 871 layer is simply a matrix-vector multiplication. This method is most
 872 commonly implemented and works well for sizes up to 5×5 .

🔍 Can we write every 2D convolutional filter as a separable convolution? The answer is no: you will notice that a separable kernel is a rank-1 matrix. The singular value decomposition (SVD) of a separable kernel A is therefore

$$A = u v^\top$$

for two vectors u, v (we incorporated the singular value into u and v). Can we however *approximate* any convolutional kernel as a sum of separable convolutions? The answer to this is yes: observe using the SVD of the kernel $A \in \mathbb{R}^{p \times p}$ that it can be written as

$$A = \sum_{i=1}^p u_i v_i^\top.$$

where u_i, v_i are the singular vectors. You don't have to pick all the factors, if you pick a few terms in this summation, you get a good spectral approximation of the matrix A . You will see in Section 5.3 how the convolutional layer in a deep network is structured and may allow the network to learn a complicated kernel A even if the operations are only separable $u_i v_i^\top$.

873 3. We can use the Fast Fourier Transform (FFT) to compute the convolution
874 as

$$x * w = \mathcal{F}^{-1} [\mathcal{F} [x] \mathcal{F} [w]].$$

875 This is efficient for large kernels, say greater than 7×7 .

876 Typically, deep learning libraries will choose an algorithm for convolution in
877 *run-time* after looking at your neural architecture; you do not have to worry
878 about the specific algorithm. A library called cuDNN from Nvidia implements
879 a bunch of convolution algorithms on GPUs efficiently. PyTorch will pick one
880 of these algorithms by checking how long it takes for the first forward-pass
881 on your deep network. But the fact remains that large kernels which allow
882 a larger receptive field (long-range correlations in the input image) are more
883 expensive to compute than smaller kernels. Architectures such as Inception
884 that we will see soon are an attempt to get a large receptive field while still
885 keeping computations in the convolutional layer small.

886 **Remark 5.5 (Stride in convolutional layers).** If you see the documentation
887 for the convolutional layer in PyTorch at (<https://pytorch.org/docs/stable/generated/torch.nn.Conv2d.html>)
888 you will also see a parameter known as stride. Stride simply means that the
889 output

$$(x * w)_k = \sum_{\tau=0}^{\infty} x_{\tau} w_{k-\tau}$$

890 is not computed at all values of k ; if the stride is set to 2, the output is computed
891 only at every alternate value of k . Note that the default stride as seen in the
892 definition of convolution is 1. Since images change very little from pixel to
893 pixel, this is a neat trick to reduce the redundancy of computing the convolution
894 again and again over similar input. The important artifact of using a stride
895 larger than 1 is that the output $(x * w)$ is no longer the same length (even after
896 padding) as the input, is half the length if the stride is 2.

897 5.3 Convolutions for multi-channel images in a 898 deep network

899 We will now study how the convolutional layer is implemented in a typical
900 deep network. Let us denote the 2D convolution operation on a single-channel
901 2D image $A \in \mathbb{R}^{w \times h}$ by a kernel $w \in \mathbb{R}^{k \times k}$ by

$$A * w = B \in \mathbb{R}^{w \times h}.$$

902 Imagine that we have an RGB input image of size $w \times h$; the RGB indicates that
903 there are three input channels, one for each color. The input to a convolutional
904 layer in a deep network is therefore an array of size $3 \times w \times h$. Typical deep
905 learning libraries, when they implement a convolutional layer with a kernel w
906 of size $k \times k$, will output an image of size $c \times w \times h$ where c are the number
907 of channels in the image at the output of the layer.

908 Effectively, a convolutional layer maps

$$\mathbb{R}^{3 \times w \times h} \ni A \mapsto B \in \mathbb{R}^{c \times w \times h}.$$

▲ You can set
torch.cudnn.benchmark = False to
stop this.

🔍 We said that convolutional filters are used to learn the correlations across nearby pixels. What would be the utility of 1×1 convolutions?

🔍 If there are 10 input channels and 25 output channels, how many parameters does a convolutional layer with a 5×5 kernel have? What is the size of the output feature map if convolution is performed with a stride of 2? Does stride change the number of parameters in a convolutional layer?

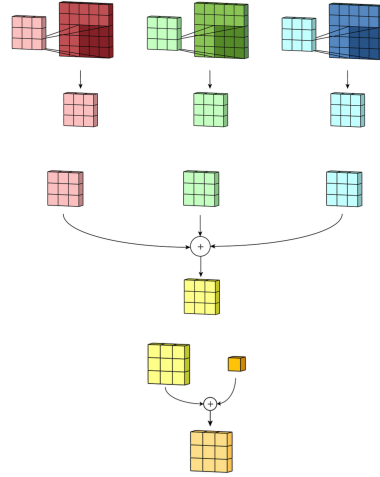


Figure 5.3: Convolutional layer in a typical deep network

909 The layer performs the operation

$$v_j + \sum_{i=1}^3 A_i * w^{ij} = B_j$$

910 where A_i for $i \in \{1, 2, 3\}$ denotes the i^{th} channel of the input image and B_j
 911 for $j \in \{1, \dots, c\}$ denotes the j^{th} channel of the output image, and the kernel
 912 $w^{ij} \in \mathbb{R}^{k \times k}$ is the convolutional kernel. The scalar $v_j \in \mathbb{R}$ denotes the bias.
 913 Effectively, there are $3c$ different kernels in one layer and the convolutional
 914 layer sums up the result of convolutions on all the input channels and adds a
 915 bias to create *each* output channel.

916 5.4 Translational equivariance using convolutions

917 We now discuss the most important reason for using convolutions in deep
 918 networks. Let us take our 1-dimensional signal x and translate it by Δ units to
 919 the right

$$x'(t + \Delta) := x(t).$$

920 You will see from the definition of convolution in (5.1) that the convolution
 921 also gets translated

$$\begin{aligned}
 (x' * w)_k &= \sum_{\tau=0}^{\infty} x'_{\tau} w_{k-\tau} \\
 &= \sum_{\tau=0}^{\infty} x_{\tau-\Delta} w_{k-\tau} \\
 &= \sum_{s=-\Delta}^{\infty} x_s w_{k-s-\Delta} \quad (s = \tau - \Delta) \\
 &= (x * w)_{k-\Delta}.
 \end{aligned}
 \tag{5.3}$$

922 In other words, if you translate the signal by Δ then the output of convolution
923 is also translated by the same amount

$$(x' * w)_{k+\Delta} = (x * w)_k.$$

924 This property is called equivariance. Equivariance also holds for 2D convolu-
925 tions. Equivariance to translations allows us to build an important property in
926 a deep network. If we have a convolutional kernel that has weights such that
927 the output is high for a certain object (star in adjoining picture, vertical/slanted
928 strips in your Gabor filter homework), the output of a convolutional layer is
929 such that the features also “move” if the input moves in the receptive field.

930 We can easily build a binary classifier using such equivariant features. If
931 we want to build a star classifier, we simply check if some features in the
932 output are large after convolution, e.g., we check if the largest feature in the
933 2D-feature map is greater than some pre-determined threshold

$$f(x, w) := \mathbf{1}_{\{\max_{i,j} \{(x*w)_{ij}\} \geq \epsilon\}}. \quad (5.4)$$

934

935 5.5 Pooling to build translational invariance

936 We would like to build a classifier such that if the object moves to some other
937 location in the input image, the output of the classifier remains unchanged, i.e.,
938 the deep network detects a test image as a cat even if it is in some other part
939 of the image in the training data. Equivariance is only one part of the story to
940 doing so. Remember that the last layer in a deep network looks like

$$f(x, w) = \text{sign}(v^\top h^L) = \text{sign}\left(\sum_{i=1}^p v_i h_i^L\right).$$

941 Even if the features h^L are equivariant when the input x is translated in the
942 2D plane, the inner product $v^\top h^L$ cannot be equivariant. Essentially, if a few
943 weights v_i are trained to check for objects like cat/dog in one particular part of
944 the image, even if the features h^L move accordingly, the output $v^\top h^L$ need
945 not be constant because the weights v_i at those new locations of features may
946 be different.

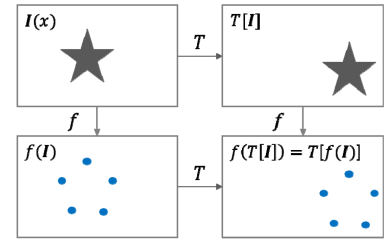
947 In other words, we want features of a deep network to be *invariant* to
948 translations in the input.

Pooling is an operation that smears out the features locally in the neighborhood of each pixel.

949 We can use our idea of setting all the weights to 1 to get what is called the
950 average pooling operation. It is a linear operation and equivalent to convolving
951 the input features using a kernel

$$w_{\text{avg-pool}} = \frac{1}{9} \begin{bmatrix} 1 & 1 & 1 \\ 1 & 1 & 1 \\ 1 & 1 & 1 \end{bmatrix}. \quad (5.5)$$

▲ Translational equivariance is much more insightful for 2D images. Let us consider an example.



▲ The pre-activation features of a convolutional layer are sometimes called the *feature map*.

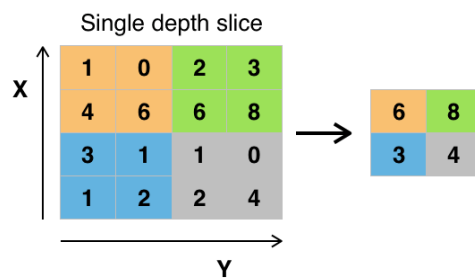
▲ Making the weights of the top layer v all equal to 1 will solve this problem, but this is of course a very poor classifier. It smears the entire input signal h^L together by just averaging the features and therefore does not have much discriminative power; it cannot easily build a multi-class classifier for instance.

952 The average-pooling kernel is fixed during training and does not have any
 953 weights, otherwise it would be just another convolutional kernel.

954 Average pooling does not solve our problem of making the features in-
 955 variant; the smeared out version simply moves less than Δ when the input
 956 translates by Δ . If we add many average pooling layers at various stages in a
 957 deep network, we make the features move even less and this may be sufficient
 958 to allow for weights v to be discriminative.

959 Max-pooling is another operation that builds invariance. It takes in an
 960 input $x \in \mathbb{R}^{w \times h}$ and computes

$$(\text{max-pool}(x))_{ij} = \max_{-k \leq s \leq k} \max_{-k \leq t \leq k} x_{i-s, j-t}. \quad (5.6)$$



Example of Maxpool with a 2×2 filter and a stride of 2

Figure 5.4: Max-pooling with a 2×2 kernel and a stride of 2 reduces the size of the input image by half. A stride of 1 would preserve the image size but would give less invariance.

961 This is a clever way of building invariance, you simply take the maximum
 962 value of the input in a window of size $k \times k$, so even if the input translates
 963 by k pixels in either direction, the output of a max-pooling layer remains
 964 the same. If we add multiple max-pooling layers at intermediate depths in a
 965 deep network, we achieve translational *invariance* in a convolutional neural
 966 network.

967 **Remark 5.6 (Max-pooling destroys information).** As we see in Figure 5.4,
 968 max-pooling destroys a lot of information in the input image. The result of
 969 max-pooling is a much smaller feature map. This results in a large loss of
 970 information in the input data and often leads to a loss of discriminative power,
 971 i.e., accuracy, during training. This trade-off between building a classifier that
 972 is invariant to changes in the input and discriminative enough to distinguish
 973 between many different categories is fundamental.

974 Max-pooling has a side-benefit, it reduces the number of operations in a
 975 deep network and the number of parameters by sequentially reducing the size
 976 of the feature map with layers. This is useful because a typical image you get
 977 from an autonomous car is easily about 10MP (10^7 pixels) and we need to
 978 boil it down into, say 10 categories that are relevant to driving, i.e., $h^L \in \mathbb{R}^{10}$.
 979 Max-pooling is a very useful for this, with the caveat that too much pooling
 980 will dramatically reduce the signal in the input image.

▲ Average pooling blurs the image. We saw this in the example in Section 5.1.2. Such blurring at intermediate layers gives *some* translational invariance by smearing out the features.

❓ Does max-pooling make sense for a fully-connected network? There is no equivariance property in such a network, so even if we do perform max-pooling, it is just like another activation function operating on the features.

❓ We have talked about invariance to translations in this lecture. Images taken from a fish-eye camera, or MRI images of the brain, are such that objects *rotate* in the field of view.



Can you think of a trick to build invariance to rotations?

Chapter 6

Data augmentation, Loss functions

Reading

1. Bishop Chapter 5.5.3, 4.3
2. Goodfellow Chapter 7.4

6.1 Data augmentation

In the previous chapter, we looked at convolutions as a way to reduce the parameters in a deep network, but more importantly as a way of building equivariance/invariance to translations. There are a lot of nuisances other than translation that do not have a group structure which precludes operations such as convolutions that we can perform to generate equivariance/invariance.

In this section, we will discuss techniques to build invariance to nuisances that are more complex than just translations, these techniques will seem brute-force but they also allow us to handle more complex nuisances. The main trick is to *augment* the data, i.e., create variants of each input datum in some simple way such that we *know* that its label is unchanged. If our original dataset is $D = \{(x^i, y^i)\}_{i=1, \dots, n}$ we create an augmented dataset

$$D^T = \{(T(x^i), y^i)\}_{i=1, \dots, n} \cup D. \quad (6.1)$$

where T is some operation of our choice. We have therefore expanded the number of samples in the training dataset to $2n$ instead of the original n . Effectively, data augmentation is a technique to create a dataset that is sampled from some other data distribution P than the original one.

1000 6.1.1 Some basic data augmentation techniques

1001 The most popular data augmentation techniques are setting T to be changes
 1002 in brightness, contrast, cropping the image to simulate occlusions, flipping
 1003 the image horizontally or vertically, jittering the pixels of the input image to
 1004 simulate noise in the CCD of the camera/weather, padding the image which
 1005 changes the borders of the input image, warping the image using a projection
 1006 that simulates the same picture taken from a different viewpoint, thresholding
 1007 the RGB color channels, zooming into an image to simulate changes in the
 1008 scale etc.

1009 You can see these operations at [https://fastai1.fast.ai/vision.transform.html#List-](https://fastai1.fast.ai/vision.transform.html#List-of-transforms)
 1010 [of-transforms](https://fastai1.fast.ai/vision.transform.html#List-of-transforms).

▲ FastAI is a wrapper on top of PyTorch and is an excellent library to learn for doing your course projects.

1011 6.1.2 How does augmentation help?

1012 A number of such augmentations are applied to the input data while training a
 1013 deep network. This increases the number of samples n we have for training
 1014 but note that different samples share a lot of information, so the effective novel
 1015 samples has not increased by much. Let us get an idea of when augmentation
 1016 is useful and when it is not. Consider a regression and classification problem
 1017 as shown below.



Figure 6.1: Cows live in many different parts of the world. A classifier that also uses background information to predict the category is likely to make mistakes when it is run in a different part of the world. Augmenting the input dataset on the left by replacing the background to include a mountain or a city is therefore a good idea if we want to run the classifier in a different part of the world. This will also force the classifier to *ignore* the background pixels when it classifies the cow, in other words the classifier is forced to become invariant to backgrounds by brute-force showing it different backgrounds.

1018 In essence, data augmentation forces the model to tackle a larger dataset
 1019 than our original dataset. The model is forced to learn what nuisances the

1020 designer would like it to be invariant to. Compare this to the previous chapter:
 1021 by replacing fully-connected layers with convolutions and pooling we made
 1022 the model invariant to translations. In principle, we could have trained a fully-
 1023 connected deep network on a very large augmented dataset with translated
 1024 objects. In principle, this would make the fully-connected network invariant
 1025 to translations as well.

1026 6.1.3 What kind of augmentation to use when?

1027 In the example with regression, we saw that the regressor on the augmented
 1028 data was essentially linear and had much less discriminative power than a
 1029 polynomial regressor. This was of course by design, we chose to augment the
 1030 data. If the test data for the problem came from the polynomial instead of our
 1031 augmented distribution, the new classifier will perform poorly.



Figure 6.2: The second panel shows the original scene with a mirror flip (i.e., across the horizontal axis) while the third panel shows the original scene after a water reflection (i.e., flip across the vertical axis). The latter is an image that is very unlikely to occur in the real world, so it is not a good idea to use it for training the model.

By being invariant to a larger set of nuisances than necessary, we are wasting the parameters of the model and risk getting a large error if the test data was not from the augmented distribution. By being invariant to a smaller set of nuisances than necessary, we are risking the situation that the test data will have some new nuisances which the classifier will perform poorly on. It is important to bear in mind that we do not always know what nuisances the model should be invariant to, the set of transformations in data augmentations necessarily depends—often critically—upon the application.

1032 Data augmentation requires a lot of domain expertise and often plays a
 1033 huge role in the performance of a deep network. You should think about what
 1034 kind of augmentations you will apply to data for speech processing, or for data
 1035 from written text.

1036 6.2 Loss functions

1037 We next discuss the various loss functions that are typically used for training
 1038 neural networks. As usual, we are given a dataset

$$D = \{(x^i, y^i)\}_{i=1, \dots, n}.$$

❓ If you are building a classifier for detecting cars, motorbikes, people etc. for autonomous driving application, do you want to be the invariant to rotations?

6.2.1 Regression

MSE loss. If the labels are real-valued $y^i \in \mathbb{R}$, e.g., we are predicting the price of housing in Boston given features of the houses (like you did in HW 0), we are solving a regression problem and the loss function to use for a deep network is also simply the regression loss.

$$\ell_{\text{mse}}(w) := \frac{1}{2} (f(x; w) - y)^2 \quad (6.2)$$

Recall, that we assume in machine learning that the training dataset contains independent and identically drawn samples. Real data often does not satisfy this iid assumption and a model fitted via regression may not work well if the data are correlated. A popular trick to handle such situations in regression to take a logarithmic transformation of the input, i.e., fit a model to $\log x$ using the loss

$$\frac{1}{2} (f(\log x; w) - y)^2;$$

we can compute the logarithm element-wise for vector valued inputs.

Huber loss. The square-residual loss in (6.2) works in most cases but it does not work well if there are outliers in the data. Outliers are data in the training set that are noisy or did not come from the true model. In such cases, we can use the Huber loss. If the residual is $r = f(x; w) - y$, the Huber loss is

$$\ell_{\text{huber}}(w; \delta) = \begin{cases} \frac{1}{2} |r|^2 & \text{if } |r| \leq \delta \\ \delta (|r| - \frac{1}{2} \delta) & \text{else.} \end{cases} \quad (6.3)$$

Observe that this does not penalize the model egregiously if the predictions are bad ($|r| \geq \delta$) for a particular datum. Doing so prevents the outliers from biasing the loss towards themselves and ruining the residuals for the other data.

MAE loss. The absolute-error loss (or ℓ_1)

$$\ell_{\text{mae}}(w) = |f(x; w) - y| \quad (6.4)$$

has a similar motivation: it does not penalize the residual on the outliers.

Using a subset-selection technique or the ℓ_{mae} loss leads to sparse weights w^* . This makes the model more interpretable than a model fitted using ℓ_{mse} loss. This is easy to understand for linear models: input dimensions corresponding to weights w_i^* that are zero do not take part in making predictions. So one may answer questions of the form “is variable x_i a relevant predictor of the target y ”.

Variable importance. For linear models, another way to answer the same question is to fit two models, one with w_i fixed to zero and all other weights fitted using the MSE loss (6.2) and another model without fixing w_i ; the difference between the average square residuals in the two cases is a measure of how important the feature x_i is for the prediction. These techniques are called variable importance methods. We can also undertake the same program for nonlinear models on non-image based data.

Quantile loss. The quantile loss is another simple trick to make the model more robust to outliers and get more information from the model than simply the prediction $f(x; w)$. Observe that if we have targets Y that are random

▲ We can perform regression in a clever way: first set all weights $w_i = 0$ and iteratively allow a subset of the weights (say the ones that improve the residuals the most) to become non-zero; non-zero weights are fitted using ℓ_{mse} . This is known as forward selection. Backward selection starts with weights w^* which minimize ℓ_{mse} and iteratively prune the weights. Both forward and backward selection are techniques to fit a model w^* with sparse weights.

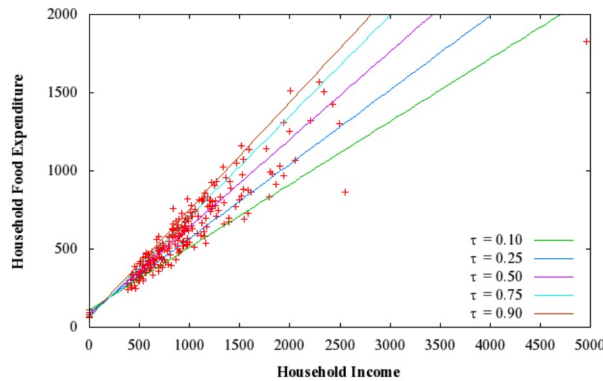
1077 variables with cumulative distribution function $F(y) = \mathbb{P}(Y \leq y)$, the τ^{th}
 1078 quantile of Y is given by

$$Q_Y(\tau) = F^{-1}(\tau) = \inf \{y : F(y) \geq \tau\}$$

1079 for $\tau \text{ in } (0, 1)$. We now learn a predictor for $Q_Y(\tau) = f(x; w)$. It turns out
 1080 (you can try to prove this) that this corresponds to the loss function

$$\begin{aligned} \ell_{\text{quantile}}(w; \tau) &= \begin{cases} r(\tau - 1) & \text{if } r < 0 \\ r\tau & \text{else.} \end{cases} & (6.5) \\ &= r(\tau - \mathbf{1}_{\{r < 0\}}). \end{aligned}$$

1081 where $r = y - f(x; w)$ is the residual. A standard technique is to fit multiple
 1082 models using the quantile loss for different quantiles, say $\tau = 0.25, 0.5, 0.75$
 1083 and give multiple predictions of the target $f(x; w^\tau)$. A typical example of
 1084 quantile linear regression looks as follows.



1085

1086 6.2.2 Classification: Cross-Entropy loss

1087 We next discuss the case when the targets are categorical and we wish to train
 1088 a discriminative model that classifies the input into one of these m categories

$$y \in \{1, \dots, m\}.$$

1089 One hot encoding.

1090 An alternative representation of the targets in classification is so-called the
 1091 *one-hot* encoding where y is transformed to

$$\text{one-hot}(y) = e_y \in \mathbb{R}^m;$$

1092 the vector e_y has a 1 at the y^{th} element and zeros everywhere else. The notation
 1093 e_y denotes the y^{th} row of the identity matrix $I_{m \times m}$.

1094 Predicting class probabilities.

1095 Instead of using the regression loss by treating y as a real-valued quantity, it
 1096 is more natural to predict the log-probability $\log p(k|x)$ for every category k
 1097 using weights w and predict the category using

$$f(x; w) = \operatorname{argmax}_k \log p_w(k|x). \quad (6.6)$$

1098 Just like we denoted the raw predictions of the model by \hat{y} in linear/logistic
1099 regression, we will denote

$$\mathbb{R}^m \ni \hat{y} = v^\top \sigma(S_L^\top \dots \sigma(S_2^\top \sigma(S_1^\top x)) \dots) \quad (6.7)$$

1100 where $v \in \mathbb{R}^{p \times m}$. As we saw in Chapter 4, \hat{y} are also called logits. Observe
1101 that the logits \hat{y} are simply vectors in \mathbb{R}^m . How can we transform these logits
1102 to get $\log p_w(k|x)$ for all $k \in \{1, \dots, m\}$ as the output of the model?

1103 Logistic loss.

1104 Linear logistic regression has a scalar output $\hat{y} \in \mathbb{R}$ which is interpreted as the
1105 log-odds of the class probabilities

$$\log \frac{p(1|x)}{p(0|x)} = \hat{y} = w^\top x. \quad (6.8)$$

1106 This expression can be rewritten as $p(1|x) = \text{sigmoid}(\hat{y})$. The likelihood of
1107 data x under this model for $y^i \in \{0, 1\}$ is

$$p_w(\{(x^1, y^1), \dots, (x^n, y^n)\}) = \prod_{i=1}^n p_w(1|x^i)^{y^i} p_w(0|x^i)^{1-y^i}.$$

1108 Maximizing this probability (MLE) is the same as minimizing the log-probability

$$\begin{aligned} \ell_{\text{logistic}}(w) &:= -\log p_w(\{(x^1, y^1), \dots, (x^n, y^n)\}) \\ &= -\sum_{i=1}^n y^i p_w(1|x^i) + (1 - y^i) p_w(0|x^i) \end{aligned} \quad (6.9)$$

1109 In other words, the logistic loss is simply maximum-likelihood estimation for
1110 the model (6.8).

1111 Binary Cross-Entropy loss.

1112 Let us turn back to neural networks and multi-class classification. Imagine
1113 if each logit of a neural network in (6.7) acts independently, i.e., it predicts
1114 whether there is class k in this input or not without paying heed to what
1115 the other logits predict. This is not very prudent, for instance, if we know
1116 beforehand that there is only one object in the input image, then such a
1117 classifier is likely to have lots of false positives. Nevertheless, observe that
1118 this is exactly like running m independent binary logistic classifiers with the
1119 same feature $h^L \in \mathbb{R}^p$. We can write the loss for such a classifier succinctly as

$$\ell_{\text{bce}}(w) = -\sum_{k=1}^m \text{one-hot}(y)_k \log p_w(k|x). \quad (6.10)$$

1120 If the ground-truth labels y^i are such that there is only one class in each input
1121 image, all entries of $\text{one-hot}(y^i)$ at other categories will be zero, so this loss
1122 penalizes only the output of one of the m independent logistic classifiers.

🔍 We saw a different expression for the logistic loss in Chapter 3

$$\ell_{\text{logistic}}(w) = \log(1 + e^{-y\hat{y}}).$$

What is the difference?

6.2.3 Softmax Layer

Observe that our classifier which employs m binary logistic classifiers for predicting all the categories independently does not predict a valid probability distribution because

$$\sum_{k=1}^m p_w(k|x)$$

is not always equal to 1. We can however posit that the model predicts logits \hat{y} that are proportional to the log-probabilities

$$\begin{aligned} \log p_w(k|x) &\propto \hat{y}_k \\ \Rightarrow p_w(k|x) &= \frac{e^{\hat{y}_k/T}}{\sum_{k'=1}^m e^{\hat{y}_{k'}/T}}. \end{aligned} \quad (6.11)$$

The result $p_w(k|x)$ is a valid distribution on k because it sums up to 1. This operation, namely taking the logits \hat{y} and constructing a probabilities out of them is called as a softmax operator. The constant T in (6.11) is called the temperature. A large value of T results in a smoother probability distribution $p_w(k|x)$ because the individual values of the logits matter less. A small value of T results in a very large weight due to the exponent on the largest logit and the distribution $p_w(k|x)$ is therefore highly spiked. The temperature is set to 1 by default in PyTorch.

The cross-entropy loss is now simply the maximum-likelihood loss after the softmax operation

$$\begin{aligned} \ell_{\text{ce}}(w) &= - \sum_{k=1}^m \text{one-hot}(y)_k \log p_w(k|x) \\ &= - \frac{\hat{y}_y}{T} + \log \left(\sum_{k'=1}^m e^{\hat{y}_{k'}/T} \right). \end{aligned} \quad (6.12)$$

Observe that the logit corresponding to the true class \hat{y}_y is being pushed higher; at the same time, if the logits of the incorrect classes are large they are being pulled *down* in the summation. This is an important point to keep in mind: the cross-entropy loss after softmax affects *all* logits, not just the logit of the correct class.

6.2.4 Label smoothing

The correct logit in (6.12) is encouraged to go to $+\infty$ while the incorrect logits are encouraged to go to $-\infty$. This can lead to dramatic over-fitting when the number of classes m is very large. Label smoothing is a trick that alleviates the problem: instead of using a one-hot encoding of the true label y , it uses the encoding

$$\text{label-smoothing}(y)_k = \begin{cases} 1 - \epsilon & \text{if } k = y, \\ \frac{\epsilon}{m-1} & \text{else.} \end{cases} \quad (6.13)$$

▲ You will often see people calling

$$\log \sum_{k'=1}^m e^{\hat{y}_{k'}/T}$$

as the “softmax” of vector \hat{y} . This is actually a more appropriate usage of the word because

$$\log \sum_{k=1}^m e^{\hat{y}_k/T} \approx \max_k \hat{y}_k$$

if one of the entries of \hat{y} is much larger than the others, or if $T \rightarrow 0$. We will however use the word “softmax” to refer to the operation of transforming \hat{y} into $p_w(k|x)$ because we do not have any need for this softened version of the max operator.

1150 The cross-entropy loss with this new encoding is now

$$\begin{aligned} \ell_{\text{label-smoothing-ce}}(w) &= - \sum_{k=1}^m \text{label-smoothing}(y)_k \log p_w(k|x) \\ &= -(1 - \epsilon) \log p_w(y|x) - \frac{\epsilon}{m-1} \sum_{k \neq y} \log p_w(k|x) \end{aligned} \quad (6.14)$$

1151 If you take the derivative of this loss with respect to \hat{y} you will see that the
1152 value of \hat{y} that minimizes the loss is

$$\hat{y}_k^* = \begin{cases} \log((m-1)(1-\epsilon)/\epsilon) + \alpha & \text{if } k = y \\ \alpha & \text{else.} \end{cases} \quad (6.15)$$

1153 where α is an arbitrary real number. Notice that logits for both the correct and
1154 the incorrect classes are finite in this case, they no longer blow up to infinity.

1155 6.2.5 Multiple ground-truth classes

1156 If there are multiple classes that are all present in the input image, i.e., if the
1157 ground truth data has multiple labels, we can easily use the vector

$$\text{multi-hot}(y) = \sum_k e_k$$

1158 for all the present classes k and set

$$\ell_{\text{bce}}(w) = - \sum_{k=1}^m \text{multi-hot}(y)_k \log p_w(k|x) \quad (6.16)$$

1159 in the BCE loss. We can also use this trick in the cross-entropy loss after the
1160 softmax operator but it will not work well because the softmax operator is
1161 designed to amplify only the largest logit in \hat{y} ; if we tried the network would
1162 still be incentivized to predict only one class instead of all classes.

Chapter 7

Bias-Variance Trade-off, Dropout, Batch-Normalization

Reading

1. Bishop 1.3, 3.2, 14.2-14.3
2. Goodfellow 5.1-5.4, 7.1-7.3
3. Dropout [Srivastava et al. \(2014\)](#)
4. Batch-Normalization [Ioffe and Szegedy \(2015\)](#)

In this chapter, we will take our first look at how machine learning classifiers generalize to new data. We will first discuss the so-called Bias-Variance Tradeoff which indicates that the variance of the predictions of a model can be reduced by increasing its bias. Regularization is a technique to give us control over this tradeoff. We will then see a few popular regularization techniques, in particular two that are important in deep learning called Dropout and Batch-Normalization.

7.1 Bias-Variance Decomposition

Ideally, we want a classifier that accurately captures the regularity in the data but also works well for unseen data. Turns out this is typically impossible to both simultaneously. We will introduce this using regression.

Given our dataset $D = \{(x^i, y^i)\}_{i=1, \dots, n}$ we fit a model $f(x; w) \in \mathcal{F}$ where \mathcal{F} is some class of models, say all neural networks with a given architecture; we will keep the dependence of f on w implicit in this section because we don't need it. We use a loss $\ell(f(x), y) = |f(x) - y|^2$ to fit this model by

1182 minimizing

$$\hat{R}(f) = \frac{1}{n} \sum_{i=1}^n |f(x^i) - y^i|^2 \quad (7.1)$$

1183 This is of course the training loss, also called the empirical risk. A classifier
1184 that minimizes $\hat{R}(f)$ works well on the training data. If we want to measure
1185 how well a model works on new data from the distribution P we are interested
1186 in the the *population risk*

$$\begin{aligned} R(f) &= \int |f(x) - y|^2 P(x, y) \, dx \, dy \\ &= \mathbb{E}_x \left[\int |f(x) - y|^2 P(y|x) \, dy \right]. \end{aligned} \quad (7.2)$$

1187 It turns out that because the loss is quadratic, we can write down the minimizer
1188 of the population risk, formally, as

$$f^*(x) = \mathbb{E}_y [y|x]. \quad (7.3)$$

1189 In other words, the optimal regressor is the conditional expectation of the
1190 targets y given a datum x . Since we do not know the data distribution P , we
1191 cannot compute the model f^* . We now compare some regression f that we
1192 may have obtained by minimizing (7.1) with the optimal f^* .

1193 Observe that

$$\begin{aligned} (f(x) - y)^2 &= (f(x) - f^*(x) + f^*(x) - y)^2 \\ &= (f(x) - f^*(x))^2 + 2(f(x) - f^*(x))(f^*(x) - y) + (f^*(x) - y)^2. \end{aligned}$$

1194 Substitute this expression in (7.2) to get

$$R(f) = \mathbb{E}_x \left[\int (f(x) - f^*(x))^2 \right] + \mathbb{E}_{(x,y) \sim P} \left[(f^*(x) - y)^2 \right] \quad (7.4)$$

1195 Observe that the cross-term

$$\mathbb{E}_x \left[\int 2(f - f^*)(f^* - y)P(y|x) \, dy \right] = 0$$

1196 vanishes because $f^*(x) = \mathbb{E} [y|x] = \int yP(y|x)dy$. In the first term, there is
1197 no y because the distribution $P(y|x)$ when integrated with respect to y is 1.
1198 The decomposition in (7.4) is insightful. The first term tells us how far our
1199 model $f(x)$ is from the optimal $f^*(x)$. The second term tells us how much
1200 the optimal model itself is from the data (x, y) . The second term is not under
1201 our control because it does not depend on $f(x)$ at all. This term

$$\text{Bayes error} = \mathbb{E}_{(x,y) \sim P} \left[(f^*(x) - y)^2 \right]. \quad (7.5)$$

1202 is irreducible error of any classifier f . It is only zero if the data (x, y) is
1203 coming from a deterministic source, i.e., there is no noise in the true targets y
1204 created by Nature and Nature's model (it is important to realize that this model
1205 is *not* f^*) is deterministic.

1206 We will now investigate the first term better. Notice that the model f is
1207 created using a finite dataset. Let us emphasize it as

$$f(x; D)$$

▲ You can think of the Bayes error as being non-zero if the sensor used to measure y is noisy, there is no way we can get deterministic data in that case. If on the other hand the sensor is perfect, e.g., a large number of humans are annotating data very carefully like we often do in modern machine learning, the Bayes error is essentially zero.

1208 and rewrite the first term in (7.4) as

$$\begin{aligned}
 (f(x; D) - f^*(x))^2 &= \left(f(x; D) - \mathbb{E}_D[f(x; D)] + \mathbb{E}_D[f(x; D)] - f^*(x) \right)^2 \\
 &= \left(f(x; D) - \mathbb{E}_D[f(x; D)] \right)^2 \\
 &\quad + \left(\mathbb{E}_D[f(x; D)] - f^*(x) \right)^2 \\
 &\quad + 2 \left(f(x; D) - \mathbb{E}_D[f(x; D)] \right) \left(\mathbb{E}_D[f(x; D)] - f^*(x) \right).
 \end{aligned}$$

1209 Recall that the dataset is a random variable as well, it is a bunch of draws
 1210 from the joint distribution P . Effectively, $f(x; D)$ which is our fitted model
 1211 is a random variable that depends on the randomness of D . We now take the
 1212 expectation over the *dataset* D on both sides of this equation.

$$\mathbb{E}_D \left[(f(x; D) - f^*(x))^2 \right] = \underbrace{\mathbb{E}_D \left[\left(\mathbb{E}_D[f(x; D)] - f^*(x) \right)^2 \right]}_{(\text{bias})^2} + \underbrace{\mathbb{E}_D \left[\left(f(x; D) - \mathbb{E}_D[f(x; D)] \right)^2 \right]}_{\text{variance}}. \quad (7.6)$$

1213 The cross-term again vanishes when we take the expectation over the dataset.
 1214 The first term is called the squared bias: it is the gap between the predictions of
 1215 our model compared to the optimal model f^* created across many experiments
 1216 each with a different dataset D . The second term is the variance and it measures
 1217 how sensitive the model $f(x; D)$ to getting a particular dataset D to train on,
 1218 if it is very sensitive a model fitted on D does not work well on most others
 1219 datasets and consequently the variance is large. We will parse these quantities
 1220 further soon.

1221 We have therefore shown that

$$R(f) = (\text{bias})^2 + \text{variance} + \text{Bayes error} \quad (7.7)$$

1222 Recall that we want to minimize the population risk $R(f)$. We cannot do much
 about the Bayes error. If the model $f(x; D)$ is large and is fitted very well

▲ Here is a good mnemonic to remember. Imagine the center of the bull's eye as the optimal classifier f^* and our darts as the model $f(x; D)$.

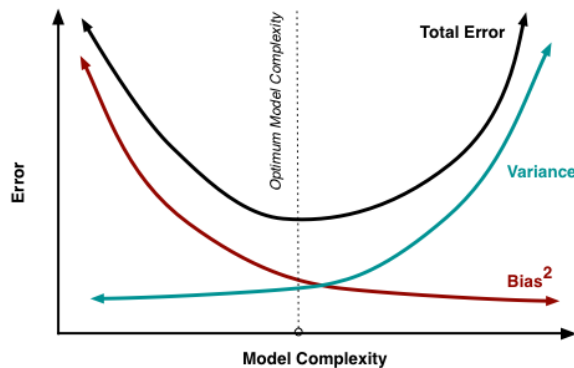
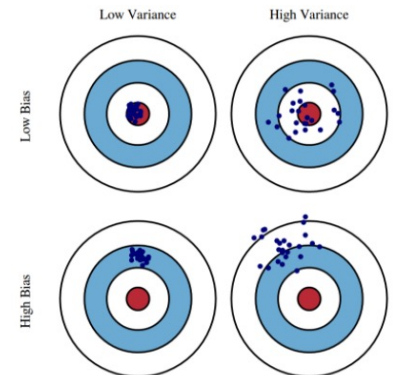


Figure 7.1: Population risk as a function of model capacity

1223 on the dataset D , i.e., if its predictions match true y (notice that the optimal
 1224 models predictions f^* are also close to y), the gap between the predictions
 1225 of the fitted model and the optimal model is small on the dataset D . In other
 1226

1227 words, if our model is large we will have a small bias. The bias of a model
 1228 decreases as we consider larger models $f(x; D)$. If our dataset is small, the
 1229 model $f(x; D)$ is likely to have a large variance because it has not seen a large
 1230 amount of data. The effect increases for larger models because they may use a
 1231 larger number of nuisances i.e., features that are not relevant to prediction of
 1232 targets. We call this over-fitting.

1233 If we plot a picture of how the bias and variance change as model capacity
 1234 (you can think of capacity simply as the number of parameters in a model for
 1235 now) increases, we see a famous U-shaped curve for the sum of squared bias
 1236 and variance shown in Figure 7.1. Given a dataset D we should pick a model
 1237 that lies at the bottom of this curve to get a good population risk; this model
 1238 makes a good tradeoff between bias and variance.

1239 The caveat is that we do not have access to a lot of different datasets to
 1240 measure the bias or the variance. This is why the bias-variance trade-off,
 1241 although fundamental in machine learning/statistics and a great thinking tool,
 1242 is of limited direct practical value.

1243 Bias-variance tradeoff for classification

1244 We have only talked about the bias-variance trade-off for regression. The
 1245 development for classification is not very different and same principles hold.
 1246 We first define an optimal classifier

$$f^*(x) = \operatorname{argmin}_{f \in \mathcal{F}} \mathbb{E}_{(x,y) \sim P} [\ell(y, f(x))]$$

1247 for a loss function ℓ . The bias, variance of a given classifier $f(x; D)$ relative
 1248 to this optimal classifier and the Bayes error are given by

$$\begin{aligned} \text{bias} &= \mathbb{E}_x [\ell(f^*(x), f(x; D))] \\ \text{variance} &= \mathbb{E}_D [\ell(f(x; D), f^{\text{avg}}(x))] \\ \text{Bayes error} &= \mathbb{E}_{(x,y) \sim P} [\ell(y, f^*(x))] \end{aligned} \quad (7.8)$$

1249 where $f^{\text{avg}}(x) = \operatorname{argmin}_f \mathbb{E}_D [\ell(y, f(x))]$; under the MSE loss this is the
 1250 average of predictions of regressors on different datasets, for the MAE loss
 1251 this is the median of the predictions of models trained on different datasets,
 1252 for the zero-one loss it is the most frequent prediction of models trained on
 1253 different datasets. We again have a trade-off that is obtained by decomposing
 1254 the population risk

$$\mathbb{E}_{(x,y) \sim P} \left[\mathbb{E}_D [\ell(y, f(x; D))] \right] = \text{bias} + c_2 \text{variance} + c_1 \text{Bayes error}.$$

1255 where c_1, c_2 are constants. You can read more about this in [Pedro \(2000\)](#).

1256 Double-descent

1257 The surprising thing is that for deep networks, we do not see this classical
 1258 bias-variance trade-off. The population risk looks like

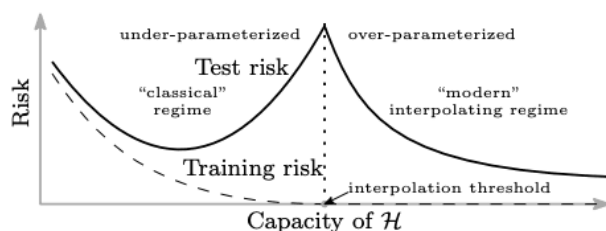


Figure 7.2: Double-descent curve: the validation error of deep networks decreases even if more and more complex models are fitted on the same data; there is no apparent over-fitting and growth in the variance of the classifier.

1259 in what is now called the “double-descent” curve. The population risk of
 1260 deep networks keeps decreasing even if we fit very large models on relatively
 1261 small datasets, e.g., CIFAR-10 has 50,000 images, the model you will fit in
 1262 HW 2 has about 1.6M weights and is considered a very small model by today’s
 1263 standards. We will see some heuristic derivation into why the population
 1264 risk may look like this for deep networks but understanding this phenomenon
 1265 which goes flat against established knowledge in machine learning is one of
 1266 the big open problems in the study of deep networks today.

1267 7.1.1 Cross-Validation

1268 We have seen that the bias-variance trade-off requires us to consider multiple
 1269 datasets. In practice, we only have *one* dataset that we collected by running an
 1270 experiment. If this data is large, we can split it into two three parts

$$\text{data} = \text{training set} \cup \text{validation set} \cup \text{test set}.$$

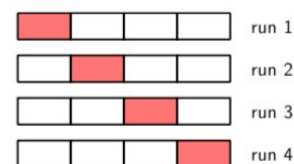
1271 The validation set is used to compare multiple models that we fit on the training
 1272 set and pick the best performing one. This model is then run on the test set
 1273 to demonstrate how well we have learned the data. The test set is necessary
 1274 because across your design efforts to fit different models, you will evaluate
 1275 on the validation set multiple times and this may lead to over-fitting on the
 1276 validation set.

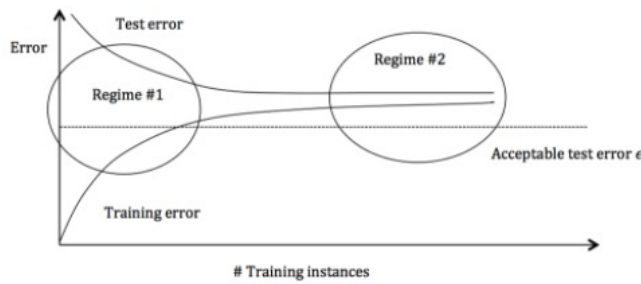
1277 If the available data is not a lot, we want to use as much of the data as
 1278 possible for training. If however only use a small fixed validation set for
 1279 comparing models, we risk making mistakes in our choices. Cross-validation
 1280 is a solution to this problem: it trains k different models, each time a fraction
 1281 $(k - 1)/k$ of the data is used as the training set and the remainder is used as
 1282 the validation set. The validation performance of k models obtained by this
 1283 process is averaged and used as a score to evaluate a particular model design
 1284 (architecture, hyper-parameters etc).

1285 Some practical tips

1286 It is useful to think of the bias-variance trade-off when you fit deep networks
 1287 in practice. If the training or test error is high, there are a number of ways to
 1288 improve performance using the bias-variance tradeoff as a thinking tool.

▲ 4-fold cross-validation.





1289

1290 In the first regime on the left, we have high validation error across cross-
 1291 validation folds and low training error. This indicates that we have a high
 1292 variance in the bias-variance trade-off. Typical techniques to counter this is to
 1293 use a smaller model, get more data, or bagging a set of models together (will
 1294 cover this in Section 7.3). In the second regime on the right, if the test error
 1295 *and* the training error are close to each other but both are large, the model is
 1296 likely to have high bias. In these cases, we should fit a more complex model
 1297 (say increase the number of weights, or pick a different architecture), add
 1298 more features to the training data (in the non-deep-learning setting) to give our
 1299 model more discriminative features to use, or use boosting (we will cover this
 1300 in Section 7.3).

1301 Cautionary Tale

1302 You will however notice that a lot of research papers in deep learning simply
 1303 use validation data as test data. Their reasons for doing so are as follows.
 1304 All researchers have the same large dataset from which they would create a
 1305 potential test set, the researchers therefore also know the ground-truth labels of
 1306 test images and it is difficult to trust them not to peek at the ground-truth labels
 1307 to choose between models. If the test data is hidden from everyone, we need a
 1308 centralized server for evaluating everyone's results. This is difficult because
 1309 research is fundamentally about discovering new knowledge. Kaggle competi-
 1310 tions or the ImageNet Challenge <http://image-net.org/challenges/LSVRC> are
 1311 few instances where such a centralized server is available.

1312 It is therefore debatable whether the current practice of using validation set
 1313 as the test set should be considered valid. On the positive side, it makes results
 1314 across different publications comparable to each other; if everyone reports the
 1315 error of their model on the same validation set, it is easy to compare Algorithm
 1316 A versus Algorithm B. On the negative side, this incentivizes extensive hyper-
 1317 parameter tuning and risks results that are over-fitted on the validation data,
 1318 e.g., new fields such as neural architecture search are particularly problematic
 1319 in this context. This is also the main reason for the current “style of research”
 1320 where folks judge the merit of machine learning research simply by checking
 1321 whether Algorithm A gets better validation error than Algorithm B on standard
 1322 datasets. This is not the correct way to do scientific research. The more
 1323 appropriate way to instantiate the scientific method is to first formulate a
 1324 hypothesis, e.g., is gene X correlated with cancer Y, then collect data that
 1325 allows us to evaluate such an hypothesis and undertake appropriate statistical
 1326 precautions report whether the hypothesis stands/does not stand.

1327 That said, there are researchers who have evaluated others' claims (ob-
 1328 tained using validation data, namely A better than B) on independent test data

1329 and reached similar conclusions, see for example <https://arxiv.org/abs/1902.10811>,
1330 so the evaluation methodology is broken but the progress is real.

1331 7.2 Weight Decay

1332 The set of models with smaller complexity are a subset of the set of models
1333 with larger complexity, e.g., if you are fitting a polynomial regression, you can
1334 consider the subset of models with coefficients of the higher-order terms equal
1335 to zero and have thus created the set linear regressors. Effectively, the space of
1336 *models* looks as follows.

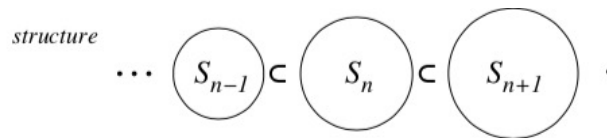


Figure 7.3: A cartoon of the space of models. The n in the picture refers to number of parameters in the model, not the number of data.

1337 Let's say we are fitting a class of models with large complexity and are
1338 unsure whether the variance in the bias-variance trade-off will be large. We
1339 can either collect more data, or we can modify the loss function to encourage
1340 the training process to pick models of lower complexity.

Restricting the space of models that the training process searches over to fit the data is called *regularization*. We will denote regularizers by

$$\text{regularizer} = \Omega(w)$$

and modify our loss function for fitting data to be

$$\ell'(w; x, y) := \ell(w; x, y) + \Omega(w).$$

1341 Weight decay is one of the simplest regularization techniques and uses

$$\Omega(w) = \frac{\alpha}{2} \|w\|_2^2. \quad (7.9)$$

1342 This is more widely known as ℓ_2 regularization because we use the ℓ_2 norm
1343 of the weights as the regularizer. It is also called Tikonov regularization, a
1344 name that comes from the literature on partial differential equations. The name
1345 weight decay comes from the neural networks literature of the 1980s. The
1346 gradient of the modified loss is

$$\nabla \ell'(w; x, y) = \nabla \ell(w; x, y) + \alpha w,$$

1347 which gives

$$w^{t+1} = (1 - \eta \alpha) w^t - \eta \nabla \ell(w^t; x, y);$$

1348 where η is the learning rate. In other words the weights w are encouraged
1349 to become smaller in magnitude when SGD takes a step using the negative
1350 gradient.

1351 If we have a linear regression problem with $f(x; w) = w^\top x$ and X, Y are
 1352 the matrices for the data and targets respectively, the regularized objective is

$$\frac{1}{2} \|Y - Xw\|_2^2 + \frac{\alpha}{2} \|w\|^2$$

1353 and you can compute the minimizer by taking derivatives and setting them to
 1354 zero to be

$$w^* = (X^\top X + \alpha I)^{-1} X^\top Y.$$

1355 In other words, weight decay for linear regression adds elements to the diagonal
 1356 of the data covariance matrix $X^\top X$. This results in a smaller inverse and
 1357 thereby a smaller magnitude of w^* . Notice that if the covariance matrix
 1358 is rank deficient, the regularized matrix is no longer rank deficient. If the
 1359 covariance matrix has a large condition number (ratio of the largest and
 1360 smaller eigenvalue), which makes taking the inverse numerically difficult, the
 1361 regularized matrix has a better condition number.

1362 7.2.1 Do not do weight decay on biases

1363 If the input data and targets in linear regression are centered we do not need a
 1364 bias parameter in our model. Notice however that if the dataset is not centered,
 1365 the bias parameter is essential. Should we perform weight decay on the bias
 1366 parameter in this case? The weight decay penalty prevents the bias parameter
 1367 to adapt to the non-zero mean of the data. This is also important to keep in
 1368 mind while training neural networks. We should not impose weight decay
 1369 regularization on the bias parameters of the convolutional and fully-connected
 1370 layers.

▲ Weight decay is closely related to other norm-based penalties, e.g., ℓ_1 regularization sets

$$\Omega_{\ell_1}(w) = \alpha \|w\|_1.$$

As we discussed briefly in Chapter 6, such a regularizer encourages the weights to become sparse. Sparsity penalties are very common in the signal processing literature (e.g., compressed sensing, phase retrieval problems) but they are less common in the deep learning literature.

1371 7.2.2 Maximum a posteriori (MAP) Estimation

1372 MAP estimation gives a Bayesian perspective to regularization in machine
 1373 learning. In maximum likelihood (ML) estimation, we were interested in
 1374 solving for weights that maximize the likelihood of the observed data:

$$w_{\text{MLE}}^* = \underset{w}{\operatorname{argmin}} -\frac{1}{n} \sum_{i=1}^n \log p_w(y^i | x^i; w).$$

1375 MAP estimation enforces some prior knowledge we may have about the
 1376 weights w . In Bayesian statistics, such prior knowledge is represented as a
 1377 probability distribution, known as the *prior*, on the parameters w *before we*
 1378 *see any data in the training process*, i.e., *a priori probability*

$$\text{prior} = p(w)$$

1379 MAP estimation is regularized ML estimation. Given a prior distribution,
 1380 we can use Bayes law to find the *posterior distribution* on the weights after
 1381 observing the data

$$p(w|D) = \frac{p(D|w) p(w)}{p(D)} \quad (7.10)$$

1382 Remember that the left hand side is a legitimate probability distribution with
1383 the denominator given by

$$Z := p(D) = \int p(D|w) p(w) dw.$$

1384 The denominator Z called the “evidence” or the partition function lies at the
1385 heart of all statistics, we will see why in Module 4.

1386 MAP estimation finds the weights that maximize this *a posteriori* proba-
1387 bility

$$\begin{aligned} w_{\text{MAP}}^* &= \underset{w}{\operatorname{argmax}} \{ \log p(D; w) + \log p(w) \} \\ &= -\frac{1}{n} \sum_{i=1}^n \log p_w(y^i | x^i; w) + \Omega(w) + \log Z(D) \\ &= -\frac{1}{n} \sum_{i=1}^n \log p_w(y^i | x^i; w) + \Omega(w). \end{aligned} \quad (7.11)$$

1388 In the second step, we have denoted the log-prior by Ω

$$\log \text{prior}(w) := \Omega(w).$$

1389 The final step follows because $Z(D)$ is not a function of the weights w and
1390 can therefore can be ignored in the optimization.

1391 Frequentist vs. Bayesian point of view

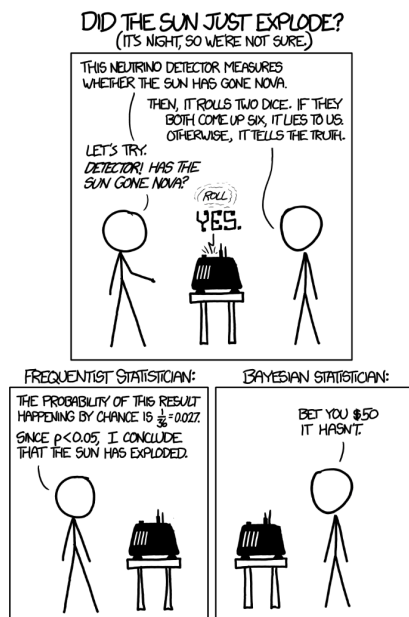
1392 This section was our first view into Bayesian probabilities, as opposed to
1393 frequentist methods where we estimate probabilities by counting how many
1394 times a certain event occurs across our experiments. Frequentist probabilities
1395 are not designed to handle all situations. For instance we may be interested in
1396 estimating the probability of a very unlikely event, say that of the sun going
1397 supernova. This event has of course not happened yet and a frequentist notion
1398 of probability where we repeat the experiment many times and estimate the
1399 probability as the fraction of times the event occurs is not appropriate. The
1400 Bayesian point of view provides a natural way to answer these questions and
1401 the key idea is to encode our belief that the sun cannot go supernova as a prior
1402 probability.

1403 An alternate way to think about this is that the weights w of a model are
1404 considered a fixed quantity that we are supposed to estimate in a frequentist
1405 setting. The likelihood $p(D; w)$ is used to compare different models w and if
1406 one wanted an estimate of how much error we are making in our estimate, we
1407 would compute the variance in the Bias-variance tradeoff namely, the variance
1408 of our estimate across different draws of the dataset D . In the Bayesian point
1409 of view, there is a single dataset D and the uncertainty of our estimate of w^*
1410 would be expressed as the variance of the posterior distribution $p(w|D)$ in
1411 Bayes law.

1412 Weight decay regularization is MAP estimation with Gaussian prior

1413 Weight decay can be seen as using a Gaussian prior

$$p_{\text{weight-decay}}(w) \propto e^{-\frac{\|w\|_2^2}{(2\alpha-1)}}.$$



1414 This is a multi-variate Gaussian distribution with mean zero and a diagonal
 1415 covariance matrix with α^{-1} on the diagonal. The denominator is a function of
 1416 α^{-1} and we do not need to worry about it while performing MAP estimation
 1417 because it does not depend on w .

1418 In other words, we have seen that weight decay in the training objective
 1419 can be thought of as a MAP estimation using a Gaussian prior instead of ML
 1420 estimation.

1421 The Gaussian prior captures our a priori estimate of the true weights:
 1422 the probability of the weights w being large is low (it is distributed as a
 1423 Gaussian/Normal distribution). The likelihood term fits the weights to the
 1424 data but instead of relying completely on the data which may result in a large
 1425 variance (in cases when data is few), we also rely on the prior while fitting the
 1426 model. This reasoning is captured in Bayes law.

1427 Similarly, a sparsity penalty is MAP estimation with a Laplace prior For
 1428 scalar random variables, the Laplace distribution is given by

$$p(w) = \frac{1}{2b} e^{-\frac{|x-\mu|}{b}}.$$

1429 If we have

$$\Omega(w) = \|w\|_1$$

1430 we can see that regularized ML, i.e., MAP estimation corresponds to using a
 1431 Laplace prior on the weights w .

1432 7.3 Dropout

1433 We will next look at a very peculiar regularization technique that is unique to
 1434 deep networks. Consider a two-layer network given by

$$\hat{y} = v^\top \text{dropout}(\sigma(S^\top x)).$$

1435 Dropout is an operation that is defined as

$$\text{dropout}_{1-p}(h) = h \odot r \tag{7.12}$$

1436 where $r \in \{0, 1\}^p$ is a binary mask and the notation \odot denotes element
 1437 multiplication. Each element of this mask r_k is a Bernoulli random variable
 1438 with probability $1 - p$

$$r_k = \begin{cases} 0 & \text{with probability } p \\ 1 & \text{with probability } 1 - p. \end{cases}$$

1439 In simple words, dropout takes the input activations h and zeros out a random
 1440 subset of these; on an average p fraction of the activations are set to zero and
 1441 the rest are kept to their original values. In pictures, it looks as follows.

▲ It is important to remember that a new dropout mask r is chosen for every input in the mini-batch.

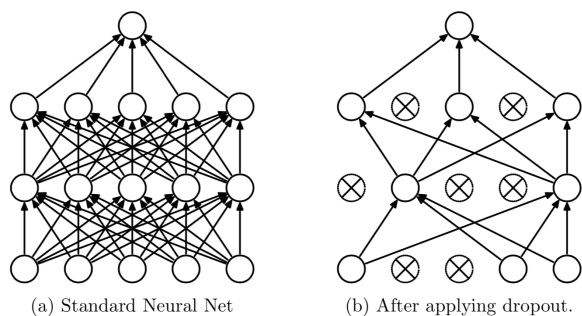


Figure 7.4: Dropout picks a random sparse subnetwork of a large deep network using the mask.

1442 The default Dropout probability is $p = 0.5$ in PyTorch, i.e., about half of
 1443 the activations are set to zero for each input. Although you will see a lot of
 1444 online code and architectures with this default value, you should experiment
 1445 with the value of p , different values often given drastically different training
 1446 and validation errors.

1447 7.3.1 Bagging classifiers

1448 Bagging, which is short for *bootstrap aggregation*, can be explained using
 1449 a simple experiment. Suppose we wanted to estimate the average height μ
 1450 of people in the world. We can measure the height of N individuals and
 1451 obtain *one* estimate of the mean μ . This is of course unsatisfying because
 1452 we know that our answer is unlikely to be the mean of the entire population.
 1453 Bootstrapping computes multiple estimates of the mean μ_k over many *subsets*
 1454 of the data N and reports the answer as

$$\mu := \text{mean}(\mu_k) + \text{stddev}(\mu_k).$$

1455 Each subset of the data is created by sampling the original data with N samples
 1456 *with replacement*. This is among the most influential ideas in statistics (Efron,
 1457 1992) because it is a very simple and general procedure to obtain the uncer-
 1458 tainty of the estimate.

1459 Effectively, the standard deviation of our new bootstrapped estimate of
 1460 the mean is simply the standard deviation in the Bias-Variance trade-off with
 1461 the big difference that we created multiple datasets D by sub-sampling with
 1462 replacement of the original dataset.

1463 Bagging is a classical technique in machine learning (Breiman, 1996) that
 1464 trains multiple predictive models $f(x; w^k)$ for $k \in \{1, \dots, M\}$, one each for
 1465 bootstrapped versions of the training dataset $\{D^1, \dots, D^M\}$. We aggregate
 1466 the outputs of all these models together to form a *committee*

$$f(x; w^1, \dots, w^M) = \frac{1}{M} \sum_{k=1}^M f(x; w^k).$$

1467 You can see that this procedure reduces the sum of the squared-bias and
 1468 variance of the model (the first term in (7.4)) in the bias-variance trade-off by

❓ The dropout mask is chosen at random for each image. Let us imagine that we have one dropout layer after every fully-connected layer. For the network shown in the figure with two hidden layers and 5 neurons at each layer, how many distinct sparse networks could be chosen for each input if $p = 0.5$?

1469 a factor of M if the errors with respect to the optimal classifier f^* of all the
 1470 models $\{w^k\}$ are zero-mean and uncorrelated. In other words, the average
 1471 error of a model can be reduced by a factor of M by simply averaging M
 1472 versions of the model.

1473 Bagging is always a good idea to keep in your mind. The winners
 1474 of most high-profile machine learning competitions, e.g., the Netflix Prize
 1475 (https://en.wikipedia.org/wiki/Netflix_Prize) or the ImageNet challenge, have
 1476 been bagged classifiers created by fitting multiple architectures on the same
 1477 dataset. Even today, random forests are among the most popular algorithms
 1478 in the industry; these are ensembles of hundreds of models called decision
 1479 trees on bootstrapped versions of data. A lot of times, if we are combining
 1480 diverse architectures in to the committee, we do not even need to bootstrap the
 1481 data. Bagging does not work when the errors of the different models are not
 1482 uncorrelated; this is however easy to fix by censoring out features in addition
 1483 to bootstrapping like it is done while training a random forests.

1484 7.3.2 Some insight into how dropout works

1485 Consider the following, very heuristic but nevertheless beautiful, argument in
 1486 the original paper on dropout (Srivastava et al., 2014).

1487 We will remove the nonlinearities and consider only a single layer linear
 1488 model with dropout directly applied to the input layer $f(x; v) = v^\top \text{dropout}(x)$.
 1489 Linear regression minimize the objective $\|y - Xw\|_2^2$ and similarly the dropout
 1490 version of linear regression for our model would minimize

$$\min_w \mathbb{E}_R [\|y - (R \odot X)w\|_2^2] \quad (7.13)$$

1491 where each row of the matrix R consist of the dropout mask for the i^{th} row x^i of
 1492 the data matrix X . Think carefully about the expectation over R on the outside,
 1493 since we choose a random dropout mask each time an input is presented to
 1494 SGD, the correct way to write dropout is using this expectation over the masks.
 1495 Each entry of R is a Bernoulli random variable with probability $1 - p$ of being
 1496 1. Note that

$$\mathbb{E}_R [R \odot X] = (1 - p)X$$

1497 and the $(ij)^{\text{th}}$ element is

$$\left(\mathbb{E}_R [(R \odot X)^\top (R \odot X)] \right)_{ij} = \begin{cases} (1 - p)^2 (X^\top X)_{ij} & \text{if } i \neq j \\ (1 - p) (X^\top X)_{ii} & \text{else.} \end{cases}$$

1498 We can use these two expressions to compute the objective in (7.13) to be

$$\mathbb{E}_R [\|y - (R \odot X)w\|_2^2] = \|y - (1 - p)Xw\|_2^2 + \underbrace{p(1 - p)w^\top \text{diag}(X^\top X)w}_{\Omega(w)}$$

1499 In other words, for linear regression, dropout is equivalent to weight-decay
 1500 where the coefficient α in (7.9) depends on the diagonal of the data covariance
 1501 and is different for different weights. If a particular data dimension varies a
 1502 lot, i.e., $(X^\top X)_{ii}$ is large, dropout tries to squeeze its weight to zero. We can
 1503 also absorb the factor of $1 - p$ into the weights w to get

$$\mathbb{E}_R [\|y - (R \odot X)w\|_2^2] = \|y - X\tilde{w}\|_2^2 + \underbrace{\left(\frac{p}{1 - p} \right) \tilde{w}^\top \text{diag}(X^\top X)\tilde{w}}_{\Omega(\tilde{w})} \quad (7.14)$$

1504 where $\tilde{w} = (1 - p)w$. This makes the regularization more explicit, if $p \approx 0$,
 1505 most activations are retained by the mask and regularization is small.

1506 Next, bagging provides a very intuitive understanding of how dropout
 1507 works in a deep network at test time. We now write out the classifier explicitly
 1508 as

$$f(x; w, r^k) = \sum_{i=1}^d w_i (x_i \odot r_i^k);$$

1509 note that the mask r^k is not a parameter of the model, we have simply chosen to
 1510 make it more explicit for the sequel. We now imagine each mask as creating a
 1511 *bootstrapped* version of the model; different masks r^k give different classifiers
 1512 even if the weights v and the input x is the same for all.

1513 It is important to realize that there is no subsampling of training dataset
 1514 happening here like classical boosting; we are instead forming multiple models
 1515 by adding randomness to how the input is propagating through the deep
 1516 network. For a linear classifier this is equivalent because

$$\sum_{i=1}^d w_i (x_i \odot r_i^k) = \sum_{i=1}^d (w_i \odot r_i^k) x_k =: f(x; w^k);$$

1517 we can either mask out the input or mask the weights and think of the masked
 1518 weights w^k as a new model.

1519 **Remark 7.1.** You will often see folks in the literature say that dropout regular-
 1520 izes by preventing co-adaptation of the neurons at each hidden layer. The moti-
 1521 vation for this statement is that the weights of the succeeding layer cannot fixate
 1522 too much upon a particular feature at the input because the feature can be ze-
 1523 roed out by the dropout mask. This prevents too much specialization of neurons
 1524 in the hidden layer and ensures that the prediction is made using a large number
 1525 of diverse features, not just a few specific ones. This is not a rigorous argument
 1526 but it is a reasonable argument in view of the experiments of Hubel and Wiesel
 1527 (see http://centennial.rucars.org/index.php?page=Neural_Basis_Visual_Perception).
 1528 The human brain is robust to large parts of it going missing/inhibited.

1529 Bagging is expensive at test time, it involves having to compute the predic-
 1530 tions of all the models in the committee. In the case of dropout, in this linear
 1531 heuristic argument, we can compute the committee prediction to be

$$\begin{aligned} f(x; w) &= \frac{1}{M} \sum_{k=1}^M \sum_{i=1}^d (w_i \odot r_i^k) x_k \\ &= \sum_{i=1}^d \left(w_i \odot \frac{1}{M} \sum_{k=1}^M r_i^k \right) x_k \\ &\approx \sum_{i=1}^d (w_i \odot (1 - p)) x_k. \end{aligned} \quad (7.15)$$

1532 This is very fortunate, it indicates that given weights w of a model trained
 1533 using dropout, we can compute the *committee average* over models created
 1534 using dropout masks simply by scaling the weights by a factor $1 - p$. This
 1535 should not be surprising, after all the equivalent training objective in (7.14)

▲ Training with dropout is equivalent to introducing weight decay on the weights. Remember however that this argument is only rigorous for linear regression models (the derivation essentially remains the same for matrix factorization). This connection of dropout with weight decay will also be apparent in Module 4 when we look at how to train a Bayesian deep network.

1536 has $\tilde{w} = (1 - p)w$ as the effective weights of the weights. Another important
 1537 point to note is that there is no masking of activations at test time.

1538 Although the argument in this section works only for linear models, we
 1539 will bravely extend the intuition to deep networks.

1540 7.3.3 Implementation details of dropout

1541 The recipe for using dropout is simple: (i) the activations at the input of each
 1542 dropout layer are zeroed out using a Bernoulli random variable of probability
 1543 $1 - p$ (the PyTorch layer takes the probability of zeroing out activations as
 1544 argument which is p in our derivations; (ii) at test time, the weights of layers
 1545 immediately preceding dropout are scaled by a factor of $1 - p$ to compute the
 1546 predictions of the “committee”.

1547 **Inverted Dropout.** It is cumbersome to remember the parameter p that was
 1548 used for training at test time. Deep learning libraries use a clever trick: they
 1549 simply scale the output activations of dropout layer by $1/(1-p)$ during training.
 1550 Training or testing the modified model using dropout gives an extra factor of
 1551 $(1 - p)$ like (7.14) and (7.15) respectively and therefore the final model can be
 1552 used as is without any further scaling of the weights or activations.

1553 The operation `model.train()` in PyTorch sets the model in the training
 1554 mode. This is a null-operation and does not do anything for fully-connected,
 1555 convolutional, softmax etc. layers. For the dropout later, it sets a boolean
 1556 variable in the layer that samples the Bernoulli mask for all the input activations
 1557 and scales the output activations by $1/(1 - p)$. The complementary operation
 1558 is `model.eval()` in PyTorch which you should use to set the model in
 1559 evaluation mode. This is again a null-operation for other layers but for the
 1560 dropout layer, it resets this boolean variable to indicate that no Bernoulli masks
 1561 should be sampled and no masking should be performed.

1562 7.3.4 Using dropout as a heuristic estimate of uncertainty

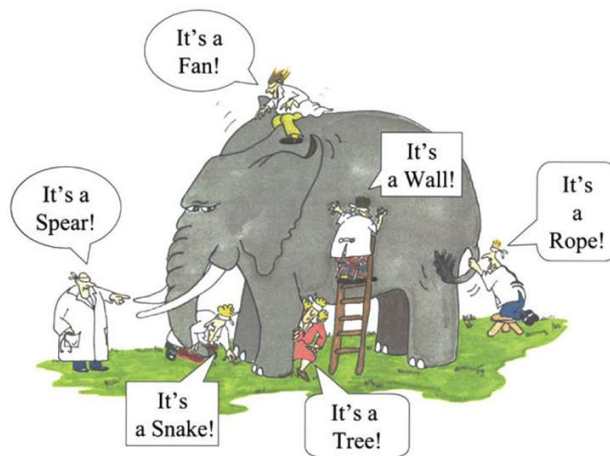
1563 We can extend the motivation from bagging to use dropout as a cheap heuristic
 1564 to get an estimate of the uncertainty of the prediction at test time. Suppose
 1565 we use dropout at test time just like we do it at training time, i.e., each time
 1566 one test input is presented to the deep network, we sample multiple Bernoulli
 1567 masks r^1, \dots, r^M and compute multiple predictions for the same test input

$$\{f(x; w, r^1), \dots, f(x; w, r^M)\}.$$

1568 The variance of these predictions can be used as heuristic of the uncertainty
 1569 of the deep network while making predictions on the test input x . This is an
 1570 estimate of the so-called *aleatoric or statistical uncertainty*. It captures our
 1571 understanding that the weights w of a trained deep network are inherently
 1572 uncertain and different training experiments, in particular, different masks r^k
 1573 will give rise to different weights. The variance across a few sampled masks
 1574 thus indicates how uncertain the model is about its predictions. Dropout is a
 1575 neat and cheap trick for this purpose; it is quite commonly used in this fashion
 1576 in medical applications where it is important to not only predict the outcome
 1577 but also characterize the uncertainty of this prediction. We will see more
 1578 powerful ways to compute aleatoric uncertainty in Module 4.

1579 **Remark 7.2.** Broadly speaking, the connection of dropout with weight decay
 1580 is contentious. If it were rigorous, we should be able to get the same perfor-
 1581 mance as dropout by using appropriate weight decay (this is a good idea for
 1582 the course project!). In practice, the validation error using dropout is very
 1583 good and cannot be achieved by tweaking weight decay. Another aspect is
 1584 that since we would like to average over lots of dropout masks in the training
 1585 process, networks with dropout should be trained for many more iterations of
 1586 SGD than networks without dropout to get the same training error. The benefit
 1587 is that the test error is much better for dropout. What exactly dropout does is
 1588 a subject of some mystery and there are other alternative explanations (e.g.,
 1589 Bayesian dropout in Module 4).

1590 Our understanding of dropout is no different than that of these blind
 1591 scientists trying to identify an elephant.



1592

1593 7.4 Batch-Normalization

1594 Batch-Normalization (BN) is another layer that is very commonly used in deep
 1595 learning. BN is very popular with more than 20,000 citations in about 5 years.

Batch normalization: Accelerating deep network training by reducing internal covariate shift

[S Ioffe, C Szegedy - arXiv preprint arXiv:1502.03167, 2015 - arxiv.org](#)

Training Deep Neural Networks is complicated by the fact that the distribution of each layer's inputs changes during training, as the parameters of the previous layers change. This slows down the training by requiring lower learning rates and careful parameter initialization, and ...

☆ 99 Cited by 21278 Related articles All 32 versions Import into BibTeX 98

1596

1597 7.4.1 Covariate shift

1598 Covariate shift is a common problem with real data. The experimental con-
 1599 ditions under which training data was gathered are subtly different from the
 1600 situation in which the final model is deployed. For instance, in cancer diagno-
 1601 sis the training set may have an over-abundance of diseased patients, often of
 1602 a specific subtype endemic in the location where the data was gathered. The
 1603 model may be deployed in another part of the world where this subtype of
 1604 cancer is not that common.

1605 The mis-match between training and test *data* distribution is called covariate
 1606 shift. Even if the labels depend on some known way $y|x$ on the covariates,

1607 i.e., given the genetic features of a person x their likelihood of a cancer y is
 1608 the same regardless of which part of the world the person is from, the fact that
 1609 we do not have training data from the entire population of the world forces the
 1610 classifier to be tested on a data distribution that is different from what it was
 1611 trained for.

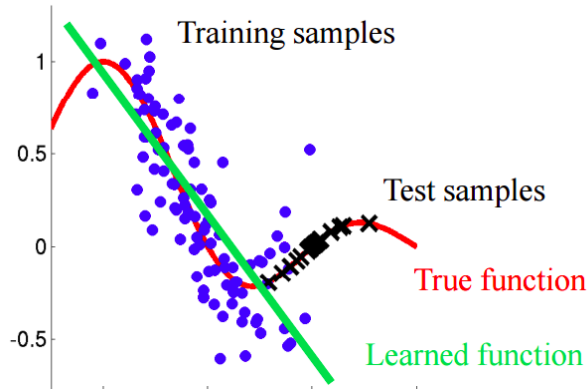


Figure 7.5: Covariate shift correction for a regression problem

1612 Covariate shift is outside our fundamental assumption in Chapter 1 that
 1613 training and test data come from the same distribution. It is however a problem
 1614 that is often seen in practice and typical ways to counter it basically look as
 1615 follows.

- 1616 1. Train a classifier \hat{w} on the available training data D .
- 1617 2. Update the trained classifier using data from the test distribution $D' =$
 1618 $\{(x^i, y^i)\}_{i=n+1, \dots, n+m}$ in addition to the original training dataset

$$w^* = \operatorname{argmin}_w \frac{1}{n+m} \sum_{i=1}^{n+m} p^i \ell^i(w) + \Omega(w - \hat{w}) \quad (7.16)$$

1619 where p^i is some weighing factor that indicates how similar the datum
 1620 (x^i, y^i) is to the *test data distribution*. The regularization $\Omega(w - w^*)$
 1621 forces the new weights w^* to remain close to the old weights \hat{w} .

1622 The above methods go under the umbrella of *doubly robust estimation*. We
 1623 will not study it in this course. The results look similar to the ones shown
 1624 in Figure 7.5.

1625 7.4.2 Internal covariate shift

1626 If we are working under the standard machine learning assumption of test
 1627 data drawn from the same distribution as the training data, then there is no
 1628 covariate shift.

1629 Recall that we whiten the inputs, say using Principal Component Analysis
 1630 (PCA), for linear regression in order to decorrelate the input features; you can
 1631 using a simple argument of how this changes the condition number of the data

1632 covariance matrix $X^\top X$ and accelerates the convergence of gradient descent
 1633 using a calculation similar to the final problem in HW 2.

1634 Deep networks are like any other model in this aspect and whitening of
 1635 the inputs is also beneficial; the ZCA transform (or Mahalanobis whitening)
 1636 is a close cousin of PCA and usually works better for image-based data. It is
 1637 natural to expect that since each layer of a deep network takes the activations
 1638 of the preceding layer as input, we should whiten the activations before the
 1639 computation in the layer. The authors of the BN paper came upon an interesting
 1640 through what is clearly a mistake. Their reasoning was based on a simple
 1641 example: if we have a mini-batch of inputs $\{x^1, \dots, x^6\}$ and our layer simply
 1642 adds a learnable bias b to this

$$h = x + b.$$

1643 If this layer whitens its output before passing it on to the next layer, we will
 1644 have

$$\hat{h} := h - \frac{1}{6} \sum_{i=1}^6 x^i.$$

1645 The output \hat{h} does not depend on the bias b . They argued, incorrectly, that the
 1646 back-propagation update of the bias \bar{b} is equal to $\bar{\hat{h}}$. This is not true of course
 1647 because

$$\bar{b} = \bar{\hat{h}} \frac{d\hat{h}}{db} = 0$$

1648 in our notation where $\bar{h} = d\ell/dh$. Nevertheless the motivation of the batch-
 1649 normalization operation is sound, we would like to whiten the input activations
 1650 to each layer of a deep network.

Batch-Normalization is a technique for whitening the output activations of each layer in a deep network.

1651 Naively, this would involve computing expressions of the form

$$\hat{h} = (\text{Cov}(h))^{-1/2} \left(h - \frac{1}{6} \sum_{i=1}^6 h^i \right).$$

1652 This is not easy to do because the features are high-dimensional vectors, the
 1653 covariance matrix $\text{Cov}(h)$ is a very large matrix. This makes computing \hat{h}
 1654 difficult for every mini-batch. Nevertheless, whitening helps and here is how
 1655 it is done in the batch-normalization module:

$$\hat{h} = \frac{h - \mathbb{E}(\{h^1, \dots, h^6\})}{\sqrt{\text{Var}(\{h^1, \dots, h^6\}) + \epsilon}}. \quad (7.17)$$

1656 The constant ϵ in the denominator prevents \hat{h} from becoming very large in
 1657 magnitude if the variance is small for a particular mini-batch. It is important
 1658 to note that both the expectation and the variance are computed for every
 1659 feature. Let us make this clear: if $h \in \mathbb{R}^{6 \times p}$, i.e., p features for this layer,

▲ This is the mistake in the original BN paper.

the training set, and $\mathbb{E}[x] = \frac{1}{N} \sum_{i=1}^N x_i$. If a gradient descent step ignores the dependence of $\mathbb{E}[x]$ on b , then it will update $b \leftarrow b + \Delta b$, where $\Delta b \propto -\partial\ell/\partial\hat{x}$. Then $u + (b + \Delta b) - \mathbb{E}[u + (b + \Delta b)] = u + b - \mathbb{E}[u + b]$.

1660 the $i^{\text{th}} \in \{1, \dots, \ell\}$ input of the mini-batch and the $j^{\text{th}} \in \{1, \dots, p\}$ of the
 1661 feature for \hat{h} is given by

$$\hat{h}_{ij} = \frac{\hat{h}_{ij} - \frac{1}{\ell} \sum_{i=1}^{\ell} h_{ij}}{\sqrt{\text{Var}(\{h_{1j}, h_{2j}, \dots, h_{\ell j}\})}}.$$

1662 Let us give names to these parameters

$$\begin{aligned} \mathbb{R}^p \ni \mu &= \mathbb{E}(\{h^1, \dots, h^\ell\}) \\ \mathbb{R}^p \ni \sigma^2 &= \text{Var}(\{h^1, \dots, h^\ell\}). \end{aligned} \quad (7.18)$$

1663 The authors of the original BN paper decided that mere normalization may not
 1664 be enough, e.g., if you normalize the activations *after a sigmoid activation*,
 1665 the layer may essentially become linear because the activations are prevented
 1666 from going too far to the right or too far too the left of the origin. This brings
 1667 the second key idea in BN, that of affine scaling of the output \hat{h} . The BN layer
 1668 really implements two

$$\hat{h} = a \left(\frac{h - \mathbb{E}(\{h^1, \dots, h^\ell\})}{\sqrt{\text{Var}(\{h^1, \dots, h^\ell\}) + \epsilon}} \right) + b. \quad (7.19)$$

1669 where $a, b \in \mathbb{R}^p$, i.e., each feature has its own multiplier a and bias b . The
 1670 final BN operation in short is therefore

$$\hat{h} = a \left(\frac{h - \mu}{\sqrt{\sigma^2 + \epsilon}} \right) + b.$$

The affine scaling parameters a, b are the only parameters in BN that are updated using backpropagation. The mean μ and variance σ^2 are unique to every mini-batch and therefore do not have any backpropagation gradient.

Execute the following code in your Jupyter notebook and check how the BN layer is implemented in PyTorch

```
import torch.nn as nn
m = nn.BatchNorm1d(15)
print(m.weight, m.bias)
print(m.running_mean, m.running_var)
```

The weight and bias here are the affine scaling parameters; and running_mean, running_var are μ, σ^2 respectively. You will see that requires_grad is True only for the former.

1671 BN for convolutional layers

1672 The activations of a convolutional layer are a 4-dimensional matrix (or a
 1673 tensor)

$$h \in \mathbb{R}^{\ell \times c \times w \times h}.$$

1674 The distinction between convolutional layers compared to fully-connected
 1675 layers is that the convolutional filter weights are shared for the whole input
 1676 channel $w \times h$. We can therefore think of each *channel as a feature* and
 1677 compute the BN mean and standard deviation over the batch dimension, as
 1678 well as the width and height. In pseudo-code, this looks as follows.

```

1679 # t is still the incoming tensor of shape [bb, c, w, H]
1680 # but mean and stddev are computed along (0, 2, 3) axes and
1681 # have just [c] shape
1682 mean = mean(t, axis=(0, 2, 3))
1683 stddev = stddev(t, axis=(0, 2, 3))
1684 for i in 0..bb-1, x in 0..h-1, y in 0..w-1:
1685     out[i,:,x,y] = normalize(t[i,:,x,y], mean, stddev)
1686

```

1688 Running updates of the mean and variance in BN

1689 BN computes the statistics over mini-batches. Even if we trained a model
 1690 using mini-batch updates we would still like to be able to use this model at
 1691 test time with a single input; it may not always be possible to wait for a few
 1692 test images to make predictions. The weights of the network are trained to
 1693 work with whitened features so we definitely need some way to whiten the
 1694 features of a test input, ignoring the whitening at test time will result in wrong
 1695 predictions.

1696 The BN layer solves this issue by maintaining a running average of the
 1697 mean and variance statistics of mini-batches during training. Effectively, the
 1698 buffers `running_mean`, `running_var` (note that these are not parameters/weights,
 1699 they are not updated using backprop) are updated after *each mini-batch* during
 1700 training as

$$\begin{aligned} \text{running_mean}^{t+1} &= \rho \text{running_mean}^t + (1 - \rho) \mu \\ \text{running_var}^{t+1} &= \rho \text{running_var}^t + (1 - \rho) \sigma^2. \end{aligned}$$

1701 The parameter ρ is called a momentum parameter for the BN layer and makes
 1702 sure that updates to `running_mean/var` are slow and one mini-batch cannot
 1703 affect the stored value too much. Note that whitening is still performed at
 1704 training time using μ, σ^2 ; we simply record the running average in the buffers
 1705 `running_mean/var`. If `model.train()` is called, then the mini-batch statistics are
 1706 used to whiten the features. If `model.eval()` is called, then the stored buffers
 1707 `running_mean/var` are used to whiten the outputs.

1708 How is all this related to internal covariate shift?

1709 You might be surprised that nothing in this section is related to covariate shift
 1710 that we discussed at the beginning. Let us try to understand heuristically why
 1711 BN is said to help with internal covariate shift.

1712 Each layer of a deep network treats its input activations as the data and
 1713 predicts the output activations. As the weights of different layers are updated
 1714 using backprop during training, the *distribution* of input activations keeps
 1715 shifting. Effectively, each layer is constantly suffering a covariate shift because
 1716 the layers below it are updated and the weights of the top layers have to adapt
 1717 to this shifting distribution. This is what is known as *internal covariate shift*.
 1718 BN normalizes the output activations to approximately have zero mean and
 1719 unit variance and therefore reduces the internal covariate shift.

1720 7.4.3 Problems with batch-normalization

1721 There are two big problems with BN.

▲ There are many caveats with this heuristic argument. The main one is to observe that the backpropagation gradient of all layers is coupled, so it is not as if the layers are updated independently of each other and cause internal covariate shifts to the other layers; the updates of all the weights in the network are coupled and it is unclear why (or even if) internal covariate shift occurs.

- 1722 1. The affine parameters are updated using backpropagation and small
1723 changes mini-batch statistics which can result in large changes to the
1724 whitened output $(h-\mu)/\sqrt{\sigma^2 + \epsilon}$ will result in very large updates to a, b .
1725 This makes the affine parameters problematic when you train networks.
1726 In general, it is a good idea to first fit a model without the affine BN
1727 parameters, you can do so by using `affine=False` in `nn.BatchNorm1d`.
- 1728 2. The mean and variance buffers of the BN layer are updated using run-
1729 nings statistics of the per-mini-batch statistics. This does not affect
1730 training because the statistics of each mini-batch are computed inde-
1731 pendently, but it does affect evaluation because the buffers are used to
1732 whiten the features of the test input. If the test input has slightly different
1733 pixel intensity statistics than the training image, then the BN buffers are
1734 not ideal for whitening and such images are classified incorrectly.

1735 **BN before ReLU or ReLU before BN**

1736 Should we apply BN before or after the nonlinearity? The purpose of a BN
1737 layer is to keep the activations close to zero in their mean and a standard-
1738 deviation of one. Imagine if we are using a ReLU nonlinearity after BN,
1739 about half of our features h have negative values which the rectification will
1740 set to zero. In this case the distribution of features given to the next layer is
1741 not zero-mean, unit-variance so we are not achieving our goal of whitening
1742 correctly. Further, it is possible that the bias parameter b in BN is negative
1743 in which case the activations could mostly be negative and ReLU will set all
1744 of them to zero and result in a large loss in information. On the other hand,
1745 if we have BN after ReLU, the input to the BN layer has a lot of zeros and
1746 we are now computing mean/variance over a number of sparse features; the
1747 mini-batch mean/variance estimated here may not be accurate therefore BN
1748 may not perform its job of correctly whitening its outputs. You can read more
1749 about similar problems at <http://torch.ch/blog/2016/02/04/resnets.html>

1750 As you can see, BN is an incredibly intricate operation without necessarily
1751 sound theoretical foundation for all the moving parts. But it works, training
1752 a deep fully-connected network is very difficult without BN, and even for
1753 convolutional layers it often makes training insensitive to the choice of learning
1754 rate. You should think about BN very carefully in your implementations; a lot
1755 of problems of the kind, “I trained my model, it gives a good training error
1756 but very poor validation error”, or “I am fine-tuning from this task, but get
1757 very poor validation error on a new task”, or other problems in reinforcement
1758 learning, meta-learning, transfer learning etc. can be boiled down to an
1759 incorrect/inaccurate understanding of batch-normalization. This is further
1760 complicated by the interaction with other operations such as Dropout, e.g.,
1761 see <https://arxiv.org/abs/1801.05134>. Studying the effect of BN in meta-
1762 learning/transfer-learning is a good idea for a course project.

1763 **How does Dropout affect BN?**

1764 Since dropout is active during training, the buffered statistics are the running
1765 mean/variance of the dropped out activations. Dropout is not used at test time,
1766 so the test time statistics, even for the same image can be quite different. A
1767 simple way to solve this problem is to run the model in training model once
1768 on the validation set (without making weight updates using backpropagation)

1769 for the BN buffers to settle to their non-dropped out values and then compute
1770 the validation error; this usually results in a marignal improvement in the
1771 validation error.

1772 **Variants of BN**

1773 There are variants of batch-normalization that have cropped out to alleviate
1774 some of its difficulties. For instance, layer normalization
1775 (<https://arxiv.org/abs/1607.06450>) normalizes across the features instead of
1776 the mini-batch which makes it work better for small mini-batches. Another
1777 variant known as group-normalization computes the mean/variance estimate
1778 in BN across multiple partitions of the mini-batch which makes the result of
1779 group-normalization independent of the batch-size. These variants work in
1780 some cases and do not work in some cases and often the specific normalization
1781 is largely dependent on the problem domain, e.g., group normalization works
1782 better for image segmentation but layer normalization and batch-normalization
1783 do not so well there.

Chapter 8

Recurrent Architectures, Attention Mechanism

Reading

1. Goodfellow 10.1-10.3, 10.5-10.7, 10.9-10.12
2. D2L.ai book Chapters 8, 9, 10
3. Paper on long short-term memory (Hochreiter and Schmidhuber, 1997)
4. Paper on the Transformer architecture (Vaswani et al., 2017)

In this chapter we will consider data that is a function of time. Typical examples of such data are videos and sentences in written/spoken language. Some typical problems that we are interested in solving given such data are classifying the activity going on in a video, classifying the object that is being described in a sentence. We can also think of generative models for such temporal data, i.e., forecasting how the video/sentence will look like a few time-steps into the future using the approaches in this chapter.

We will look at three kinds of neural architectures, namely Recurrent Neural Networks (RNNs), and the Long Short-Term Memory (LSTM) and Attention modules, that are typically used to model such data.

8.1 Recursive updates in a Kalman filter, sufficient statistics

Consider a scalar signal in time $h_t \in \mathbb{R}$ that evolves according to some dynamics

$$h_{t+1} = ah_t + \xi_t;$$

with the scalar $a \in \mathbb{R}$ that we have modeled and the noise $\xi_t \in \mathbb{R}$ reflects our understanding that the scalar a in our model of evolution of the signal h_t may

1803 not be the same as that of Nature. We model this discrepancy by setting ξ_t to
 1804 be zero-mean Gaussian noise that is i.i.d across time

$$\xi_t \sim N(0, \sigma_\xi^2).$$

1805 Let us say that our dataset consists of observing the signal for some time
 1806 $\{x_1, x_2, \dots, x_t\}$. Think of h_t being the location of a car at time t and our
 1807 dataset being the observation of the trajectory of vehicle up to time t . Assume
 1808 that we do not observe the true trajectory of the vehicle, but observe some
 1809 noisy estimate of the state at each time

$$x_t = h_t + \nu_t$$

1810 where $\nu_t \sim N(0, \sigma_\nu^2)$ is the noise in our observation.

1811 In this section, we will estimate the true signal at the next time instant
 1812 \hat{h}_{t+1} . A good estimate is the one that minimizes the MSE loss with the true
 1813 (unknown) signal

$$\underset{\hat{h}_{t+1}}{\operatorname{argmin}} \mathbb{E}_{\xi_1, \nu_1, \dots, \xi_{t+1}, \nu_{t+1}} \left[\left(h_{t+1} - \hat{h}_{t+1} \right)^2 \mid \underbrace{x_1, \dots, x_t, x_{t+1}}_{\text{“dataset”}} \right]. \quad (8.1)$$

1814 The expectation is taken over the noise because there could be many trajectories
 1815 that the system could have taken, each corresponding to a particular realization
 1816 of the noise.

1817 Our estimate should only depend on the dataset

$$\hat{h}_{t+1} = \text{function}(x_1, \dots, x_t, x_{t+1}).$$

1818 Since predictions are likely to be required across a long range of time, we
 1819 want to construct a *recursive* update for \hat{h}_{t+1} that takes in the estimate at the
 1820 previous time-step \hat{h}_t and updates it using the most recent observation x_{t+1} .

1821 Kalman filter updates sufficient statistics

1822 Like we computed the optimal predictor in the bias-variance tradeoff for
 1823 regression as the conditional distribution of the labels given the data, it is
 1824 possible to prove that the best estimate \hat{h}_{t+1} is the conditional mean given
 1825 past data

$$\hat{h}_{t+1} = \mathbb{E}[h_{t+1} \mid x_1, x_2, \dots, x_{t+1}].$$

1826 Not surprisingly, to estimate the location of the car at time $t + 1$, you need to
 1827 watch the entire past trajectory of the car.

1828 However, surprisingly, a powerful and deep result in control theory is
 1829 that for our problem (where the model of the signal is linear with additive
 1830 Gaussian noise and our observations x_t are a linear function of h_t corrupted
 1831 with Gaussian noise) we only need to recursively update of the first two
 1832 moments of our estimate. If we have

$$\hat{h}_{t+1} = N(\mu_{t+1}, \sigma_{t+1}^2)$$

1833 where

$$\begin{aligned} \mu_{t+1} &= \mathbb{E} \left[\hat{h}_{t+1} \mid x_1, \dots, x_{t+1} \right] \\ \sigma_{t+1} &= \operatorname{var} \left(\hat{h}_{t+1} \mid x_1, \dots, x_{t+1} \right). \end{aligned} \quad (8.2)$$

▲ In machine learning parlance, this setup is called online learning where data occur sequentially one after other and you train/update the model to incorporate the latest datum; future predictions of this model are made using this updated model.

1834 and update the mean and variance recursively using their values at the previous
1835 time-step as

$$\begin{aligned}\mu_{t+1} &= \mu_t + k_t (x_{t+1} - a\hat{h}_t) \\ \sigma_{t+1} &= \sigma_t^2 (1 - k_t) \\ k_t &= \frac{a^2 \sigma_t^2 + \sigma_\nu^2}{a^2 \sigma_t^2 + \sigma_\nu^2 + \sigma_\xi^2}.\end{aligned}\tag{8.3}$$

1836 You can derive this part very easily. Show that if the objective in (8.1) was
1837 minimal at time t , then the expressions in (8.3) also minimize it at time $t + 1$.
1838 This algorithm is known as the Kalman filter is one of the most widely used
1839 algorithms for estimation of signals based on their observation. The key
1840 property to remember for us from the Kalman filter is the following.

The two quantities μ_t, σ_t capture *all* the information from the past trajectory x_1, \dots, x_t . Instead of creating our MSE estimate \hat{h}_t using the entire data as shown in (8.1), if we maintain these two quantities and recursively update them using (8.3) we obtain the best MSE estimate.

In other words, μ_t, σ_t are sufficient statistics of the data x_1, \dots, x_t for the problem of estimating the next state h_{t+1} . The notion *sufficient statistic* means that you do not need anything beyond these two to estimate any function of the data x_1, \dots, x_{t+1} . A statistic is simply any function of data, therefore a sufficient statistic is a quantity such that if you have it, you can throw away all the data without losing any information. Not all statistics are sufficient, and not all sufficient statistics look like a few moments of data; for more interesting signals the sufficient statistics are non-trivial and difficult to find.

The structure of neural architectures for sequence modeling is intimately related to the above result. Just like a CNN learns the best features that classify the input data, a recurrent model learns the best statistics of the past sequence (sufficient) that predict the future elements of the sequence.

1841 8.2 Recurrent Neural Networks (RNNs)

1842 The data to an RNN is a set of n sequences

$$D = \{(x_1^i, y_1^i), (x_2^i, y_2^i), \dots, (x_T^i, y_T^i)\}_{i=1, \dots, n}.$$

1843 Each sequence has length T and each element of the sequence $x_t^i \in \mathbb{R}^d$. There
1844 can be labels at every time-step, e.g., these labels can be, say, ground-truth
1845 annotations of the activity “playing with a basketball” going on the video at that
1846 time, or also forecasting the inputs by one (or more) time-steps $y_t^i := x_{t+1}^i$.

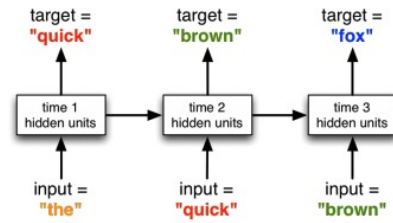


Figure 8.1: A recurrent model predicting the next word in a sentence.

1847 Focus on one particular sequence $\{(x_1, y_1), \dots, (x_T, y_T)\}$ from the dataset.
 1848 To predict the labels y_t at each time instant, the RNN would like to maintain a
 1849 statistic, let us denote it by

$$h_t^i = \varphi((x_1, y_1), \dots, (x_t, y_t)).$$

1850 where φ is some function that we would like to build. Similar to a Kalman
 1851 filter we *hope to learn* a sufficient statistic, in this case sufficiency means that
 1852 the quantity h_t can predict the target y_t . Again, we would like to update the
 1853 statistic recursively.

$$h_{t+1} = \varphi(h_t, x_{t+1}); \quad (8.4)$$

1854 notice the similarity with the updates in (8.3) where updates to μ_t, σ_t also used
 1855 the latest observation x_{t+1} . We will also have the RNN use the latest input
 1856 x_{t+1} . You can think of h_t as a summary of the past sequence or some memory
 1857 that is updated recursively. This summary/statistic is also called the “hidden
 1858 state” in the RNN literature.

1859 We do not know what function φ to pick so we are going to learn it using
 1860 parameters. We will set

$$h_{t+1} = \sigma(w_h h_t + w_x x_{t+1}); \quad (8.5)$$

1861 where $w_h \in \mathbb{R}^{p \times p}$, $w_x \in \mathbb{R}^{p \times d}$ are weights that multiply the previous statist-
 1862 ic and the current input to calculate the current statistic. Again $\sigma(\cdot)$ is a
 1863 nonlinearity that is applied element-wise.

1864 **Weights of an RNN are not a function of time.** It is important to observe
 1865 that the weights w_h, w_x do not change as the sequence moves forward. The
 1866 same function is used to update the statistic at different points of time; notice
 1867 that this does not mean that the statistic h_t^i remains the same across t . In this
 1868 sense, an RNN is effectively the same neural model unrolled into the future as
 1869 it takes in inputs of a sequence.

1870 Output predictions can now be made as usual by learning weights

$$\hat{y}_t = v^\top h_t. \quad (8.6)$$

1871 The loss function of an RNN is a sum of the error in the predictions for all
 1872 time-steps

$$\sum_{t=1}^T \ell(y_t, \hat{y}_t) \quad (8.7)$$

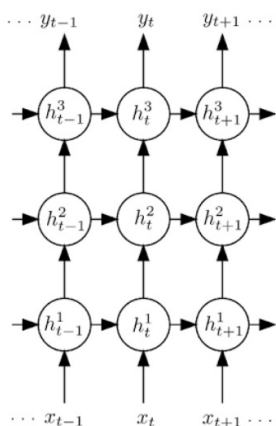
1873 and we can train the RNN by updating weights w_h, w_x using backpropagation.
 1874 In some problems, you may only have targets for the final time-step y_T (say

▲ Note that just like we cannot claim that the features learned by a CNN are sufficient features, i.e., the only information from the data necessary to predict the targets, we cannot *claim* that h_t is a sufficient statistic of the past sequence. If the RNN/CNN is making predictions accurately, then it is reasonable to expect that we have learned something close to a sufficient statistic.

1875 predicting whether it is going to rain right now or not based on the weather
 1876 data of the past few hours); this does not change much conceptually, we will
 1877 simply have only one term in the summation of the loss above.

1878 Multi-layer RNNs

1879 We have created a single-layer RNN in (8.5). We can use the same idea to
 1880 create a multi-layer RNN the same way that we did for CNNs. We combine
 1881 different parts of the hidden state/statistic and use these as features. In an
 1882 RNN, it is traditional to combine the features both from the lower layer and
 1883 features from the previous time-step of the same layer. As a picture it looks as
 follows



1884

1885 We can write an expression for this as

$$h_t^{l+1} = \sigma(w_{tt} h_{t-1}^{l+1} + w_{hh} h_t^l).$$

1886 Again we have used trainable weights $w_{tt} \in \mathbb{R}^{p \times p}$ and $w_{hh} \in \mathbb{R}^{p \times p}$ to
 1887 compute the hidden state/statistic/activations of the top layer. For a multi-layer
 1888 RNN with L layers, the predictions at each time step are given by

$$\hat{y}_t = v^\top h_t^L.$$

1889 The utility of having multiple layers in an RNN is similar to that of a CNN,
 1890 more layers let us create more complex predictors than the recurrent perceptron-
 1891 style predictor in (8.6) by learning a richer set of features.

1892 8.2.1 Backpropagation in an RNN

1893 Let us see how to compute the gradient of the loss function with respect to the
 1894 weights of an RNN in order to train the model using SGD. We will consider a
 1895 sequence of two time-steps for a single-layer RNN

$$\begin{aligned} h_1 &= \sigma(ux_1) \quad \text{where we set } h_0 = 0 \\ \hat{y}_1 &= vh_1 \\ h_2 &= \sigma(ux_2 + wh_1) \\ \hat{y}_2 &= vh_2 \end{aligned} \tag{8.8}$$

🔗 How should we initialize the first hidden vector h_0 in an RNN? We have not seen any element of the sequence yet, so the value of h_0 has no meaning per se. Typically, h_0 is initialized either using Gaussian noise; it is sometimes also initialized to zeros.

1896 The weights we would like to update are u, v and w . Let us say that the loss
 1897 function is only computed at the final time-step $t = 2$ as $\ell := \ell(y_2, \hat{y}_2) =$
 1898 $\|y_2 - \hat{y}_2\|^2$. Using our notation for backpropagation we have

$$\begin{aligned} \frac{d\ell}{d\ell} &= \bar{\ell} = 1 \\ \bar{\hat{y}}_2 &= \bar{\ell} \frac{d\ell}{d\hat{y}_2} \\ &= -(y_2 - \hat{y}_2). \\ \bar{v} &= \bar{\hat{y}}_2 \frac{d\hat{y}_2}{dv} \\ &= -(y_2 - \hat{y}_2) h_2 \\ \bar{h}_2 &= \bar{\hat{y}}_2 v \\ \bar{u} &= \bar{h}_2 \sigma'(ux_2 + wh_1) x_2 \\ &\vdots \end{aligned}$$

1899 You should write down the update steps completely for an RNN making
 1900 predictions at each time-step, using the loss function

$$\ell := \|y_1 - \hat{y}_1\|^2 + \|y_2 - \hat{y}_2\|^2$$

1901 and see how the gradient of the loss at each time-step with respect to weights
 1902 “accumulates” in \bar{w}, \bar{v} and \bar{u} . Backpropagation in RNNs is also called backpropagation-
 1903 through-time (BPTT). There is nothing special going on inside BPTT, it is
 1904 simply backpropagation applied to a computational graph that is unrolled in
 1905 time.

1906 8.2.2 Handling long-term temporal dependencies

1907 Implementations of BPTT for RNNs has a number of numerical issues.

1908 Gradient vanishing

1909 Notice that the gradient

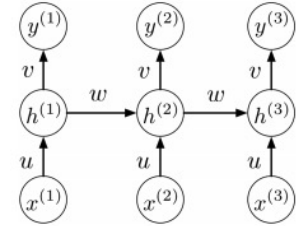
$$\begin{aligned} \bar{u} &= \bar{h}_2 \sigma'(ux_2 + wh_1) x_2 \\ &= -(y_2 - \hat{y}_2) v \sigma'(ux_2 + wh_1) x_2. \end{aligned}$$

1910 in our backprop equations depends on the gradient of non-linearity. If we have
 1911 a sigmoid non-linearity and the input activations to it $ux_2 + wh_1$ have large
 1912 magnitude, the output h_2 will be saturated. This results in \bar{u}, \bar{h}_2 having small
 1913 magnitudes. Further notice that \bar{u} also depends upon products of the weights v
 1914 and the inputs x_2 . If you unroll this further for a few more time-steps (like we
 1915 did in HW2) you will see that even future activations h_t are recursive products
 1916 of past activations with weights. It is easy to observe that if we have a matrix
 1917 A and a vector x the product

$$\lim_{k \rightarrow \infty} A^k x \tag{8.9}$$

1918 goes to zero if the largest eigenvalue of A is less than 1, i.e., $\lambda_{\max} = \|A\|_2 < 1$.
 1919 The product goes to positive/negative infinity if the largest eigenvalue is greater

▲ Computational graph of a single-layer RNN. Please ignore the notation in this figure and see (8.8).



1920 than 1 if x has a non-zero inner product with the corresponding eigenvector.
 1921 In other words, if the length of the sequence is long, the recursive computation
 1922 in an RNN entails that the activations can blow up to infinity in both cases,
 1923 this can also lead to gradient explosion; they can also become zero which can
 1924 result in gradient vanishing.

1925 The same is also true for CNNs with many layers: the weights of the lower
 1926 layers get their backprop gradient after it goes through multiple nonlinearities
 1927 (ReLU leads to saturation as well if the input is negative) and can therefore
 1928 receive a small gradient. While typical CNNs have 10 or so layers, typical
 1929 RNNs handle sequences of length 50–100 (or more). The chance of having
 1930 vanishing gradients to the weights is thus much higher in RNNs.

1931 You would think that if the objective is a sum of the loss at each time;
 1932 this alleviates the problem of gradient vanishing. But there is a deeper point
 1933 we are trying to make here. The backprop gradient is an indication of how
 1934 much we should change u, h_2 to make more accurate predictions at some
 1935 future time-step y_t . If $t \gg 2$, the value of h_2 does not play a strong role in
 1936 making predictions too far into the future. In other words, the predictions
 1937 of the RNN become myopic we do not learn statistics that are a function of
 1938 the entire past trajectory, the statistics are highly dominated by the near past
 1939 which makes it difficult to capture long-range correlations in the sequence and
 1940 predict high-level concepts.

1941 Which nonlinearities are good for RNNs?

1942 Think about which nonlinearities are good for training RNNs. Gradient vanishing
 1943 is a large problem with sigmoids whereas both gradient vanishing and
 1944 gradient explosion can occur for ReLU nonlinearities. You might be tempted
 1945 to design a nonlinearity that does not saturate on either side of the origin but
 1946 such nonlinearities look closer to and closer to an identity mapping and as we
 1947 have seen a linear model is much less powerful than a nonlinear model. In
 1948 other words, gradient explosion/vanishing is a problem in BPTT for RNNs but
 1949 there is really no effective solution to it.

1950 Gradient clipping

1951 We can avoid gradient explosion from ruining the weights being updated by
 1952 gradient descent using gradient clipping. There are many ways of implement-
 1953 ing this idea. The most prevalent one is to clip the ℓ_2 norm of the gradient to a
 1954 pre-specified value. The SGD update is modified to be

$$w^{t+1} = w^t - \eta \text{clip}_c(\nabla \ell^{\omega_t}(w^t))$$

1955 where $\nabla \ell^{\omega_t}(w^t)$ is the gradient of the objective on the sample with index
 1956 $\omega_t \in \{1, \dots, n\}$ in the dataset computed at weights ω_t and clipping performs
 1957 the operation

$$\text{clip}_c(v) = \frac{cv}{\|v\|_2 + \epsilon}$$

1958 where c is a pre-specified value and it is the ℓ_2 norm of the clipped gradient.
 1959 The scalar ϵ in the denominator prevents numerical issues when the gradient
 1960 magnitude is small.

▲ The function `clip_grad_norm` performs gradient clipping. When you observe it closely you will realize that it is really scaling the gradient and should therefore be called gradient scaling.

1961 Sometimes you instead clip the per-weight gradient at values $[-c, c]$, i.e.,
 1962 if the gradient vector is $v \in \mathbb{R}^p$ and v_k is the gradient at the k^{th} element

$$\text{clip}_c(v) = [\min(\max(-c, v_1), c), \dots, \min(\max(-c, v_p), c)].$$

1963 **Orthogonal initializations**

1964 All eigenvalues of an orthogonal matrix have an absolute value of 1. If A is an
 1965 orthogonal matrix, we have

$$A^\top A = I.$$

1966 This helps when we perform repeated multiplication with the weight matrices
 1967 in forward-backward propagation because the norm of the intermediate
 1968 products does not change

$$\|A^k x\|_2 = \|x\|$$

1969 if A is orthogonal. The weight matrices of an RNN are typically initialized
 1970 as orthogonal matrices; this is easy to do by first initializing the matrix using
 1971 random Gaussian entries as usual and then setting the actual weights to be the
 1972 left singular vectors after computing an SVD of the matrix.

🔗 If the weights of an RNN are initialized as orthogonal matrices, do they remain so all through training after multiple steps of SGD?

1973 **Moving window over the data**

1974 We wrote down SGD updates as sampling a random (input,target) pair from
 1975 the dataset at each iteration. The data for an RNN consists of a number of
 1976 trajectories/sequences. We can sample one (or a mini-batch) of such sequences
 1977 and a contiguous chunk of each of those sequences as a mini-batch in an RNN

$$\begin{aligned} D_{\text{mini-batch}} = & \{(x_1^i, y_1^i), \dots, (x_{25}^i, y_{25}^i)\} \cup \\ & \{(x_5^j, y_5^j), \dots, (x_{30}^j, y_{30}^j)\} \cup \\ & \{(x_{13}^k, y_{13}^k), \dots, (x_{38}^k, y_{38}^k)\} \cup \\ & \vdots \end{aligned}$$

1978 The hidden state h_0 of the RNN is initialized to zero/randomly at the beginning
 1979 for all these trajectories.

1980 We can also play a neat trick while sampling mini-batches in an RNN to
 1981 give it the ability to handle more long-range correlations. The mini-batch is
 1982 treated as a moving window over the data and it is rolled forward sequentially,
 1983 i.e.,

$$\begin{aligned} D_{\text{mini-batch 1}} = & \{(x_1^i, y_1^i), \dots, (x_{25}^i, y_{25}^i)\} \cup \\ & \{(x_1^j, y_1^j), \dots, (x_{25}^j, y_{25}^j)\} \cup \\ & \{(x_1^k, y_1^k), \dots, (x_{25}^k, y_{25}^k)\} \cup \dots \end{aligned}$$

1984 and the next mini-batch is chosen to be

$$\begin{aligned} D_{\text{mini-batch 2}} = & \{(x_{25}^i, y_{25}^i), \dots, (x_{50}^i, y_{50}^i)\} \cup \\ & \{(x_{25}^j, y_{25}^j), \dots, (x_{50}^j, y_{50}^j)\} \cup \\ & \{(x_{25}^k, y_{25}^k), \dots, (x_{50}^k, y_{50}^k)\} \cup \dots \end{aligned}$$

1985 In this case, we simply copy the hidden state/statistic h_{25} of the previous mini-
 1986 batch as the initialization h_0 for the next mini-batch. While creates strong
 1987 correlations in the consecutive mini-batches and data for SGD is not sampled
 1988 iid, it is a clever trick to increase the effective range of temporal correlations
 1989 modeled in the RNN without essentially any special operations. You can see
 1990 an implementation of this idea at
 1991 https://github.com/pytorch/examples/blob/master/word_language_model/main.py#L131
 1992

Roughly speaking, data that consists of sequences of length up to 25
 can be trained with RNNs.

1993 8.3 Long Short-Term Memory (LSTM)

1994 Innovations on top of the basic RNN architecture try to improve their ability
 1995 to handle long-range correlations in the data. We saw that the updates to the
 1996 hidden state/statistic h_t is the key to doing so. The architectures called LSTMs,
 1997 and their simpler counterparts called GRUs, are mechanisms that give us more
 1998 control to update the hidden state.

1999 8.3.1 Gated Recurrent Units (GRUs)

2000 GRUs “gate” the hidden state, i.e., the architecture has a mechanism to control
 2001 when the hidden state gets updated and when it does not. For instance, if the
 2002 first symbol in our sequence is very predictive of the future of the sequence
 2003 we want the RNN to learn to not update the hidden state, and similarly if there
 2004 are irrelevant words in the middle of the sequence we want the hidden state to
 2005 not be updated at those time-steps. A GRU also has a mechanism to “reset”
 2006 the hidden state that reduces the influence of the previous hidden state on the
 2007 next hidden state.

2008 Recall that the hidden state for an RNN with a single layer is updated as

$$h_{t+1} = \sigma(w_h h_t + w_x x_{t+1}).$$

2009 A GRU has two more variables that are called the reset variable and the
 2010 zero variable respectively, each created from previous x_t, h_t using learnable
 2011 weights

$$\begin{aligned} r_{t+1} &= \text{sigmoid}(w_{xr} x_t + w_{hr} h_t) \\ z_{t+1} &= \text{sigmoid}(w_{xz} x_t + w_{hz} h_t). \end{aligned} \quad (8.10)$$

2012 The entires of r_t, z_t are between $(0, 1)$. The update to the hidden state in an
 2013 RNN is modified to be

$$h_{t+1} = z_{t+1} h_t + (1 - z_{t+1}) \odot \tanh(w_h (r_{t+1} \odot h_t) + w_x x_{t+1}). \quad (8.11)$$

2014 If entires of z_{t+1} are close to 1, the old state is propagated almost unchanged
 2015 to result in h_{t+1} ; information from x_{t+1} is essentially ignored in this case.
 2016 In z_{t+1} are close to zero, the reset gate is used to decide what the next state
 2017 h_{t+1} is: if r_{t+1} is close to one, the update is the same as that of a conventional
 2018 RNN, if r_{t+1} is close to zero, the previous hidden state does not play any role
 2019 in the update and the update is only dependent on the observation x_{t+1} .

▲ The idea that the hidden state is the memory in sequence models is more clear in this context. In some cases we may want to update our memory after observing a particular part of the sequence, in some cases we want to keep the memory unchanged while in some cases we may wish to reinitialize the memory before observing the future data.

▲ GRUs are very useful recurrent models because they are more general than RNNs but at the same time much simpler than other models such as LSTMs. In most cases, it is a good idea to first try to fit the data using a GRU before using more complex models.

8.3.2 LSTMs

The design of an LSTM was inspired by logic gates in a computer and is a bit complicated; the original LSTM paper is an assigned reading for this lecture. LSTMs are powerful models in sequence modeling and in spite of being developed all the way back in 1997, they are among the few deep learning models that remained popular through the second AI winter and are still the workhorse of the NLP industry today.

An LSTM has three new variables on top of an RNN, these are called the “input, forget, and output” gates respectively

$$\begin{aligned} i_{t+1} &= \sigma(w_{hi} h_t + w_{xi} x_{t+1}) \\ f_{t+1} &= \sigma(w_{hf} h_t + w_{xf} x_{t+1}) \\ o_{t+1} &= \sigma(w_{ho} h_t + w_{xo} x_{t+1}) \end{aligned} \quad (8.12)$$

where all the above weight matrices are learnable parameters. In the GRU we had the convex combination using the zero gate in (8.11) to prevent forgetting. In an LSTM we use the two gates f_t, i_t for this purpose. The hidden state of an LSTM is propagated as

$$h_{t+1} = o_{t+1} \odot c_{t+1} \quad (8.13)$$

where the variable

$$c_{t+1} = f_{t+1} \odot c_t + i_{t+1} \odot \tanh(w_{hc} h_t + w_{xc} x_{t+1}) \quad (8.14)$$

is thought of as a memory cell. Understanding crisply what an LSTM ought to learn is a bit difficult but we can think of an LSTM as parameterizing the operations of GRU; convex combination in (8.11) is replaced by a weighted combination using the input and forget gates in (8.14) while the output gate in (8.13) is identity in a GRU.

Just like we can handle multiple layers in an RNN, we can also have multiple layers in an GRU. Each layer gets its own gates; temporal propagation is performed using the above equations and only the hidden state h_t is propagated up to the deeper layers.

You will notice that a lot of non-linearities in GRUs/LSTMs are sigmoids and hyperbolic tangents. This is because these gates are interpreted as Boolean variables that the model is supposed to learn. There are two lessons to draw from this. First, if you are modeling some computation and would like to learn a Boolean variable, it is a good idea to compute a learnable function of the inputs and use a sigmoid nonlinearity. Second, vanishing gradients are a problem with LSTMs/GRUs as well, the various mechanisms (reset/zero in GRUs and input/forget/output in LSTMs) alleviate this to an extent but do not eliminate vanishing gradients. Roughly speaking, we can use LSTMs to model sequences of up to length 50.

8.4 Bidirectional architectures

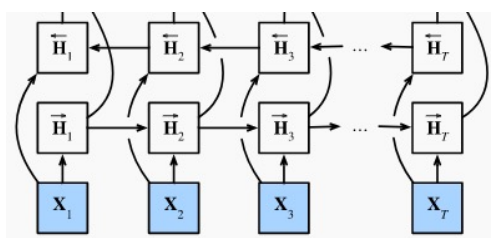
Until now, we have imagined that we would like to predict the future words in a sequence or design a predictor that uses a statistic of the sequence to predict the output. Our recurrent models were causal in the temporal direction, i.e., future elements of the sequence did not play a role in the outputs and updates

of the model at time t . This is indeed how a lot of computation is performed, e.g., if you want to predict the next location of a vehicle in a video, you should not build a predictor that uses future frames because this model cannot be run at test time without access to the future frames. However, there are also problems in which you have access to some future observation and estimate the present state. For instance, you may fill in the following blanks totally differently depending upon the context of the future words.

I am very
 I am very for school.
 I am very , I need a big dinner.

Bidirectional models help us distinguish between the three situations and allow predicting context-specific output. Just like we motivated recurrent models using a Kalman filter and sufficient statistics of the past sequence, we can also derive an analogy with what is called Kalman smoothing (predicting the current state given the past observations *and* the future observations).

Building bidirectional models using RNNs is easy. We have two RNNs running in opposite directions as shown in the following picture.



We maintain two sets of weights, one for the forward RNN and the other for the backward RNN. This gives two hidden states, one in the forward direction and another in the backward direction

$$h_{t+1}^{\text{forward}} = \sigma(w_h^{\text{forward}} h_t^{\text{forward}} + w_x^{\text{forward}} x_{t+1})$$

$$h_t^{\text{backward}} = \sigma(w_h^{\text{backward}} h_{t+1}^{\text{backward}} + w_x^{\text{backward}} x_t).$$

The concatenation of these two hidden states is now the sufficient statistic of the entire sequence. So the output \hat{y}_t is now a function of both these hidden states

$$\hat{y}_t = v^{\text{forward}\top} h_t^{\text{forward}} + v^{\text{backward}\top} h_t^{\text{backward}}. \quad (8.15)$$

Let us emphasize that these two directions have nothing to do with back-propagation. There is a backpropagation for the backward directions as well, which updates $\overline{h_{t+1}^{\text{backward}}}$ using $\overline{h_t^{\text{backward}}}$. You should do the following exercise: imagining that the loss is only computed on the predictions at time t , i.e., $\ell = \ell(y_t, \hat{y}_t)$ and think of how the backpropagation gradient flows in a bidirectional RNN.

Just like we have bidirectional RNNs, we can also build bidirectional GRUs and LSTMs.

8.5 Attention mechanism

The human perception system is quite limited by its sensors, we do not have eyes at the back of our heads. It is also limited by computation, the human

2095 brain consumes only about 12W of power when it works, about 30% of this
 2096 power is consumed by the visual system.

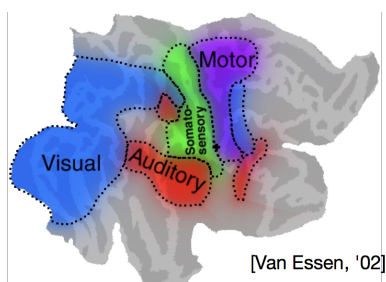


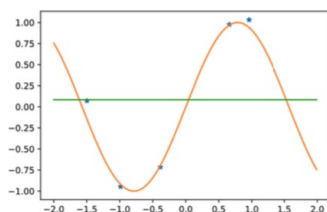
Figure 8.2: This is a picture of the human brain by a famous neuroscientist named David Van Essen. Around the early 90s it became clear that brains consist of different parts, each specialized to processing different kinds of data. The visual system takes up a bulk (30%) of the real estate.

2097 Our perceptual system is very powerful considering the limits of this com-
 2098 putation. We discussed reasons for this in Chapter 1, the ability to move gives
 2099 us the ability to specialize the processing on different parts of the environment
 2100 instead of passively processing all the incoming data from the sensors. For
 2101 instance, when you are driving, you look over your shoulder only before you
 2102 merge on the right, you do not really care to remember where every car in your
 2103 vicinity is at any given point of time. Similarly, experiments on race car drivers
 2104 reveal that even at high speeds they do not pay attention to all parts of the
 2105 environment, a driver typically only cares about two variables, the heading of
 2106 the car while going into a turn and the distance to the apex of the turn. When
 2107 you watch TV, you are paying attention to only a small part of the TV screen.
 2108 You can read more about these experiments at <http://ilab.usc.edu/surprise> and
 2109 in the work of many other researchers who study such problems.

2110 The human perceptual system is tuned to pay attention to only parts of
 2111 the input data that is relevant. Attention in machine learning is an attempt to
 2112 model this phenomenon. It turns out that since understanding which part of a
 2113 long sequence is relevant to making a prediction at a particular time instant,
 2114 attention is well-suited to mitigating the problems with long-range correlations
 2115 in sequence data. We will not go very deep into the architectural intricacies of
 2116 attention models (you can read the suggested reading material) but we provide
 2117 an introduction that makes it easy to understand the papers.

2118 8.5.1 Weighted regression estimate

2119 Consider a regression problem where the true function is drawn in orange and
 2120 the dataset is shown in blue.



2121

2122 If we wanted to predict the targets the green line given by

$$\hat{y} = \frac{1}{n} \sum_{i=1}^n y^i.$$

2123 is the world's dumbest estimator; it predicts the output irrespective of the
2124 input x . We can do better using the so-called Watson-Nadaraya estimator in
2125 statistics. We compute the weighted combination

$$\hat{y}(x) = \sum_{i=1}^n k(x, x^i) y^i$$

2126 where kernel $k(x, x^i)$ computes some similarity between the input x^i in the
2127 dataset and the test input x ; the kernel weighs the target y^i higher if x is close
to x^i .

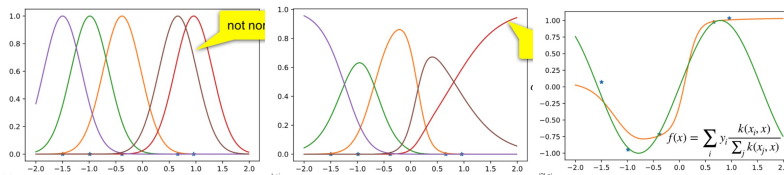


Figure 8.3: The left panel shows the Gaussian kernel $k(\cdot, x^i)$ for different inputs in the dataset. The kernel is not normalized so we cannot match the target values y^i easily using a weighted combination of the kernels. The second panel fixes this by picking a normalized kernel $k(x, x^i) := \frac{k(x, x^i)}{\sum_j k(x, x^j)}$. The estimate of the target $\hat{y}(x)$ using a weighted combination of this normalized kernel is a non-parametric estimator of the targets.

2128

2129 The Watson-Nadaraya estimator in Figure 8.3 is a simple interpolation
2130 mechanism and it is also consistent, i.e., as the amount of data $n \rightarrow \infty$, the
2131 regression error goes to zero. There are no weights in this model. All the
2132 intricacy lies in choosing the kernel over the data.

An attention layer can be thought of as learning the weighing function in our regression estimate, and a weighted average instead of an unweighted average.

2133 8.5.2 Attention layer in deep networks

2134 Let us consider a typical kind of attention that is heavily employed in deep
2135 learning. It is called the dot-product attention mechanism. This takes in two
2136 matrices as input: $k \in \mathbb{R}^{T \times P}$ which is called the “key” and $v \in \mathbb{R}^{T \times P}$ which
2137 are called “values”. Given a query vector $q \in \mathbb{R}^P$ the attention module outputs

$$\sum_{i=1}^T \sigma(k_i^\top q) v_i \quad (8.16)$$

2138 where k_i denotes the i^{th} row of the matrix and likewise for the values. Observe
2139 that the summation is a weighted combination of all the values v_i with weights

2140 given by the similarity of the query with each of the keys k_i . Just like the
 2141 Watson-Nadaraya estimator, we would like these weights to be normalized, so
 2142 we choose

$$\sigma(k_i^\top q) = \text{softmax}_i(k_i^\top q);$$

2143 the softmax normalization is performed over the time-axis i . In simple words,
 2144 the expression is a weighted combination of the values where the kernel
 2145 is computed using a simple dot product and normalization of the kernel is
 2146 performed using softmax. If a particular query vector q is similar to one of the
 2147 keys k_i , that value v_i gets upweighted in the summation.

2148 If the query vector is one of the keys k_i , we have the so-called **self-**
 2149 **attention operation**.

2150 How can we use this in a deep network? First let us consider a standard
 2151 convolutional network with features $h^l \in \mathbb{R}^{m \times c}$ at the l^{th} layer; we have
 2152 reshaped the width and height of the feature map into a single dimension of
 2153 size m , the number of channels is c . If we set the keys, values and queries to
 2154 be learnable quantities

$$\begin{aligned} \mathbb{R}^{m \times c} \ni k &= \sigma(w_k^\top h^l) \\ \mathbb{R}^{m \times c} \ni q &= \sigma(w_q^\top h^l) \\ \mathbb{R}^{m \times c} \ni v &= \sigma(w_v^\top h^l) \end{aligned} \quad (8.17)$$

2155 where $\sigma(\cdot)$ is some nonlinearity, say ReLU, then the output of the attention
 2156 block would be given by a weighted summation over the features for each
 2157 pixel given by

$$h_j^{l+1} = \sum_{i=1}^m \text{softmax}(k_i^\top q_j) v_i. \quad (8.18)$$

2158 This is a just a more complex version of the correlation operator. It creates
 2159 output features $h_j^{l+1}; j \in \{1, \dots, m\}$ that captures the similarities between
 2160 the queries and the keys.

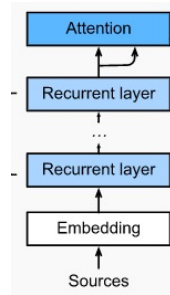
▲ Draw a picture of the computation in an attention module

2161 8.5.3 Attention as one of the layers of a recurrent networks

2162 The attention layer is much more popular for sequence modeling because it
 2163 offers a very powerful way to mitigate the problem with vanishing/exploding
 2164 gradients for long sequences. For a sequence of length T , the attention
 2165 layer computes the same operation as in (8.18). Observe that this expression,
 2166 rewritten here with the number of features $m := T$ corresponding to the time
 2167 dimension and the feature size $c := p$

$$h_j^{l+1} = \sum_{i=1}^T \text{softmax}(k_i^\top q_j) v_i$$

2168 has hidden state h_j^{l+1} that depends on the hidden states of the lower layer
 2169 $h_i^l, i \in \{1, \dots, T\}$. Effectively, the attention layer acts as a temporal shortcut
 2170 that makes the hidden states of an RNN dependent on both past and future
 2171 hidden states for the sequence. In a picture, this looks as follows.



2172

2173 The recurrent layers compute features in a causal fashion but the attention
2174 layer connects all the time-steps together. If you think of how backpropagation
2175 gradient flows down from the output layer via the attention, you will realize
2176 that the gradient of the loss computed at step t , say $\ell(y_t, \hat{y}_t)$ flows back to
2177 the hidden states h_2 using two paths; the first is the standard BPTT path of
2178 the recurrent layers while the second one is a more direct path of the cross-
2179 correlation operation in the attention layer. This is a huge benefit because it
2180 essentially eliminates problems with gradient vanishing and allows recurrent
2181 model very long sequences. Modifications of this attention module can easily
2182 handle sequences of a few hundred words.

2183 To conclude, attention is a powerful operation and has become very popular
2184 in the past 1-2 years. It has been used predominantly for NLP models but
2185 also works surprisingly well as a replacement for convolutional layers for
2186 image-based data. One can think of the attention module as a fully-connected
2187 layer that performs very strong weight sharing.

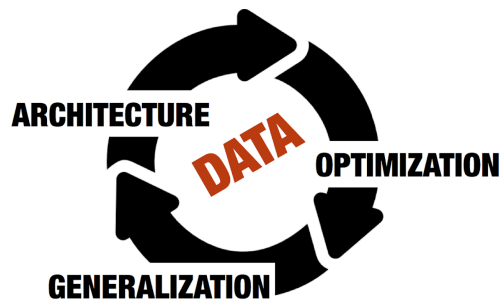
2188 You can read Chapter 10.3 in the D2L.ai book and the original paper on
2189 a popular attention-based architecture called the Transformer to know more
2190 about this operation.

2191 Chapter 9

2192 Background on 2193 Optimization, Gradient 2194 Descent

2195 We have covered the cliff-notes of the practice of deep learning in the previous
2196 eight chapters. It is by no means a complete overview. The practice of deep
2197 learning is an enticing, mysterious, and sometimes frustrating. The more time
2198 you spend playing with code the more you will learn about deep learning. New
2199 ideas are routinely discovered using very simple experiments that each of you
2200 is capable of running in your Colab now.

2201 As we discussed, there three main concepts in machine learning. First, the
2202 class of functions $f(x; w)$ that you use to make predictions, this is called the
2203 hypothesis class or the architecture. Second, the algorithm you use to find the
2204 best model in this class of functions that fits your data; this uses tools from
2205 optimization theory. Third is the generalization performance of your classifier.
2206 Machine Learning is about picking a good hypothesis class, finding the best
2207 model within this class and making sure that the model generalizes.



2208

2209 The above process is relatively well-understood for simpler models such
2210 as SVMs but the story is quite murky for deep networks. Often in practice,
2211 it is never clear which architecture you should pick for your problem (many
2212 of you have asked this question in the office hours for instance). Training a
2213 deep network involves a number of bells and whistles (some of which like
2214 Batch-Normalization and Dropout that we have seen) and if at the end of this
2215 exercise we get a high validation error, it is unclear how one should change

2216 the parts of the process to improve performance. Disentangling this vicious
2217 cycle is what “understanding deep learning” is all about.

2218 **Goal** Module 2 will develop an understanding of optimization and gener-
2219 alization for more generic machine learning models first. It will end with an
2220 insight into understanding their interplay for deep networks. Module 2 has a
2221 different flavor, it is more theoretical. Our goal is to grasp the general concepts
2222 behind these theoretical results and understand the training process of deep
2223 networks better. This will also help us train deep networks much better in
2224 practice.

2225 9.1 Convexity

2226 Consider a function $\ell : \mathbb{R}^p \rightarrow \mathbb{R}$ that is convex, i.e., for any w, w' that lie in
2227 the domain (which is assumed to be a convex set) of f and any $\lambda \in [0, 1]$ we
2228 have

$$\ell(\lambda w + (1 - \lambda)w') \leq \lambda \ell(w) + (1 - \lambda)\ell(w'). \quad (9.1)$$

2229 A function $\ell(w)$ is concave if $-\ell(w)$ is convex. Some examples of convex
2230 functions are

- 2231 • affine functions $Aw + b$, norms $\|w\|_p = (\sum_{i=1}^p |w_i|^p)^{1/p}$, or $\|w\|_\infty =$
2232 $\max_k |w_k|$.
- 2233 • exponential e^w for $w \in \mathbb{R}$
- 2234 • powers w^α for $w > 0$ and $\alpha \geq 1$ or $\alpha \leq 0$
- 2235 • powers of absolute values $|w|^p$ for $w \in \mathbb{R}$ and $p \geq 1$

2236 **Strictly convex functions** Strictly convex functions have the property that
2237 for all $w \neq w'$ in the domain (which is assumed to be convex) and $\lambda \in (0, 1)$

$$\ell(\lambda w + (1 - \lambda)w') < \lambda \ell(w) + (1 - \lambda)\ell(w').$$

2238 **First-order condition for convexity** If ℓ is differentiable, the definition
2239 of convexity in (9.1) is equivalent to the following first-order condition. A
2240 differentiable function ℓ with convex domain is convex iff

$$\ell(w') \geq \ell(w) + \langle \nabla \ell(w), w' - w \rangle. \quad (9.2)$$

2241 for all w, w' in the domain. Note that the first-order condition is equivalent
2242 to the definition of convexity in (9.1) for differentiable functions. The proof
2243 is long but easy; you can see https://www.princeton.edu/aaa/Public/Teaching/ORF523/S16/ORF523_S16_Lec7_gh.pdf for the proof. For strictly convex
2244 functions the inequality is strict
2245

$$\ell(w') > \ell(w) + \langle \nabla \ell(w), w' - w \rangle.$$

2246 **Monotonicity of the gradient for convex functions** The first-order con-
 2247 dition for convexity gives a useful, and equivalent, characterization of the
 2248 gradient. Write (9.2) for w, w' in two opposite directions

$$\begin{aligned}\ell(w) &\geq \ell(w') + \langle \nabla \ell(w'), w - w' \rangle \\ \ell(w') &\geq \ell(w) + \langle \nabla \ell(w), w' - w \rangle\end{aligned}$$

2249 and add them to get

$$\langle \nabla \ell(w) - \nabla \ell(w'), w - w' \rangle \geq 0. \quad (9.3)$$

2250 It is also true that monotonicity of the gradient implies convexity (try to prove
 2251 it).

2252 **Second-order condition for convexity** If ℓ is twice-differentiable with a
 2253 convex domain, it is convex iff

$$\nabla^2 \ell(w) \succeq 0 \quad (9.4)$$

2254 for all w in the domain. The symbol \succeq denotes positive semi-definiteness of
 2255 the Hessian matrix $\nabla^2 \ell(w)$

$$(\nabla^2 \ell(w))_{ij} = \frac{\partial^2 \ell(w)}{\partial w_i \partial w_j}.$$

2256 For strictly convex functions, the inequality in (9.4) is strict, i.e., the Hessian
 2257 is positive definite. As an example, the least squares objective $\ell(w) = \|y -$
 2258 $Xw\|_2^2$ is convex because

$$\nabla^2 \ell(w) = 2X^\top X$$

2259 which is positive definite for any non-singular X .

2260 **Strongly convex functions** A function is strongly convex if there exists an
 2261 $m > 0$ such that

$$\ell(w) - \frac{m}{2} \|w\|_2^2 \text{ is convex.} \quad (9.5)$$

2262 It is easy to see that strict convexity implies convexity. Since the function
 2263 $\ell(w) - m/2 \|w\|_2^2$ is convex, it satisfies the definition of convexity:

$$\begin{aligned}\ell(\lambda w + (1 - \lambda)w') - \frac{m}{2} \|\lambda w + (1 - \lambda)w'\|_2^2 \\ \leq \lambda \left(\ell(w) - \frac{m}{2} \|w\|_2^2 \right) + (1 - \lambda) \left(\ell(w') - \frac{m}{2} \|w'\|_2^2 \right).\end{aligned} \quad (9.6)$$

2264 **But**

$$\frac{\lambda m}{2} \|w\|_2^2 + \frac{(1 - \lambda)m}{2} \|w'\|_2^2 - \frac{m}{2} \|\lambda w + (1 - \lambda)w'\|_2^2 > 0$$

2265 for $\lambda \in (0, 1)$ for all $w \neq w'$ because $\|w\|_2^2$ is strictly convex which shows
 2266 that if we have a strongly convex function ℓ it also satisfies

$$\ell(\lambda w + (1 - \lambda)w') < \lambda \ell(w) + (1 - \lambda) \ell(w').$$

2267 In other words, we have

strong convexity \Rightarrow strict convexity \Rightarrow convexity.

2268 Observe that strongly convexity in (9.6) is a stronger version of Jensen's in-
 2269 equality. Strongly convex functions are easier to optimize for algorithms. It
 2270 will also always be much easier to prove a result in optimization on strongly
 2271 convex functions. It is easy to see using the second-order condition for con-
 2272 vexity that an m -strongly convex function has

$$\nabla^2 \ell(w) \succeq mI_{p \times p}.$$

2273 We will use the following first-order condition for strongly convex func-
 2274 tions often. A function is m -strongly convex if and only if

$$\ell(w') \geq \ell(w) + \langle \nabla \ell(w), w' - w \rangle + \frac{m}{2} \|w' - w\|^2 \quad (9.7)$$

2275 for any w, w' in the domain.

2276 9.2 Introduction to Gradient Descent

2277 In this chapter, we will write $\ell(w)$ to denote the training objective, i.e., if we
 2278 have a classifier $f(x; w)$ and a dataset $D = \{(x^i, y^i)\}_{i=1, \dots, n}$ of n samples
 2279 we will denote

$$\ell(w) := \frac{1}{n} \sum_{i=1}^n \ell(w; x^i, y^i).$$

2280 The objective ℓ will always be a function of the entire dataset but we will keep
 2281 the dependence implicit. Note that the number of samples n is usually quite
 2282 large in deep learning, so the summation above has a large number of terms
 2283 on the right-hand side.

2284 Gradient descent is a simple algorithm to minimize $\ell(w)$. Before we study
 2285 its properties, it will help to refresh the following few facts.

2286 9.2.1 Conditions for optimality

2287 **Local and global minima** A point w is a local minimum of the function
 2288 $\ell(w)$ for all w' in a neighborhood of w we have $\ell(w) \leq \ell(w')$. The point
 2289 is a global minimum of the function ℓ if this condition is true for all w' in the
 2290 domain, not just the ones in the neighborhood.

2291 **Local minima are global minima for convex functions** This is easy to see
 2292 using an argument by contradiction. If w is a local minimum that is not the
 2293 global minimum, there exists a point w' in the domain such that $\ell(w') < \ell(w)$.
 2294 The domain of the function is convex, so pick a point $v = \lambda w' + (1 - \lambda)w$
 2295 and see that

$$\ell(v) - \ell(w) \leq \lambda(\ell(w') - \ell(w))$$

2296 using the definition of convexity. Since w is only a local minimum, we can
 2297 pick λ to be small enough that the left hand side is non-negative. This shows
 2298 that $\ell(w') \geq \ell(w)$ but this means that w is a global minimum and we have a
 2299 contradiction.

2300 **Global minimum is unique for strictly convex functions** If a function is
 2301 strictly convex on a convex domain the optimal solution (if it exists) must be
 2302 unique. Indeed, if there were two solutions w, w' that were both minimizers
 2303 we would have

$$\ell(w) = \ell(w') \leq \ell(w'') \quad \forall w'' \quad (9.8)$$

2304 We can now apply the definition of convexity to the point $v = (w + w')/2$ to
 2305 get

$$\ell(v) < \frac{1}{2}\ell(w) + \frac{1}{2}\ell(w') = \ell(w).$$

2306 which contradicts (9.8). The least-squares objective is strictly convex, so the
 2307 solution is unique global minimizer of the objective.

2308 **First-order optimality condition** If w is a local minimum of a continuously
 2309 differentiable function ℓ , then it satisfies

$$\nabla \ell(w) = 0. \quad (9.9)$$

2310 If further ℓ is convex, then $\nabla \ell(w) = 0$ is a sufficient condition for global
 2311 optimality from the above discussion.

2312 9.2.2 Different types of convergence

2313 Let us assume that we have a continuously differentiable convex function ℓ
 2314 and let

$$w^* = \underset{w}{\operatorname{argmin}} \ell(w)$$

2315 be the global minimizer of this function.

2316 We would like to develop an iterative scheme that takes in the initialization
 2317 of the weights w^0 and updates them to obtain a sequence

$$w^0, w^1, \dots, w^t, \dots$$

2318 Along this sequence we are interested in understanding the

- 2319 1. convergence of the function value $\ell(w^t)$ to the minimal value $\ell(w^*)$,
- 2320 and
- 2321 2. convergence of the iterates $\|w^t - w^*\|$.

2322 **Descent direction** We are going to perform a sequence of updates given by

$$w^{t+1} = w^t + \eta d^t \quad (9.10)$$

2323 where d^t is called the descent direction and the scalar parameter $\eta > 0$ is called
 2324 the step-size and determines how far we travel using this descent direction.
 2325 Any direction such that

$$\langle \nabla \ell(w^t), d^t \rangle < 0$$

2326 is a good descent direction because this leads to a reduction in the value of the
 2327 function $\ell(w^{t+1})$ after the weight update. There are numerous ways to pick a
 2328 good descent direction. Among the simplest ones is gradient descent which

2329 descends along the direction of the negative gradient and thereby performs the
2330 following set of updates

$$w^{t+1} = w^t - \eta \nabla \ell(w^t) \quad (9.11)$$

2331 given an initial value w^0 . The step-size (also called the learning rate) is chosen
2332 by the user. The step-size need not always be fixed, for instance you chose
2333 it to be a function of the number of weight updates t in the homework. A
2334 good step-size is one that does not overshoot the minimum w^* . For instance,
2335 after having chosen a particular descent direction d^t we can compute the best
2336 step-size to use at time t by solving

$$\eta^t = \underset{\eta \geq 0}{\operatorname{argmin}} \ell(w^t + \eta d^t).$$

2337 This is known as line-search in the optimization literature. You may have seen
2338 Newton's method

$$w^{t+1} = w^t - (\nabla^2 \ell(w^t))^{-1} \nabla \ell(w^t). \quad (9.12)$$

2339 which does not have a user-tuned step-size and further modifies the descent
2340 direction to be the product of the inverse Hessian with the gradient.

2341 9.3 Convergence rate for gradient descent

2342 We will next understand how quickly gradient descent converges to the global
2343 minimum. There are two concrete goals of this analysis

- 2344 1. to be able to pick the step-size to avoid overshooting without doing
2345 line-search, and
- 2346 2. characterize how many iterations of gradient descent to run until we are
2347 guaranteed to be within some distance of the global minimum.

2348 9.3.1 Some assumptions

2349 Before we begin, we will make a few simplifying assumptions on the function
2350 $\ell(w)$. These are quite typical in optimization and ensure that we are not dealing
2351 with pathological functions that make minimizing them arbitrarily hard.

- 2352 1. **Lipschitz continuity/bounded gradients** We will assume that ℓ is Lip-
2353 schitz continuous

$$|\ell(w) - \ell(w')| \leq B \|w - w'\|_2. \quad (9.13)$$

2354 for some $B > 0$. You might also see this condition written as

$$\|\nabla \ell(w)\| \leq B$$

2355 for differentiable functions.

▲ Draw a picture of overshooting using a large step-size.

🔗 Can you think of an algorithm for minimizing a function that does not use the gradient of the function to compute the descent direction?

2356 **2. Smoothness** We will always consider functions such that their gradients
2357 are L -Lipschitz, i.e.,

$$\|\nabla \ell(w) - \nabla \ell(w')\|_2 \leq L\|w - w'\|_2. \quad (9.14)$$

2358 If ℓ is twice-differentiable, this is equivalent to assuming

$$\nabla^2 \ell(w) \preceq L I_{p \times p}. \quad (9.15)$$

2359 From the Cauchy-Schwarz inequality which states that

$$\langle u, v \rangle \leq \|u\| \|v\|$$

2360 for two vectors u, v , we have the following implication of smoothness:

$$\langle \nabla \ell(w) - \nabla \ell(w^*), w - w^* \rangle \leq L\|w - w^*\|^2. \quad (9.16)$$

2361 A related concept is called **co-coercivity** of the gradient. The gradient
2362 being L -Lipschitz is equivalent to co-coercivity of the gradient with
2363 parameter $1/L$

$$\frac{1}{L}\|\nabla \ell(w) - \nabla \ell(w')\|^2 \leq \langle \nabla \ell(w) - \nabla \ell(w'), w - w' \rangle. \quad (9.17)$$

2364 We can see that co-coercivity implies Lipschitz continuity of the gradi-
2365 ents $\nabla \ell(w)$ using (9.16) and (9.17). The reverse is also true, Lipschitz-
2366 continuity of the gradient implies the Descent Lemma Lemma 9.1 which
2367 is seen by applying the Descent Lemma twice for the two functions
2368 $g(u) = \ell(u) - \langle \nabla \ell(w'), u \rangle$ and $h(u) = \ell(u) - \langle \nabla \ell(w), u \rangle$.

2369 9.3.2 GD for convex functions

2370 We begin with the so-called Descent Lemma.

2371 **Lemma 9.1 (Descent Lemma).** For an L -smooth function, we have

$$\ell(w') \leq \ell(w) + \langle \nabla \ell(w), w' - w \rangle + \frac{L}{2}\|w' - w\|^2. \quad (9.18)$$

2372 for any two w, w' in the domain.

2373 **Proof.** First, you should compare this with the first-order characterization of
2374 convexity

$$\ell(w') \geq \ell(w) + \langle \nabla \ell(w), w' - w \rangle.$$

2375 The two conditions can be used to sandwich the value of $\ell(w^{t+1})$ given the
2376 value of $\ell(w^t)$ in gradient descent with room for a quadratic term $\frac{L}{2}\|w' - w\|^2$.
2377 This also gives some intuition as to what L -smooth really means; a large value
2378 of L means that the function ℓ decreases quickly. Let $v = w + \lambda(w' - w)$ and
2379 use Taylor's theorem to see that

$$\ell(w') = \ell(w) + \int_0^1 \langle \nabla \ell(v), w' - w \rangle \, d\lambda \quad (9.19)$$

2380 Subtract $\langle \nabla \ell(w), w' - w \rangle$ from both sides to get

$$\ell(w') - \ell(w) - \langle \nabla \ell(w), w' - w \rangle = \int_0^1 \langle \nabla \ell(v) - \nabla \ell(w), w' - w \rangle \, d\lambda.$$

2381 Observe that

$$\begin{aligned}
|\ell(w') - \ell(w) - \langle \nabla \ell(w), w' - w \rangle| &= \left| \int_0^1 \langle \nabla \ell(v) - \nabla \ell(w), w' - w \rangle \, d\lambda \right| \\
&\leq \int_0^1 |\langle \nabla \ell(v) - \nabla \ell(w), w' - w \rangle| \, d\lambda \\
&\leq \int_0^1 \|\nabla \ell(v) - \nabla \ell(w)\| \|w' - w\| \, d\lambda \\
&\leq L \int_0^1 \lambda \|w' - w\|^2 \, d\lambda \\
&= \frac{L}{2} \|w' - w\|^2.
\end{aligned}$$

2382 This completes the proof after removing the absolute value on the left-hand
2383 side. \square

2384 We can use the Descent Lemma twice on two points to w, w' to get (9.16).
2385 Another direct consequence of the Descent Lemma is the following corollary
2386 that relates the value $\ell(w)$ at any point w in the domain to that of the global
2387 minimum.

2388 **Corollary 9.2.** For L -smooth convex function ℓ , if w^* is the global minimizer,
2389 then

$$\frac{1}{2L} \|\nabla \ell(w)\|^2 \leq \ell(w) - \ell(w^*) \leq \frac{L}{2} \|w - w^*\|^2. \quad (9.20)$$

2390 **Proof.** Since $\nabla \ell(w^*) = 0$, the right-hand side follows directly from the
2391 Descent Lemma. To get the left-hand side, let us optimize the upper bound in
2392 the Descent Lemma using $w' = w + \lambda v$ with $\|v\| = 1$ as follows

$$\begin{aligned}
\ell(w^*) &= \inf_{w'} \ell(w') \leq \inf_{w'} \left\{ \ell(w) + \langle \nabla \ell(w), w' - w \rangle + \frac{L}{2} \|w' - w\|^2 \right\} \\
&= \inf_{\|v\|=1} \inf_{\lambda} \left\{ \ell(w) + \lambda \langle \nabla \ell(w), v \rangle + \frac{L}{2} \lambda^2 \right\} \\
&= \inf_{\|v\|=1} \left\{ \ell(w) - \frac{1}{2L} (\langle \nabla \ell(w), v \rangle)^2 \right\} \\
&= \ell(w) - \frac{1}{2L} \|\nabla \ell(w)\|^2.
\end{aligned}$$

2393 \square

2394 In other words, the gap between the function values $\ell(w) - \ell(w^*)$ is upper-
2395 bounded by the gap to the minimizer $\frac{L}{2} \|w - w^*\|^2$ and lower-bounded by the
2396 norm of the gradient $\frac{1}{2L} \|\nabla \ell(w)\|^2$.

2397 **Lemma 9.3 (Monotonic progress for gradient descent).** For gradient des-
2398 cent $w^{t+1} = w^t - \eta \nabla \ell(w^t)$, if we pick the step-size

$$\eta \leq \frac{1}{L} \quad (9.21)$$

2399 we have

$$\ell(w^{t+1}) \leq \ell(w^t) - \frac{\eta}{2} \|\nabla \ell(w^t)\|^2. \quad (9.22)$$

2400 Further,

$$\ell(w^{t+1}) - \ell(w^*) \leq \frac{1}{2\eta} (\|w^t - w^*\|^2 - \|w^{t+1} - w^*\|^2) \quad (9.23)$$

2401 which implies

$$\|w^{t+1} - w^*\|^2 \leq \|w^t - w^*\|^2. \quad (9.24)$$

2402 **Proof.** Substitute $\eta \leq 1/L$ in the Descent Lemma and simplify to get (9.22).
2403 The second result is obtained by

$$\begin{aligned} 0 \leq \ell(w^{t+1}) - \ell(w^*) &\leq \ell(w^t) - \ell(w^*) - \frac{\eta}{2} \|\nabla \ell(w^t)\|^2 \\ &\leq \langle \nabla \ell(w^t), w^t - w^* \rangle - \frac{\eta}{2} \|\nabla \ell(w^t)\|^2 \\ &= \frac{1}{2\eta} (\|w^t - w^*\|^2 - \|w^t - w^* - \eta \nabla \ell(w^t)\|^2) \\ &= \frac{1}{2\eta} (\|w^t - w^*\|^2 - \|w^{t+1} - w^*\|^2). \end{aligned}$$

2404 Observe that since the left-hand side is positive, the claim in (9.24) is true. \square

2405 We have therefore shown that if the step-size is not too large (the smoothness parameter of the function determines how large the step-size can be) then gradient descent always improves the value of the function with each iteration (9.22). It also improves the distance of the weights to the global minimum at each iteration (9.24).

2410 **Lemma 9.4 (Convergence rate for gradient descent, convex function).** For
2411 gradient descent $w^{t+1} = w^t - \eta \nabla \ell(w^t)$ with step-size $\eta < 1/L$, we have

$$\ell(w^{t+1}) - \ell(w^*) \leq \frac{1}{2t\eta} \|w^0 - w^*\|^2. \quad (9.25)$$

2412 **Proof.** We sum up the expression in (9.23) for all times t to get

$$\begin{aligned} \sum_{s=1}^t \ell(w^s) - \ell(w^*) &\leq \frac{1}{2\eta} \sum_{s=1}^t (\|w^{s-1} - w^*\|^2 - \|w^s - w^*\|^2) \\ &= \frac{1}{2\eta} (\|w^0 - w^*\|^2 - \|w^t - w^*\|^2) \\ &\leq \frac{1}{2\eta} \|w^0 - w^*\|^2. \end{aligned}$$

2413 We know from (9.22) that $\ell(w^t)$ is non-increasing, so we can write

$$\ell(w^t) - \ell(w^*) \leq \frac{1}{t} \sum_{s=1}^t (\ell(w^s) - \ell(w^*)) \leq \frac{1}{2t\eta} \|w^0 - w^*\|^2.$$

2414 \square

If we want to find a weights with

$$\ell(w^t) - \ell(w^*) \leq \epsilon$$

for a convex function, we need to run gradient descent for at least

$$\mathcal{O}(1/\epsilon)$$

iterations. This is an important result to remember.

2415 9.3.3 Gradient descent for strongly convex functions

2416 Things are much better if the function we are minimizing is strongly con-
2417 vex. First we have the following lemma for strongly-convex functions which
2418 involves a rewriting co-coercivity condition for strongly convex functions.

2419 **Lemma 9.5 (Co-coercivity for strongly convex function).** If $\ell(w)$ is m -
2420 strongly convex, and L -smooth, then the function $g(w) = \ell(w) - \frac{m}{2}\|w\|^2$
2421 is convex and $L - m$ -smooth. The co-coercivity condition for $\nabla g(w)$ can
2422 therefore be re-written as

$$\langle \nabla \ell(w) - \nabla \ell(w'), w - w' \rangle \geq \frac{mL}{m+L} \|w - w'\|^2 + \frac{1}{m+L} \|\nabla \ell(w) - \nabla \ell(w')\|^2. \quad (9.26)$$

2423 **Proof.** The convexity of $g(w)$ is immediate to see from the definition of strong
2424 convexity of $\ell(w)$. Use the monotonicity of the gradient of $g(w)$ to get

$$\begin{aligned} 0 &\leq \langle \nabla g(w) - \nabla g(w'), w - w' \rangle \\ &= \langle \nabla \ell(w) - \nabla \ell(w'), w - w' \rangle - m\|w - w'\|^2 \\ &\leq (L - m)\|w - w'\|^2. \end{aligned}$$

2425 We can now rewrite the co-coercivity condition for $\nabla g(w)$ with the smooth-
2426 ness parameter $L - m$ and simplify to get (9.26). \square

2427 **Lemma 9.6 (Convergence rate of gradient descent for strongly convex**
2428 **functions).** For strongly convex functions we have pick a step-size

$$0 < \eta < \frac{2}{m+L}$$

2429 to get

$$\|w^{t+1} - w^*\|^2 \leq \left(1 - \eta \frac{2mL}{m+L}\right) \|w^t - w^*\|^2. \quad (9.27)$$

2430 which gives

$$\|w^t - w^*\|^2 \leq c^t \|w^0 - w^*\|^2 \quad (9.28)$$

2431 where $c = \left(1 - \eta \frac{2mL}{m+L}\right)$.

2432 **Proof.** We expand the left hand-side in (9.27) to get

$$\begin{aligned} \|w^{t+1} - w^*\|^2 &= \|w^t - \eta \nabla \ell(w^t) - w^*\|^2 \\ &= \|w^t - w^*\|^2 - 2\eta \langle \nabla \ell(w^t), w^t - w^* \rangle + \eta^2 \|\nabla \ell(w^t)\|^2 \\ &\leq \left(1 - \eta \frac{2mL}{m+L}\right) \|w^t - w^*\|^2 + \eta \left(\eta - \frac{2}{m+L}\right) \|\nabla \ell(w^t)\|^2 \\ &\leq \left(1 - \eta \frac{2mL}{m+L}\right) \|w^t - w^*\|^2. \end{aligned}$$

2433 We have substituted the co-coercivity condition from (9.26) for the inner-
 2434 product with $w' := w^t$ and $w := w^*$ to get the first inequality. This implies
 2435 that the distance to the global minimum $\|w^t - w^*\|$ decreases multiplicatively;
 2436 compare this with (9.24) where the progress is additive. The additional as-
 2437 sumption of strong convexity therefore means that we are making very quick
 2438 progress towards the global minimum. We can use this inequality repeatedly
 2439 for all iterations t to get

$$\|w^t - w^*\|^2 \leq c^t \|w^0 - w^*\|^2$$

2440 where $c = \left(1 - \eta \frac{2mL}{m+L}\right)$. □

Strong convexity enables much faster progress towards the global minimum. If we want $\|w^t - w^*\| \leq \epsilon$ we need

$$\mathcal{O}(\log(1/\epsilon))$$

iterations of gradient descent. This is *much* less than that for a convex function. This is called *linear* convergence because we need a constant number of iterations to reduce the gap to the optimal in half. The naming convention is a bit unusual here but you will see that if we plot $\log\|w^t - w^*\|$ (or $\log(\ell(w^t) - \ell(w^*))$) on the Y-axis and number of iterations t on the X-axis, we get a straight line for gradient descent on strongly-convex functions; you can see this from (9.28).

We say that the convergence rate of gradient descent for non-strongly convex functions is *sub-linear*. The longer we run GD for convex functions, the slower its progress.

Further, if we pick the largest step-size $\eta = 2/(m+L)$ we get

$$c = \left(\frac{\kappa - 1}{\kappa + 1}\right)^2 < 1. \quad (9.29)$$

where $\kappa = L/m$ is the condition number of the Hessian (it is the ratio of the largest eigenvalue and the smallest eigenvalue). Larger the condition number κ , closer to 1 the multiplicative constant c and *slower* the convergence rate of gradient descent.

▲ Plot the convergence rate of gradient descent for convex and strongly-convex functions.

▲ In the optimization literature, an algorithm with

$$\lim_{t \rightarrow \infty} \frac{\ell(w^{t+1}) - \ell(w^*)}{\ell(w^t) - \ell(w^*)} = \rho$$

is said to be sub-linear if $\rho \in (0, 1)$, linear if $\rho = 1$ and super-linear if $\rho = 0$.

2441 A few more points to note

- 2442 1. The step-size is limited by $m+L$ but the convergence rate depends on
 2443 $\kappa = L/m$. Smaller the value of c , faster the convergence.
- 2444 2. Larger the L , smaller the ideal step-size η
- 2445 3. You can get the upper bound

$$\ell(w^t) - \ell(w^*) \leq \frac{L}{2} \|w^t - w^*\|^2 \leq \frac{c^t L}{2} \|w^0 - w^*\|^2 \quad (9.30)$$

2446 using (9.20).

2447 You will also see the convergence rate written in many papers as

$$\|w^t - w^*\| \leq e^{-4t/\kappa} \|w^0 - w^*\|. \quad (9.31)$$

2448 You can get this inequality by using the fact that $1 + x \leq e^x$ in (9.29). We can
 2449 use this to pull out the dependence on κ in the convergence rate; for strongly
 2450 convex functions, gradient descent requires

$$\mathcal{O}(\kappa \log(1/\epsilon))$$

2451 iterations to reach within an ϵ -neighborhood of the global minimum $\ell(w^*)$.
 2452 This suggests that smaller the condition number κ fewer the iterations required.

2453 We can intuitively understand why convergence of gradient descent is
 2454 slower for a large condition number. A large condition number means that
 2455 some directions of the objective ℓ are highly curved while some others are
 2456 very flat. It is difficult to pick one single scalar step-size in such situations that
 2457 makes quick progress along the flat directions but also does not overshoot the
 2458 highly curved directions. You might imagine that clever schemes to change the
 2459 step-size depending upon the local geometry of the function $\ell(w^t)$ could help
 2460 solve this issue and indeed it does, but such adaptive schemes are expensive to
 2461 implement computationally. We will see some algorithms that pick different
 2462 step-sizes for different weights in Chapter 11.

▲ Draw a picture of this phenomenon for a quadratic objective $\ell(w) = \langle w, Aw \rangle$ for matrices $A \succ 0$ with different condition numbers κ .

2463 9.4 Limits on convergence rate of first-order meth- 2464 ods

2465 It is a powerful and deep result that we cannot do better than a linear conver-
 2466 gence rate for optimization methods that only use the gradient of the function
 2467 $\ell(w)$. More precisely, for any first-order method, i.e., any method where the
 2468 iterate at step t given by w^t is chosen to be

$$w^t \in w^0 + \text{span} \{ \nabla \ell(w^0), \dots, \nabla \ell(w^t) \},$$

2469 we have the following theorem by Yurii Nesterov.

2470 **Theorem 9.7 (Nesterov's lower bound).** If $w \in \mathbb{R}^p$, for any $t \leq (p-1)/2$
 2471 and every initialization of weights w^0 there exist functions $\ell(w)$ that are
 2472 convex, differentiable, L -smooth with finite optimal value $\ell(w^*)$ such that any
 2473 first-order method has

$$\ell(w^t) - \ell(w^*) \geq \frac{3}{32} \frac{L \|w^0 - w^*\|^2}{(t+1)^2}.$$

2474 Let us read the statement of the theorem carefully. It states that *fixed* a time
 2475 t and initial condition w^0 , we can *find* a convex function $\ell(w)$ such that it takes
 2476 gradient descent at least $\mathcal{O}(1/\epsilon^2)$ to reach an ϵ -neighborhood of the optimal
 2477 value $\ell(w^*)$. The implication of this theorem is as follows. The convergence
 2478 rate $\mathcal{O}(1/\epsilon)$ we obtained for convex functions is not the best rate we can
 2479 get. Nesterov's lower bound suggests that there should be gradient-based
 2480 algorithms that only require $\mathcal{O}(1/\sqrt{\epsilon})$ iterations. Such methods will be the
 2481 topic of the next Chapter.

2482 Chapter 10

2483 Accelerated Gradient 2484 Descent

Reading

1. The blog-post titled “Why momentum really works?” at <https://distill.pub/2017/momentum>

2485 In the previous chapter we saw two results that characterize how many
2486 iterations gradient descent requires to reach within an ϵ -neighborhood of the
2487 global optimum for convex functions. If the function $\ell(w)$ is convex, GD
2488 with a step-size at most $1/L$ requires $\mathcal{O}(1/\epsilon)$ iterations. If the function $\ell(w)$
2489 is strongly convex, then the step-size can be as large as $2/(m + L)$ and GD
2490 requires $\mathcal{O}(\kappa \log(1/\epsilon))$ iterations where

$$\kappa = \frac{L}{m}$$

2491 is the condition number of the Hessian $\nabla^2 \ell(w)$. A large value of κ means
2492 that there are some directions where the function is highly curved and others
2493 where it is relatively flat. The main point to remember is that we often do
2494 not know a good value for m, L . Since the step-size of GD depends upon the
2495 curvature of the function; if the step-size is too large then GD overshoots on
2496 the highly curved directions and if the step-size is too small then GD makes
2497 slow progress along a direction.

2498 We will study two algorithms in this chapter which accelerate the progress
2499 of gradient descent.

2500 10.1 Polyak’s Heavy Ball method

2501 The most natural place to begin is to imagine gradient descent as a kinematic
2502 equation. Let w^t be the iterate of GD at time t , let us associate to it an auxiliary

2503 variable called the “velocity” v^t

$$v^t := \frac{w^{t+1} - w^t}{\eta}. \quad (10.1)$$

2504 Gradient descent can then be written as

$$v^t = -\nabla \ell(w^t), \quad (10.2)$$

2505 which allows us to think of the term $-\nabla \ell(w^t)$ is the force that acts on a
 2506 particle to update its position from w^t to w^{t+1} . This particle has no inertia, so
 2507 the force applied directly affects its position. If the magnitude of this gradient
 2508 is small in a certain direction, the velocity is also small in that direction.

2509 We now give our particle some inertia. Instead of the force directly affect-
 2510 ing the position we will write down Newton’s second law of motion ($F = ma$)
 2511 for a particle with unit mass $m = 1$ as

$$\begin{aligned} -\nabla \ell(w^t) &=: \frac{v^{t+1} - v^t}{\eta} \\ &= \frac{1}{\eta} (w^{t+1} - 2w^t + w^{t-1}) \\ \Rightarrow w^{t+1} &= w^t - \eta \nabla \ell(w^t) + (w^t - w^{t-1}). \end{aligned} \quad (10.3)$$

2512 Notice the third term on the right-hand side above, it is the gap between the
 2513 current weights w^t and the previous weights w^{t-1} , if we have

$$\langle w^t - w^{t-1}, \nabla \ell(w^t) \rangle < 0,$$

2514 i.e., the change from the previous time-step is along the descent direction,
 2515 then the weights w^{t+1} get an extra boost. If instead, the change from the
 2516 previous direction is not along the gradient descent direction, then the third
 2517 term reduces the magnitude of the gradient. The third term is effectively the
 2518 inertia of gradient updates. This method is therefore called Polyak’s Heavy
 2519 Ball method.

We give ourselves some more control over how inertia enters the update equation using a hyper-parameter ρ

$$w^{t+1} = w^t - \eta \nabla \ell(w^t) + \rho (w^t - w^{t-1}). \quad (10.4)$$

If $\rho = 0$, we do not use any inertia and Polyak’s method boils down to gradient descent. Typically, we choose $\rho \in (0, 1)$. This inertia is called *momentum* in the optimization literature and ρ is called the momentum coefficient.

2520 Polyak’s method is simple yet very powerful. In the previous chapter, we
 2521 showed a lower-bound of Nesterov which indicates that first-order optimization
 2522 algorithm (that only depends on the gradient of the objective) cannot be faster
 2523 than $\mathcal{O}(1/\sqrt{\epsilon})$. It turns out that Polyak’s method converges at this rate, i.e., if
 2524 we want

$$\|w^t - w^*\| \leq \epsilon$$

2525 we need to run Polyak's Heavy Ball method for $\mathcal{O}(1/\sqrt{\epsilon})$ iterations for convex
 2526 functions. If the function is strongly convex, the number of iterations comes
 2527 down to

$$\mathcal{O}(\sqrt{\kappa} \log(1/\epsilon)).$$

2528 Both of these are improvements upon their convergence rates for gradient
 2529 descent. These improvements are also quite a lot, we need quadratically fewer
 2530 iterations than gradient descent in Polyak's method and the only incremental
 2531 cost of doing so is that we have to maintain a copy of the weights w^{t+1} while
 2532 implementing the updates in (10.4).

2533 **An alternative way to write Polyak's updates** We can rewrite the updates
 2534 in (10.4) using a dummy variable u^t as

$$\begin{aligned} u^t &= (1 + \rho)w^t - \rho w^{t-1} \\ w^{t+1} &= u^t - \eta \nabla \ell(w^t). \end{aligned} \quad (10.5)$$

2535 This is how these updates are implemented in PyTorch. This is convenient:
 2536 effectively, the code needs to maintain only the difference $u^t = (1 + \rho)w^t -$
 2537 ρw^{t-1} in a buffer u^t and subtract the gradient $\nabla \ell(w^t)$ from this update to
 2538 result in the new updates. GD can be implemented with a simple change by
 2539 setting $u^t := w^t$. The dummy variable is initialized to $u^0 = w^0$.

A yet another way to write Polyak's updates We can also rewrite the updates in (10.5) as

$$\begin{aligned} u^{t+1} &= \rho u^t - \nabla \ell(w^t) \\ w^{t+1} &= w^t + \eta u^{t+1}. \end{aligned} \quad (10.6)$$

This set of updates brings out idea of momentum more clearly. The variable u^t in this case is exactly the velocity v^t that we have seen above except that it is updated slightly different than our expression ($F = ma$) in the first equation. The first term

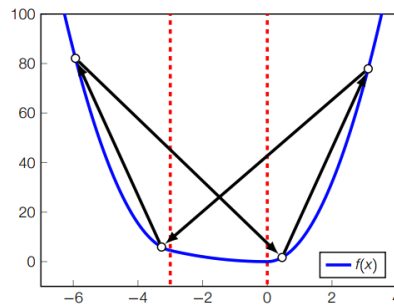
$$u^{t+1} = \rho u^t - \nabla \ell(w^t)$$

reduces the velocity u^t by a factor ρ before adding the gradient to it.

▲ Draw Polyak's updates for a two-dimensional function.

2540 10.1.1 Polyak's method can fail to converge

2541 The caveat with relying on the inertia of the particle to make progress is that
 2542 near the global minimum, when the iterates overshoot the global minimum, the
 2543 inertia is often very different from the gradient. Polyak's method can become
 2544 unstable and can result in oscillations under such conditions, e.g.,



2545

2546 However it is a very simple method to accelerate gradient descent and works
2547 great in practice.

2548 10.2 Nesterov's method

2549 Nesterov's method is an advanced version of Polyak's method and removes
2550 the oscillations towards the end. Let us understand these oscillations better.
2551 We saw that incorporating a notion of inertia in Polyak's method gave us
2552 accelerated convergence; this is intuitive, if the velocity is along the descent
2553 direction the particle descends faster. The same inertia hurts towards the end
2554 because the velocity can be very different than the gradient when the particle
2555 overshoots the minimum.

2556 A simple way to fix this is to incorporate damping (friction) into New-
2557 ton's law of motion; you can read about the simple harmonic oscillator at
2558 https://en.wikipedia.org/wiki/Harmonic_oscillator. We are going to write

$$ma = F - cv.$$

2559 where m is the mass, c is the coefficient of damping, a and v are acceleration
2560 and velocity respectively and F is the force as usual. The effective force
2561 decreases with the velocity. Doing so does not slow down the weight updates
2562 much when the gradient magnitude is large at the beginning of training. But
2563 when the gradient magnitude is small (when the particle is in the neighborhood
2564 of the global minimum), this friction prevents excessive overshooting.

2565 With that background, let us see how Nesterov's updates for gradient
2566 descent look.

We will write a similar set up of updates as that of (10.6). Nesterov's

updates correspond to

$$\begin{aligned} u^{t+1} &= \rho u^t - \nabla \ell(w^t + \eta \rho u^t) \\ w^{t+1} &= w^t + \eta u^{t+1}. \end{aligned} \tag{10.7}$$

The only difference between (10.7) and (10.6) is the term in blue; effectively the gradient is computed as if the weights w^t moved using the velocity u^t ; and then this new velocity u^{t+1} is used to obtain the new updates w^{t+1} . Nesterov's method solves the problem of instability in Polyak's method by essentially computing the gradient (the blue term) as given by the current velocity. You can see how this *slows down* the updates if the velocity is well-aligned with the gradient; we are reducing the benefit of inertia/momentum. However, doing so prevents overshooting as the iterates reach the neighborhood of the global minimum.

2567 **An alternative way to write Nesterov's updates** We can rewrite the up-
2568 dates in (10.7) to look like those in (10.5), to get

$$\begin{aligned} u^t &= (1 + \rho)w^t - \rho w^{t-1} \\ w^{t+1} &= u^t - \eta \nabla \ell(u^t). \end{aligned} \tag{10.8}$$

2569 Again the blue term is the only difference between Polyak's method and
2570 Nesterov's method. The term u^t is conceptually a forecasted version of the
2571 weights w^t because notice that

$$u^t = w^t + \rho(w^t - w^{t-1}).$$

2572 The new weights w^{t+1} are now obtained by thinking of u^t as the actual weights.
2573 We initialize $w^{t+1} = w^t$ to w^0 for $t = 0$.

2574 10.2.1 Yet another way to write Nesterov's updates

2575 We now tie back Nesterov's updates to our introductory narrative on friction.
2576 We will set the damping coefficient (ρ) in (10.8) to a special value

$$\rho = \frac{t-1}{t+2};$$

2577 effectively as $t \rightarrow \infty$ the friction becomes larger and larger. This simplifies
2578 our updates to

$$\begin{aligned} u^t &= w^t + \frac{t-1}{t+2} (w^t - w^{t-1}) \\ w^{t+1} &= u^t - \eta \nabla \ell(u^t). \end{aligned}$$

2579 which upon collapsing together give

$$w^{t+1} - w^t = \frac{t-1}{t+2} (w^t - w^{t-1}) - \eta \nabla \ell(u^t). \tag{10.9}$$

2580 We now choose a different way of interpreting these updates. We will imagine
2581 that the sequence

$$\{w^0, w^1, \dots, w^t, w^{t+1}, \dots\}$$

2582 is the discretization of a smooth curve

$$\{W(\tau) : \tau \in [0, \infty)\}.$$

2583 How is this curve $W(\tau)$ related to the original sequence? We are going to
2584 study the updates under the setting

$$\tau := \sqrt{\eta} t. \quad (10.10)$$

2585 Essentially the time of the discrete-time updates (10.9) increments in intervals
2586 of 1, but the time of the curve $W(\tau)$ is real-number. Each increment in
2587 discrete-time corresponds to $\sqrt{\eta}$ increment of the time τ for the curve $W(\tau)$.
2588 This gives

$$\begin{aligned} W(\tau) &= w^t \\ W(\tau + \sqrt{\eta}) &= w^{t+1}. \end{aligned}$$

2589 We now do a Taylor expansion for the continuous curve $X(\tau)$ to get

$$\begin{aligned} w^{t+1} - w^t &= W(\tau + \sqrt{\eta}) - W(\tau) \\ &= \dot{W}(\tau)\sqrt{\eta} + \frac{1}{2}\ddot{W}(\tau)\eta + \mathcal{O}(\sqrt{\eta}). \end{aligned} \quad (10.11)$$

2590 Here

$$\dot{W}(\tau) = \frac{d}{d\tau}W(\tau), \quad \ddot{W}(\tau) = \frac{d^2}{d\tau^2}W(\tau)$$

2591 are the first and second derivative of the curve with respect to time and $\mathcal{O}(\sqrt{\eta})$
2592 denotes higher-order terms. Similarly

$$\begin{aligned} w^t - w^{t-1} &= W(\tau) - W(\tau - \sqrt{\eta}) \\ &= \dot{W}(\tau)\sqrt{\eta} - \frac{1}{2}\ddot{W}(\tau)\eta + \mathcal{O}(\sqrt{\eta}). \end{aligned}$$

2593 Note that due to our special scaling of time we have

$$\frac{t-1}{t+2} = 1 - \frac{3}{t+2} \approx 1 - \frac{3}{t} = 1 - \frac{3\sqrt{\eta}}{\tau}.$$

2594 We now do a Taylor expansion of the loss term $\nabla \ell(u^t)$ to get

$$\begin{aligned} \nabla \ell(u^t) &= \nabla \ell \left(w^t + \frac{t-1}{t+2} (w^t - w^{t-1}) \right) \\ &= \nabla \ell(w^t) + \text{higher order terms} \\ &= \nabla \ell(W(\tau)) + \mathcal{O}(\sqrt{\eta}). \end{aligned} \quad (10.12)$$

Substitute (10.11) and (10.12) in (10.9) to get

$$\begin{aligned} \dot{W}(\tau) + \frac{1}{2}\ddot{W}(\tau)\sqrt{\eta} + \mathcal{O}(\sqrt{\eta}) &= \left(1 - \frac{3\sqrt{\eta}}{\tau} \right) \left(\dot{W}(\tau) - \frac{1}{2}\ddot{W}(\tau)\sqrt{\eta} + \mathcal{O}(\sqrt{\eta}) \right) \\ &\quad - \sqrt{\eta} \nabla \ell(W(\tau)) + \mathcal{O}(\sqrt{\eta}). \end{aligned}$$

2595 This equation is true for all values of η , so we can compare the coefficients of
2596 $\sqrt{\eta}$ on both sides to get

$$\ddot{W} + \frac{3}{\tau}\dot{W} + \nabla \ell(W) = 0. \quad (10.13)$$

2597 This equation looks very similar to Newton's law with friction $ma + cv = F$.
 2598 Again, the term $\nabla \ell(W)$ is acting as the force, the second derivative \ddot{W} is the
 2599 acceleration and the friction term $\frac{3}{t}\dot{W}$ increases with velocity. We have shown
 2600 that for a particularly chosen value of the momentum coefficient, Nesterov's
 2601 updates result in an ordinary differential equation that looks much like that
 2602 simple harmonic oscillator that most of you have seen before in high-school.
 2603 This approach gives an alternative, and very simple, way of understanding
 2604 Nesterov's updates which is nice because the updates in (10.7) and (10.8) were
 2605 quite non-intuitive and created by Nesterov through a sheer *tour de force*.

2606 **Remark 10.1.** Derive a similar ordinary differential equation for Polyak's
 2607 updates using the same setting of friction $(t - 1)/(t + 2)$ as that in (10.9).
 2608 You will notice that if viewed in continuous-time Polyak's updates are exactly
 2609 the same as Nesterov's updates. This suggests that that the continuous-time
 2610 construct is a more abstract point-of-view and eliminates the subtle differences
 2611 between the updates between the two algorithms.

2612 Such continuous-time constructs are however very useful to understand
 2613 what these updates actually do, e.g., we know that Nesterov's (and Polyak's)
 2614 updates correspond to having friction in Newton's law which is not apparent by
 2615 looking at the equations in (10.8). It is also very easy to obtain the convergence
 2616 rate of the continuous-time version; it is an ordinary differential equation and
 2617 we can use a lot of tools from dynamical systems, in particular Lyapunov
 2618 functions. It will amuse you to know that obtaining the convergence rate for
 2619 Nesterov's updates using the continuous-time version (10.13) takes about half
 2620 a page.

2621 10.2.2 How to pick the momentum parameter?

2622 Nesterov's updates converge at a rate that is similar to that of Polyak's updates.
 2623 For convex functions, we need

$$\mathcal{O}(1/\sqrt{\epsilon})$$

2624 iterations to get within the ϵ -neighborhood of the global minimum if we set

$$\rho = (t - 1)/(t + 2)$$

2625 in (10.6). If we are minimizing a strongly-convex function we can pick the
 2626 momentum coefficient to depend on m, L : we can set

$$\rho = \frac{\sqrt{\kappa} - 1}{\sqrt{\kappa} + 1} \quad (10.14)$$

2627 and $\eta < 2/(m + L)$. Doing so entails that we need only

$$\mathcal{O}(\sqrt{\kappa} \log(1/\epsilon))$$

2628 weight updates to reach within an ϵ -neighborhood of the global minimum. The
 2629 expression in (10.14) gives some insight in how momentum accelerates things.
 2630 If $\kappa \approx 1$, i.e., the Hessian of the objective is well-conditioned without a big
 2631 diversity in the curvature in different directions, we do not really need friction
 2632 $\rho \approx 0$ to avoid overshooting close to the minimum; progress in all directions
 2633 is balanced. On the other hand, if $\kappa \gg 1$, the objective is badly conditioned
 2634 and the friction coefficient $\rho \approx 1$ should be large to avoid overshooting near
 2635 the global minimum.

2636 **How to pick ρ in practice?** If we know what m, L are for a given problem
2637 (you will see an example of this in HW 4), it is straightforward to pick the
2638 momentum coefficient and get accelerated convergence of gradient descent.
2639 If we do not know m, L , we pick some constant value of ρ . For instance,
2640 $\rho = 0.9$ is popularly used in most deep learning libraries. Typically, the
2641 momentum coefficient is not increased with the number of weight updates
2642 using $(t - 1)/(t + 2)$. You will see some heuristics for modifying the momentum
2643 coefficient in this week's recitation.

2644

Chapter 11

2645

Stochastic Gradient Descent

Reading

1. “Stochastic gradient descent tricks” by [Bottou \(2012\)](#). Great paper with lots of little tricks of how to use SGD in practice.
2. Up to Section 4.2 of “Optimization methods for large-scale machine learning” by [Bottou et al. \(2018\)](#). This is advanced material, you do not need to be able to follow it completely.
3. http://fa.bianp.net/teaching/2018/eecs227at/stochastic_gradient.html
4. Stochastic Weight Averaging (SWA) by [Izmailov et al. \(2018\)](#).

2646

Stochastic Gradient Descent (SGD) has its roots in stochastic optimization.

2647

A stochastic optimization problem looks like

$$w^* = \underset{w}{\operatorname{argmin}} \mathbb{E}_{\xi}[\ell(w, \xi)] \tag{11.1}$$

2648

where ξ is a random variable. This is a very old and rich area, there was lots of action in it already in the 1950s, e.g., ([Kushner and Yin, 2003](#); [Robbins and Monro, 1951](#)). It is also a highly relevant problem: for instance, when a plane goes from Los Angeles to Philadelphia, the route that the plane takes depends on the local weather conditions along its path and airlines will optimize this route using a stochastic optimization problem of the above form. The variable w will be the trajectory of the plane and ξ are the weather conditions which we do not know exactly but may perhaps have estimated a distribution for them. Such problems are very common in other fields like operations research, e.g., optimizing the time at which an Amazon package arrives with various disturbances such as delays in shipping, missing inventory in the warehouse etc.

2660

In machine learning, we are interested in solving a slightly different problem called the finite-sum problem. Given a finite dataset $D = \{(x^i, y^i)\}_{i=1, \dots, n}$

2661

2662 we minimize

$$\ell(w) := \frac{1}{n} \sum_{i=1}^n \ell^i(w) \quad (11.2)$$

2663 where we will use the shorthand

$$\ell^i(w) := \ell(w; x^i, y^i)$$

2664 to denote the loss on the datum (x^i, y^i) with weights w . Essentially, the
 2665 random variable ξ in (11.1) represents the samples in the training dataset;
 2666 with important differences being that neither do we know anything about the
 2667 distribution of the input data, nor do we have an infinite number of samples.

2668 It is difficult to do gradient descent if the number of samples n is large
 2669 because the gradient is a summation of a large number of terms

$$\nabla \ell(w) = \frac{1}{n} \sum_{i=1}^n \nabla \ell^i(w).$$

2670 If the mini-batch size is 1, i.e., at each iteration we sample one of the training
 2671 samples denoted by

$$\omega_t \in \{1, \dots, n\}$$

2672 we update the weights using

$$w^{t+1} = w^t - \eta \nabla \ell^{\omega_t}(w^t). \quad (11.3)$$

2673 For a larger mini-batch of size ℓ let us denote the samples in the mini-batch by

$$\{(x^{\omega_t^1}, y^{\omega_t^1}), \dots, (x^{\omega_t^\ell}, y^{\omega_t^\ell})\}$$

2674 where each $\omega_t^k \in \{1, \dots, n\}$ is the index chosen uniformly randomly from
 2675 the training dataset. We will choose these indices with replacement (analyzing
 2676 SGD for sampling without replacement is quite hard). The gradient on this
 2677 sampled mini-batch is denoted by

$$\nabla \ell_\ell(w) := \frac{1}{\ell} \sum_{i=1}^{\ell} \ell^{\omega_t^i}(w) \quad (11.4)$$

2678 and we update the weights as usual using

$$w^{t+1} = w^t - \eta \nabla \ell_\ell(w^t).$$

2679 If $\ell = 1$, we will denote the gradient by $\nabla \ell_\omega$ to keep the notation clear.

2680 **What is an epoch in PyTorch?** We will not think of epochs when we
 2681 develop the theory for SGD. An epoch is a construct introduced in deep
 2682 learning libraries for bookkeeping purposes. It also ensures that if Algorithm A
 2683 obtains so and so training/validation error after 100 epochs, it can be compared
 2684 directly with Algorithm B which obtains the same training/validation error
 2685 after, say, 120 epochs, e.g., one can say Algorithm A is faster than Algorithm
 2686 B at training a network. Instead of sampling a mini-batch of data uniformly
 2687 randomly with replacement, PyTorch shuffles the entire training set at the
 2688 beginning of each epoch and samples the mini-batch *with replacement* during

2689 each epoch. This is reasonable but there will be some discrepancies in the
 2690 performance of SGD as predicted by theory and obtained by PyTorch on deep
 2691 networks, especially if the mini-batch size is large.

2692 Although we will not discuss this, SGD using mini-batches sampled
 2693 with replacement is faster than with mini-batches sampled without replace-
 2694 ment (Recht and Ré, 2012).

2695 11.1 SGD for least-squares regression

2696 Let us understand SGD for one dimensional least-squares, our data and targets
 2697 are $x^i, y^i \in \mathbb{R}$ and the objective is

$$\ell(w) = \frac{1}{2n} \sum_{i=1}^n (x^i w - y^i)^2 \quad (11.5)$$

2698 for the weights $w \in \mathbb{R}$. Notice that the objective is a sum of n different
 2699 quadratics, each quadratic is minimized by *different* weights

$$w^*(i) := \frac{y^i}{x^i};$$

2700 in other words, each sample in the training dataset would like the weight to
 2701 be y^i/x^i to minimize its residual and the least-squares objective which sums
 2702 up their individual residuals forces them to made trade-offs. Focus on two
 2703 quantities

$$w_{\min} = \min_i \{w^*(i)\}, \quad w_{\max} = \max_i \{w^*(i)\}.$$

2704 Notice that the interval $(-\infty, w_{\max})$ is the region where the descent direction
 2705 on any sample in the dataset moves the weights w^t to the right. The interval
 2706 (w_{\max}, ∞) is the region where the descent direction on any sample moves
 2707 the weights to the left. If weights are initialized in the latter region, $w^0 \gg$
 2708 $\max_i w^*(i)$, successive iterations of SGD will quickly bring the weights to

$$w^t \in (w_{\min}, w_{\max}) \quad (11.6)$$

2709 which we will call the “zone of confusion”. Similarly, if weights are initialized
 2710 $w^0 \ll w_{\min}$, they will move right until iterates reach the zone of confusion.

After $w^t \in (w_{\min}, w_{\max})$, there is no real convergence of the weights,

▲ Draw the objective here for different values of w^i and understand how SGD works for this problem.

if the learning rate η is fixed, since the samples ω_t are sampled uniformly randomly, depending upon which sample was chosen to compute the gradient the weights move to the right or the left and therefore keep shuttling back and forth in this region.

Notice that the objective in (11.5) is convex because it is the sum of convex functions so there is a unique global minimum namely

$$w^* = \frac{\sum_{i=1}^n x^i y^i}{\sum_{i=1}^n (x^i)^2}.$$

If one were to execute gradient descent on this same problem $w^{t+1} = w^t - \eta \nabla \ell(w^t)$, we will converge to this value. But since SGD samples a different sample at each iteration, SGD never converges, it remains in this large zone (w_{\min}, w_{\max}) .

2711 11.2 Convergence of SGD

2712 If the learning rate is large, SGD makes quick progress outside the zone
2713 of confusion but bounces around a lot inside the zone of confusion. If the
2714 learning rate is too small, SGD is slow outside the zone of confusion but does
2715 not bounce around too much inside the zone. You can explore how the learning
2716 rate changes the dynamics of SGD at

2717 http://fa.bianp.net/teaching/2018/eecs227at/stochastic_gradient.html.

2718 In this section, we will study under what conditions SGD converges to the
2719 global minimum and how the learning rate of SGD should be reduced to make
2720 it converge quickly. We will first analyze SGD with mini-batch size of 1.

2721 **Strongly convex functions** The proofs for convex functions are tedious, so
2722 we will only consider strongly convex functions in this section. As usual the
2723 strong convexity parameter is m and smoothness parameter is L . One key
2724 thing to notice that these that constants L, m refer to the full objective, i.e.,

$$\|\nabla \ell(w) - \nabla \ell(w')\| \leq L\|w - w'\|$$

2725 and

$$\ell(w) - \frac{m}{2}\|w\|^2 \text{ is convex.}$$

2726 Here $\ell(w)$ is the *full objective*

$$\ell(w) = \frac{1}{n} \sum_{i=1}^n \ell^i(w).$$

2727 **What is the appropriate notion of convergence?** The key difference be-
2728 tween updates of SGD and those of GD is that SGD updates also depend on
2729 the random variable ω_t . The iterate w_t is a *random variable* and therefore
2730 instead of simply bounding the gap $\ell(w^t) - \ell(w^*)$ we will have to obtain an
2731 upper bound for

$$\mathbb{E}_{w^t} [\ell(w^t)] - \ell(w^*).$$

2732 Similar to the case of SGD, let us construct a descent lemma for one
2733 iteration of SGD update.

Lemma 11.1 (Descent Lemma for SGD).

$$\begin{aligned} \mathbb{E}_{\omega_t} [\ell(w^{t+1}) - \ell(w^t) \mid w^t] &\leq -\eta \left\langle \nabla \ell(w^t), \mathbb{E}_{\omega_t} [\nabla \ell^{\omega_t}(w^t)] \right\rangle \\ &\quad + \frac{L\eta^2}{2} \mathbb{E}_{\omega_t} [\|\nabla \ell^{\omega_t}(w^t)\|^2]. \end{aligned} \quad (11.7)$$

2734 **Proof.** First, compare this with the descent lemma for gradient descent (if we
2735 substitute $w^{t+1} - w^t = -\eta \nabla \ell(w^t)$ from Chapter 9)

$$\ell(w^{t+1}) - \ell(w^t) \leq -\eta \langle \nabla \ell(w^t), \nabla \ell(w^t) \rangle + \frac{L\eta^2}{2} \|\nabla \ell(w^t)\|^2$$

2736 The only difference now is that in the case of SGD we have

$$w^{t+1} - w^t = -\eta \nabla \ell^{\omega_t}(w^t).$$

2737 The most important difference however is that the descent term, namely the
2738 left-hand side in (11.7) is conditioned on the random variable w^t . The proof of
2739 this lemma is easy, we simply substitute the expression for the weight updates
2740 of SGD and take an expectation over the index of datum sampled by SGD ω_t
2741 on both sides of the inequality. \square

2742 The implication of the above lemma is that SGD updates need more refined
2743 conditions under which we can claim monotonic progress towards the global
2744 minimum. Effectively, we need to make sure that the right-hand side is
2745 negative, *always* irrespective of what the value of the random variable w^t is.
2746 We would like to upper bound the right-hand side by a deterministic quantity
2747 ideally.

2748 11.2.1 Typical assumptions in the analysis of SGD

2749 1. **Stochastic gradients are unbiased.** Assume that the stochastic gradi-
2750 ent is unbiased

$$\nabla \ell(w) = \mathbb{E}_{\omega} [\nabla \ell^{\omega}(w)] \quad (11.8)$$

2751 for all w in the domain. This is akin to assuming that the way we
2752 sample images in the mini-batch is such that the average is always
2753 pointing towards the true gradient with a similar magnitude. This is a
2754 natural condition and will only change if the sampling distribution is not
2755 uniform. This assumption allows to control the first term in the descent
2756 lemma.

2757 2. **Second moment of gradient norm does not grow too quickly.** We
2758 will assume that there exist scalars σ_0 and σ such that

$$\mathbb{E}_{\omega_t} [\|\nabla \ell^{\omega}(w)\|^2] \leq \sigma_0 + \sigma \|\nabla \ell(w)\|^2. \quad (11.9)$$

2759 This assumption allows to control the second term in the descent lemma
2760 for SGD. It assumes that the stochastic estimate of the gradient in
2761 SGD $\nabla \ell^{\omega_t}(w)$ is not too different than the full gradient $\nabla \ell(w)$. In

2762 the neighborhood of a critical point (locations where the full gradient
2763 $\nabla \ell(w) = 0$), the stochastic gradient is allowed to grow in a similar
2764 fashion as the true gradient except with a scaling factor $\sigma > 0$ and a
2765 constant σ_0 .

2766 Let us see how the descent lemma changes with these additional assump-
2767 tions.

2768 **Lemma 11.2 (Descent Lemma for SGD with additional assumptions).** If
2769 SGD gradients are unbiased and the second moment of the stochastic gradients
2770 can be bounded, we have

$$\begin{aligned}
& \mathbb{E}_{\omega_t} [\ell(w^{t+1}) - \ell(w^t) \mid w^t] \\
& \leq -\eta \left\langle \nabla \ell(w^t), \mathbb{E}_{\omega_t} [\nabla \ell^{\omega_t}(w^t)] \right\rangle + \frac{L\eta^2}{2} \mathbb{E}_{\omega_t} [\|\nabla \ell^{\omega_t}(w^t)\|^2] \\
& \leq -\eta \|\nabla \ell(w^t)\|^2 + \frac{L\eta^2}{2} \mathbb{E}_{\omega_t} [\|\nabla \ell^{\omega_t}(w^t)\|^2] \\
& = -\eta \left(1 - \frac{\eta L \sigma}{2}\right) \|\nabla \ell(w^t)\|^2 + \frac{\eta^2 L \sigma_0}{2}.
\end{aligned} \tag{11.10}$$

2771 The proof is given in (11.10) itself. Compare this to the corresponding
2772 result we have derived for gradient descent in Chapter 9

$$\ell(w^{t+1}) - \ell(w^t) \leq -\frac{\eta}{2} \|\nabla \ell(w^t)\|^2.$$

2773 In addition to the negative term $-\frac{\eta}{2} \|\nabla \ell(w^t)\|^2$, we have two additional posi-
2774 tive terms

$$\frac{\eta^2 L \sigma}{2} \|\nabla \ell(w^t)\|^2 + \frac{\eta^2 L \sigma_0}{2};$$

2775 this indicates that depending upon the magnitude of these terms we may not get
2776 monotonic improvement of the objective for SGD. There is no such concern
2777 for gradient descent, we get monotonic progress at all parts of the domain.

We need to pick the learning rate η in such a way that balances the the right-hand side of (11.10) and makes it negative.

2778 11.2.2 Convergence rate of SGD for strongly-convex func- 2779 tions

2780 **Theorem 11.3 (Optimality gap for SGD).** If we pick a step-size

$$\eta \leq \frac{1}{L\sigma}$$

2781 for m -strongly convex and L -smooth function $\ell(w)$ then the expected optimal-
2782 ity gap satisfies

$$\begin{aligned}
& \mathbb{E}_{\omega_1, \omega_2, \dots, \omega_t} [\ell(w^{t+1})] - \ell(w^*) \\
& \leq \frac{\eta L \sigma_0}{2m} + (1 - \eta m)^t \left(\ell(w^0) - \ell(w^*) - \frac{\eta L \sigma_0}{2m} \right).
\end{aligned} \tag{11.11}$$

We will not cover the proof of this theorem, it is a direct application of the descent lemma. See Bottou et al. (2018, Theorem 4.6) for an elaborate proof.

This theorem beautifully demonstrates the interplay between the step-size and the variance of SGD gradients. If there is no stochasticity, i.e., $\sigma_0 = 0$ and $\sigma = 1$, we get the same result as that of gradient descent, namely, the function value $\ell(w^{t+1})$ converges at a *linear rate* $(1 - \eta m)^t$. Some points to notice

1. The random variable w^{t+1} depends upon all the indices $\omega_1, \omega_2, \dots, \omega_t$ that were sampled during updates of SGD and therefore the expectation in (11.11) should be over all these random variables.
2. When the stochastic gradient is noisy, we have a non-zero σ_0 we can no longer get to the global minimum, there is a first term which does not decay with time.
3. If we pick a small η , we get closer to the global minimum but go there quite slowly. On the other hand, we can pick a large η and get to a neighborhood of the global minimum quickly but we will then have a large error leftover at the end.

How can we make SGD converge and drive down the first term in (11.11) to zero? A simple trick is to reduce the learning rate η with time. We do not want to decay the learning rate too quickly however because the second term in (11.11) is small, i.e., optimality gap is reduced quickly by its multiplicative nature, for a large value of the learning rate. A good schedule to pick is

$$\sum_{t=1}^{\infty} \eta_t = \infty, \quad \text{and} \quad \sum_{t=1}^{\infty} \eta_t^2 < \infty. \quad (11.12)$$

Heuristic for training neural networks The two terms in the convergence rate of SGD explain the widely used heuristic of “divide the learning rate by some constant” if the training error seems plateaued. We are reducing the size of the ball in which SGD iterates bounce around by doing so.

Theorem 11.4 (Convergence rate of SGD for decaying step-size). For a schedule

$$\eta_t = \frac{\beta}{t + t_0} \text{ where } \beta > \frac{1}{m} \text{ and } t_0 \text{ is such that } \eta_1 < \frac{1}{L\sigma}$$

then the expected optimality gap satisfies

$$\mathbb{E}_{\omega_1, \omega_2, \dots, \omega_t} [\ell(w^{t+1})] - \ell(w^*) = \mathcal{O}\left(\frac{1}{t + t_0}\right). \quad (11.13)$$

We will not do the proof. If you are interested, see Bottou et al. (2018, Theorem 4.7). Compare this to the convergence rate of $\mathcal{O}(\kappa \log(1/\epsilon))$ for gradient descent for strongly-convex functions. Notice that we converge only at a sub-linear rate for SGD even for strongly convex loss functions. SGD is a much slower algorithm than GD.

2812 **Convergence rate for mini-batch SGD** The mini-batch gradient $\nabla \ell_\ell(w)$
 2813 is still an unbiased estimate of the full-gradient

$$\mathbb{E}[\nabla \ell_\ell(w)] = \nabla \ell(w)$$

2814 but the second assumption in SGD improves a bit. Since the mini-batch
 2815 gradient is averaged over ℓ samples we have

$$\mathbb{E}[\|\nabla \ell_\ell(w)\|^2] \leq \frac{\sigma_0}{\ell} + \frac{\sigma}{\ell} \|\nabla \ell(w)\|^2$$

2816 if σ_0, σ were the constants in (11.9). This changes the convergence rate
 2817 in Theorem 11.3 to

$$\begin{aligned} & \mathbb{E}_{\omega_1, \omega_2, \dots, \omega_t} [\ell(w^{t+1})] - \ell(w^*) \\ & \leq \frac{\eta L \sigma_0}{2m\ell} + (1 - \eta m)^t \left(\ell(w^0) - \ell(w^*) - \frac{\eta L \sigma_0}{2m\ell} \right). \end{aligned} \quad (11.14)$$

2818 Note that the maximum learning rate in Theorem 11.3 is inversely proportional
 2819 to σ so we can also pick a larger learning rate $\eta < \frac{\ell}{L\sigma}$. If we do so, the first
 2820 and last terms above are not affected by the batch-size but multiplicative term
 2821 $(1 - \eta m)^t$ is. Since

$$(1 - \eta m)^t \leq e^{-tm\eta}$$

2822 we see that increasing the learning rate by a factor of ℓ will reduce the number
 2823 of iterations required to reach the zone of confusion by a factor of ℓ . Of
 2824 course, this comes with the caveat that each iteration also requires $\mathcal{O}(\ell)$ more
 2825 computation to compute the gradient compared to single-sample SGD.

2826 11.2.3 When should one use SGD in place of GD?

2827 Theorem 11.4 indicates that SGD is a very slow algorithm, GD is much faster
 2828 than SGD to minimize strongly convex functions. This gap also exists if we do
 2829 not have strong convexity: we did not prove this but SGD requires $\mathcal{O}(1/\epsilon^2)$ to
 2830 reach an ϵ -neighborhood of the global optimum for convex functions whereas
 2831 GD requires a much smaller $\mathcal{O}(1/\epsilon)$. One might wonder why we should use
 2832 SGD at all.

2833 It is critical to remember that the objective in machine learning is a sum of
 2834 many terms

$$\ell(w) = \frac{1}{n} \sum_{i=1}^n \ell^i(w)$$

2835 One iteration of SGD requires us to compute only $\nabla \ell^{\omega_t}(w)$ whereas one
 2836 update of GD requires us to compute the full gradient $\nabla \ell(w)$. One weight
 2837 update of GD is $\mathcal{O}(n)$ more expensive than one weight update using SGD. Let
 2838 us do a back-of-the-envelope computation for convex functions. If we want
 2839 to reach an ϵ -neighborhood of the global minimum of a convex function, we
 2840 need $\mathcal{O}(1/\epsilon)$ iterations of GD, which requires

$$\mathcal{O}\left(\frac{n}{\epsilon}\right)$$

2841 operations. SGD needs $\mathcal{O}(1/\epsilon^2)$ iterations and therefore requires

$$\mathcal{O}\left(\frac{1}{\epsilon^2}\right)$$

2842 operations to reach the ϵ -neighborhood. This indicates that if our chosen ϵ -ball
2843 is

$$\epsilon \lesssim \frac{1}{n}$$

2844 GD requires fewer overall operations. But if ϵ -ball is larger than this, we
2845 should use SGD because it is computationally cheaper.

2846 SGD is particularly suited to machine learning compared to GD for the
2847 following reason. Let $\epsilon^i = \ell^i(w^t) - \ell^i(w^*)$ be the residual on the i^{th} datum
2848 in the training dataset. Observe that our ϵ -neighborhood is

$$\epsilon = \ell(w^t) - \ell(w^*) = \frac{1}{n} \sum_{i=1}^n \epsilon^i.$$

2849 If ϵ^i is constant and does not depend on the number of training samples n
2850 (i.e., say we are happy with the average error over the training dataset being
2851 2% even and do not seek a smaller one even if we collect more data) then we
2852 should use SGD to train our model because it is cheaper. This is not always
2853 the case for other problems, e.g., if you are doing computational tomography
2854 (capturing multiple images from a CT-scan machine and trying to reconstruct
2855 the heart/lung region in the thoracic cavity), we may seek a more and more
2856 accurate answer, i.e., small ϵ if we have more data.

2857 11.3 Accelerating SGD using momentum

2858 The convergence rate of SGD is quite bad, it is sub-linear. Roughly speaking,
2859 the successive iterates of SGD are computed using different mini-batches; the
2860 gradient on each such mini-batch is a noisy approximation of the full-gradient
2861 on the training dataset (that of GD). This makes the SGD iterates noisy and one
2862 may improve the convergence rate of SGD by simply averaging the weights.
2863 This leads to a simple technique to accelerate SGD which we discuss next.

2864 **Polyak-Ruppert averaging** Consider the updates

$$\begin{aligned} w^{t+1} &= w^t - \eta_t \nabla \ell_\delta(w^t) \\ u^t &= \frac{w^0 + w^1 + \dots + w^t}{t}. \end{aligned} \tag{11.15}$$

2865 In a series of papers, [Polyak \(1990\)](#); [Polyak and Juditsky \(1992\)](#); [Ruppert](#)
2866 [\(1988\)](#) showed that the quantity

$$\mathbb{E}_{\omega_1, \dots, \omega_{t-1}} [\ell(u^t)] - \ell(w^*)$$

2867 converges faster than the quantity

$$\mathbb{E}_{\omega_1, \dots, \omega_{t-1}} [\ell(w^t)] - \ell(w^*);$$

2868 both of these still converge at rate $\mathcal{O}(1/\epsilon^2)$ but the former has a smaller
2869 constant. This is quite surprising and useful: essentially we are still performing
2870 mini-batch updates for the weights w^t but instead of thinking of w^t as the
2871 answer, we think of u^t as the output of SGD. This averaging of iterates does
2872 not change the SGD algorithm. Computing this output requires us to remember

2873 all the past iterations w^0, \dots, w^t but we can easily approximate that step by
 2874 exponential averaging of the *weights*

$$u^t = \rho u^{t-1} + (1 - \rho) w^t;$$

2875 exponential averaging is likely to achieve the same purpose with a much
 2876 smaller memory requirement.

2877 Further, this idea of using averaged iterates to speed up stochastic opti-
 2878 mization algorithms is quite general and also works for algorithms other than
 2879 SGD. The paper on Stochastic Weight Averaging by [Izmailov et al. \(2018\)](#)
 2880 performs weight averaging (with quite different motivations) and works very
 2881 well in practice.

2882 11.3.1 Momentum methods do not accelerate SGD

2883 We saw that momentum is very useful to accelerate the convergence of gradient
 2884 descent. The power of momentum lies in making faster progress using the
 2885 inertia of the particle: if the velocity and the current gradient are aligned with
 2886 each other (as is the case at the beginning of training when the iterates are far
 2887 from the global optimum) momentum speeds up things. Towards the end of
 2888 training when gradients are typically mis-aligned with the velocity, we need
 2889 friction (as in Nesterov’s updates) to reduce this effect.

2890 Observe that in SGD, the gradient is *always* incorrect; it is after all only
 2891 a noisy stochastic approximation of the full gradient on the dataset. Since
 2892 the velocity $w^t - w^{t-1}$ was computed using the previous stochastic gradient,
 2893 there is no reason to believe that this velocity is accurate and will speed up
 2894 SGD. Here is a very important point ([Kidambi et al., 2018](#); [Liu and Belkin, 2018](#))
 2895 that you should remember.

Momentum methods (Polyak’s or Nesterov’s) do not significantly
 accelerate SGD.

2896 To be more precise, we saw that for Nesterov’s updates in GD for strongly-
 2897 convex functions we have a result of the form

$$\|w^t - w^*\| \leq e^{-t/\sqrt{\kappa}} \|w^0 - w^*\|$$

2898 while the constant without momentum is larger, it is $e^{-t/\kappa}$. This term is
 2899 directly related to the second term in [Theorem 11.4](#). The above authors
 2900 come up with counterexamples to show that Nesterov’s updates with SGD
 2901 only improve this multiplicative term to something like $e^{-ct/\kappa}$ for some c ; in
 2902 other words using Nesterov’s updates with SGD only lead to a constant factor
 2903 improvements in the convergence rate.

2904 Accelerating stochastic optimization algorithms is done via the use of
 2905 control variates ([Le Roux et al., 2012](#)). Broadly speaking these methods
 2906 work by using the previous gradients in SGD $\{\nabla \ell^{\omega_1}(w^1), \dots, \nabla \ell^{\omega_t}(w^t)\}$ to
 2907 compute some surrogate for the current full gradient $\nabla \ell(w^t)$ and compute the
 2908 descent direction using both this surrogate full gradient and the standard SGD
 2909 gradient.

2910 **Why do we use Nesterov’s method to train deep networks?** It is worth-
 2911 while to think why we use Nesterov’s momentum to train deep networks: (i)
 2912 we know that momentum does not help speed up training, and (ii) momentum
 2913 is simply a faster way to minimize the same objective ℓ so it does not have
 2914 any regularization properties that help generalization either. We do not have a
 2915 definitive answer to this question yet but here is what we know.

2916 Datasets that we use in deep learning represent quite narrow distributions
 2917 (natural images of animals, household objects etc.). For instance, the two
 2918 images below are essentially the same in spite of belonging to different classes.



2919

2920 Most weights of a deep network will have a similar gradient for these images as
 2921 input, the weights for which the gradient will differ are likely to be the weights
 2922 at the top few layers of the network. This entails that even if the stochastic
 2923 gradients are computed on different mini-batches, they are essentially quite
 2924 similar to each other, and thereby to the full-gradient. More precisely, the
 2925 covariance of mini-batch gradients

$$\text{Cov}(\nabla \ell_{\delta}(w), \nabla \ell_{\delta'}(w)) = \mathbb{E}_{\delta, \delta'} \left[(\nabla \ell_{\delta}(w) - \nabla \ell(w)) (\nabla \ell_{\delta'}(w) - \nabla \ell(w))^{\top} \right]$$

2926 is a matrix with very few non-zero eigenvalues; only about 0.5% of the
 2927 eigenvalues are non-zero (Chaudhari and Soatto, 2017) even for large networks.
 2928 This means that the SGD gradient while training deep networks is essentially
 2929 the full gradient and we should expect momentum to accelerate convergence
 2930 in practice.

2931 11.4 Understanding SGD as a Markov Chain

2932 The preceding development tells us how SGD works and how many iterations
 2933 of SGD we need to get within an ϵ -neighborhood of the global minimum
 2934 for convex functions. Things are not this easy to understand for non-convex
 2935 functions; essentially if we have two minima u^*, v^*

$$\nabla \ell(u^*) = \nabla \ell(v^*) = 0$$

2936 depending upon where GD/SGD are initialized they can converge to different
 2937 places. In this section, we will look at an alternative way of understanding
 2938 how SGD works for non-convex functions. The development here will be
 2939 much more abstract than the preceding section because we want to capture the
 2940 overall properties of SGD.

2941 11.4.1 Gradient flow

2942 Let us first talk about gradient descent. Just like we constructed a model for
 2943 Nesterov’s updates using a differential equation, we will first construct a model
 2944 for gradient descent using a differential equation. The updates are given by

$$w^{t+1} - w^t = -\eta \nabla \ell(w^t).$$

▲ A non-convex function with two local minima. The one on the left is the global minimum but gradient descent may not always reach here.



2945 If we again imagine a continuously differentiable curve $W(\tau)$ as a model for
 2946 these discrete-time updates and time

$$d\tau := \eta$$

2947 we can write a differential equation of the form

$$\frac{dW}{d\tau} = \dot{W}(\tau) = -\nabla \ell(W(\tau)); \quad W(0) = w^0. \quad (11.16)$$

2948 This is called gradient flow. If we wanted to execute gradient flow on a
 2949 computer, we can do so using Euler discretization

$$\dot{W}(\tau) \approx \frac{W(\tau + \Delta\tau) - W(\tau)}{\Delta\tau} = -\nabla \ell(W(\tau)).$$

2950 for any value of the time-step $\Delta\tau$. If the time-step $\Delta\tau = \eta$ we get exactly
 2951 gradient descent. More precisely, gradient flow is the limit of gradient descent
 2952 as the learning rate $\eta \rightarrow 0$. It is important to always remember that gradient
 2953 flow is a model for GD, not GD itself. Our goal in the remainder of the section
 2954 is to develop a similar model for SGD.

2955 11.4.2 Markov chains

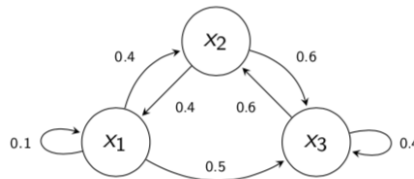
2956 Consider the Whack-The-Mole game: a mole has burrowed a network of three
 2957 holes w^1, w^2, w^3 into the ground. It keeps going in and out of the holes and
 2958 we are interested in finding which hole it will show up next so that we can give
 2959 it a nice whack.

- Three holes:

$$X = \{x_1, x_2, x_3\}.$$

- Transition probabilities:

$$T = \begin{bmatrix} 0.1 & 0.4 & 0.5 \\ 0.4 & 0 & 0.6 \\ 0 & 0.6 & 0.4 \end{bmatrix}$$



2960

2961 This is an example of a Markov chain. There is a transition matrix P which
 2962 determines the probability P_{ij} of the mole resurfacing on a given hole w^j
 2963 given that it resurfaced at hole w^i the last time. The matrix P^t is the t -step
 2964 transition matrix

$$P_{ij}^t = \mathbb{P}(w^t = w^j \mid w^{(0)} = w^i).$$

2965 If there exist times t, t' such the both the probabilities

$$\mathbb{P}(w^t = w^j \mid w^{(0)} = w^i) \quad \mathbb{P}(w^{t'} = w^i \mid w^{(0)} = w^j)$$

2966 are non-zero the two states w^i and w^j are said to “communicate”

$$w^i \leftrightarrow w^j$$

2967 The set of states in the Markov chain that *all* communicate with each other
 2968 are an equivalence class. This means that the Markov chain can visit any state

2969 from any other state in this equivalence class with non-zero probability, we
 2970 just might have to wait for a really long time if $P_{ij}^t \approx 0$ for two states w^i, w^j .
 2971 If all the states in the Markov chain belong to the same equivalence class, it
 2972 is called irreducible. A related concept is that of “positive recurrence”, i.e.,
 2973 if the Markov chain was at a state w at some time, it comes back to the same
 2974 state after some finite time. Since the process is Markov it forgets that is just
 2975 came back to the same state and therefore positive recurrence also means that
 2976 if we consider an infinitely long trajectory of a Markov chain, the chain visits
 2977 the same state infinitely many times along this trajectory. You can see the
 2978 animations at <https://setosa.io/ev/markov-chains> to build more intuition.

2979 **Invariant distribution of a Markov chain** The probability of being in a
 2980 state w^i at time $t + 1$ can be written as

$$\mathbb{P}(w^{t+1} = w^i) = \sum_{j=1}^N \mathbb{P}(w^{t+1} = w^i \mid w^t = w^j) \mathbb{P}(w^t = w^j).$$

2981 This equation governs how the probabilities $\mathbb{P}(w^t = w^i)$ change with time t .
 2982 Let’s do the calculations for the Whack-The-Mole example. Say the mole was
 2983 at hole w^1 at the beginning. So the probability distribution of its presence

$$\pi^{(t)} = \begin{bmatrix} \mathbb{P}(w^t = w^1) \\ \mathbb{P}(w^t = w^2) \\ \mathbb{P}(w^t = w^3) \end{bmatrix}$$

2984 is such that

$$\pi^1 = [1, 0, 0]^\top.$$

2985 We can now write the above formula as

$$\pi^{(t+1)} = P^\top \pi^{(t)}$$

2986 and compute the distribution $\pi^{(t)}$ for all times

$$\begin{aligned} \pi^2 &= P^\top \pi^1 = [0.1, 0.4, 0.5]^\top; \\ \pi^3 &= P^\top \pi^2 = [0.17, 0.34, 0.49]^\top; \\ \pi^4 &= P^\top \pi^3 = [0.153, 0.362, 0.485]^\top; \\ &\vdots \\ \pi^\infty &= \lim_{t \rightarrow \infty} P^t \pi^1 \\ &= [0.158, 0.355, 0.487]^\top. \end{aligned}$$

2987 If such a distribution π^∞ exists, the Markov chain is said to have “equilibrat-
 2988 ed” or reached an invariant distribution. The numbers $\mathbb{P}(w^{t+1} = w^i)$ stop
 2989 changing with time. We can compute this invariant distribution by writing

$$\pi^\infty = P^\top \pi^\infty.$$

2990 Does such a limiting invariant distribution π^∞ always exist? It turns out that if
 2991 a Markov chain has a finite number of states then the invariant distribution π^∞
 2992 always exists; this is easy to show yourself. If the Markov chain is irreducible
 2993 and aperiodic, then the invariant distribution is also unique. We can also
 2994 compute the π^∞ given a transition matrix P : the invariant distribution is the
 2995 (right-)eigenvector of the matrix P^\top corresponding to the eigenvalue 1.

2996 **Periodicity of a Markov chain** A state of a Markov chain is periodic with
 2997 period k if the probability of coming back to the same state is zero for times
 2998 that *are not* integral multiples of k and the probability of coming back to the
 2999 same state is non-zero for all times that *are* integral multiples of k . To take a
 3000 simple example, every number of a clock is a periodic state; the Markov chain
 3001 comes back to that state at regular intervals. If we cannot find such a time k
 3002 for a given state, then the state is aperiodic. It is easy to see that if there exists
 3003 an aperiodic state in one communicating class, then all the other states in that
 3004 class also have to be aperiodic. It is useful to remember that if a particular
 3005 state has a non-zero probability of self-transition, then the state is aperiodic.

3006 **Example 11.5.** Consider a Markov chain on two states where the transition
 3007 matrix is given by

$$P = \begin{bmatrix} 0.5 & 0.5 \\ 0.4 & 0.6 \end{bmatrix}.$$

3008 This is an irreducible Markov chain because you can hop between any two
 3009 states with non-zero probability within one step. It is also recurrent: this is
 3010 intuitive because say the Markov chain was in state 1, it is easy for it to come
 3011 back to this state after a few hops. After the chain comes back to state 1, the
 3012 Markov property means the chain forgets all the past steps and will again
 3013 come back to state 1. The expected number of times the Markov chain comes
 3014 back to state 1 is infinite. Each of the two states has a non-zero probability of
 3015 self-transition, so both of them are aperiodic.

3016 We are therefore guaranteed that a unique invariant distribution exists for
 3017 this Markov chain. In this case it is

$$\begin{aligned} \pi^1 &= 0.5\pi^1 + 0.4\pi^2 \\ \pi^2 &= 0.5\pi^1 + 0.6\pi^2. \end{aligned}$$

3018 Note that the constraint for π being a probability distribution, i.e., $\pi^1 + \pi^2 = 1$
 3019 is automatically satisfied by the two equations. We can solve for π^1, π^2 to get

$$\pi^1 = 4/9 \quad \pi^2 = 5/9.$$

3020 **Time spent at a particular state by the Markov chain** We can observe a
 3021 long trajectory of a Markov chain and compute the number of times the chain
 3022 is in a particular state w^i . This is directly proportional to $\pi^\infty(w^i)$. In other
 3023 words, if the invariant distribution gives small probability to a particular state,
 3024 if we stop the Markov chain at an arbitrary time during its trajectory, we are
 3025 very unlikely to find the Markov chain at this state.

3026 11.4.3 A Markov chain model of SGD

3027 The updates of SGD with mini-batch size ℓ are given by

$$w^{t+1} - w^t = -\eta \nabla \ell_\ell(w^t).$$

3028 Notice that conditional on the iterate w^t , the next iterate w^{t+1} is independent
 3029 of w^{t-1} , all these three quantities are random variables because they depend
 3030 on the input data $\omega_0, \dots, \omega_t$ sampled by SGD in the previous time-steps. You
 3031 should never make the mistake of saying that gradient descent is a Markov
 3032 chain; there is no randomness in the iterates of GD.

3033 **Transition probability of SGD** What is the transition probability

$$\mathbb{P}(w^{t+1} | w^t)$$

3034 for SGD? If we take the conditional expectation on both sides

$$\mathbb{E}_{\mathfrak{b}} [w^{t+1} - w^t | w^t] = -\eta \mathbb{E}_{\mathfrak{b}} [\nabla \ell(w^t)] = -\eta \nabla \ell(w^t);$$

3035 in other words, on-average the change in weights at w^t is proportional to the
3036 full gradient $\nabla \ell(w^t)$. Notice that the change in weights exactly the same for
3037 GD; this should not be surprising after all, if the gradient of SGD is unbiased
3038 then SGD is GD “on-average”.

3039 **Variance of SGD weight updates** The variance is computed as follows

$$\begin{aligned} \text{Var}_{\mathfrak{b}} (w^{t+1} - w^t | w^t) &= \eta^2 \text{Var}_{\mathfrak{b}} (\nabla \ell_{\mathfrak{b}}(w^t) | w^t) \\ &= \eta^2 \mathbb{E}_{\mathfrak{b}} \left[(\nabla \ell_{\mathfrak{b}}(w^t) - \nabla \ell(w^t)) (\nabla \ell_{\mathfrak{b}}(w^t) - \nabla \ell(w^t))^{\top} \right] \end{aligned}$$

3040 Notice that the variance of the weight updates in SGD is proportional to the
3041 square of the learning rate. We have seen this before, larger the learning rate
3042 more noisy the weight update as compared to the update using the full-gradient
3043 $\eta \nabla \ell(w^t)$. The variance is a large matrix $\in \mathbb{R}^{p \times p}$; this matrix depends on the
3044 current weight w^t .

3045 If we are sampling the data inside a mini-batch with replacement the
3046 stochastic gradients are independent for different samples ω^1 and ω^2 in the
3047 mini-batch

$$\nabla \ell^{\omega^1}(w) \perp \nabla \ell^{\omega^2}(w).$$

3048 In other words

$$\mathbb{E}_{\omega^1, \omega^2} \left[(\nabla \ell^{\omega^1}(w^t) - \nabla \ell(w^t)) (\nabla \ell^{\omega^2}(w^t) - \nabla \ell(w^t))^{\top} \right] = 0.$$

3049 You can use this to show that

$$\begin{aligned} \text{Var}_{\mathfrak{b}} (w^{t+1} - w^t | w^t) &= \eta^2 \text{Var}_{\omega^1, \dots, \omega^{\mathfrak{b}}} \left(\frac{1}{\mathfrak{b}} \sum_{i=1}^{\mathfrak{b}} \nabla \ell^{\omega^i}(w^t) \right) \\ &= \frac{\eta^2}{\mathfrak{b}^2} \sum_{i=1}^{\mathfrak{b}} \text{Var}_{\omega^i} (\nabla \ell^{\omega^i}(w^t)) \quad (11.17) \\ &= \frac{\eta^2}{\mathfrak{b}} \text{Var}_{\omega} (\nabla \ell^{\omega}(w^t)). \end{aligned}$$

3050 The last step follows because we are sampling inputs ω^i uniformly randomly
3051 and therefore gradients $\nabla \ell^{\omega^i}(w^t)$ are not just independent but also identically
3052 distributed. In other words, a mini-batch size of \mathfrak{b} reduces the variance by a
3053 factor of \mathfrak{b} .

3054 **SGD is like GD with Gaussian noise** We now *model* the transition proba-
3055 bility $\mathbb{P}(w^{t+1} | w^t)$ as a Gaussian distribution. Let us denote by W^t, W^{t+1}
3056 etc. the updates of this model. We now have

$$W^{t+1} = W^t + \xi^t$$

3057 where ξ^t is Gaussian noise

$$\xi^t \sim N\left(-\eta \nabla \ell(w^t), \frac{\eta^2}{\mathfrak{b}} \text{Var}(\nabla \ell(w^t))\right).$$

3058 In other words, on-average SGD updates weights like gradient descent, by a
3059 term $-\eta \nabla \ell(w^t)$ but SGD's updates also have a variance.

3060 Such equations are called stochastic difference equations and they are quite
3061 difficult to understand compared to non-stochastic difference equations (what
3062 we see in gradient descent). So we will make a drastic simplification in our
3063 model. We will say that the variance of the mini-batch gradients is identity.
3064 Our model for SGD is

$$W^{t+1} = W^t - \eta \nabla \ell(W^t) + \frac{\eta}{\sqrt{\mathfrak{b}}} \xi^t \quad (11.18)$$

3065 where we have zero-mean unit-variance Gaussian noise $\xi^t \sim N(0, I_{p \times p})$.

3066 **Remark 11.6.** The above model for SGD is a Markov chain except that the
3067 states in the Markov chain is infinite; the number of states in the Whack-The-
3068 Mole example were finite. It is easy to see that the above model is not exactly
3069 SGD: (i) we assumed the the transition probability was a Gaussian which need
3070 not be the case while training a deep network, (ii) we further assumed that
3071 the Gaussian noise does not depend on w^t and has identity covariance. You
3072 can implement the above model on a computer, first you compute the *full*
3073 *gradient* $\nabla \ell(w^t)$ and then sample Gaussian noise ξ^t to update the weights to
3074 W^{t+1} . This is obviously not equivalent to SGD which updates weights using
3075 the stochastic gradient $\nabla \ell_{\mathfrak{b}}(w^t)$.

3076 11.4.4 The Gibbs distribution

3077 In a Markov chain we were interested in the invariant distribution because that
3078 gives us a way to understand where the chain spends most of its time. We can
3079 compute the invariant distribution for our model of SGD. It is a very powerful
3080 result (which we will not do) and leads to the so-called Gibbs distribution. The
3081 probability density of the invariant distribution is given by

$$\rho^\infty(w) = \frac{1}{Z(\beta)} e^{-\beta \ell(w)}. \quad (11.19)$$

3082 The quantity

$$\beta = \frac{2\mathfrak{b}}{\eta} \quad (11.20)$$

3083 and $Z(\beta)$ is a normalizing constant for probability density

$$Z(\beta) = \int_{\mathbb{R}^p} e^{-\beta \ell(w)} \mathrm{d}w.$$

3084 Let us list a few properties of the Gibbs distribution that are apparent
3085 simply by looking at the above expression.

- 3086 1. The invariant distribution is reached asymptotically and is the limiting
3087 distribution of the weights. For instance the sum of the weights along an
3088 infinitely long trajectory converges to the mean of the Gibbs distribution

$$\lim_{T \rightarrow \infty} \frac{1}{T} \sum_{t=1}^T W^t = \int_w w \rho^\infty(w) \mathrm{d}w. \quad (11.21)$$

3089 Similarly, the second moment of the weights along a long trajectory of
 3090 SGD converges to the second moment of the Gibbs distribution; and
 3091 same for the variance.

$$\lim_{T \rightarrow \infty} \frac{1}{T} \sum_{t'=1}^T \sum_{t=1}^T (W^{t'}) (W^t)^\top = \int_{w, w'} w w'^\top \rho^\infty(w) \rho^\infty(w') \, dw dw'. \quad (11.22)$$

3092 2. The probability that the iterates of SGD are found at a location w is
 3093 proportional to $e^{-\beta \ell(w)}$. If the training loss $\ell(w)$ is high, this probability
 3094 is low and if the training loss is low, the probability is high. The Gibbs
 3095 distribution therefore shows that if we let SGD run until it equilibrates
 3096 we have a high chance of finding the iterates that have a small training
 3097 loss. This observation is powerful because it does not require us to
 3098 assume that $\ell(w)$ is convex. However this statement does require the
 3099 assumption that the steps-size η of SGD does not go to zero; after all
 3100 SGD iterates *stop* if $\eta = 0$.

3101 3. The quantity $1/\beta$ is quite common in physics where it is called the
 3102 “temperature”. This temperature $\beta^{-1} = \frac{\eta}{2\ell}$ fundamentally governs how
 3103 the Gibbs distribution looks. Higher the temperature, more the noise in
 3104 the iterates and vice-versa. If the learning rate η is large or the batch-size
 3105 ℓ is small, it is easy for *our model of SGD* to jump over hills. This is
 3106 the reason why the Gibbs distribution will be spread around the entire
 3107 domain at high temperature. On the other hand, if temperature is very
 3108 small, the Gibbs distribution puts a large probability mass in places
 3109 where the training loss is small and the probability of finding iterates
 3110 at other places in the domain diminishes. In particular, if $\beta \rightarrow \infty$, the
 3111 Gibbs distribution only puts non-zero probability on the global minima
 3112 of the loss function $\ell(w)$.

3113 4. Written in another way, if we want the Gibbs distribution to remain the
 3114 same we should ensure that

$$\beta^{-1} = \frac{\eta}{2\ell} \text{ is a constant.}$$

3115 If you increased the batch-size by two times, you should also double the
 3116 learning rate if you desire that the solutions of SGD are qualitatively
 3117 similar.

3118 5. We have achieved something remarkable by looking at the Gibbs distri-
 3119 bution. We have discovered an algorithm to find the global minimum of
 3120 a non-convex loss function.

- 3121 • Start from some initial condition w^0 ;
- 3122 • Take lots of steps of SGD with learning rate η until SGD reaches
 3123 its invariant distribution, i.e., until it equilibrates;
- 3124 • Reduce the step-size η and repeat the previous step

3125 This is only a formal algorithm but in theory it will converge to the
 3126 global minimum of a non-convex function $\ell(w)$ if the number of steps
 3127 is very large. The catch of course is that at each step we have to wait
 3128 until SGD equilibrates. For many problems, it may take an inordinately
 3129 long amount of time for SGD to equilibrate.

It is very important to remember that when we train a deep network we are executing one run of SGD. The invariant distribution is an abstract concept that does not really exist on your computer. We have constructed this model to help us understand how updates of SGD behave.

11.4.5 Convergence of a Markov chain to its invariant distribution

For gradient descent and SGD, we had quantities like $\|w^t - w^*\|$ or $\ell(w^t) - \ell(w^*)$ that let us measure the progress towards the global minimum. For a non-convex problem, there may not exist a unique global minimum, or there may be multiple local minima in the domain where the gradient vanishes. We discussed in the preceding section how the invariant distribution of SGD is achieved even if the loss $\ell(w)$ is non-convex. In this section, we will see a simple tool to measure progress towards this distribution.

Let us define a quantity called the Kullback-Leibler (KL) divergence between two probability distributions. For two probability distributions $p(w)$ and $q(w)$ supported on a discrete set $w \in W$, the KL-divergence is given by

$$\text{KL}(p \parallel q) = \sum_{w \in W} p(w) \log \frac{p(w)}{q(w)}. \quad (11.23)$$

This formula is well-defined only if for all w where $q(w) = 0$, we also have $p(w) = 0$. The KL-divergence is a measure of the distance between two distributions, it is zero if and only if $p(w) = q(w)$ for all $w \in W$. It is always positive (you can show this easily using Jensen's inequality). However, the KL-divergence is not a metric because it is not symmetric

$$\text{KL}(p \parallel q) \neq \text{KL}(q \parallel p) = \sum_{w \in W} q(w) \log \frac{q(w)}{p(w)}.$$

For probability densities, the KL-divergence

$$\text{KL}(p \parallel q) = \int_w p(w) \log \frac{p(w)}{q(w)} dw \quad (11.24)$$

is defined analogously and has the same properties.

We will now show a very powerful result: the KL-divergence of the state distribution of a Markov chain decreases monotonically as the Markov chain converges to its invariant distribution. Although, this result is true for SGD as well, we will only prove it for a Markov chain with finite states. Let the initial distribution of the Markov chain be π^0 , its transition matrix be P and its invariant distribution be π^∞ . We will assume that the Markov chain is such that the invariant distribution exists (it is irreducible and recurrent).

Let us also assume that a reverse transition matrix

$$P_{ij}^{\text{rev}} = \mathbb{P}(w^t = w^i | w^{t+1} = w^j).$$

3157 exists; such Markov chains are called reversible. For any states w, w' this
3158 transition matrix satisfies the definition of conditional probability

$$\mathbb{P}(w^{t+1} = w' | w^t = w) \mathbb{P}(w^t = w) = \mathbb{P}(w^t = w | w^{t+1} = w') \mathbb{P}(w^{t+1} = w').$$

3159 In our notation, this becomes

$$P_{ww'}^{\text{rev}} = \frac{P_{w'w} \pi(w')}{\pi(w)} = \frac{P_{w'w} \pi(w')}{\sum_{w'} P_{w'w} \pi(w')}.$$

3160 **Lemma 11.7.** For a reversible Markov chain with an invariant distribution
3161 π^∞ , $\text{KL}(\pi^\infty \parallel \pi^t)$ decreases monotonically:

$$\text{KL}(\pi^\infty \parallel \pi^{t+1}) \leq \text{KL}(\pi^\infty \parallel \pi^t). \quad (11.25)$$

3162 **Proof.** The proof is a simple calculation.

$$\begin{aligned} \text{KL}(\pi^\infty \parallel \pi^{t+1}) &= \sum_w \pi^\infty(w) \log \frac{\pi^\infty(w)}{\pi^{t+1}(w)} \\ &= \sum_w \pi^\infty(w) \log \frac{\pi^\infty(w)}{\sum_{w'} P_{w'w} \pi^t(w')} \\ &= - \sum_w \pi^\infty(w) \log \frac{\sum_{w'} P_{w'w} \pi^t(w')}{\pi^\infty(w)} \\ &= - \sum_w \pi^\infty(w) \log \left(\sum_{w'} P_{ww'}^{\text{rev}} \frac{\pi^t(w')}{\pi^\infty(w')} \right) \quad (\text{substitute definition of } P^{\text{rev}} \text{ for distribution } \pi^\infty) \\ &\leq - \sum_w \pi^\infty(w) \sum_{w'} P_{ww'}^{\text{rev}} \log \frac{\pi^t(w')}{\pi^\infty(w')} \quad (\text{Jensen's inequality}) \\ &= \sum_{w'} \sum_x P_{ww'}^{\text{rev}} \pi^\infty(w) \log \frac{\pi^\infty(w')}{\pi^t(w')} \quad (\text{flip the negative sign, exchange sum}) \\ &= \sum_{w'} \pi^\infty(w') \log \frac{\pi^\infty(w')}{\pi^t(w')} \\ &= \text{KL}(\pi^\infty \parallel \pi^t). \end{aligned}$$

3163 The distance to the invariant distribution π^∞ decreases at each step of the
3164 Markov chain. A similar statement is true for the reverse KL divergence:

$$\text{KL}(\pi^{t+1} \parallel \pi^\infty) \leq \text{KL}(\pi^t \parallel \pi^\infty).$$

3165

□

The above result is also true for SGD which, as we discussed, can

be modeled as a Markov chain with infinite states. It gives us some very important intuition. Just like gradient descent makes monotonic progress towards the global minimum w^* , a Markov chain (or SGD) makes monotonic progress towards its invariant distribution. The big difference between them is that while we required that the loss function $\ell(w)$ is convex for gradient descent to guarantee this monotonic progress, the loss need not be convex for the case of the Markov chain model of SGD.

This result *does not* mean that SGD makes monotonic progress towards the global minimum $w^* = \operatorname{argmin}_w \ell(w)$. We choose to look at SGD not as one particle undergoing (stochastic) gradient descent updates but rather as a Markov chain. The probability distribution of states of this Markov chain is then a legitimate object (the distribution π^t is the distribution of weights W^t obtained after many independent run of SGD from different initializations). Although π^t is *not* meaningful across *one* run of SGD, we can use it to get an abstract understanding of how SGD also makes monotonic progress as it converges if we imagine many *independent* runs of SGD occurring simultaneously.

3166 Chapter 12

3167 Shape of the energy 3168 landscape of neural 3169 networks

Reading

1. Goodfellow Chapter 13
2. “Neural Networks and Principal Component Analysis: Learning from Examples Without Local Minima” by [Baldi and Hornik \(1989\)](#)
3. “Entropy-SGD: Biasing gradient descent into wide valleys” by [Chaudhari et al. \(2016\)](#)

3170 In this chapter, we will try to understand the shape of the objective for
3171 training neural networks. We would like to characterize the difficulty of
3172 training neural networks. We know that the objective is not convex and training
3173 a network is difficult because of it. But how non-convex is the objective? The
3174 questions we want to answer here are of the following form.

- 3175 1. How many global minima exist?
- 3176 2. How many local minima and saddle points exist?
- 3177 3. What is the loss at the local minima or saddle points? If we train with
3178 gradient descent or stochastic gradient descent, what loss can we expect
3179 to obtain even if we don’t reach the global minimum?
- 3180 4. What is the local geometry of the loss function?
- 3181 5. What is the global topology of the loss function?

3182 This will help understand how SGD seems to train deep networks so
3183 efficiently and why we often get very good generalization error after training.
3184 As a pre-cursor to how the picture of the energy landscape of a neural network
3185 looks like, here’s one picture from [Li et al. \(2018\)](#):

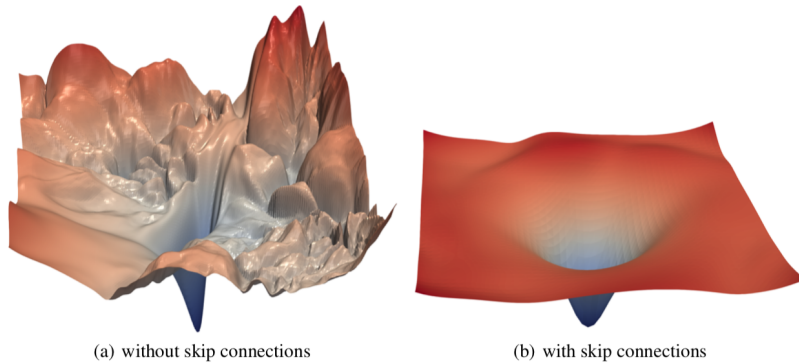


Figure 12.1: A picture of the training loss. The picture on the left was created by sampling two directions randomly out of the millions of weights for a residual network without skip-connections and computing the training loss by discretization of this two-dimensional space. The picture on the right is a similar picture for the resnet with skip-connections intact. In this picture, we see that while the training loss is very complex on the left-hand side with lots of local minima and saddle points, the loss is much more benign on the right-hand side.

12.1 Introduction

Let us introduce a few quantities that will help characterize the energy landscape. We will consider the case when the function $\ell(w)$ is twice-differentiable.

Global minima are all points in the set

$$\{w : \ell(w) \leq \ell(w') \text{ for all } w'\}.$$

Note that there may exist many different locations all with the same loss $\ell(w)$, they would all be global minima in this case. Local minima are all points in the set

$$\{w : \nabla \ell(w) = 0, \nabla^2 \ell(w) \succeq 0\}.$$

i.e., all points w where the Hessian $\nabla^2 \ell(w)$ is positive semi-definite. Note that the two conditions (i) first-order stationarity $\nabla \ell(w) = 0$ and (ii) positive semi-definiteness of the Hessian $\nabla^2 \ell(w) \succeq 0$ also have to be satisfied for all global minima. Critical points are all locations which satisfy only first order stationarity

$$\{w : \nabla \ell(w) = 0\}.$$

Saddle points are critical points but which are neither local minima nor local maxima

$$\{w : \nabla \ell(w) = 0, \nabla^2 \ell(w) \text{ is neither positive nor negative semi-definite}\}.$$

Non-convex functions, in general, can have all these different kinds of locations in the energy landscape and this makes minimizing the objective difficult. Our goal in this chapter is to learn theoretical and empirical results that help paint a mental picture of what the energy landscape looks like.

🔍 Draw the Gibbs distribution of SGD if $\ell(w)$ has multiple global minima.

🔍 Draw the Gibbs distribution of SGD if $\ell(w)$ has multiple global minima and multiple local minima.

3204 12.2 Deep Linear Networks

3205 Let us consider the simplest case of linear neural networks first. We will have
 3206 a two-layer neural network which takes in inputs x^i and aims to predict targets
 3207 y^i . For simplicity, we will consider the case when both

$$x^i, y^i \in \mathbb{R}^d.$$

3208 and use the regression loss

$$\ell(A, B) = \frac{1}{2n} \sum_{i=1}^n \|y^i - AB x^i\|_2^2 \quad (12.1)$$

3209 We use the standard trick of appending a 1 to the input x^i so that we don't
 3210 have to carry around biases in our equations.

3211 The matrices A, B are the weights of the neural network with

$$A \in \mathbb{R}^{d \times p}, B \in \mathbb{R}^{p \times d}.$$

3212 We will consider the case when $p \leq d$. We are interested in finding A and B
 3213 and will develop some results from Baldi & Hornik's paper.

3214 **Least squares solution** A simple calculation reveals that for a single-layer
 3215 network the solution of the problem

$$L^* = \operatorname{argmin}_L \frac{1}{2n} \sum_{i=1}^n \|y^i - Lx^i\|_2^2$$

3216 is

$$L^* = \Sigma_{yx} \Sigma_{xx}^{-1} \quad (12.2)$$

3217 where

$$\Sigma_{yx} = \sum_i y^i x^{i\top}$$

$$\Sigma_{xx} = \sum_i x^i x^{i\top}.$$

3218 The matrices Σ_{yx} and Σ_{xx} are the data covariance matrices.

3219 **Projection of a vector onto a matrix** It will be useful to define a projection
 3220 matrix. Say we have a vector v that we want to project on the span of the
 3221 columns of a full-rank matrix

$$M = [m_1 \quad m_2 \quad \dots \quad m_n].$$

3222 If this projection is $\hat{v} \in \operatorname{span}\{m_1, \dots, m_n\}$, we know that it has to satisfy

$$(v - \hat{v}) \perp m_k \text{ for all } k \leq n \quad \Rightarrow \quad m_k^\top (v - \hat{v}) = 0.$$

3223 The vector \hat{v} is also obtained by a combination of the columns of M , so there
 3224 exists a vector c which allows us to write

$$\hat{v} = Mc.$$

3225 These together imply

$$c = (M^\top M)^{-1} M^\top \hat{v}$$

3226 and finally

$$\hat{v} = \underbrace{M(M^\top M)^{-1} M^\top}_{\text{projection matrix}} v \\ =: P_M v.$$

3227 where the matrix P_M is called the projection matrix corresponding to the
3228 matrix M .

3229 **Back to deep linear networks** We know from the homework problem that
3230 there is no unique solution to the problem

$$A^*, B^* = \operatorname{argmin}_{A, B} \frac{1}{2n} \sum_{i=1}^n \|y^i - AB x^i\|_2^2.$$

3231 If A^*, B^* are solutions, so are $A^*P, P^{-1}B^*$ for any invertible matrix P . We
3232 also showed in the homework that the objective is not convex. But if we fix
3233 either A or B and only optimize over the other, the loss is convex. Notice that
3234 the rank of AB is at most p .

3235 **Fact 12.1 (Critical points of B if A is fixed).** For any A , the function $\ell(A, B)$
3236 is convex in B and has a minimum at

$$(A^\top A) \hat{B}(A) \Sigma_{xx} = A^\top \Sigma_{yx}.$$

3237 If Σ_{xx} is invertible and A is full-rank, then we can write

$$\hat{B}(A) = (A^\top A)^{-1} A^\top \Sigma_{yx} \Sigma_{xx}^{-1}. \quad (12.3)$$

3238 Note that these are all locations when the gradient

$$\frac{\partial \ell}{\partial B} = 0.$$

3239 **Fact 12.2 (Critical points of A if B is fixed).** We have an analogous version
3240 of the previous fact for A : if B is fixed, the loss is convex in A , for full-rank
3241 Σ_{xx} and B , then for $\frac{\partial \ell}{\partial A} = 0$, we should have

$$AB \Sigma_{xx} B^\top = \Sigma_{yx} B^\top. \quad (12.4)$$

3242 or

$$\hat{A}(B) = \Sigma_{yx} B^\top (B \Sigma_{xx} B^\top)^{-1}. \quad (12.5)$$

3243 **Fact 12.3 (Critical points of (A, B)).** We now solve the equations (12.3)
3244 and (12.5) to get a critical point, i.e., the gradient of the objective in both A
3245 and B is zero. First

$$W = AB = P_A \Sigma_{yx} \Sigma_{xx}^{-1}. \quad (12.6)$$

3246 from (12.3). Next, multiply on both sides of (12.4) by A^\top and substitute the
3247 above value of W to get that the matrix A should satisfy

$$P_A \Sigma = \Sigma P_A = P_A \Sigma P_A.$$

3248 where

$$\Sigma = \Sigma_{yx} \Sigma_{xx}^{-1} \Sigma_{xy}.$$

▲ Note that $P_M^2 = P_M$, i.e., if we project the vector twice onto the column space of M , the second projection does nothing. Also, any projection matrix P is symmetric. To see this, consider two vectors v, w and the dot products

$$\langle Pv, w \rangle, \text{ and } \langle v, Pw \rangle.$$

In both cases, one of the vectors lies completely in the column space of M and therefore the dot product ignores any component that is orthogonal to the column space of M . This means

$$\langle Pv, w \rangle = \langle v, Pw \rangle = \langle Pv, Pw \rangle.$$

We can now rewrite the first equality to obtain

$$(Pv)^\top w = v^\top (Pw) \\ \Rightarrow v^\top P^\top w = v^\top Pw$$

and since this is true for any two vectors v, w , we have that $P = P^\top$.

3249 **Fact 12.4 (If W is a critical point, then it can be written as a projection**
 3250 **of the least squares solution $\Sigma_{yx}\Sigma_{xx}^{-1}$ on the subspace spanned by some p**
 3251 **eigenvectors of Σ).** This is an important fact. Let us say we have a full-rank Σ
 3252 with distinct eigenvalues $\lambda_1 > \dots > \lambda_d$. Let u_{i_k} be the eigenvector associated
 3253 with the i_k^{th} eigenvalue of Σ . So given any set of p eigenvalues

$$\mathcal{I} = \{i_1, \dots, i_p\} \text{ with } 1 \leq i_k \leq d \text{ for all } k.$$

3254 we can define a matrix of rank p

$$U_{\mathcal{I}} = [u_{i_1} \quad u_{i_2} \quad \dots \quad u_{i_p}].$$

3255 Then one can show that the matrices A and B are critical points if and only if
 3256 there is a set \mathcal{I} and an invertible matrix $C \in \mathbb{R}^{p \times p}$ such that

$$\begin{aligned} A &= U_{\mathcal{I}} C \\ B &= C^{-1} U_{\mathcal{I}}^{\top} \Sigma_{yx} \Sigma_{xx}^{-1}. \end{aligned} \quad (12.7)$$

3257 You can find the proof in the Appendix of Baldi & Hornik's paper. Because
 3258 $U_{\mathcal{I}}$ is a matrix of orthonormal vectors we also have

$$P_{U_{\mathcal{I}}} = U_{\mathcal{I}} U_{\mathcal{I}}^{\top}$$

3259 and therefore

$$W = P_{U_{\mathcal{I}}} \Sigma_{yx} \Sigma_{xx}^{-1}$$

3260 which is the same form for W as (12.6) in Fact 3 and L^* in (12.2). In other
 3261 words, the solution $W = AB$ in a two-layer linear network is given by our
 3262 original least squares regression matrix followed by an orthogonal projection
 3263 onto the subspace spanned by p eigenvectors of Σ .

3264 **Fact 12.5 (If W is the global minimum for a two-layer network, then it is**
 3265 **a projection of the solution for a single-layer network onto the subspace**
 3266 **spanned by the top p eigenvectors of Σ).** You can further show that the
 3267 objective

$$\ell(A, B) = \text{trace}(\Sigma_{yy}) - \sum_{i_k \in \mathcal{I}} \lambda_{i_k}. \quad (12.8)$$

3268 at a critical point (A, B) . The first term is a constant with respect to the
 3269 parameters of the network A, B . The second term is a sum of the eigenvalues
 3270 of the matrix Σ at indices that we picked in our set $U_{\mathcal{I}}$. What is the index set
 3271 that minimizes this loss? It is simply the largest p eigenvalues of Σ . This is also
 3272 a unique value for the loss because we have assumed that all the eigenvalues
 3273 are distinct. This also solidifies the connection of this model with Principal
 3274 Component Analysis (PCA), the matrix W is projecting on the sub-space
 3275 spanned by the top p eigenvectors in the auto-associative case.

3276 **Fact 12.6 (There are exponentially many saddle points for a two-layer**
 3277 **network).** There are a total of $\binom{d}{p}$ possible index sets \mathcal{I} . One of them as we
 3278 saw above corresponds to a global minimum. It can be shown that all the
 3279 others are saddle points. Note that there are exponentially many saddle points.
 3280 This is an important fact to remember: there are exponentially many saddle
 3281 points in a hierarchical architecture. Smaller the number of neurons in the
 3282 hidden layer p (also the upper bound for the rank of the weight matrices),

🔗 Based on the previous two facts, what can you say about the solution W if $p \geq d$ and Σ is invertible? Since the two-layer network simply projects on the p eigenvalues of Σ , if $p \geq d$ and Σ is invertible, the solution already lies in the column-space of Σ and therefore $W = L^*$.

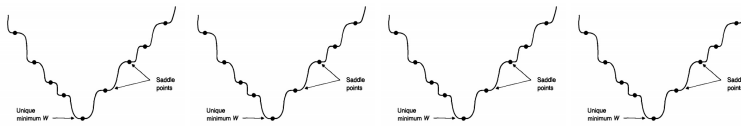
3283 fewer are the number of saddle points but this also creates a dimensionality
 3284 bottleneck in the feature space. If p is too small as compared to d we lose
 3285 large amounts of information necessary to classify the image and the network
 3286 may not work well.

3287 **Fact 12.7 (No local minima in a deep linear network, all minima are**
 3288 **global minima).** The proof of the previous fact (see the Appendix of [Baldi](#)
 3289 [and Hornik \(1989\)](#)) shows that any index set $\mathcal{I} \neq \{1, \dots, p\}$ cannot be a local
 3290 minimum. There are no local minima for a deep linear network, only global
 3291 minima and saddle points. This is often said as “linear networks have no bad
 3292 local minima”.

3293 **Fact 12.8 (The global minimum is not unique).** This is perhaps the most
 3294 important point of this chapter. The loss at the global minimum is unique,
 3295 not the global minimum itself. Any full-rank square matrix $C \in \mathbb{R}^{p \times p}$ of our
 3296 choice gives a pair of solutions (A, B) . How many such solutions are there?
 3297 There are lots and lots of such solutions, in fact, given any solution with a
 3298 particular C if we can perturb the C without losing rank (quite easy to do
 3299 by, say, changing the eigenvalues slightly) we get another solution of a linear
 3300 network.

3301 **Fact 12.9 (All the previous results are true for multi-layer linear net-**
 3302 **works).** The same results are true for deep linear networks ([Kawaguchi,](#)
 3303 [2016](#)). These results also hold if $\dim(y_i) = 1$, i.e., for the regression case.

We used a simple two-layer linear network to obtain an essentially complete understanding of how the loss function looks like. A schematic looks as follows.



There are lots of locations where the global minimum of the function is achieved. There are lots of saddle points in the energy landscape. The Gibbs distribution for this energy landscape has a lot of modes, one each at the global minima.

3304 How does weight-decay

$$\Omega(A, B) = \lambda (\|A\|_F^2 + \|B\|_F^2)$$

3305 change the energy landscape of deep linear networks? It changes the number
 3306 of global minima, only the ones that have the smallest ℓ_2 norm remain in the
 3307 energy landscape. It also reduces the number of saddle points because the
 3308 Hessian at saddle points has an extra additive term that involves λ .

3309 12.3 Extending the picture to deep networks

3310 Let us think carefully about the non-uniqueness of the solution for a two-layer
3311 network. We know that all critical points are of the form

$$A = U_{\mathcal{I}}C,$$
$$B = C^{-1}U_{\mathcal{I}}^{\top}\Sigma_{yx}\Sigma_{xx}^{-1}.$$

3312 The gradient at these critical points is zero. Given a particular C , we can
3313 perturb it slightly and obtain a new critical point (a new saddle point, or a new
3314 global minimum) and this keeps the objective unchanged. Effectively, we have
3315 a connected set of global minima and saddle points for a deep linear networks.

3316 If one were to try to visualize this energy landscape and extend the picture
3317 heuristically to deep networks with nonlinearities, we can think of the global
3318 minimum as looking like the basin of the Colorado river.



3319

3320 The important point to remember from this picture is that all the points at
3321 the basin of the river are solutions that obtain a good training loss. Although
3322 gradient-based algorithms (GD/SGD etc.) do not allow us to travel along the
3323 river (the gradient is zero along it), if the river basin snakes around in the
3324 entire domain, no matter where the network is initialized, we always have a
3325 global minimum close to the initialization. Essentially, the objective of deep
3326 networks is not convex, but current results indicate that it is quite benign. And
3327 this is perhaps the reason why it is so easy to train them.

Chapter 13

Generalization performance of machine learning models

This chapter gives a preview of generalization performance of deep networks. We will take a more abstract view of learning algorithms here and focus only on binary classification. We will first introduce a “learning model”, i.e., a formal description of what learning means. The topics we will discuss stem from the work of two people: **Leslie Valiant** who developed the most popular learning model called Probably Approximately Correct Learning (PAC-learning) and **Vladimir Vapnik** who is a Russian statistician who developed a theory (called the VC-theory) that provided a definitive answer on the class of hypotheses that were learnable under the PAC model.

13.1 The PAC-Learning model

Our goal in machine learning is to use the training data in order to construct a model that generalizes well, i.e., has good performance outside of the training data. Formally, we search over a hypothesis space \mathcal{F} , e.g., a specific neural net architecture, using the available data to find a good hypothesis $f \in \mathcal{F}$. As we motivated in Chapter 2, without further assumptions, we cannot guarantee that this hypothesis works well on test data. We therefore assume two things in this chapter:

1. Nature provides independent and identically distributed samples $x \in \mathcal{X}$ from some (unknown to the learner) distribution P .
2. Nature labels these samples with $c(x)$ which is again unknown to the learner.

Both training and test data are samples from Nature’s distribution P . We will also assume that even if the true labeler $c(x)$ is unknown to us, we know that it belongs to a chosen hypothesis class \mathcal{C} and is deterministic, i.e., Bayes error is zero. Changing this assumption does not change the crux of this theory.

Consider a learning algorithm, denoted by L . Given a dataset $D = \{(x^i, c(x^i))\}_{i=1}^n$ and a hypothesis class \mathcal{C} , the population risk (for classifi-

3359 cation) of the hypothesis output by this learning algorithm is

$$R(h) = \mathbb{E}_{x \sim P} [\mathbf{1}_{\{f(x) \neq c(x)\}}]$$

3360 Let us assume that the learning algorithm is deterministic for now, i.e., given
3361 a training dataset D it returns a unique answer f . Let us assume that the
3362 hypothesis class that the learner searches over, named \mathcal{F} is the same as the
3363 hypothesis class \mathcal{C} . What do we want from this algorithm?

3364 We expect that it works well for all hypotheses Nature could use to label
3365 data $c \in \mathcal{C}$ and all datasets D drawn from P . The PAC-Learning model
3366 postulates the following desiderata upon the learning algorithm.

3367 1. We are okay with an answer f with error

$$R(f) \in [0, 1/2)$$

3368 because we only have access to finitely many training data. This is
3369 the “approximate correct” part of the PAC-Learning. However the error
3370 should decrease as n increases.

3371 2. The dataset D is a random variable. This implies that the hypothesis
3372 outputted by the learning algorithm $f(D)$ is also a random variable. The
3373 above statement therefore should hold with some large probability over
3374 draws of the dataset D . In other words, there can be a small probability
3375 that a non-representative dataset D is drawn and we do not expect
3376 the learner to output a good hypothesis with $R(f) < 1/2$. However
3377 the probability of such failure, let us call it $\delta \in [0, 1/2)$, should also
3378 become smaller if more data is provided. This is the “probably” part of
3379 PAC-Learning.

3380 We now have a definition of what it means to be a good learning algorithm.

3381 **Definition 13.1 (PAC-learnable hypothesis class).** A hypothesis class \mathcal{C} is
3382 PAC-learnable if there exists an algorithm L such that for every $c \in \mathcal{C}$, for
3383 every $\epsilon, \delta \in [0, 1/2)$, if L is given access to $n(\epsilon, \delta)$ i.i.d. training data from P
3384 and their corresponding labels c then it outputs a hypothesis $h_D \in \mathcal{C}$ such that

$$\mathbb{P}_D (R(f) < \epsilon) \geq 1 - \delta.$$

3385 We want the learner to be statistically efficient, i.e., as our desiderata ϵ, δ
3386 get smaller, we should expect $n(\epsilon, \delta)$ to not grow too quickly. For instance, we
3387 would like $n(\epsilon, \delta)$ to be a polynomial function of $1/\epsilon$ and $1/\delta$. The minimum
3388 number of samples $n(\epsilon, \delta)$ required to learn a hypothesis class \mathcal{C} is called the
3389 sample complexity of \mathcal{C} . One is also typically interested in the computational
3390 complexity of finding f , e.g., to avoid a brute-force algorithm L that searches
3391 over the entire hypothesis class $\mathcal{F} = \mathcal{C}$; we will not worry about it here.

3392 It is important to notice that PAC-learning assumes nothing about *how* L is
3393 going to use the data, e.g., whether it runs SGD or what surrogate loss it uses,
3394 or even whether it performs Empirical Risk Minimization. In this sense, the
3395 above learning model is very abstract and we should expect only qualitative
3396 answers from this theory.

3397 **Example 13.2 (Learning Monotone Boolean Formulae).** Let $x = [x_1, \dots, x_d]$
3398 be the datum and $c(x)$ be a conjunction, e.g.,

$$c(x) = x_1 \wedge x_3 \wedge x_4.$$

3399 To take a few examples, $c(10011) = 0$ and $c(11110) = 1$. Such formulae are
 3400 called monotone because no literals show up as negated in the formula.

3401 We can have the hypothesis class \mathcal{F} to be the set of all possible conjunc-
 3402 tions of d variables x_1, \dots, x_d . Each literal x_i can be in the conjunction or
 3403 not, so the total number of hypotheses in \mathcal{F} is 2^d .¹ Observe that since this is
 3404 exponential in d , an algorithm L that brute-force searches over \mathcal{F} will have a
 3405 large computational complexity. Also observe that since the true hypothesis
 3406 $c \in \mathcal{F}$, there exists an answer f that the algorithm L can output that achieves
 3407 zero training error, i.e.,

$$\min_{f \in \mathcal{F}} \frac{1}{n} \sum_{i=1}^n \mathbf{1}_{\{f(x^i) \neq c(x^i)\}} = 0.$$

3408 But for a fixed amount of data n , there is some probability that the minimizing
 3409 hypothesis f has zero training error but large population risk. As the number
 3410 of data n is large, we expect this event to be less and less probable.

3411 Consider an algorithm L that does the following. It starts with the hypoth-
 3412 esis

$$f^0(x) = x_1 \wedge x_2 \wedge \dots \wedge x_d$$

3413 with all literals and for every datum with a label 1, it deletes all literals x_i that
 3414 are not in this datum to update the hypothesis f ; this makes sense because if
 3415 the deleted literals were zero in some input, f and c would predict different
 3416 outputs. Remember that since $c(x) \in \mathcal{F}$, we cannot have a datum with input
 3417 $1111 \dots 1$ and output 0.

3418 What kind of errors does this algorithm make? If some literal x_i was
 3419 deleted, it is because it had the value $x_i = 0$ on a positively labeled sample.
 3420 So, it should be deleted, otherwise the hypothesis will output 0. So, we only
 3421 output a wrong hypothesis if more literals present than those in $c(x)$. So, the
 3422 output $f(x)$ can only make an error on data labeled 1 by $c(x)$, never on the
 3423 ones labeled zero. Our algorithm therefore only has false negatives.

3424 We now see why requesting more samples diminishes the probability of
 3425 this event happening. Let $p_i = \mathbb{P}_{x \sim P} [c(x) = 1, x_i = 0 \text{ in } x]$. Therefore

$$R(h) \leq \sum_{x_i \in f} p_i$$

3426 If some p_i is small, then it does not contribute much to the error. If some
 3427 p_i is large then we make sure to see enough samples so that we remove that x_i
 3428 from f . After all, it only takes one appearance of this event to delete this x_i ,
 3429 and the event has probability p_i which is large. Rigorously, if all x_i in f have
 3430 $p_i < \epsilon/d$ then $R(h) < \epsilon$. On the other hand, if some x_i has $p_i > \epsilon/d$ then the
 3431 probability of having this x_i in f is the probability that the event of p_i never
 3432 happens in the draw of n samples. But this new probability is smaller than
 3433 $1 - \epsilon/d$. And the event will never happen in n i.i.d. draws with probability at
 3434 most $(1 - \epsilon/d)^n \leq e^{-n\epsilon/d}$. Using the union bound, since there are at most
 3435 d literals in f , the probability that there is at least one such “bad event” is at
 3436 most $de^{-n\epsilon/d}$.

¹Actually the total number of conjunctions is $2^d + 1$ because for the null-conjunction (without any literals) we can have the constant $c(x) = 0$ or $c(x) = 1$ for all x . We should therefore explicitly make sure $c(111 \dots 11) = 0$ is not in the true labeling function. But we ignore this corner case, and silently assume that only the hypothesis $c(x) = 1 \forall x$ is in our class \mathcal{C} .

3437 If this bad event never happens the population risk is less than ϵ . Of course,
 3438 such a bad event happening would be devastating. For some distributions it
 3439 could lead the error up to 1. However, in our PAC-learning setting we can
 3440 accept this as long as it happens rarely with probability at most δ . Since

$$de^{-n\epsilon/d} < \delta \iff n \geq \frac{d}{\epsilon} \log \frac{d}{\delta}$$

3441 we are guaranteed to meet the PAC criteria: of error less than ϵ with probability
 3442 at least $1 - \delta$.

3443 Note that both the sample complexity and computational complexity are
 3444 polynomial. We have thus shown that the class of Monotone Boolean Formulae
 3445 is (ϵ, δ) -PAC learnable.

3446 13.2 Concentration of Measure

3447 Two very important results from probability theory that we will use are the
 3448 Union Bound and the Chernoff Bound.

3449 13.2.1 Union Bound (or Boole's Inequality)

3450 For any countable set of events, $\{A_1, \dots, A_n, \dots\}$,

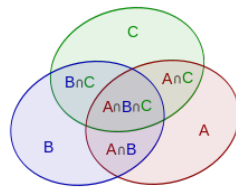
$$\mathbb{P}\left(\bigcup_i A_i\right) \leq \sum_i \mathbb{P}[A_i].$$

3451 This is a rather loose, but useful, upper bound and is (mostly) embedded in
 3452 the assumptions of what we call a "probability measure" in probability theory
 3453 (σ -subadditivity). This essentially means that it can be used without any extra
 3454 assumptions in practice.

3455 By the inclusion-exclusion principle for finite set of events $\{A_1, \dots, A_n\}$,

$$\mathbb{P}\left(\bigcup_{i=1}^n A_i\right) = \sum_{i=1}^n \mathbb{P}(A_i) - \sum_{1 \leq i < j \leq n} \mathbb{P}(A_i, A_j) + \dots + (-1)^{n-1} \mathbb{P}(A_1, A_2, \dots, A_n)$$

3456 We can get better approximations of the union, if we use the first $k \leq n$ terms
 3457 above. If we stop at odd k , we get an upper bound. If we stop at even k we get
 3458 a lower bound. The error of the approximation is decreasing with k .



3459

3460 13.2.2 Chernoff Bound

3461 Let A_1, \dots, A_n be a sequence of i.i.d. random variables. We focus on the
 3462 case of Bernoulli random variables where $\mathbb{P}(A_i = 1) = p$. We would like

▲ If we want a better approximation of the probability of the union of multiple events and we know more about the problem at hand we can use what are called Bonferroni inequalities.

❓ Where did we use the union bound in the proof for the PAC-learnability of the class of monotone Boolean functions?

❓ Try to prove that

$$\mathbb{P}\left(\bigcap_{i=1}^n A_i\right) \geq 1 - \sum_{i=1}^n \mathbb{P}(A_i^c)$$

3463 to estimate p from samples. One way to do this is to compute the empirical
3464 average

$$\hat{p} = \frac{1}{n} \sum_{i=1}^n A_i$$

3465 and estimate how close it is to the true p . We know that as $n \rightarrow \infty$

3466 **Weak Law** For all $\epsilon > 0$ we have

$$\mathbb{P}(|\hat{p} - p| > \epsilon) \rightarrow 0.$$

3467 This is also known as convergence in probability.

3468 **Strong Law** We have almost sure convergence, i.e.,

$$\mathbb{P}\left(\lim_{n \rightarrow \infty} \hat{p} = p\right) = 1.$$

3469 **Central Limit Theorem** As $n \rightarrow \infty$, the quantity $\sqrt{n}(\hat{p} - p)$ is distributed
3470 as a Normal distribution with mean zero and variance $p(1 - p)$. Notice that
3471 as opposed to the law of large numbers, the central limit theorem also gives
3472 us a rate of convergence, i.e., how many samples n are necessary if want the
3473 difference to be close to a Normal distribution. If we set $\sigma^2 = p(1 - p)$ we
3474 can rewrite the Central Limit Theorem as

$$\mathbb{P}(|\hat{p} - p| > \epsilon) \leq 2e^{-n\epsilon^2/(2\sigma^2)}.$$

3475

3476 **Chernoff Bound** Since $\sigma^2 = p(1 - p) < 1/4$ we have from CLT that

$$\mathbb{P}\left(\left|\frac{1}{n} \sum_i A_i - p\right| > \epsilon\right) \leq 2e^{-2n\epsilon^2}.$$

3477 An easy way to remember the Chernoff bound is that if we want the average
3478 of n random variables to be ϵ -close to their expected value with probability at
3479 least $1 - \delta$, then we need

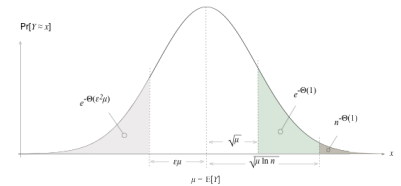
$$n = \Omega\left(\frac{1}{\epsilon^2} \log \frac{1}{\delta}\right)$$

3480 samples.

3481 Concentration of measure is an exciting area of probability theory and
3482 similar results can be obtained for other distributions, other functions than aver-
3483 aging of random variables A_1, \dots, A_n etc. Popular inequalities are Markov's
3484 Inequality, Chebyshev's Inequality and Chernoff Bounds (and Hoeffding's
3485 Inequality as an important special case). They are written in terms of increas-
3486 ing tightness, but also of increasing assumptions of what we need to know
3487 in order compute them. You can read a very good introduction to this topic
3488 at <https://terrytao.wordpress.com/2010/01/03/254a-notes-1-concentration-of-measure/>.
3489

3490 In general, Markov's inequality only needs the expectation, Chebyshev's
3491 Inequality needs the variance too, while Chernoff bounds usually need the

▲ This picture makes it easy to remember concentration inequalities for an n -dimensional Gaussian random variable Y .



❓ Do you see any patterns in the Chernoff bound with sample complexity in PAC-learning?

3492 whole moment generating function. They are all applications of Markov's
 3493 Inequality on higher order statistics. The value of Chernoff bounds is in-
 3494 creasingly more important when we talk about distributions of few sufficient
 3495 statistics, like the Bernoulli distribution (or any exponential distribution).

3496 13.3 Uniform convergence

3497 We now lift the assumption that Nature's labeling function $c \in \mathcal{C}$. After all,
 3498 even if there exists such a true deterministic c we can never be sure that it is
 3499 inside \mathcal{F} , say the class of neural networks of a specific architecture that we are
 3500 using. This model is called the Agnostic PAC-Learning model.

3501 We will stay within the confinements of Empirical Risk Minimization
 3502 where we are provided with some samples where we output the hypothesis
 3503 with the smallest training error

$$\hat{R}(f) = \frac{1}{n} \sum_{i=1}^n \mathbf{1}_{\{f(x^i) \neq y^i\}} \quad \text{minimizing this gives } f_{\text{ERM}} \in \mathcal{F}.$$

3504 The population risk is

$$R(f) = \mathbb{E}_{(x,y) \sim P} [\mathbf{1}_{\{f_{\text{ERM}}(x) \neq y\}}] \quad \text{minimizing this gives } f^* \in \mathcal{F}.$$

3505 Observe that f^* is *not* the Bayes optimal predictor that we saw in the bias-
 3506 variance tradeoff. This is because the former is restricted to the hypothesis
 3507 class \mathcal{F} while the latter has no such restriction to lie in \mathcal{F} , it is simply the
 3508 optimal hypothesis that minimizes the population risk.

Our goal while computing a *generalization bound* is to ask the following question: if we obtain an ERM hypothesis f_{ERM} with a good training error, then does this also mean that the population risk of the best hypothesis in the class \mathcal{F} is small?

3509 The above question is central, answering it in the affirmative ensures that
 3510 we are using a correct hypothesis class (say neural architecture) and that the
 3511 error on the training dataset is a good indicator of the performance on the
 3512 entire distribution. This involves the following two steps.

3513 1. First, we need to make sure that the difference

$$\left| \hat{R}(f_{\text{ERM}}) - R(f_{\text{ERM}}) \right| \rightarrow 0, \quad n \rightarrow \infty.$$

3514 This is easy, it is akin to the concentration of measure we saw in the
 3515 previous section.

3516 2. Second, we need to ensure that

$$\hat{R}(f_{\text{ERM}}) \approx R(f^*)$$

3517 with high probability for every training dataset of n samples using which
 3518 f_{ERM} is computed. If this is true, it tells us something about the ERM
 3519 procedure itself, i.e., it tells us whether minimizing the empirical risk

3520 $\hat{R}(f)$ is a good thing if we want to build a classifier that works well on
3521 the population.

3522 This is difficult to do, after all f_{ERM} and f^* are totally different hypoth-
3523 esis. Vapnik set up a powerful construction to do this. He showed that
3524 a *sufficient* condition to achieve the above is that for all hypotheses in
3525 \mathcal{F} , the empirical risk and population risk are similar. This is known as
3526 uniform convergence.

3527 Let us now develop the two points above. Since data are drawn iid, we can
3528 use the Chernoff bound to get that

$$\forall f \in \mathcal{F}, \mathbb{P} \left(\left| \hat{R}(f) - R(f) \right| > \epsilon \right) \leq 2e^{-2n\epsilon^2}.$$

3529 If the hypothesis class is finite \mathcal{F} , we can use the union bound to show that for
3530 *any* hypothesis, the training error and population risk are close.

$$\begin{aligned} & \mathbb{P} \left(\exists f \in \mathcal{F} : \left| \hat{R}(f) - R(f) \right| > \epsilon \right) \\ & \leq \sum_{f \in \mathcal{F}} \mathbb{P} \left(\left| \hat{R}(f) - R(f) \right| > \epsilon \right) \\ & \leq |\mathcal{F}| 2e^{-2n\epsilon^2}. \end{aligned}$$

3531 If we want this above probability of a bad event to be less than δ we
3532 therefore need

$$n \geq \frac{1}{2\epsilon^2} \log \frac{2|\mathcal{F}|}{\delta} \quad (13.1)$$

3533 training data. Notice how this bound changed from the Monotone Boolean
3534 function example: we need $\mathcal{O}(1/\epsilon)$ times more samples to get the uniform
3535 convergence result.

3536 Suppose we had a classifier f with 2% gap ($\epsilon = 0.02$) between the training
3537 error $\hat{R}(f)$ and the validation error (which is a proxy for the population risk
3538 $R(f)$), if we want to reduce this gap by half to 1% ($\epsilon = 0.01$), we need
3539 4 times as many training data. We could also reduce this gap by fitting a
3540 classifier with small $|\mathcal{F}|$ but in this case, both the training and validation error
3541 will increase even if their gap decreases.

3542 Next, we need a relation between the population risk of f_{ERM} and the best
3543 possible predictor $f^* \in \mathcal{F}$ in our hypothesis class. Observe that

$$\begin{aligned} R(f_{\text{ERM}}) & \leq \hat{R}(f_{\text{ERM}}) + \epsilon && \text{(Chernoff bound on } f_{\text{ERM}}) \\ & \leq \hat{R}(f^*) + \epsilon && (f_{\text{ERM}} \text{ has the smallest training error)} \\ & \leq R(f^*) + 2\epsilon && \text{(Chernoff bound on } f^*). \end{aligned}$$

3544 The two Chernoff bound inequalities hold with probability at least $1 - \delta$ so
3545 the final inequality

$$R(f_{\text{ERM}}) \leq R(f^*) + 2\epsilon$$

3546 holds with probability at least $1 - 2\delta$. Substitute this in (13.1) to get

$$R(f_{\text{ERM}}) \leq R(f^*) + 2\sqrt{\frac{1}{2n} \log \frac{4|\mathcal{F}|}{\delta}} \quad (13.2)$$

3547 with probability $1 - \delta$. A result of this kind is called a Vapnik-Chernovenkis
3548 (VC) bound or a PAC bound.

3549 Let us consider our monotone Boolean formulae example again. Since
 3550 $|\mathcal{F}| = 2^d$, if the input dimension is $d = 1000$ and we set $\delta = 10^{-3}$, the VC-
 3551 bound predicts the following. In this case, we should imagine running ERM
 3552 to pick the best hypothesis f_{ERM} , not the elimination algorithm we discussed
 3553 in the section on monotone Boolean formulae.

- 3554 1. With $n = 1000$ data, we have $R(f_{\text{ERM}}) \leq R(f^*) + 1.42$. This is
 3555 vacuous/non-informative since the population risk is an expectation of
 3556 indicator variables and should therefore be less than 1.
- 3557 2. With $n = 10^5$, we have $R(f_{\text{ERM}}) \leq R(f^*) + 0.45$. This is informative,
 3558 it means that the population risk of the classifier obtained by ERM is
 3559 within 44% of the population risk of the best classifier f^* in that class.
 3560 Of course it is only meaningful if f^* generalizes well, i.e., if $R(f^*)$ is
 3561 small. This will happen if the hypothesis class \mathcal{F} is large enough.
- 3562 3. With $n = 10^6$, we have $R(f_{\text{ERM}}) \leq R(f^*) + 0.04$.

3563 13.4 Vapnik-Chernovenkis (VC) dimension

3564 In the above section, the concept/hypothesis class was assumed to be finite
 3565 $|\mathcal{C}| < \infty$. The union bound of course breaks if this is not the case. Notice that
 3566 once we pick a neural architecture (hypothesis class), the number of possible
 3567 models (hypotheses), each with different weight vectors, is infinite. Observe
 3568 that in the monotone Boolean formulae example, the algorithm L was using
 3569 the training data to eliminate hypothesis from \mathcal{C} , this is not going to work
 3570 \mathcal{C} is not finite. It is therefore a natural question whether we can still learn a
 3571 hypothesis class with a finite number of training data.

3572 Vladimir Vapnik and Alexey Chernovenkis (Vapnik, 2013) developed the
 3573 so-called VC-theory to answer the above question. Technically, VC-theory
 3574 transcends PAC-Learning but we will discuss only one aspect of it within the
 3575 confinements of the PAC framework. VC-theory assigns a “complexity” to
 3576 each hypothesis $f \in \mathcal{C}$.

3577 **Shattering a set of inputs** We say that the set of inputs $D = \{x^1, \dots, x^n\}$
 3578 is *shattered* by the concept class \mathcal{C} , if we can achieve every possible labeling
 3579 out of the 2^n labellings using some concept $c \in \mathcal{C}$. The size of the largest set
 3580 D that can be shattered by \mathcal{C} is called the VC-dimension of the class \mathcal{C} . It is
 3581 a measure of the complexity/expressiveness of the class; it counts how many
 3582 different classifiers the class can express.

3583 If we find a configuration of n inputs such that when we assign *any* labels
 3584 to these data, we can still find a hypothesis in \mathcal{C} that can realize this labeling,
 3585 then

$$\text{VC}(\mathcal{C}) \geq n.$$

3586 On the other hand, if for every possible configuration of $n + 1$ inputs, we can
 3587 always find a labeling such that no hypothesis in \mathcal{C} can realize this labeling,
 3588 then

$$n \leq \text{VC}(\mathcal{C}).$$

3589 If we find some n for which both of the above statements are true, then

$$\text{VC}(\mathcal{C}) = n.$$

3590 Some examples.

3591 • d -dim Linear Threshold Functions: $\text{VC-dim} = d + 1$.

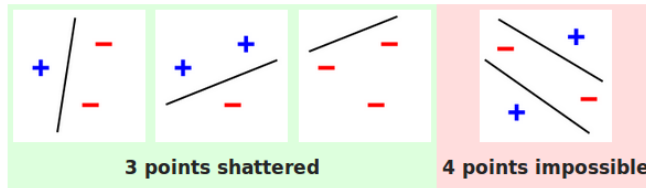


Figure 13.1: $d=2$: See that for the lower bound, we found some configuration of the 3 points, such that a linear threshold function always separates the points consistently with the labels; for any possible labeling. 3 such labellings are shown, convince yourselves that it can be done for all 8 cases. Observe that we cannot do the same for 4 points. In the figure above one such unrealizable configuration is given (With the “XOR” labeling). To prove the upper bound we need to talk about ANY configuration though. See that the only other case for 4 points, is that one point is inside the convex hull generated from the other 3. Find the labeling that cannot be obtained with linear classifiers in this case.

3592 • 2 dimensional axis aligned rectangles: $\text{VC-dim} = 4$ (exercise)

3593 • Monotone Boolean Formulae: $\text{VC-dim} = d$ (exercise).

3594 • If the hypothesis class is finite, then

$$\text{VC}(\mathcal{F}) \leq \log |\mathcal{F}|.$$

3595 • If $x \in \mathbb{R}$ and our concept class includes classifiers of the form

$$\text{sign}(\sin(wx))$$

3596 where w is a learned parameter, then

$$\text{VC} = \infty.$$

3597 • For a neural network with p weights and sign activation function

$$\text{VC} = \mathcal{O}(p \log p).$$

It is a deep result that if the VC-dimension of concept class is finite $V = \text{VC}(\mathcal{F}) < \infty$, then this class has the uniform convergence property (for any $f \in \mathcal{F}$, the empirical and population error are close). Therefore, we can learn this concept class agnostically (without worrying about whether Nature’s labeling function c is in our hypothesis class \mathcal{F} or not) in the PAC framework with

$$n = \Omega \left(\frac{V}{\epsilon^2} \log \frac{V}{\epsilon} + \frac{1}{\epsilon^2} \log \frac{1}{\delta} \right)$$

training data. If a hypothesis class has infinite VC-dimension, then it is not PAC-learnable and it also does not have the uniform convergence property.

3598 The above result written in another form looks as follows. For a (finite or
3599 infinite) hypothesis class \mathcal{F} with finite VC-dimension $V = \text{VC}(\mathcal{F})$

$$R(f_{\text{ERM}}) \leq R(f^*) + 2\sqrt{\frac{1}{n} (2V - \log \delta)} \quad (13.3)$$

3600 with probability at least $1 - \delta$. This is an important expression to remember:
3601 the number of samples n required to learn a concept class scales linearly with
3602 the VC-dimension V . A more refined version of this bound looks like

$$R(f_{\text{ERM}}) \leq R(f^*) + 2\sqrt{\frac{1}{n} \left(V \left(\log \frac{2n}{V} + 1 \right) + \log \frac{4}{\delta} \right)}. \quad (13.4)$$

3603 **Bounds on the VC-dimension of deep neural networks** For general clas-
3604 sifiers, it is typically difficult to compute the VC dimension. One instead finds
3605 upper and lower bounds for the VC dimension to be used in inequalities of the
3606 form (13.4). Bounds on the VC-dimension of deep network architectures are
3607 available (Bartlett et al., 2019). With p weights and L layers, an essentially
3608 tight VC-dimension looks like

$$\Omega \left(p L \log \frac{p}{L} \right) = \text{VC}(\mathcal{F}) = \mathcal{O}(p L \log p)$$

3609 for deep networks with ReLU nonlinearities.

3610 This bound is not entirely useful in the VC-theory however. For instance,
3611 the ALL-CNN network you used in your homework with $p \approx 10^6$ and $L = 10$
3612 has $\text{VC} \approx 10^8$. If we use the coarse VC-bound in (13.3) with $n = 50,000$
3613 samples, we have

$$R(f_{\text{ERM}}) \leq R(f^*) + 40$$

3614 which is a vacuous generalization bound. However, remember that this is
3615 simply an *upper bound* on the generalization error of ERM. It is clear from
3616 empirical results in the literature (including your homework problems) that
3617 deep networks indeed generalize well to new data outside the training set and
3618 that means $R(f_{\text{ERM}})$ is small.

3619 The gap in applying VC-theory to deep networks therefore likely stems
3620 from the need for uniform convergence: we may not need that the empirical
3621 and population risk are close for *all* hypotheses in the class. If we only
3622 have uniform convergence within a small subset $F \subset \mathcal{F}$ and if $\text{VC}(F) \ll$
3623 $\text{VC}(\mathcal{F})$ and if the training algorithms like SGD always find ERM minimizers
3624 $f_{\text{ERM}} \in F$, then VC-theory/PAC-Learning do predict that deep networks will
3625 generalize well. Understanding this is the subject of a large body of ongoing
3626 research.

3627

Chapter 14

3628

Variational Inference

Reading

1. Sections 1-2 of “Variational Inference: A Review for Statisticians” by [Blei et al. \(2017\)](#).
2. Sections 1-5 of “Auto-Encoding Variational Bayes” by [Kingma and Welling \(2013\)](#)
3. Chapter 2 of Durk Kingma’s thesis: <https://pure.uva.nl/ws/files/17891313/Thesis.pdf>.
4. Bishop Chapter 11.5-11.6
5. Bishop Chapter 10-10.3
6. Lots of great intuition at <http://ruishu.io/2018/03/14/vae/>

3629

We have been primarily concerned with models for classification and regression as yet in this course. The task there is to match the target (a class identity or a real-valued outcome). We now change tracks to consider generative modeling, these are models that are trained to synthesize new data. Effectively, the task here is not *match* a target datum, but given a training dataset of images/text, create a model that outputs similar images/text at test time. We will first take a look at variational methods and generative modeling using these methods in this chapter and do implicit generative models such as Generative Adversarial Networks in the next chapter.

3638

14.1 The model

3639

Imagine how you would draw the image of a dog x on paper. First, you would decide in your mind, its breed, its age, the color of its fur etc. Let us call these quantities “latent factors”. Latent factors can also include things that are not specific to the dog, e.g., the background of your painting (grass, house, beach

3640

3641

3642

3643 etc.), the weather on that day (cloudy, sunny etc.), the viewpoint (zoomed
3644 in/far away). We will denote all such quantities by

$z :=$ latent factors.

3645 Having decided upon all these factors, you realize your painting x . The
3646 painting x is not unique given latent factors z , e.g., two people can start off
3647 with the same latent factors and draw two totally different pictures.



3648

3649 We therefore model the generative process as a obtaining samples from a
3650 probability distribution

$$p(x|z).$$

3651 Given a latent factor z and an image x , the quantity $p(x|z)$ denotes the like-
3652 lihood of the sample. Given the painting image x , we do not know what the
3653 latent factors are. For instance, it is not easy to say whether the following
3654 image is that of a cat or a dog.



3655

In other words, the latent factors of data x are not known to us if we do not take part in the generative process. Nature is in charge of generating the data and our goal here is to guess the parameters of this generative model to be able to synthesize new samples that look as if Nature generated them.

3656 There can be lots of latent factors z . So let us control this complexity and
3657 assume that we know a prior over the latent factors

prior $p(z)$

3658 that models our belief of how likely a factor “dog with color blue” is in Nature.

Let us imagine Nature’s generative model as running in two steps

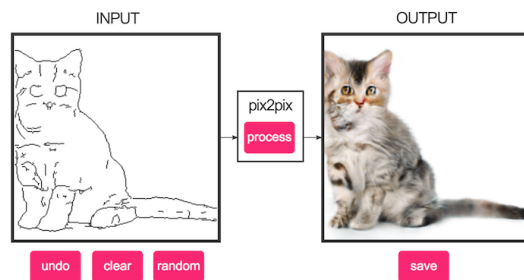
1. First, sample a latent factor z from some distribution, and then
2. sample a datum $x \sim p(x|z)$.

The central point to appreciate is that we know neither Nature's distribution for sampling latents z nor its generative model $p(x|z)$. We will need to fit both these quantities using a training dataset of images/text.

3659 The purpose of doing so can be many-fold, e.g., we may want to generate
 3660 new data to amplify the size of our training set, given a part of the input image
 3661 (say due to occlusions, or image corruption) we may want to complete the rest
 3662 of it.



3663



3664

3665 Most such applications require the knowledge of the latent factors that gener-
 3666 ated the data. Therefore, formally, we are interested in computing the posterior
 3667 distribution

$$\text{posterior } p(z|x)$$

3668 given the prior distribution $p(z)$ and samples in a training dataset $D =$
 3669 $\{x^i\}_{i=1}^n$. Notice that we do not need labels for this problem, effectively
 3670 labels $y^i = x^i$ itself because our generative model should of course be very
 3671 good at generating samples from the training data.

3672 14.2 Some technical basics

3673 14.2.1 Variational calculus

3674 We will first take a brief look at what is called variational calculus.

3675 A function is something takes in a variable as input and returns the value
 3676 of the function as the output, e.g., $\mathbb{R} \ni f(x) = 5x^2$ for $x \in \mathbb{R}$. Similarly, a

3677 *functional* is an object that takes in a *function* as an input and returns a real
3678 number as the output. An example of this is entropy

$$\mathbb{R} \ni H[p] = - \int p(x) \log p(x) \, dx$$

3679 which takes in a probability density p as the input and returns a real num-
3680 ber. Entropy is therefore a *functional*. Just like standard calculus where we
3681 take derivatives/minimize over functions, we can also take derivatives of the
3682 functional.

3683 The functional derivative $\frac{\delta H[p]}{\delta p}(x)$ is defined in a funny way as

$$\int \frac{\delta H[p]}{\delta p}(x) \varphi(x) \, dx = \lim_{\epsilon \rightarrow 0} \frac{H[p + \epsilon \varphi] - H[p]}{\epsilon}$$

3684 for any arbitrary function φ . Essentially, you perturb the argument to the
3685 functional p by some epsilon and see how much the functional changes. The
3686 change in the functional is measured using the test function φ by integrating
3687 its changes $\frac{\delta H(p)}{\delta p}(x)$ at each point x in the domain. There may be certain
3688 conditions that the perturbation φ needs to satisfy, e.g., since $p + \epsilon \varphi$ should also
3689 be probability density, the functional derivative above should only consider
3690 test functions φ such that

$$\forall \epsilon \int (p(x) + \epsilon \varphi(x)) \, dx = 1 \Rightarrow \int \varphi(x) \, dx = 0.$$

3691 The KL-divergence between two probability densities,

$$\text{KL}(p \parallel q) = \int p(x) \log \frac{p(x)}{q(x)} \, dx,$$

3692 is another such functional; it has two arguments p and q .

3693 Variational optimization is concerned with minimizing functionals. For
3694 instance, if we have a problem

$$w^* = \underset{w \in \mathbb{R}^p}{\text{argmin}} \ell(w)$$

3695 in standard optimization, a variational optimization problem with KL-divergence
3696 as the loss given a fixed density p looks like

$$q^* = \underset{q \in \mathcal{Q}}{\text{argmin}} \text{KL}(q \parallel p). \quad (14.1)$$

3697 The variable of optimization is the probability density q and we will denote the
3698 domain of the variable by \mathcal{Q} . Since we want q to be a legitimate probability
3699 density, we should choose

$$\mathcal{Q} \subseteq \mathcal{P}(\mathcal{X})$$

3700 where $\mathcal{P}(\mathcal{X})$ denotes the set of all probability densities on some domain \mathcal{X} .

3701 **Picking the domain and objective in variational optimization** Picking a
3702 good domain \mathcal{Q} to minimize over is important. It is similar to the notion of
3703 the a hypothesis class in machine learning. If \mathcal{Q} is too big, it is difficult to
3704 solve the optimization problem but we obtain a better value to $\text{KL}(q \parallel p)$. If \mathcal{Q}

3705 is too small, the optimization problem may be easy but we may not match the
 3706 desired distribution p very well. Imagine if p is a mixture of two Gaussians
 3707 and we pick \mathcal{Q} to be a family of uni-modal Gaussian distributions. Since the
 3708 KL-divergence is zero if and only if the two distributions are equal, we are
 3709 never going to be able to minimize it completely. On the other hand, if we
 3710 pick \mathcal{Q} to be the family of distributions with 2 or more Gaussian modes, then
 3711 we can perfectly match p . Essentially, the crux of variational inference boils
 3712 down to picking a good family of distributions \mathcal{Q} that makes solving (14.1)
 3713 easy.

3714 **What functional should we use to measure the distance between q and p ?**
 3715 The KL-divergence is popular and easy to use in practice but there are many
 3716 others. For example, when we studied the Gibbs distribution we briefly talked
 3717 about something called “Wasserstein metric”: if one imagines a mountain of
 3718 dirt given by distribution q and another mountain of dirt p , the Wasserstein
 3719 distance $W_2(q, p)$ is the amount of work done in transporting the dirt from q
 3720 to p ; it is also called the “earth mover’s distance”. The Wasserstein metric
 3721 is as legitimate a distance between two distributions as the Kullback-Leibler
 3722 divergence.

3723 14.2.2 Laplace approximation

3724 Laplace approximation is a very useful trick that is similar to variational
 3725 inference. Here is how it works: suppose we have to estimate approximately
 3726 an expectation of our random variable $\varphi(w)$

$$w \sim e^{-n\ell(w)} \quad \mathbb{E} [\varphi(w)] = \int e^{-nf(w)} \varphi(w) dw$$

3727 for some large value of n . The above integral takes many values, some have
 3728 small $\ell(w)$ and some have large $\ell(w)$. The values of w where $\ell(w)$ is small
 3729 are the ones that have the highest $e^{-n\ell(w)}$, especially as $n \rightarrow \infty$, and therefore
 3730 the ones that we should pay most attention while approximating the integral.
 3731 For large n , Laplace approximation replaces the above integral by simply

$$\begin{aligned} \int e^{-n\ell(w)} \varphi(w) dw &\approx \int \varphi(w) e^{-n(\ell(w^*) + \frac{1}{2}(w-w^*)^\top \nabla^2 \ell(w^*)(w-w^*))} dw \\ &= e^{-n\ell(w^*)} \int \varphi(w) e^{-\frac{n}{2}(w-w^*)^\top \nabla^2 \ell(w^*)(w-w^*)} dw \end{aligned} \quad (14.2)$$

3732 where $w^* = \operatorname{argmin} \ell(w)$ is the global minimum of $\ell(w)$. The integral is now
 3733 with respect to a Gaussian distribution and can be done more easily.

3734 How does a variational approximation differ from the Laplace approxima-
 3735 tion? Let us look at an example.

3736

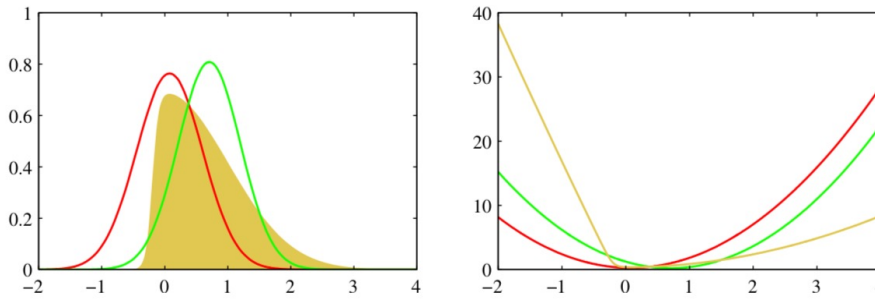


Figure 10.1 Illustration of the variational approximation for the example considered earlier in Figure 4.14. The left-hand plot shows the original distribution (yellow) along with the Laplace (red) and variational (green) approximations, and the right-hand plot shows the negative logarithms of the corresponding curves.

3737

14.2.3 Digging deeper into KL-divergence

3738

Let us take an example to understand KL-divergence better.

3739

Figure 14.1 compares two forms of KL-divergence. The green contours represent equi-probability lines (1,2,3 standard deviations) for a two-dimensional correlated Gaussian $p(z_1, z_2)$. Red contours represent similar equi-probability lines for the variational approximation of this distribution using an uncorrelated Gaussian distribution

3740

3741

3742

3743

3744

$$q(z) = q_1(z_1)q_2(z_2)$$

3745

where both q_1, q_2 are one-dimensional Gaussians. The variational family $q \in \mathcal{Q}$ thus consists of factored uncorrelated Gaussians and we are trying to find the best member of this family that approximates the *correlated* true distribution $p(z)$.

3746

3747

3748

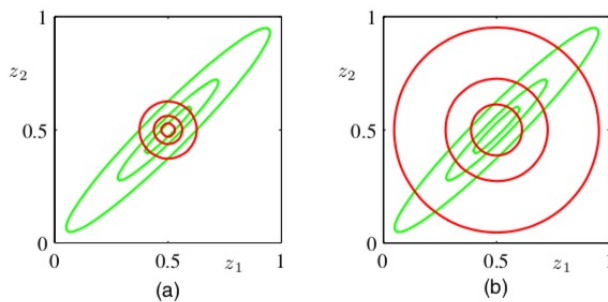


Figure 14.1: Comparison between the variational approximation of a correlated Gaussian using forward and reverse KL divergence and a factored Gaussian family.

3749

Left panel (a) in Figure 14.1 shows the result using the forward KL-divergence minimization

3750

$$q^* = \text{KL}(q \parallel p).$$

3751

while the right panel (b) shows the result for the reverse KL-divergence minimization

3752

$$q^* = \text{KL}(p \parallel q).$$

3753

We see that both these forms capture the mean of the true distribution $p(z)$ correctly. The variance of the two approximations is quite different depending upon which form we employ.

3754

3755

🔗 Use the expression of the KL-divergence to convince yourself why the forward KL under-estimates the variance while the reverse KL over-estimates the variance in Figure 14.1.

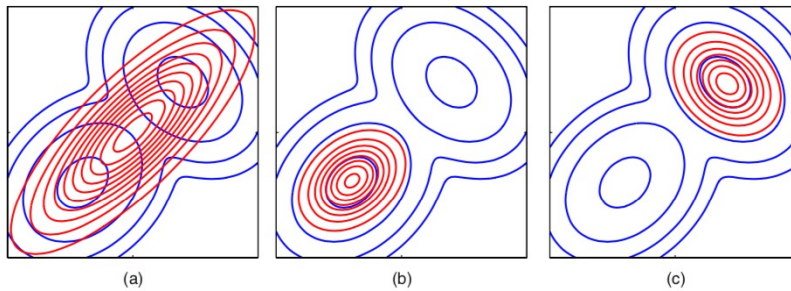


Figure 14.2: Approximating a multi-modal distribution using a uni-modal variational family.

3756 We next consider the case when a multi-modal probability distribution
 3757 $p(z)$ is approximated using a unimodal Gaussian distribution. Both these
 3758 examples are very often seen in practice, the distribution of true data/latent
 3759 factors is often correlated and multi-modal. We have seen one instance of
 3760 this: the distribution of weights of a deep network in the Gibbs distribution is
 3761 multi-modal because of multiple global minima.

3762 In panel (a) of Figure 14.2, the reverse KL divergence $\text{KL}(p || q)$ is used to
 3763 obtain the red contours of q^* . In contrast the forward KL divergence $\text{KL}(p || q)$
 3764 is used to obtain q^* in panels (b) and (c). Note that the distribution p is bi-
 3765 modal and the variational problem is no longer convex in this case; depending
 3766 upon the initial condition using q , one may get different solutions shown in
 3767 panels (b) and (c).

3768 KL-divergence is not the only distance used in variational inference and
 3769 there are many many other ones. You should think of these different ways to
 3770 measure distances between probability distributions in variational inference
 3771 as different surrogate losses; which one we use is highly problem dependent
 3772 although the forward KL-divergence $\text{KL}(q || p)$ is the most common.

3773 14.3 Evidence Lower Bound (ELBO)

3774 We now go back to the generative model.

We will formalize our goal in generative modeling as computing

Nature's true posterior distribution of latent factors

$$p(z|x).$$

We have access to a training dataset $D = \{(x^i)\}_{i=1}^n$. We do not know (i) what form Nature's posterior distribution takes, e.g., Gaussian, multi-modal distribution etc. and (ii) we do not know the true latent factors z that Nature uses. So we are going to approximate the true posterior using some variational family of our choice

$$\mathcal{Q} \ni q^*(z|x) \approx p(z|x).$$

This is the basic idea of variational inference: to approximate a complex distribution $p(z|x)$ using a member of from a simpler family of our choosing \mathcal{Q} . In practice, this variational family \mathcal{Q} will be parameterized by a deep network.

3775 With this background, the mathematical process of executing the above
3776 program is quite simple. We will simply minimize the KL-divergence

$$q^*(z|x) = \operatorname{argmin}_{q \in \mathcal{Q}} \frac{1}{n} \sum_{i=1}^n \operatorname{KL}(q(z|x^i) || p(z|x^i)). \quad (14.3)$$

3777 We next rewrite this KL-divergence above in a special form.

$$\begin{aligned} 0 &\leq \operatorname{KL}(q(z|x^i) || p(z|x^i)) \\ &= \mathbb{E}_{z \sim q(z|x^i)} \left[\log \frac{q(z|x^i)}{p(z|x^i)} \right] \\ &= - \mathbb{E}_{z \sim q(z|x^i)} [\log p(z|x^i)] + \mathbb{E}_{z \sim q(z|x^i)} [\log q(z|x^i)] \\ &= - \mathbb{E}_{z \sim q(z|x^i)} [\log p(z, x^i) - \log p(x^i)] + \mathbb{E}_{z \sim q(z|x^i)} [\log q(z|x^i)] \\ &= \log p(x^i) - \mathbb{E}_{z \sim q(z|x^i)} [\log p(z, x^i)] + \mathbb{E}_{z \sim q(z|x^i)} [\log q(z|x^i)]. \\ \Rightarrow \log p(x^i) &\geq \mathbb{E}_{z \sim q(z|x^i)} [\log p(z, x^i)] - \mathbb{E}_{z \sim q(z|x^i)} [\log q(z|x^i)] \end{aligned}$$

3778 This is quite interesting. The left-hand side of this inequality is the log-
3779 likelihood of the data under Nature's distribution, i.e., it is fixed and independent
3780 of what we do. The left-hand side is also called the evidence. The right
3781 hand-side

$$\operatorname{ELBO}(q, x^i) := \mathbb{E}_{z \sim q(z|x^i)} [\log p(z, x^i)] - \mathbb{E}_{z \sim q(z|x^i)} [\log q(z|x^i)]. \quad (14.4)$$

3782 is a lower bound on the evidence and therefore called the Evidence Lower
3783 Bound (ELBO).

Next comes a key step: a good generative model should be such that

the evidence of the training data, i.e., the log-likelihood of this data under Nature's distribution, should be large under the model. We therefore want to maximize the ELBO on our training data

$$q^*(z|x) = \operatorname{argmax}_{q \in \mathcal{Q}} \frac{1}{n} \sum_{i=1}^n \text{ELBO}(q, x^i). \quad (14.5)$$

to find the posterior distribution of the latent factors $q^*(z)$. Maximizing ELBO is equivalent to minimizing the KL-divergence $\text{KL}(q(z|x^i) || p(z|x^i))$.

3784 We will again solve the optimization problem in (14.5) using stochastic
3785 gradient descent. Before we study how to do that, let us consider what model
3786 we have developed so far. The solution to this problem

$$q^*(z|x) \approx p(z|x)$$

3787 approximates Nature's posterior distribution. If we maximize ELBO well,
3788 given an input x , samples $z \sim q^*(z|x)$ are likely to be the latent factors that
3789 Nature could have chosen while rendering this image. But we still do not know
3790 how to synthesize an image x for these latent factors. We now rewrite ELBO
3791 in a different form to understand this.

$$\begin{aligned} \text{ELBO}(q, x^i) &= \mathbb{E}_{z \sim q(z|x^i)} [\log p(z, x^i)] - \mathbb{E}_{z \sim q(z|x^i)} [\log q(z|x^i)] \\ &= \mathbb{E}_{z \sim q(z|x^i)} [\log p(x^i|z) + \log p(z)] - \mathbb{E}_{z \sim q(z|x^i)} [\log q(z|x^i)] \\ &= \mathbb{E}_{z \sim q(z|x^i)} [\log p(x^i|z)] - \text{KL}(q(z|x^i) || p(z)). \end{aligned}$$

3792 This form of ELBO

$$\text{ELBO}(q, x^i) = \mathbb{E}_{z \sim q(z|x^i)} [\log p(x^i|z)] - \text{KL}(q(z|x^i) || p(z)) \quad (14.6)$$

3793 is very interesting. The first term is Nature's log-likelihood of datum x^i given
3794 the latent factor z sampled from *our* candidate posterior q . The second term
3795 is the discrepancy between our variational approximation of the posterior
3796 $q^*(z|x^i) \approx p(z|x^i)$ and Nature's true marginal distribution over latent factors
3797 $p(z)$. This alternative form of ELBO is conceptually very similar to what we
3798 do in standard classification, e.g.,

$$\operatorname{argmin}_w \left\{ \ell(w) + \frac{\alpha}{2} \|w\|^2 \right\}.$$

3799 We would like our $q(z|x^i)$ to be close to Nature's prior distribution $p(z)$ but at
3800 the same time be such that samples from $q(z|x^i)$ have a high log-likelihood
3801 $p(x^i|z)$ of synthesizing images in the training set. The KL-term is therefore a
3802 regularizer for the first data-fitting term.

3803 14.3.1 Parameterizing ELBO

3804 What variational family \mathcal{Q} should we choose? Say we parametrized each
3805 distribution $q(z|x^i)$ by its mean and diagonal of the covariance.

$$\mathbb{R}^m \ni z \sim q(z|x^i) = N(\mu(x^i), \sigma^2(x^i)I) \in \mathcal{Q}(x^i)$$

3806 where $\mu(x^i), \sigma^2(x^i) \in \mathbb{R}^m$. The ELBO in (14.6) is totally independent for
 3807 each x^i in the training dataset, so all $i \in \{1, \dots, n\}$ we can solve for

$$\mu^*(x^i), \sigma^2(x^i) = \operatorname{argmax}_{\mu, \sigma^2} \operatorname{ELBO}(N(\mu(x^i), \sigma^2(x^i)I), x^i).$$

3808 But this is not a good idea: the parameters μ, σ^2 are distinct for each input x^i
 3809 and effectively they are being trained using a dataset of only input image x^i .

Amortized variational inference is a clever trick that ties together the variational families $Q(x^i)$. We will be using a deep network with parameters $u \in \mathbb{R}^p$ that takes x^i as the input and gives $\mu(x^i; u), \sigma^2(x^i; u)$ as the outputs

$$\text{Encoder} : x^i \xrightarrow[\text{parameters } u]{} \mu(x^i; u), \sigma^2(x^i; u).$$

The variational family $Q(x^i)$ that we are considering is therefore the set of distributions expressed by this deep network with p parameters. The family $Q(x^i)$ is still distinct for each datum x^i but they are all tied together by the same weights u .

Encoder. We will call this deep network the encoder because it takes in an input x^i and encodes it into $\mu(x^i; u), \sigma^2(x^i; u)$ which parameterize the distribution of the latent factors.

3810 **Decoder.** Observe that although we have now parameterized the distribution
 3811 $q(z|x^i)$ using a deep network with weights u , we still do not know how to
 3812 model the term $p(x^i|z)$. After all, this is Nature's log-likelihood.

3813 We have a dataset $\{(x^i, z^i)\}_{i=1}^n$ that consists of the images x^i and their
 3814 corresponding latents z^i sampled from our encoder. We are going to model
 3815 Nature's rendering process $p(x|z)$ using a deep network. This is a program
 3816 that we have done many times in the past, e.g., we model the targets in
 3817 classification y^i as samples from the softmax distribution with images x^i as
 3818 the input and train the weights using maximum-likelihood (as you may recall,
 3819 this is equivalent to the cross-entropy loss).

3820 We can repeat that program here: we are going to learn a deep network

$$\text{Decoder} : p_v(x^i|z) \approx p(x^i|z).$$

3821 with parameters $v \in \mathbb{R}^p$ that models Nature's likelihood $p(x^i|z)$.

3822 **Different possible decoders for MNIST** Depending upon the type of data
 3823 x^i , we will code up the deep network in different ways. For instance, if each
 3824 pixel of $x^i \in \mathbb{R}^{28 \times 28}$ is grayscale $[0, 255]$ like it is in MNIST, the output of
 3825 the decoder is a multinomial with size $28 \times 28 \times 256$.

3826 If we take the training dataset as binarized MNIST (if pixel jk is less
 3827 than 128 set it to 0, else set it to 1), then the output of the decoder has size
 3828 $28 \times 28 \times 2$ and we can fit this using a logistic distribution at each pixel

$$p_v(x^i|z) = \prod_{j,k=1}^{28} \underbrace{p_v(x_{jk}^i|z)}_{\text{logistic distribution for pixel } x_{jk}^i \in \{0,1\}}$$

▲ The distribution of labels y^i in classification was one-hot vectors, so the softmax layer created a multinomial distribution on the classes.

3829 The log-likelihood term in (14.6) will then correspond to the logistic loss as
3830 discussed in the Homework.

3831 **Using a mean-field prior** $p(z)$. We do not know what the prior distribution
3832 $p(z)$ in (14.6) is. We will choose a simple prior

$$p(z) = \prod_{j=1}^m p_j(z_j) \quad (14.7)$$

3833 where $p_i(z_i)$ is the distribution of the i^{th} latent factor z_i . Such distributions are
3834 called mean-field priors (where the distribution of a vector $z \in \mathbb{R}^m$ is modeled
3835 as independent distributions on its components). We will further choose each
3836 distribution

$$p_j(z_j) = N(0, 1)$$

3837 to be a zero-mean standard Gaussian distribution. This is a Gaussian mean-
3838 field prior. Just like the choice of a regularizer is critical in machine learning
3839 for obtaining good generalization, the choice of a prior is critical in variational
3840 inference for synthesizing good images from the generative model.

3841 14.4 Gradient of the ELBO

3842 We now have all the ingredients in place for training a variational generative
3843 model. Let us summarize our setup.

- 3844 1. Encoder parameters u are weights of a deep network that takes in x^i
3845 as input and outputs parameters $\mu(x^i), \sigma^2(x^i)$ of the latent distribution.
3846 We have tacitly assumed the latent posterior $p(z|x^i)$ to be a Gaussian
3847 here; if you have a problem where you wish to have a different latent,
3848 e.g., all the latent genes that could have caused a particular cancer, then
3849 you want to output the parameters of that distribution from the encoder.
- 3850 2. The decoder models the likelihood $p_v(x^i|z)$ using parameters v .
- 3851 3. The prior $p(z)$ will be a mean-field Gaussian distribution. The prior has
3852 no parameters in our case, although you may see research papers where
3853 the prior also has its own parameters. A popular choice is to use

$$\text{ELBO}_\beta(q, x^i) = \mathbb{E}_{z \sim q(z|x^i)} [\log p(x^i|z)] - \beta^{-1} \text{KL}(q(z|x^i) || p(z))$$

3854 in place of the standard ELBO. The hyper-parameter $\beta > 0$ gives more
3855 control over the strength of the prior; this is of course akin to picking
3856 the weight-decay coefficient.

▲ The concept of variational inference and ELBO are much more general than generative models or the encoder-decoder structure that we have developed. Go through the assigned reading material to learn more.

The ELBO when rewritten in terms of the encoder and decoder pa-

parameters looks as follows.

$$\text{ELBO}(u, v; x^i) = \mathbb{E}_{z \sim q_u(z|x^i)} [\log p_v(x^i|z)] - \text{KL}(q_u(z|x^i) || p(z)). \quad (14.8)$$

Our goal is to fit the weights u, v using

$$u^*, v^* = \underset{u, v \in \mathbb{R}^p}{\text{argmax}} \frac{1}{n} \sum_{i=1}^n \text{ELBO}(u, v; x^i). \quad (14.9)$$

The number of parameters of the encoder and decoder can be different but for clarity we imagine them to be the same.

3857 (14.9) is an optimization problem and in this section, we will see how to
3858 compute the gradient of the objective so that we can solve the problem using
3859 SGD.

3860 14.4.1 The Reparameterization Trick

3861 **Focus on the gradient with respect to u of the first term of ELBO**

$$\nabla_u \mathbb{E}_{z \sim q(z|x^i)} [\varphi(z)].$$

3862 We have written $\log p_v(x^i|z) = \varphi(z)$ to keep the notation clear; we do not
3863 care about the exact form of the integrand in this section.

3864 If we draw a computational graph for the forward propagation of this term,
3865 it looks as follows

$$u, x^i \rightarrow \text{sample } z \text{ from } q_u(z|x^i) \rightarrow \varphi(z).$$

3866 The intermediate sampling step is troublesome, we do not really know how to
3867 use the chain rule of calculus across sampling, i.e., given

$$\overline{\varphi(z)} := \frac{d}{d_u} \varphi(z)$$

3868 we need to compute $\overline{u} = d\ell/d_u u$. We only know how to apply the chain rule
3869 for *deterministic operations* of the form

$$u, x^i \rightarrow z = \text{some deterministic function } g(u, x^i) \rightarrow \varphi(z),$$

3870 in which case we use the standard backprop across the function g .

The Reparameterization Trick enables us to obtain backpropagation gradients across sampling operations via a creative use of the Laplace approximation of the distribution $q_u(z|x^i)$.

3871 We know from the Laplace approximation that we can compute an ex-
3872 pectation over z using a Gaussian centered at the global maximum of the

3873 distribution $q_u(z|x^i)$ with variance equal to the inverse Hessian at that maxi-
 3874 mum. Motivated by this, the Reparameterization Trick *rewrites* the random
 3875 variable z as

$$z = \mu(x^i; u) + \sigma(x^i; u) \odot \epsilon$$

3876 where

$$\epsilon \sim N(0, I_{m \times m})$$

3877 is a sample from a standard multi-variate Gaussian distribution and the notation
 3878 \odot denotes element-wise product. Effectively, we imagine that the encoder
 3879 outputs

$$\begin{aligned} \mu(x^i; u) &= \operatorname{argmax}_z q_u(z|x^i) \\ \sigma^2(x^i; u) &= \operatorname{diag} \left([\nabla_z^2 q_u(z|x^i)]^{-1} \right). \end{aligned}$$

3880 Just like the integral in (14.2) was performed over the Gaussian, the integral
 3881 over z can be rewritten as an integral over ϵ

$$\begin{aligned} \nabla_u \mathbb{E}_{z \sim q_u(z|x^i)} [\varphi(z)] &= \nabla_u \mathbb{E}_{\epsilon \sim N(0, I)} [\varphi(\mu(x^i; u) + \sigma(x^i; u) \odot \epsilon)] \\ &= \mathbb{E}_{\epsilon \sim N(0, I)} [\nabla_u \varphi(\mu(x^i; u) + \sigma(x^i; u) \odot \epsilon)] \\ &\approx \frac{1}{N} \sum_{j=1}^N \nabla_u \varphi(\mu(x^i; u) + \sigma(x^i; u) \odot \epsilon^j), \text{ where } \epsilon^j \sim N(0, I). \end{aligned}$$

3882 We can take the gradient operator inside the expectation in this case because ϵ
 3883 no longer depends on the weights u . The term $\nabla_u \varphi(\mu(x^i; u) + \sigma(x^i; u) \odot \epsilon^j)$
 3884 is a deterministic operation given a sample z^j and can be computed using
 3885 standard backpropagation.

3886 14.4.2 Score-function estimator of the gradient

3887 Let us look at an alternative way to compute the same gradient.

$$\begin{aligned} \nabla_u \mathbb{E}_{z \sim q_u(z|x^i)} [\varphi(z)] &= \nabla_u \int \varphi(z) q_u(z|x^i) \, dz \\ &= \int \varphi(z) \nabla_u q_u(z|x^i) \, dz \\ &= \int \varphi(z) \frac{\nabla_u q_u(z|x^i)}{q_u(z|x^i)} q_u(z|x^i) \, dz \\ &= \int \varphi(z) \nabla_u \log q_u(z|x^i) q_u(z|x^i) \, dz \\ &= \mathbb{E}_{z \sim q_u(z|x^i)} [\varphi(z) \nabla_u \log q_u(z|x^i)] \\ &\approx \frac{1}{N} \sum_{j=1}^N \varphi(z^j) \nabla_u \log q_u(z^j|x^i), \text{ with } z^j \sim q_u(z|x^i). \end{aligned} \tag{14.10}$$

3888 The term

$$\frac{\nabla_u q_u(z|x^i)}{q_u(z|x^i)} = \nabla_u \log q_u(z|x^i) \tag{14.11}$$

3889 is called the score function of a probability distribution q_u . The above cal-
 3890 culation is quite beautiful: calculating the gradient of the expectation of any

3891 quantity $\varphi(z)$ is equal to the expectation of the same quantity weighted by the
3892 score function

$$\nabla_u \mathbb{E}_{z \sim q_u} [\varphi(z)] = \mathbb{E}_{z \sim q_u} [\varphi(z) \nabla_u \log q_u].$$

3893 Due to this trick, we can compute the gradient using N samples

$$z^j \sim p_u(z|x^i) \quad (14.12)$$

3894 from the encoder; this is easy if, say, the encoder outputs the mean and
3895 standard-deviation of the distribution of the latents. Given z^j , the gradient

$$\nabla_u \log q_u(z^j|x^i)$$

3896 is just the standard back-propagation gradient of the quantity $\log q_u(z^j|x^i)$
3897 with respect to weights u of the deep network and can be computed using
3898 autograd.

The key difference between the Reparameterization Trick and the score-function estimator is that in the latter, we do not need to make sure that the gradient $d\ell/dz^j$ can be back-propagated across the sampling operation. The score-function estimator directly computes the gradient of the entire expectation by a weighted average across the samples.

Having two different ways of computing the same gradient may seem redundant but they both are suited to very different applications. The Reparameterization Trick is not accurate in cases when the distribution $q_u(z|x^i)$ is multi-modal because we have only one mean $\mu(x^i)$ around which the samples are drawn. The score-function trick does not have this problem because so long as iid samples are drawn in (14.12) (using any method, e.g., importance sampling) we obtain true estimate of the gradient. The problem in score-function estimator lies in that the denominator $q_u(z|x^i)$ in (14.11) can take very small values if the particular sample z is unlikely. The summation (14.10) is a combination of many N , some very large in magnitude and some very small; the variance of score-function estimate of the gradient in (14.10) can therefore be quite large in most problems.

Typically, the Reparameterization Trick is commonly used in generative models while both the Reparameterization Trick and the score-function estimator are used widely in Reinforcement Learning.

3899 14.4.3 Gradient of the remaining terms in ELBO

3900 The gradient with respect to weights v of the decoder of the first term in ELBO

$$\nabla_v \mathbb{E}_{z \sim q_u(z|x^i)} [\log p_v(x^i|z)]$$

3901 is simply the standard backpropagation gradient (the sampling distribution of
3902 the encoder does not depend on the weights of the decoder).

3903 Let us focus on the second term

$$\text{KL} \left(q_u(z|x^i) \parallel \prod_{j=1}^m p_j(z_j) \right). \quad (14.13)$$

3904 where $p_j(z_j) = N(0, 1)$ are terms of the mean-field prior. The gradient of this
3905 term with respect to weights of the decoder is zero

$$\nabla_v \text{KL} \left(q_u(z|x^i) \parallel \prod_{j=1}^m p_j(z_j) \right) = 0.$$

3906 Following the reasoning in the Reparameterization Trick, we are positing that
3907 $q_u(z|x^i)$ is a Gaussian distribution:

$$q_u(z|x^i) = N(\mu(x^i; u), \sigma^2(x^i; u)I).$$

3908 Notice that $\sigma^2(x^i; u) \in \mathbb{R}^m$ is the diagonal of the covariance and therefore
3909 the individual marginals $q_u(z_j|x^i)$ and $q_u(z_{j'}|x^i)$ for two indices j, j' are
3910 independent. We can therefore write

$$q_u(z|x^i) = \prod_{j=1}^m N(\mu_j(x^i; u), \sigma_j^2(x^i; u)). \quad (14.14)$$

3911 The KL-divergence of a univariate Gaussian $N(\mu_1, \sigma_1^2)$ with respect to the
3912 standard Gaussian is

$$\text{KL}(N(\mu, \sigma^2) \parallel N(0, 1)) = \log \frac{1}{\sigma} + \frac{\sigma^2 + \mu^2}{2} - \frac{1}{2}. \quad (14.15)$$

3913 The general formula is

$$\text{KL}(N(\mu_1, \sigma_1^2) \parallel N(\mu_2, \sigma_2^2)) = \log \frac{\sigma_2}{\sigma_1} + \frac{\sigma_1^2 + (\mu_1 - \mu_2)^2}{2\sigma_2^2} - \frac{1}{2}.$$

3914 Due to (14.14), the KL-divergence in (14.13) is a sum of the KL-divergences
3915 of the individual univariate Gaussians

$$\text{KL}(q_u(z|x^i) \parallel p(z)) = -\frac{1}{2} \sum_{j=1}^m (\log \sigma_j^2(x^i; u) - \sigma_j^2(x^i; u) + \mu_j^2(x^i; u) + 1). \quad (14.16)$$

3916 The right-hand side of this equation is only a function of u and its gradient can
3917 be calculated using standard back-propagation.

3918 This completes our development of ELBO. Using the gradient calculated
3919 in this section, we can use SGD to maximize the objective in (14.5) and train
3920 a generative model.

3921 14.5 Some comments

3922 Although the mathematics of ELBO seems complicated, it is quite easy to
3923 implement generative models using variational inference in practice. You did
3924 for a simple MNIST problem in the homework/recitation but if the encoder
3925 and decoder are convolutional and deconvolutional architectures respectively,
3926 we can get very sophisticated generative models.

🔗 Prove that

$$\begin{aligned} \text{KL} \left(\prod_{j=1}^m q_j(z_j) \parallel \prod_{j=1}^m p_j(z_j) \right) \\ = \sum_{j=1}^m \text{KL}(q_j(z_j) \parallel p_j(z_j)). \end{aligned}$$



Figure 14.3: Samples from a state-of-the-art VAE trained on ImageNet (Razavi et al., 2019)

3927 Variational inference and information-theoretic methods are a rich (and
3928 old) area of research and there are many modifications/innovations to ELBO,
3929 e.g., read Alemi et al. (2018) for some simple yet deep modifications.

Chapter 15

Generative Adversarial Networks

Reading

1. Andrew Ng's notes on generative models
<http://cs229.stanford.edu/notes/cs229-notes2.pdf>
2. The original GAN paper by Goodfellow et al. (2014)
3. "The Numerics of GANs" by Mescheder et al. (2017)

In the previous chapter, we used variational methods to build a generative model for the data. In this case, we are given samples $D = \{x^i\}_{i=1}^n$ and would like to build a model that can synthesize new data. For every data x that a decoder synthesizes at test time using latent variables z , we can calculate the likelihood

$$x \sim p_v(x|z), \text{ for any } z \sim N(0, I).$$

This likelihood is an indicator of how unlikely the data x is under z . Models for which we can calculate such likelihood are called explicit generative models, i.e., they give a sample x and also report its likelihood. In this chapter, we will look at an alternative class of generative models that are implicit, i.e., they only give a sample x but do not report its likelihood.

A Generative Adversarial Network (GAN) consists of two neural networks: a Generator and a Discriminator. The Generator works in the same way as the decoder in a variational auto-encoder. Given a sample z from some distribution, most commonly a standard normal, we train a neural network to generate a sample

$$x = g_v(z).$$

GANs differ from explicit models in how they train the generator, the discriminator is used for this purpose. We will look at this next.

15.1 Two-sample tests and Discriminators

We will first take a short trip into an area of statistics known as decision theory. Consider two datasets coming from two distributions $p(x)$ and $q(x)$

$$D_1 = \{x^1, \dots, x^n, : x^k \sim p(x)\}$$

$$D_2 = \{x^1, \dots, x^n, : x^k \sim q(x)\}.$$

We would like to check if these two distributions are the same given access to only their respective datasets D_1 and D_2 . Let us define the *null hypothesis* which claims that the two distributions are the same.

$$H_0 : p = q$$

The alternate hypothesis is

$$H_1 : p \neq q.$$

The goal of the so-called “two-sample test” is to decide whether H_0 is true or not. A typical two-sample test will construct a statistic (recall from Chapter 7 that a statistic is any function of the data)

$$\hat{t}$$

out of the two datasets, e.g., their individual means, their variances, and will use this statistic to *accept or reject* the null hypothesis, i.e., decide whether H_0 is true or false.

Let’s say that we pick a threshold t_α , and the test statistic \hat{t} is the difference of the means

$$\hat{t} = \left| \frac{1}{n} \sum_{x \in D_1} x - \frac{1}{n} \sum_{x \in D_2} x \right|.$$

Level of a test A statistician will then say that the null hypothesis is valid with *level* α if

$$\mathbb{P}_{D_1 \sim p, D_2 \sim p} (\hat{t} > t_\alpha) \leq \alpha. \quad (15.1)$$

In other words, if the null hypothesis were true (both D_1 and D_2 are drawn from the same distribution p) and if the probability of our empirical statistic \hat{t} being larger than some *chosen* threshold t_α is smaller than some *chosen* probability α , then we know that the two distributions are the same despite only having finite data to check. The threshold α is called the *p-value* in the statistics literature and you will have seen statements like “gene marker XX is correlated with disease YY with *p-value* of 10^{-3} ” or “smokers and non-smokers have different distributions of cancers with *p-value* of 10^{-3} ”.

Power of a test The power of a two-sample test is the probability of rejecting the null hypothesis when it is actually false. We want tests with a large power, i.e., we like

$$\mathbb{P}_{D_1 \sim p, D_2 \sim q} (\hat{t} > t_\alpha) \quad (15.2)$$

being large if the two datasets D_1 and D_2 are drawn from two different distributions p and q respectively.

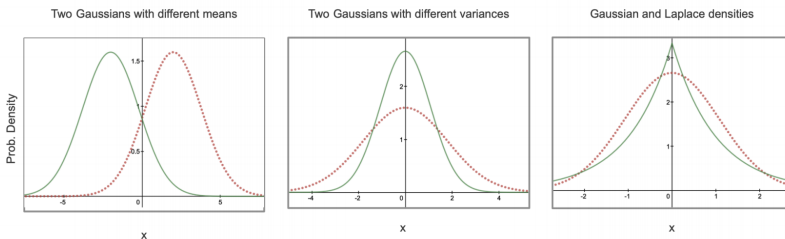
▲ The concept of a hypothesis here is different from what we saw in generalization/VC-theory. Hypothesis in decision theory simply means our hunch about a particular situation, e.g., $p = q$.

The key point to remember about two-sample tests is that they let us check if two distributions are the same without knowing anything about the distributions. We only need access to the samples and can run this test. This is fundamentally different than say

$$\text{KL}(q || p) = \int q(x) \log \frac{q(x)}{p(x)} dx$$

where we need to know the probabilities $q(x), p(x)$ to compute the distance between distributions.

3980 **Example 15.1.** A two-sample test requires three things, a statistic \hat{t} , a level α
 3981 and a threshold for the statistic t_α . The latter two are numbers that a statistician
 3982 can pick, e.g., picking $\alpha = 0.05$ is an accepted standard in most biological
 3983 studies.



3984

3985 15.2 Building the Discriminator in a GAN

Finding two-sample test statistics for arbitrary distributions is difficult, especially for high-dimensional problems where the samples are natural images. The key idea behind a Generator Adversarial Network (GAN) is to learn the statistic \hat{t} .

A good statistic is the one that lets us distinguish between data that comes from Nature's distribution and data that is synthesized by our generative model. This statistic, which is called the discriminator in GAN, is a critic of the generative model's results. It has a *high power* in (15.2) if the generated samples are different from those of Nature. Why? Because in this case for most thresholds t_α that we can pick, the power of the two-sample test in (15.2) will be large.

The discriminator should also be sound, i.e., if the two distributions are indeed the same (e.g., if our generator is as good as Nature's renderer), the discriminator should have a *low level* α in (15.1).

3986 We are going to train a binary classifier

$$d_u : \mathcal{X} \mapsto [0, 1]$$

3987 that will act as the discriminator in a GAN. You should think of the decision
 3988 boundary of this binary classifier as the difference of the test statistic and our
 3989 threshold $\hat{t} - t_\alpha$.

3990 We next create a dataset to train this classifier. Given n images from
 3991 Nature's distribution $p(x)$ and the distribution of our generator's images $q(x)$,
 3992 we will label the former with $y = 1$ and the latter with $y = 0$ to create a joint
 3993 dataset:

$$\begin{aligned} D_1 &= \{(x^i, 1)_{i=1, \dots, n} : x^i \sim p(x)\} \\ D_2 &= \{(x^i, 0)_{i=1, \dots, n} : x^i \sim q(x)\} \\ D &= D_1 \cup D_2. \end{aligned}$$

3994 Fitting d_u on this problem can be done simply using the logistic loss wherein
 3995 d_u is modeling the log-odds

$$\log \frac{\mathbb{P}(y = 1|x)}{\mathbb{P}(y = 0|x)} = d_u(x).$$

3996 The logistic loss is therefore

$$u^* = \operatorname{argmin}_u -\frac{1}{n} \sum_{x \sim D_1} \log d_u(x) - \frac{1}{n} \sum_{x \sim D_2} \log(1 - d_u(x)). \quad (15.3)$$

3997 Observe that this is the same logistic loss that we are used to; the only dif-
 3998 ference being that the entire dataset has $2n$ samples with all the ones in D_1
 3999 having labels $y = 1$ and all the ones in D_2 having labels $y = 0$.

4000 **What is the ideal discriminator?** The population risk corresponding to the
 4001 discriminator's objective in (15.3) is

$$d^* = \operatorname{argmax}_d \mathbb{E}_{x \sim p} [\log d(x)] + \mathbb{E}_{x \sim q} [\log(1 - d(x))]. \quad (15.4)$$

4002 We can take the variational derivative of this objective (just like you did in
 4003 HW 3 to compute the optimal classifier in the bias-variance tradeoff) to get

$$d^*(x) = \frac{p(x)}{p(x) + q(x)}. \quad (15.5)$$

4004 Observe that the ideal discriminator is $1/2$ if the two distributions p and q are
 4005 the same. The intuitive reason for this is that if the data D were really coming
 4006 from the same distribution, we would never be able to fit a logistic classifier to
 4007 get better than 50% error because D_1 and D_2 have different labels in spite of
 4008 having similar input data.

4009 Think of you would use our discriminator to build a two-sample test for a
 4010 given dataset. If given two datasets D_1 and D_2 labeled as above

$$\hat{t} := \frac{1}{n} \sum_{x \in D_1} \mathbf{1}_{\{d_u(x) > 0\}} + \frac{1}{n} \sum_{x \in D_2} \mathbf{1}_{\{d_u(x) < 0\}}$$

4011 and the threshold $t_\alpha = 1/2$. This construction is an example of what is called
 4012 a "classifier-based two-sample test"; you can read more about it at [Lopez-Paz](#)
 4013 [and Oquab \(2016\)](#).

It can be shown that if the two distributions are not the same, the

▲ Notice how rigorous theory is used as an inspiration for developing GANs. This is a common theme that you will see in the deep learning literature; the models may seem *ad hoc* and sprung out of sheer intuition, but the reason they work well is often because there are sound theoretical principles behind them. Building this skill requires studying the classical curriculum (ML, statistics, optimization) but being creative in applying this curriculum with deep networks.

▲ For a functional

$$L[d] = \int \log d(x)p(x) \, dx$$

the variational derivative is

$$\frac{\delta L}{\delta d}(x) = \frac{p(x)}{d(x)}.$$

Similarly, the variational derivative for

$$L[d] = \int \log(1 - d(x))q(x) \, dx$$

is

$$\frac{\delta L}{\delta d}(x) = \frac{q(x)}{1 - d(x)}.$$

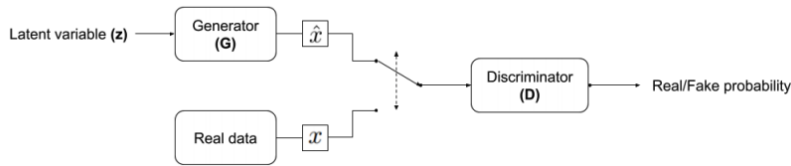


Figure 15.1: Schematic of the architecture in a GAN

power of the two-sample test is an increasing function of the statistic \hat{t} . Therefore if we wanted to maximize the power, maximizing the test statistic \hat{t} of the discriminator is a good idea. This makes the discriminator more and more sensitive to the differences between samples from p and q .

4014 15.3 Building the Generator of a GAN

The second key idea in a GAN is that the generator

$$g_v : \mathcal{Z} \rightarrow \mathcal{X}$$

that maps the latent space $\mathcal{Z} \subset \mathbb{R}^m$ to data space \mathcal{X} is trained to *minimize* the power of the two-sample test.

The generator g_v wants to synthesize data that look like they came from Nature's distribution $p(x)$. As the generator's distribution q comes closer to p , the accuracy of the discriminator d_u will degrade (it cannot distinguish between them as easily) and thereby discriminator will be forced to make its test statistic more sensitive to subtle differences between the two distributions.

4015 15.4 Putting the discriminator and generator together

4017 The GAN objective combines two objectives: the discriminator updates its
4018 weights u to maximize the power and the generator updates its weights v to
4019 minimize the power. We will write the population version of the optimization
4020 problem as follows.

$$\min_v \max_u E_{x \sim p(x)} [\log d_u(x)] + E_{x \sim q(x)} [\log (1 - d_u(x))] \quad (15.6)$$

4021 Let us fill in a few more details. The dataset of real images consists of samples
4022 from Nature's distribution $p(x)$, so we will write it as a finite sum over our
4023 dataset $D = \{x^i \sim p\}_{i=1}^n$. The generator uses samples z from some generic
4024 distribution, e.g., a standard Gaussian distribution.

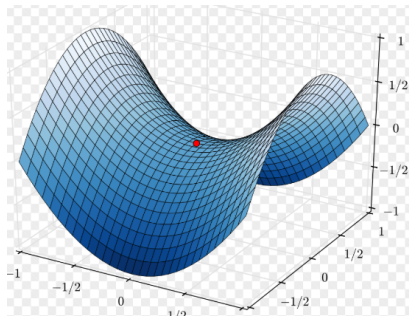
$$\min_v \max_u \frac{1}{n} \sum_{x \in D} [\log d_u(x)] + E_{z \sim N(0, I)} [\log (1 - d_u(g_v(z)))] \quad (15.7)$$

4025 **Training a GAN** The objective in (15.7) is an example of a min-max op-
 4026 timization problem. Such problems are quite difficult to solve and this is
 4027 why training GANs is quite difficult. In practice, we typically resort to a few
 4028 crude tricks. We sample a mini-batch of real images $\{x^1, \dots, x^b\}$ and another
 4029 mini-batch of noise vectors $\{z^1, \dots, z^b\}$. Using these two mini-batches

- 4030 1. we update the generator g_v using the gradient of the objective with respect
 4031 to v .
- 4032 2. update the discriminator d_u using the gradient of the loss with respect to u .

4033 There is no need for the Reparametrization Trick here because there is no
 4034 expectation being taken over parametrized distributions. This is a big benefit
 4035 of the GAN formulation as compared to variational inference; the former does
 4036 not have to be careful while picking a variational family and complex deep
 4037 networks can be used as the generator or the discriminator easily. Let us next
 4038 make a few comments about the objective in (15.7).

4039 **Solving min-max problems is difficult** This is a min-max problem: the
 4040 generator is minimizing the objective and the discriminator is maximizing the
 4041 objective. Such problems are hard to solve in optimization especially with
 4042 gradient descent techniques. Consider an example of a saddle point



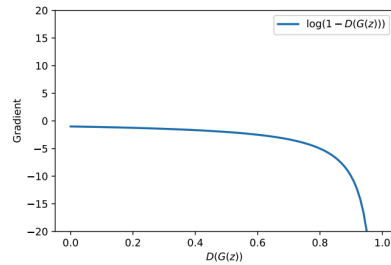
4043
 4044 where the loss function increases in one direction and decreases in the other
 4045 direction. Finding the solution of the min-max objective involves finding the
 4046 saddle point. It is easy to appreciate that depending on how many steps of
 4047 gradient descent we take for either of the min/max players we risk falling
 4048 down or climbing up the hill. There are many many other other factors that
 4049 make solving such problems hard, e.g., learning rate, momentum, stochastic
 4050 gradients if we are using mini-batches. Hyper-parameters are very tricky to
 4051 pick while training GANs and this is often called “instability of training”.

4052 **A harsh discriminator inhibits the training of the generator** The gener-
 4053 ator has a much more difficult task than the discriminator. During early stages
 4054 of training, the generator needs to learn how to synthesize images whereas
 4055 the discriminator can easily distinguish between bad images generated by
 4056 the generator and good ones from our original dataset using very similar test
 4057 statistics, e.g., an average of the RGB values all the pixels.

4058 The gradient of the second term in the objective is

$$\nabla_v \log(1 - d_u(g_v(z))) = -\frac{\nabla_v d_u(g_v(z))}{1 - d_u(g_v(z))}.$$

4059 As a function of $d_u(g_v(z))$ the second term in the objective thus looks like



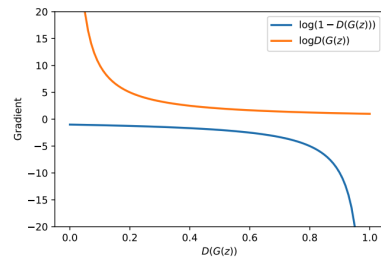
4060

4061 In other words, the gradient with respect to the generator's weights v is
 4062 essentially zero if the generator is not working well (this is the case when
 4063 $d_u(g_v(z))$ predicts a large negative value). This does not allow the generator
 4064 to learn well; it is essentially like your advisor shooting down all your ideas.

4065 Most GAN implementations therefore modify the second term in the
 4066 objective to be

$$- \mathbb{E}_{z \sim N(0, I)} [\log d_u(g_v(z))]$$

4067 which does not suffer from the small gradient problem.



4068

4069 **Synthesizing new images from a GAN** The generator samples latent fac-
 4070 tors $z \sim N(0, I)$ at test time to synthesize new images. The discriminator is
 4071 not used at test time.

4072 15.5 How to perform validation for a GAN?

4073 For variational generative models, we can use the log-likelihood of synthesized
 4074 images to obtain some understanding of whether the model is working well. If
 4075 the log-likelihood of new images is similar to the log-likelihood of images in
 4076 the training data then the new images are good at least as far as the model is
 4077 concerned even if they may have perceptual artifacts.

4078 Doing so is not so easy for implicit models because they do not output the
 4079 likelihood of the generated samples. Run the generator a few times to eyeball
 4080 the quality of images it generates.



4081

4082 But this is a very heuristic and qualitative metric.

4083 **Frechet Inception Distance (FID)** A number of other metrics exist for eval-
 4084 uating generative models. One popular one is the so-called Frechet Inception
 4085 Distance (FID) where we take any pre-trained model for classification, in this
 4086 case people typically use the Inception architecture, and evaluate

$$\text{FID}(p, q) = \|\mu_p - \mu_q\|_2^2 + \text{trace} \left(\Sigma_p + \Sigma_q - 2(\Sigma_p \Sigma_q)^{1/2} \right).$$

4087 where μ_p, Σ_p are the mean and covariace of the features of an Inception
 4088 network when real images are fed to it and similarly μ_q, Σ_q are the mean/
 4089 covariance of the features when GAN-generated images are fed to the same
 4090 network.

4091 The above formula is the Wasserstein distance between the two densities
 4092 p, q . There are many similar techniques such as the Maximum Mean Dis-
 4093 crepancy (MMD) that can be used to understand the discrepancy between the
 4094 two distributions once the features are computed using some pre-trained model
 4095 on their respective images.

4096 Roughly speaking, the evaluation methodology in generative models, espe-
 4097 cially for images, is quite flawed. This is not a new phenomenon in machine
 4098 learning/statistics because it is a intrinsically difficult problem to measure
 4099 when two distributions are the same given only finite data from them. The
 4100 problem is exacerbated in deep generative models because deep networks
 4101 are very good at over-fitting, e.g., GANs can often end up memorizing the
 4102 training data, they can generate very realistic images that are essentially the
 4103 same as those in the training data. Nevertheless, a lot of techniques exist to
 4104 make GANs synthesize high-quality images. See some examples at [Brock
 4105 et al. \(2018\)](#); [Karras et al. \(2017\)](#).

The key behind the empirical success of GANs is to convert a problem

about estimating distributions, sampling from them etc. into a classification problem. Deep networks are extremely good at classification as compared to other problems like regression, reconstruction etc. and GANs leverage this remarkably. This is a trick that you will do well to remember when you use deep networks in the future: typically you will always get better results if you manage to rewrite your problem as a classification problem. I suspect the real reason for this is that we do not have good regularization techniques for deep networks for non-classification problems.

4106 **15.6 The zoo of GANs**

4107 Due to the numerous issues with GANs, there have been a large number of
4108 variants and attempts to improve their empirical performance. They fall mainly
4109 into the following categories.

- 4110 1. Optimization tricks to train the generator-discriminator pair in a more stable
4111 fashion.
- 4112 2. New loss functions that change the binary cross-entropy loss of the discrim-
4113 inator to something else. A majority of papers, including the example we
4114 saw above, fall into this category.
- 4115 3. Characterizing the kind of critical points, equilibria of the training process;
4116 this is a similar line of analysis as the study of the energy landscape of deep
4117 networks for standard supervised learning.
- 4118 4. Connections with variational inference suggest that GANs and their training
4119 techniques are essentially variational inference in disguise (Nowozin et al.,
4120 2016).
- 4121 5. Coming up with new ways of evaluating generative models.

4122 In addition to the above lines, there are many other novel and interesting
4123 applications such as Cycle-GANs and conditional-GANs.

Bibliography

- Aizerman, M. A. (1964). Theoretical foundations of the potential function method in pattern recognition learning. *Automation and remote control*, 25:821–837.
- Alemi, A., Poole, B., Fischer, I., Dillon, J., Saurous, R. A., and Murphy, K. (2018). Fixing a broken elbo. In *International Conference on Machine Learning*, pages 159–168. PMLR.
- Baldi, P. and Hornik, K. (1989). Neural networks and principal component analysis: Learning from examples without local minima. *Neural networks*, 2(1):53–58.
- Bartlett, P. L., Harvey, N., Liaw, C., and Mehrabian, A. (2019). Nearly-tight vc-dimension and pseudodimension bounds for piecewise linear neural networks. *J. Mach. Learn. Res.*, 20:63–1.
- Blei, D. M., Kucukelbir, A., and McAuliffe, J. D. (2017). Variational inference: A review for statisticians. *Journal of the American Statistical Association*, 112(518):859–877.
- Bottou, L. (2012). Stochastic gradient descent tricks. In *Neural networks: Tricks of the trade*, pages 421–436. Springer.
- Bottou, L., Curtis, F. E., and Nocedal, J. (2018). Optimization methods for large-scale machine learning. *Siam Review*, 60(2):223–311.
- Breiman, L. (1996). Bagging predictors. *Machine learning*, 24(2):123–140.
- Breiman, L. (2001). Random forests. *Machine learning*, 45(1):5–32.
- Brock, A., Donahue, J., and Simonyan, K. (2018). Large scale gan training for high fidelity natural image synthesis. *arXiv preprint arXiv:1809.11096*.
- Chaudhari, P., Choromanska, A., Soatto, S., LeCun, Y., Baldassi, C., Borgs, C., Chayes, J., Sagun, L., and Zecchina, R. (2016). Entropy-sgd: Biasing gradient descent into wide valleys. *arXiv:1611.01838*.
- Chaudhari, P. and Soatto, S. (2017). Stochastic gradient descent performs variational inference, converges to limit cycles for deep networks. *arXiv preprint arXiv:1710.11029*.
- Cortes, C. and Vapnik, V. (1995). Support vector machine. *Machine learning*, 20(3):273–297.
- Efron, B. (1992). Bootstrap methods: another look at the jackknife. In *Breakthroughs in statistics*, pages 569–593. Springer.
- Fukushima, K. (1988). Neocognitron: A hierarchical neural network capable of visual pattern recognition. *Neural networks*, 1(2):119–130.
- Goodfellow, I., Pouget-Abadie, J., Mirza, M., Xu, B., Warde-Farley, D., Ozair, S., Courville, A., and Bengio, Y. (2014). Generative adversarial nets. In *Advances in neural information processing systems*, pages 2672–2680.

- Hinton, G. E., Osindero, S., and Teh, Y.-W. (2006). A fast learning algorithm for deep belief nets. *Neural computation*, 18(7):1527–1554.
- Hochreiter, S. and Schmidhuber, J. (1997). Long short-term memory. *Neural computation*, 9(8):1735–1780.
- Hubel, D. H. and Wiesel, T. N. (1968). Receptive fields and functional architecture of monkey striate cortex. *The Journal of physiology*, 195(1):215–243.
- Ioffe, S. and Szegedy, C. (2015). Batch normalization: Accelerating deep network training by reducing internal covariate shift. *arXiv preprint arXiv:1502.03167*.
- Izmailov, P., Podoprikin, D., Gariipov, T., Vetrov, D., and Wilson, A. G. (2018). Averaging weights leads to wider optima and better generalization. *arXiv preprint arXiv:1803.05407*.
- Karras, T., Aila, T., Laine, S., and Lehtinen, J. (2017). Progressive growing of gans for improved quality, stability, and variation. *arXiv preprint arXiv:1710.10196*.
- Kawaguchi, K. (2016). Deep learning without poor local minima. In *Advances in neural information processing systems*, pages 586–594.
- Kidambi, R., Netrapalli, P., Jain, P., and Kakade, S. (2018). On the insufficiency of existing momentum schemes for stochastic optimization. In *2018 Information Theory and Applications Workshop (ITA)*, pages 1–9. IEEE.
- Kingma, D. P. and Welling, M. (2013). Auto-encoding variational bayes. *arXiv preprint arXiv:1312.6114*.
- Krizhevsky, A., Sutskever, I., and Hinton, G. E. (2012). Imagenet classification with deep convolutional neural networks. In *Advances in neural information processing systems*, pages 1097–1105.
- Kushner, H. and Yin, G. G. (2003). *Stochastic approximation and recursive algorithms and applications*, volume 35. Springer Science & Business Media.
- Le Roux, N., Schmidt, M. W., Bach, F. R., et al. (2012). A stochastic gradient method with an exponential convergence rate for finite training sets. In *NIPS*, pages 2672–2680.
- LeCun, Y., Bengio, Y., and Hinton, G. (2015). Deep learning. *nature*, 521(7553):436–444.
- LeCun, Y., Boser, B., Denker, J. S., Henderson, D., Howard, R. E., Hubbard, W., and Jackel, L. D. (1989). Backpropagation applied to handwritten zip code recognition. *Neural computation*, 1(4):541–551.
- LeCun, Y., Bottou, L., Bengio, Y., and Haffner, P. (1998). Gradient-based learning applied to document recognition. *Proceedings of the IEEE*, 86(11):2278–2324.
- Li, H., Xu, Z., Taylor, G., Studer, C., and Goldstein, T. (2018). Visualizing the loss landscape of neural nets. In *Advances in Neural Information Processing Systems*, pages 6389–6399.
- Liu, C. and Belkin, M. (2018). Mass: an accelerated stochastic method for over-parametrized learning. *arXiv preprint arXiv:1810.13395*.
- Lopez-Paz, D. and Oquab, M. (2016). Revisiting classifier two-sample tests. *arXiv preprint arXiv:1610.06545*.
- McCulloch, W. S. and Pitts, W. (1943). A logical calculus of the ideas immanent in nervous activity. *The bulletin of mathematical biophysics*, 5(4):115–133.
- Mescheder, L., Nowozin, S., and Geiger, A. (2017). The numerics of gans. In *Advances in Neural Information Processing Systems*, pages 1825–1835.
- Minsky, M. and Papert, S. A. (2017). *Perceptrons: An introduction to computational geometry*. MIT press.

- Nowozin, S., Cseke, B., and Tomioka, R. (2016). f-gan: Training generative neural samplers using variational divergence minimization. In *Advances in neural information processing systems*, pages 271–279.
- Pedro, D. (2000). A unified bias-variance decomposition and its applications. In *17th International Conference on Machine Learning*, pages 231–238.
- Pickering, A. (2010). *The cybernetic brain: Sketches of another future*. University of Chicago Press.
- Polyak, B. T. (1990). A new method of stochastic approximation type. *Avtomatika i telemekhanika*, (7):98–107.
- Polyak, B. T. and Juditsky, A. B. (1992). Acceleration of stochastic approximation by averaging. *SIAM Journal on Control and Optimization*, 30(4):838–855.
- Rahimi, A. and Recht, B. (2008). Random features for large-scale kernel machines. In *Advances in neural information processing systems*, pages 1177–1184.
- Raina, R., Madhavan, A., and Ng, A. Y. (2009). Large-scale deep unsupervised learning using graphics processors. In *Proceedings of the 26th annual international conference on machine learning*, pages 873–880.
- Razavi, A., van den Oord, A., and Vinyals, O. (2019). Generating diverse high-fidelity images with vq-vae-2. In *Advances in Neural Information Processing Systems*, pages 14866–14876.
- Recht, B. and Ré, C. (2012). Beneath the valley of the noncommutative arithmetic-geometric mean inequality: conjectures, case-studies, and consequences. *arXiv preprint arXiv:1202.4184*.
- Robbins, H. and Monro, S. (1951). A stochastic approximation method. *The annals of mathematical statistics*, pages 400–407.
- Rosenblatt, F. (1958). The perceptron: a probabilistic model for information storage and organization in the brain. *Psychological review*, 65(6):386.
- Rumelhart, D. E., Hinton, G. E., and Williams, R. J. (1985). Learning internal representations by error propagation. Technical report, California Univ San Diego La Jolla Inst for Cognitive Science.
- Ruppert, D. (1988). Efficient estimations from a slowly convergent robbins-monro process. Technical report, Cornell University Operations Research and Industrial Engineering.
- Salakhutdinov, R. and Larochelle, H. (2010). Efficient learning of deep boltzmann machines. In *Proceedings of the thirteenth international conference on artificial intelligence and statistics*, pages 693–700.
- Scholkopf, B. and Smola, A. J. (2018). *Learning with kernels: support vector machines, regularization, optimization, and beyond*. Adaptive Computation and Machine Learning series.
- Springenberg, J. T., Dosovitskiy, A., Brox, T., and Riedmiller, M. (2014). Striving for simplicity: The all convolutional net. *arXiv:1412.6806*.
- Srivastava, N., Hinton, G., Krizhevsky, A., Sutskever, I., and Salakhutdinov, R. (2014). Dropout: a simple way to prevent neural networks from overfitting. *The journal of machine learning research*, 15(1):1929–1958.
- Turing, A. M. (2009). Computing machinery and intelligence. In *Parsing the Turing Test*, pages 23–65. Springer.
- Vapnik, V. (2013). *The nature of statistical learning theory*. Springer science & business media.
- Vaswani, A., Shazeer, N., Parmar, N., Uszkoreit, J., Jones, L., Gomez, A. N., Kaiser, L., and Polosukhin, I. (2017). Attention is all you need. In *Advances in neural information processing systems*, pages 5998–6008.
- Wiener, N. (1965). *Cybernetics or Control and Communication in the Animal and the Machine*, volume 25. MIT press.